

2013

Synthetic efforts toward the eastern hemisphere of theonellamide C

Douglas D. Wong

Louisiana State University and Agricultural and Mechanical College

Follow this and additional works at: https://digitalcommons.lsu.edu/gradschool_dissertations



Part of the [Chemistry Commons](#)

Recommended Citation

Wong, Douglas D., "Synthetic efforts toward the eastern hemisphere of theonellamide C" (2013). *LSU Doctoral Dissertations*. 210.
https://digitalcommons.lsu.edu/gradschool_dissertations/210

This Dissertation is brought to you for free and open access by the Graduate School at LSU Digital Commons. It has been accepted for inclusion in LSU Doctoral Dissertations by an authorized graduate school editor of LSU Digital Commons. For more information, please contact gradetd@lsu.edu.

SYNTHETIC EFFORTS TOWARD THE EASTERN HEMISPHERE OF THEONELLAMIDE C

A Dissertation

Submitted to the Graduate Faculty of the
Louisiana State University and
Agricultural and Mechanical College
in partial fulfillment of the
requirements for the degree of
Doctor of Philosophy

in

The Department of Chemistry

by

Douglas D. Wong

B.S., Louisiana State University, 2003

December 2013

To My Family:

To my mom and dad, Helena and Roger, who showed me that with hard work and dedication anything is possible.

To my sister, Teresa, whose wisdom guides me.

To my brother, Alex, whose example inspires me.

To my sister, Lisa, whose honesty influences me.

ACKNOWLEDGMENTS

First and foremost, I would like to express my deepest gratitude for my advisor, Dr. Carol M. Taylor, for her years of guidance and support. Rarely will you find a person more passionate about her chemistry than Carol. I have learned from Carol that when you hold something in such high regard, you must work tirelessly in order to protect what is important. I am indebted to Carol for helping me strengthen my chemical intuition and professional foundation. I am also thankful for her “never too busy for her students” approach, more evidence that for Carol, it has and always will be about the chemistry. I honestly don’t know how I got to this point, but, I am grateful for every opportunity given to me.

My appreciation goes to members of the Taylor research group, Benson, Ning, Saroj, Chamini and Chyree for scientific discussions, friendship and support. The past six years have not been easy but all of you have made this process exponentially better. I feel truly blessed to call each and every one of you friend. I also thank Molly of Dr. Waldrop group for explaining all things biology to an organic chemist. Special thanks to Alex of Dr. Vicente group for his friendship and encouragement.

I would like to thank my committee members, Dr. William Crowe, Dr. Graca Vicente and Dr. Evgueni Nesterov for their advice and helpful suggestions. A heartfelt thanks to the late Dr. Dale Treleven and Dr. Thomas Weldeghiorghis for their assistance in the acquisition and interpretation of more complex NMR spectra. I wish to thank Dr. Connie David for her help in all things related to mass spectrometry. I would be remiss if I did not thank the Department of Chemistry at LSU and the National Science Foundation for their financial support.

TABLE OF CONTENTS

ACKNOWLEDGMENTS	iii
LIST OF TABLES	vii
LIST OF FIGURES	viii
LIST OF SCHEMES.....	xi
LIST OF ABBREVIATIONS AND SYMBOLS	xv
ABSTRACT.....	xx
CHAPTER 1:	
THE THEONELLAMIDES (TNMs) AND RELATED COMPOUNDS	1
1.1 Isolation and Biological Activity	1
1.2 Structure Determination of Selected Amino Acids of TNM F ⁶	6
1.3 The Relationship between Isotheopalauamide and Theopalauamide ⁹	10
1.4 Early Biological Studies	11
1.5 Synthetic Studies of TNM F by Shioiri and co-workers.....	13
1.5.1 Synthesis of the Southern Hemisphere* of TNM F	14
1.5.2 Synthesis of the Northern Hemisphere of TNM F	15
1.6 Recent Biological Studies	16
1.7 Goals of the Current Work.....	23
1.8 References.....	24
CHAPTER 2:	
ASYMMETRIC SYNTHESIS OF <i>ERYTHRO</i> - β -HYDROXYASPARAGINE (<i>EHYASN</i>)	27
2.1 Proteinogenic vs Nonproteinogenic Amino Acids.....	27
2.2 Nonribosomal Peptide Synthesis	28
2.3 Identification and Occurrence of HyAsn in Nature	30
2.4 Previous Syntheses of 3-Hydroxyaspartic Acid.....	31
2.5 Previous Syntheses of β -Hydroxy-L-asparagine.....	33
2.5.1 Previous Syntheses of <i>Erythro</i> - β -Hydroxyasparagine	33
2.5.2 Previous Syntheses of <i>Threo</i> - β -Hydroxyasparagine	34
2.6 Retrosynthetic Analysis	37
2.7 The Sharpless Asymmetric Aminohydroxylation	38
2.8 Synthesis of <i>eHyAsn</i>	44
2.9 The <i>eHyAsn</i> -Phe Dipeptide	46
2.10 Experimental Section	48
2.10.1 Experimental Procedures	49
2.10.2 Spectra.....	55
2.11 References.....	71
CHAPTER 3:	
EARLY APPROACHES TO THE SYNTHESIS OF ABOA	75
3.1 Previous Synthesis of Aboa by Tohdo <i>et al</i> ¹	75
3.2 A Challenging Application of the Sharpless Aminohydroxylation Reaction	77
3.3 The Regioreversed Sharpless Aminohydroxylation Reaction	79

3.4	Attempted Synthesis of Triene 175 , an Aboa Precursor	81
3.5	A Model System for the Regioreversed SAH.....	84
3.6	The Nitroaldol Reaction.....	85
3.7	Wolf's Asymmetric Nitroaldol Reaction	87
3.8	The Second Approach for the Synthesis of Aboa: Application of Wolf's Nitroaldol Reaction	89
3.9	A Model System for Wolf's Nitroaldol Reaction	89
3.10	Experimental Section	92
	3.10.1 Experimental Procedures	92
	3.10.2 Spectra.....	103
3.11	References.....	125
CHAPTER 4:		
RECENT APPROACHES TO THE SYNTHESIS OF APOA AND ABOA.....		129
4.1	The Third Approach to the Synthesis of Aboa and Apoa	129
4.2	Preparation of the Phosphonate Ester Fragments for Aboa and Apoa Synthesis.....	130
4.3	Preparation of the Aldehyde Fragment for Aboa and Apoa Synthesis	133
4.4	Probing Anion Formation and the HWE Reaction	140
4.5	The Key HWE Reaction	146
4.6	A Model System for Protecting Group Manipulations and Functional Group Interconversions	149
4.7	Attempted Elaboration to Apoa, Synthesis of an Advanced Primary Alcohol Intermediate 279	151
4.8	An Alternate Approach for the Synthesis of Apoa	158
4.9	Efforts to Synthesize Aldehyde 281 from 254 Through a TBS or Alloc Protected Intermediate	159
4.10	Future Work for the Completion of Apoa and Aboa	161
4.11	Experimental Section	162
	4.11.1 Experimental Procedures	162
	4.11.2 Spectra.....	176
4.12	References.....	204
CHAPTER 5:		
PEPTIDE FRAGMENT ASSEMBLY FOR THEONELLAMIDE C		207
5.1	Introduction.....	207
5.2	Peptide and Peptide-Based Drugs	207
5.3	How to Make an Amide Bond	212
5.4	Retrosynthesis for the Eastern Hemisphere of TNM C	214
5.5	The Risk of Epimerization During Fragment Condensation.....	216
5.6	Synthesis of the Fmoc- <i>allo</i> -Thr(OTBS)-Ser(OTBS)-Phe-OBn Tripeptide	217
5.7	Synthetic Efforts Towards the Eastern Hemisphere of TNM C: a β -Phe Analog.....	222
5.8	Future Work and Perspectives	224
	5.8.1 Future Work: Construction of Both Naturally Occurring Theonellamide Eastern Hemispheres, The Apoa and Aboa Containing Congeners.....	224
	5.8.2 Future TNM C Perspectives: Utilizing the Amphotericin B Blueprint.....	226
5.9	Experimental Section	227
	5.9.1 Experimental Procedures	227
	5.9.2 Spectra.....	231
5.10	References.....	235

APPENDIX: LETTERS OF PERMISSION.....	239
THE VITA	256

LIST OF TABLES

Table 1.1	Amino Acid Composition of TNMs A-F (10 and 12-16), Theonegramide (11) and Theopalauamide (9). Copyright 2007, Elsevier, reprinted with permission (p. 241).	4
Table 2.1	A Substrate Based Approach for Control of Regioselectivity by Janda and Co-Workers	41
Table 2.2	McLeod and Co-Workers' Investigation on Factors Affecting Regioselectivity Using Similarly Substituted Esters.....	44
Table 2.3	<i>e</i> HyAsn-Phe Dipeptide Formation: Optimization Study	48
Table 3.1	Wittig Reaction Between Benzaldehyde and Carboxy Ylides Varying in Methylene Chain Length to Examine Trends in <i>E/Z</i> Stereoselectivity as Performed by Maryanoff <i>et al.</i> ²⁶	83
Table 4.1	Hutton and Co-workers' ¹⁷ Optimization Study for Generation of Oxazolidine 250	139
Table 4.2	Helquist and Co-workers' ¹⁸ Access to 4-Methyldienoate Derivatives Using LiHMDS in HWE Reactions	140
Table 4.3	Collignon <i>et al.</i> ¹⁹ Generation of 2-Diethylphosphonyl Homoallylic Alcohols Using LDA in HWE Reactions.....	143
Table 4.4	HWE Reaction of Commercially Available Bases with <i>p</i> -Bromobenzaldehyde	144
Table 4.5	Nicolaou and Co-worker's ²⁰ Use of (<i>E</i>)-Diethyl Cinnamylphosphonate <i>En Route</i> to Endiandric Acids A-G	145
Table 4.6	Optimization Study for the HWE Reaction	148
Table 4.7	¹ H and ¹³ C NMR Data for Z-277 in CDCl ₃	157

LIST OF FIGURES

Figure 1.1	Some Representative Natural Products from the Lithistid Sponges.....	1
Figure 1.2	Current Classification of Lithistid Sponges.....	2
Figure 1.3	Swinholide A and Theopalauamide Derived from Purified Cell Types of <i>T. Swinhoei</i> . Copyright 1998, John Wiley and Sons, reprinted with permission (p. 240).....	3
Figure 1.4	Chemical Structures of TNM F and Theonegramide	4
Figure 1.5	Structures of Varying Amino Acids for the Theonellamides and Related Compounds	5
Figure 1.6	β -L-Arabinose and β -D-Arabinose in their Pyranose Forms Compared to D-Galactose	6
Figure 1.7	Aboa Structure Elucidation: NMR Data Correlations for Bond Connectivity	10
Figure 1.8	Theonellamides Induced Vacuole Formation in Rat Embryonic 3Y1 Fibroblasts. Copyright 2002, Springer, reprinted with permission (p. 243).....	12
Figure 1.9	Chemical-Genetic Profiling. Copyright 2012, Elsevier, reprinted with permission (p. 244)	17
Figure 1.10	Recent TNM Biological Studies, Part 1. Copyright 2009, Nature Publishing Group, reprinted with permission (p. 248). Copyright 2006, Elsevier, reprinted with permission (p. 246).....	18
Figure 1.11	Recent TNM Biological Studies, Part 2. Copyright 2009, Nature Publishing Group, reprinted with permission (p. 248).	19
Figure 1.12	Recent TNM Biological Studies, Part 3. Copyright 2009, Nature Publishing Group, reprinted with permission (p. 248).....	20
Figure 1.13	Recent TNM Biological Studies, Part 4. Copyright 2010, Nature Publishing Group, reprinted with permission (p. 249).	21
Figure 1.14	Recent TNM Biological Studies, Part 5. Copyright 2010, Nature Publishing Group, reprinted with permission (p. 249).....	22
Figure 2.1	The Standard Amino Acids	27
Figure 2.2	Structures of β -Hydroxyaspartic Acid, <i>e</i> HyAsn and <i>t</i> HyAsn.....	30
Figure 2.3	Lysobactin and Ramoplanin A1	34
Figure 2.4	Janda and Co-Workers ³³ Proposed a Catalytically Active Complex for the SAH Reaction. Copyright 2009, Elsevier, reprinted with permission (p. 251).....	41
Figure 3.1	Representative Products of the Regioreversed SAH	80

Figure 3.2	HPLC Chromatogram of Sharpless Aminohydroxylation Reaction After Flash Chromatography.....	95
Figure 3.3	HPLC Chromatogram of Nitroaldol Reaction After Flash Chromatography	99
Figure 3.4	HPLC Chromatogram of 201 Diastereomer 1	100
Figure 3.5	Chiral HPLC Chromatogram of 201 Diastereomer 1	100
Figure 3.6	HPLC Chromatogram of 200	101
Figure 3.7	HPLC Chromatogram of 201 Diastereomer 2	102
Figure 3.8	HPLC Chromatogram of 201 Diastereomer 2	102
Figure 4.1	Chiral HPLC Chromatogram for SAH Reaction Products after Preparative HPLC to Separate Regioisomers	134
Figure 4.2	¹ H NMR Chemical Shifts for the N-H Proton of 209 and its Regioisomer	134
Figure 4.3	Phosphonate Ester Fragment for Apoa and a Desmethyl Analog	140
Figure 4.4	¹ H NMR Spectra of Starting Apoa Phosphonate Ester (Blue) and Dideuterated Apoa Phosphonate Ester (Red)	142
Figure 4.5	Chemical Structures of <i>E</i> - 277 and <i>Z</i> - 277	153
Figure 4.6	Tohdo's Olefin Assignments Based on nOe Measurements of Precursors	153
Figure 4.7	Helquist's Double Bond Assignments Based on ROESY NMR Results	154
Figure 4.8	HSQC spectrum of <i>Z</i> - 277	155
Figure 4.9	HMBC spectrum of <i>Z</i> - 277	155
Figure 4.10	ROESY spectrum of <i>Z</i> - 277	156
Figure 5.1	Summary of Synthetic Work Presented.....	207
Figure 5.2	Challenging Motifs in Peptide Chemistry	209
Figure 5.3	Natural Peptides as Approved Peptide Drugs.....	210
Figure 5.4	Graphic Depiction of Aliskiren Binding to the Active Site of Renin. Copyright 2008, Nature Publishing Group, reprinted with permission (p. 256).....	212
Figure 5.5	Common Peptide Coupling Reagents and Additives Used in This and Previous Chapters	213
Figure 5.6	Synthesis of the Eastern Hemisphere of TNM F by Shioiri <i>et al.</i> ^{32,33} 11 Steps (5 Deprotections and 6 Couplings) → 3.6% Overall Yield.....	214

Figure 5.7 Three Macrocycles Related to the Eastern Hemisphere of TNM C 222

LIST OF SCHEMES

Scheme 1.1	Amino Acids of TNM F Assigned the <i>L</i> -Configuration by Chiral GC-MS	7
Scheme 1.2	Aboa Structure Elucidation: Functional Group Determination	8
Scheme 1.3	Aboa Structure Elucidation: Absolute Stereochemistry Assignment	9
Scheme 1.4	Important ROESY Correlations for Both Conformational Isomers	11
Scheme 1.5	Preparation of TNM A-Conjugated Gel Beads and the Two Proteins Bound on Subsequent Reaction with Rabbit Liver Tissue Extracts	12
Scheme 1.6	Biological Functions of 17 β -Hydroxysteroid Dehydrogenase IV and Glutamate Dehydrogenase	13
Scheme 1.7	DPPA (DEPC) Reaction Mechanism	14
Scheme 1.8	Synthesis of the Southern Hemisphere of TNM F	15
Scheme 1.9	Synthesis of the Northern Hemisphere of TNM F	16
Scheme 1.10	Major Disconnections for TNM C	24
Scheme 2.1	Some Examples of PTM: Specific Covalent Modifications.....	28
Scheme 2.2	Roles of 3 Primary Domains in a NRPS Module	29
Scheme 2.3	Cho and Ko's ¹⁰ Cyclic Iminocarbonate Intermediate for a Projected 3-Hydroxyaspartic Acid Synthesis	31
Scheme 2.4	Shioiri and Co-workers' ¹¹ <i>L</i> -threo- β -Hydroxyaspartic Acid Synthesis <i>En Route</i> to Alterobactin A.....	32
Scheme 2.5	Lectka <i>et al.</i> ¹² BQ Catalyzed Synthesis of β -Substituted Aspartic Acid Precursors.....	32
Scheme 2.6	Okai and Izumiya's ^{6,13} Synthesis of <i>e</i> HyAsn Using an Enzyme-Catalyzed Reaction.....	33
Scheme 2.7	Sendai and Co-workers' ¹⁴ Synthesis of <i>e</i> HyAsn Using an Enzyme-Catalyzed Reaction	34
Scheme 2.8	Lectka and Co-workers' ¹⁷ BQ Catalyzed Synthesis of <i>t</i> HyAsn	35
Scheme 2.9	VanNieuwenhze <i>et al.</i> ¹⁸ Synthesis of <i>t</i> HyAsn.....	36
Scheme 2.10	Boger and Co-workers' ^{19,20} Synthesis of <i>t</i> HyAsn Using a Stereoselective Reaction.....	37
Scheme 2.11	Retrosynthetic Analysis of <i>e</i> HyAsn	37
Scheme 2.12	Sharpless Chemistry	38

Scheme 2.13 Reaction Mechanism for the Sharpless Aminohydroxylation Reaction. Copyright 2010, John Wiley and Sons, reprinted with permission (p. 250).....	39
Scheme 2.14 Aminohydroxylation of Cinnamates Using (DHQ) ₂ PHAL.....	40
Scheme 2.15 The Catalytically Active Complexes as Supported by B3LYP/6-31G* Calculations. Copyright 2009, Elsevier, reprinted with permission (p. 251).....	43
Scheme 2.16 Part 1 of <i>e</i> HyAsn Synthesis.....	45
Scheme 2.17 Precedents for Oxidative Cleavage of the PMP Group in the Presence of Cbz	45
Scheme 2.18 Part 2 of <i>e</i> HyAsn Synthesis.....	46
Scheme 2.19 γ -Hydroxyacids Can Form γ -Lactones Under Acidic Conditions.....	46
Scheme 2.20 Side Reaction of Unprotected Asn Residues: β -Cyanoalanine Derivative Formation. Copyright 2009, Elsevier, reprinted with permission (p. 253).....	47
Scheme 3.1 Tohdo <i>et al.</i> ¹ Retrosynthesis of Aboa.....	75
Scheme 3.2 Synthesis of Aboa by Tohdo <i>et al.</i> ¹	76
Scheme 3.3 The Original Retrosynthetic Analysis	77
Scheme 3.4 Challenges in the Aminohydroxylation Reaction of 147 (Left) with Selected Dihydroxylation Reaction Precedents (Right)	78
Scheme 3.5 Attempted Synthesis of 175	81
Scheme 3.6 Application of the Regioreversed SAH on a Model Compound.....	84
Scheme 3.7 Nitroaldol Reaction Products are Precursors to Useful Moieties in Organic Synthesis.....	85
Scheme 3.8 Walsh and Kowzowski's Proposed Mechanism ³⁸ for Shibasaki's Li ₃ (THF) _{<i>n</i>} (BINOLate) ₃ La(OH) ₂ Catalyzed Nitroaldol Reaction. Copyright 2008, University Science Books, reprinted with permission (p. 255)	86
Scheme 3.9 Synthesis and Physical Characteristics of Wolf's Bisoxazolidine Catalyst	87
Scheme 3.10 Wolf's Nitroaldol Reaction Generates: (<i>R</i>)-Nitro Alcohols with 190 /ZnMe ₂ ⁴⁰ (<i>S</i>)-Nitro Alcohols with 190 /CuOAc ⁴³	88
Scheme 3.11 Wolf's Nitroaldol Reaction Between Benzaldehyde and Nitroethane: Preferential Formation of the <i>Syn</i> Diastereomer ⁴⁰	89
Scheme 3.12 The Second Retrosynthetic Analysis.....	89
Scheme 3.13 Nitroaldol Reaction Between <i>Trans</i> -Cinnamaldehyde and Methyl 3-Nitropropanoate Under Wolf Conditions	91

Scheme 4.1	The Third Retrosynthesis of Aboa and Apoa	129
Scheme 4.2	Precedents for the Proposed S _N 1 Reaction	130
Scheme 4.3	Competing Mechanistic Pathways for the Bromination Reaction.....	131
Scheme 4.4	Synthesis of the Phosphonate Ester Fragment for Apoa	132
Scheme 4.5	Synthesis of the Phosphonate Ester Fragment for Aboa	132
Scheme 4.6	Synthesis of β-amino alcohol 209	133
Scheme 4.7	TBS Protection of 209 Using TBSOTf and TBSCl.....	135
Scheme 4.8	Results for the DIBALH Reduction of 235	136
Scheme 4.9	Kandula and Kumar <i>En Route</i> to (+)-L-733,060.....	136
Scheme 4.10	Precedents for Deprotonation of Acidic Carbamate Protons Followed by Addition Reactions.....	137
Scheme 4.11	Example of an Aldehyde Containing a Di-Boc-Protected Primary Amine Used for an Olefination Reaction.....	137
Scheme 4.12	Attempted Synthesis of 247	138
Scheme 4.13	Completion of the Aldehyde Fragment for Apoa and Aboa Synthesis	139
Scheme 4.14	Formation of an Unexpected Dideuterated Product	141
Scheme 4.15	Proposed Mechanism for the Deuteration Product.....	142
Scheme 4.16	HWE Reaction of the Model and Apoa Phosphonate Ester with Garner's Aldehyde.....	146
Scheme 4.17	Mechanism of the HWE Reaction	147
Scheme 4.18	Comparison of the Model System to Apoa for Further Modifications.....	149
Scheme 4.19	Initial and Improved Conditions for Reactions of Interest	150
Scheme 4.20	An Explanation for the Accelerating Effect of H ₂ O in Dess-Martin Oxidations	151
Scheme 4.21	Formation of a Side Product Following Oxazolidine Group Deprotection	152
Scheme 4.22	Formation of Primary Alcohol 279	158
Scheme 4.23	An Alternate Retrosynthesis of Apoa.....	159
Scheme 4.24	Attempted Synthesis of Primary Alcohol 286 Using a TBS Protecting Group.....	160
Scheme 4.25	Synthesis of Aldehyde 281 Using an Alloc Protecting Group	161

Scheme 4.26 Plans to Complete Apoa and Aboa.....	161
Scheme 5.1 Inhibition of RAS can Occur at Three Different Stages.....	211
Scheme 5.2 The Retrosynthetic Analysis for Commercial Production of Aliskiren. Copyright 2008, Nature Publishing Group, reprinted with permission (p.256).....	212
Scheme 5.3 Amide Bond Formation Via Activation	213
Scheme 5.4 Eastern Hemisphere of TNM C: Retrosynthesis and Protecting Group Strategy.....	215
Scheme 5.5 Mechanism of Racemization: Oxazolone Formation	216
Scheme 5.6 Fmoc- <i>allo</i> -Thr(OTBS)-Ser(OTBS)-Phe-OBn Tripeptide Construction	217
Scheme 5.7 Reaction Mechanism for Carbodiimide-Mediated Peptide Ligation.....	218
Scheme 5.8 Fmoc- <i>allo</i> -Thr(O ^t Bu)-Ser(O ^t Bu)-OH Dipeptide Formation Via DCC/NHS Activation	219
Scheme 5.9 HATU Activation and Coupling	220
Scheme 5.10 Side Reaction Associated with the Use of HATU.....	220
Scheme 5.11 Neighboring Group Participation: H-Bonding Accelerates Rate of Coupling of OAt Esters.....	221
Scheme 5.12 TBS Protection of the Hydroxyl Group in Fmoc-Ser-OH.....	221
Scheme 5.13 Progress Toward the Eastern Hemisphere of TNM C: a β -Phe Analog.....	223
Scheme 5.14 Plans to Complete Both Theonellamide Eastern Hemispheres	225
Scheme 5.15 Linking AmB's Past to TNM C's Future	226

LIST OF ABBREVIATIONS AND SYMBOLS

Å	angstrom
AA	amino acid
Aboa	(3 <i>S</i> ,4 <i>S</i> ,5 <i>E</i> ,7 <i>E</i>)-3-amino-8-(4-bromophenyl)-4-hydroxy-6-methylocta-5,7-dienoic acid
Ac	acetyl
ACE	angiotensin-converting-enzyme
AD-mix- α	1 kg contains: $K_3Fe(CN)_6$, 699.6 g; K_2CO_3 , 293.9 g; and $[(DHQ)_2-PHAL]$, 5.52g; and $K_2O_5O_2(OH)_4$, 1.04 g
AD-mix- β	Contents are as for AD-mix- α except the ligand: $[(DHQD)_2-PHAL]$
A-domain	adenylation-domain
Ahad	(2 <i>S</i> ,4 <i>R</i>)-2-amino-4-hydroxyadipic acid
Alloc	allyloxycarbonyl
AmB	amphotericin B
Apoa	(3 <i>S</i> ,4 <i>S</i> ,5 <i>E</i> ,7 <i>E</i>)-3-amino-4-hydroxy-6-methyl-8-phenylocta-5,7-dienoic acid
ARBs	angiotensin II receptor blockers
BINOL	1,1'-Bi(2-naphthol)
Bn	benzyl
Boc	<i>tert</i> -butyloxycarbonyl
BOP	benzotriazol-1-yloxytris(dimethylamino)-phosphonium hexafluorophosphate
BORSM	based on recovered starting material
BQ	benzoylquinine
^t Bu	<i>tert</i> -butyl
°C	degrees Celsius
<i>C. albicans</i>	<i>Candida albicans</i>

CAN	cerium (IV) ammonium nitrate
Cbz	carbobenzyloxy
CD	circular dichroism
C-domain	condensation-domain
<i>C</i> → <i>N</i>	carbon-to-nitrogen
COSY	correlation spectroscopy
CSA	camphorsulfonic acid
DBN	1,5-diazabicyclo[4.3.0]non-5-ene
DBU	1,8-diazabicyclo[5.4.0]undec-7-ene
DCC	dicyclohexylcarbodiimide
DCU	dicyclohexylurea
<i>de</i>	diastereomeric excess
DEPC	diethyl phosphorocyanidate
DIBALH	diisobutylaluminum hydride
DIPEA	<i>N,N</i> -diisopropylethylamine
DMAP	4-dimethylaminopyridine
DMF	dimethylformamide
DMI	1,3-dimethyl-2-imidazolidinone
DMP	Dess-Martin periodinane
DNP	dinitrophenylhydrazine
DPPA	diphenylphosphoryl azide
EDC	1-(3-dimethylaminopropyl)-3-ethylcarbodiimide hydrochloride
<i>ee</i>	enantiomeric excess
EGF	epidermal growth factor
<i>eHyAsn</i>	<i>erythro</i> -hydroxyasparagine
EI	electron ionization

ESI	electrospray ionization
FAB	fast atom bombardment
FGI	functional group interconversion
FK463	Micafungin
Fmoc	9-fluorenylmethoxycarbonyl
Gal	galactose
GC	gas chromatography
GO	Gene Ontology
τ -HAL	τ -histidinoalanine
HAPyU	<i>O</i> -(7-azabenzotriazol-1-yl)-1,1,3,3-tetramethyleuronium hexafluorophosphate
HATU	<i>O</i> -(7-azabenzotriazol-1-yl)-1,1,3,3-tetramethyluronium hexafluorophosphate
HBPyU	<i>O</i> -(benzotriazol-1-yl)oxybis-(pyrrolidino)uronium hexafluorophosphate
HBTU	<i>O</i> -(benzotriazol-1-yl)-1,1,3,3-tetramethyluronium hexafluorophosphate
HMBC	heteronuclear multiple bond correlation spectroscopy
HMDS	hexamethyldisilazane
HOAt	1-hydroxy-7-azabenzotriazole
HOBt	1-hydroxybenzotriazole
HPLC	high performance liquid chromatography
HSQC	heteronuclear single quantum coherence spectroscopy
HRMS	high resolution mass spectrometry
HWE	Horner-Wadsworth Emmons
HyAsn	hydroxyasparagine
Hz	hertz
IC ₅₀	half maximal inhibitory concentration
IR	infrared spectroscopy
L1210	mouse lymphocytic leukemia cells

LAPase	leucine aminopeptidase
LDA	lithium diisopropylamide
LiHMDS	lithium hexamethyldisilazide
<i>m</i>	<i>meta</i>
Me	methyl
MOA	mode of action
MoBY-ORF	molecular barcoded yeast open reading frame
2-MP	2-methoxypropene
MS	mass spectrometry
<i>Mtb</i>	<i>Mycobacterium tuberculosis</i>
MVD1	mevalonate pyrophosphate decarboxylase
<i>m/z</i>	mass-to-charge ratio
NHS	<i>N</i> -hydroxysuccinimide
NMR	nuclear magnetic resonance
nOe	nuclear Overhauser effect
NRPSs	nonribosomal peptide synthetases
<i>p</i>	<i>para</i>
PC	phosphatidylcholine
PCP	peptidyl carrier protein
PE	phosphatidylethanol
PMP	<i>para</i> -methoxyphenyl
ppm	parts per million
PPTS	pyridinium <i>p</i> -toluenesulfonate
PS	phosphatidylserine
PTM	post-translational modification
q	quartet

RAS	renin-angiotensin system
R _f	retention factor
ROESY	rotating frame Overhauser effect spectroscopy
rt	room temperature
s	singlet
SAD	Sharpless asymmetric dihydroxylation
SAE	Sharpless asymmetric epoxidation
SAH	Sharpless asymmetric aminohydroxylation
<i>S. cerevisiae</i>	<i>Saccharomyces cerevisiae</i>
SM	sphingomyelin
S _N 1	unimolecular nucleophilic substitution
<i>S. pombe</i>	<i>Schizosaccharomyces pombe</i>
TBAF	tetra- <i>n</i> -butylammonium fluoride
TBS	<i>t</i> -butyldimethylsilyl
TFA	trifluoroacetic acid
THF	tetrahydrofuran
<i>t</i> HyAsn	<i>threo</i> -hydroxyasparagine
TLC	thin layer chromatography
TNM	theonellamide
TOCSY	total correlation spectroscopy
TOF	time of flight
trityl	triphenylmethyl
Troc	2,2,2-trichloroethoxycarbonyl
<i>T. swinhoei</i>	<i>Theonella swinhoei</i>
UV	ultraviolet
YEPD	yeast extract peptone dextrose

ABSTRACT

The theonellamides (TNMs) A-F are bicyclic dodecapeptides isolated from marine sponges of the genus *Theonella* and were shown to display potent antifungal activity. Despite considerable synthetic effort to produce TNM F by the Shioiri group in the early 1990s, a total synthesis of a TNM has yet to be reported. This dissertation describes our efforts toward some of the required amino acid residues of TNM C and the eastern hemisphere.

The production of *erythro*- β -hydroxyasparagine (*eHyAsn*) followed the synthesis of *threo*- β -HyAsn by Boger and co-workers, utilizing a key Sharpless aminohydroxylation reaction. The *eHyAsn* building block, Boc-*eHyAsn*(OTBS)-OH, was coupled with HCl.Phe.OMe using EDC/HOBt/NEt₃/THF to afford Boc-*eHyAsn*(OTBS)-Phe-OMe in 68% yield.

Our two early approaches toward the (3*S*,4*S*,5*E*,7*E*)-3-amino-8-(4-bromophenyl)-4-hydroxy-6-methylocta-5,7-dienoic acid (Aboa) residue are presented. The first relied on a challenging regioreversed Sharpless aminohydroxylation reaction and the second on a nitroaldol condensation. Results from individual model systems indicated that the levels of diastereo- and enantioselectivity for each approach were not acceptable.

The most recent approach to Apoa and Aboa utilized a key Horner-Wadsworth Emmons reaction followed by two conceptual sets of protecting group manipulations. The optimized conditions for the HWE reaction of (4*S*,5*R*)-*tert*-butyl 5-formyl-4-(2-(4-methoxyphenoxy)ethyl)-2,2-dimethyloxazolidine-3-carboxylate with (*E*)-diethyl (4-phenylbut-3-en-2-yl)phosphonate led to a 40% yield with a 4.5:1 *E/Z* ratio of olefin products. Currently, an advanced primary alcohol intermediate (three steps from Apoa) has been verified by HRMS. We also briefly explored an approach whereby the conjugated system could potentially be introduced after the oxidative removal of the PMP group.

The preparation of the Fmoc-*allo*-Thr(OTBS)-Ser(OTBS)-Phe-OBn tripeptide resulted from coupling commercially available amino acid residues in an *N*→*C* stepwise fashion followed by exchange

of both *O*^tBu protecting groups with their TBS counterparts. Since the A_{poa} and A_{boa} residues were not yet available, we sought to synthesize an analog of the eastern hemisphere of TNM C containing β-Phe as this would generate a macrocycle with the same ring size. Synthetic efforts toward this analog have produced the cyclization precursor as verified by HRMS. Once A_{poa}/A_{boa} is complete, the deprotection and coupling conditions outlined for the β-Phe analog can be applied towards the assembly of both A_{poa}- and A_{boa}-containing eastern hemispheres.

CHAPTER 1: THE THEONELLAMIDES (TNMs) AND RELATED COMPOUNDS

1.1 Isolation and Biological Activity

Lithistid sponges have been an important source of many different classes of compounds with potent biological activities.^{1,2} These sponges occur in both shallow and deep water environments and have produced over 300 natural products to-date. These structurally complex compounds include cyclic and linear peptides, polyketides, alkaloids, sterols, and lipids (Figure 1.1).

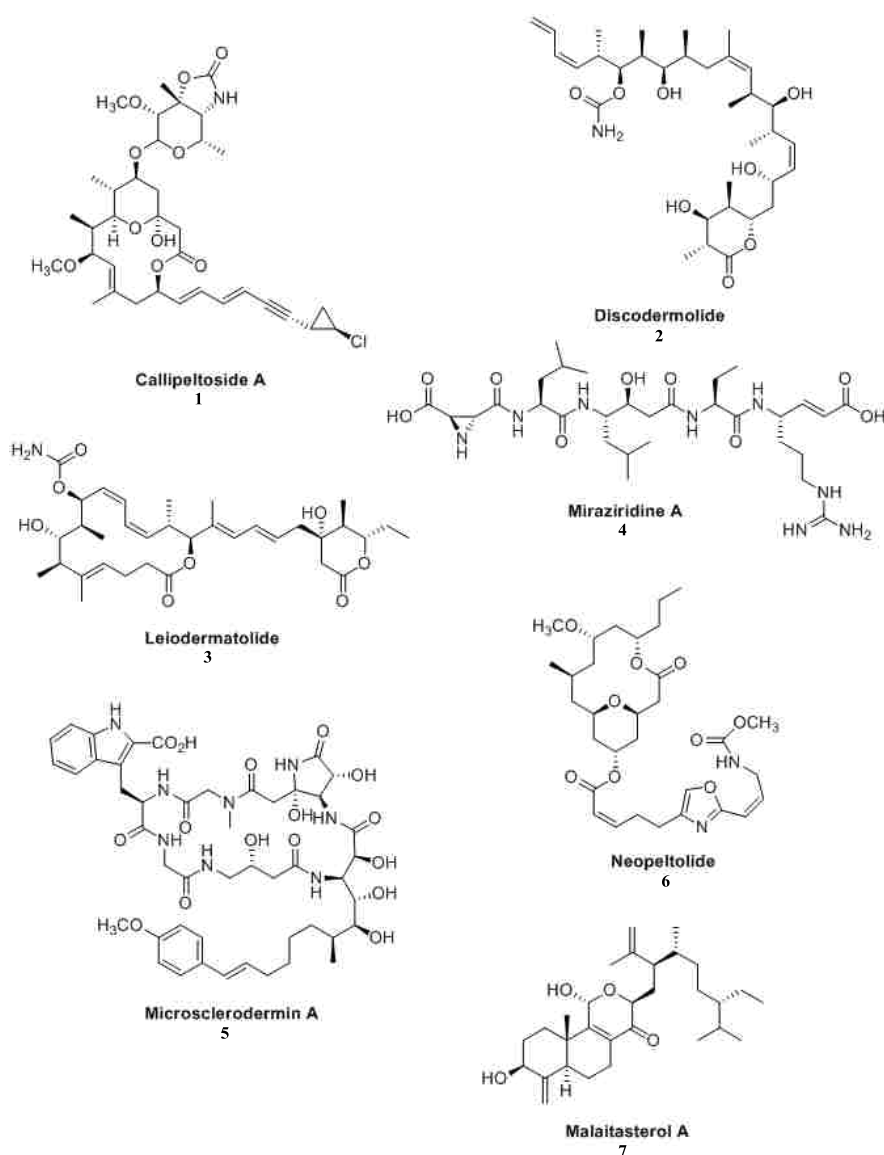


Figure 1.1 – Some Representative Natural Products from the Lithistid Sponges

The Order Lithistida (Figure 1.2) is an assemblage of sponges grouped together based on fused or interlocking spicules called desmas that make up their skeleton.³ The skeleton of desmas provides the sponges with a firm or rock-hard consistency and also separates the sponge into internal (endosome) and external (ectosome) tissues.

Phylum Porifera

Class Demospongiae

Order Lithistida

Family Theonellidae

Genera Discodermia, Racodiscula, Siliquaruaspongia, Theonella

Figure 1.2 – Current Classification of Lithistid Sponges

Early work by Bewley and co-workers⁴ reported that a number of symbiotic bacteria live in association with the sponge *Theonella swinhoei*.⁵ The sponge *T. swinhoei* contains four cell populations: unicellular cyanobacteria, unicellular heterotrophic bacteria (eubacteria), sponge cells, and filamentous heterotrophic bacteria (filaments). The unicellular cyanobacteria occur only in the ectosome while the filamentous bacteria reside only in the endosome. Heterotrophic eubacteria and sponge cells occur in both endosome and ectosome. The separation of external and internal tissues was followed by dissociation (passage through a juicer) and differential centrifugation of the cell suspension. This led to cell types of >90% purity. Chemical analysis (HPLC and ¹H NMR spectroscopy) of the four cell fractions showed that the unicellular cyanobacteria and sponge cells lacked any bioactive metabolites. The polyketide swinholide A **8** (and demonstrated an *in vitro* IC₅₀ value against KB and L1210 tumor cells 0.04 and 0.03 μg mL⁻¹, respectively) was present in the fraction of eubacteria and theopalauamide **9** was localized in the filamentous bacteria (Figure 1.3).⁴

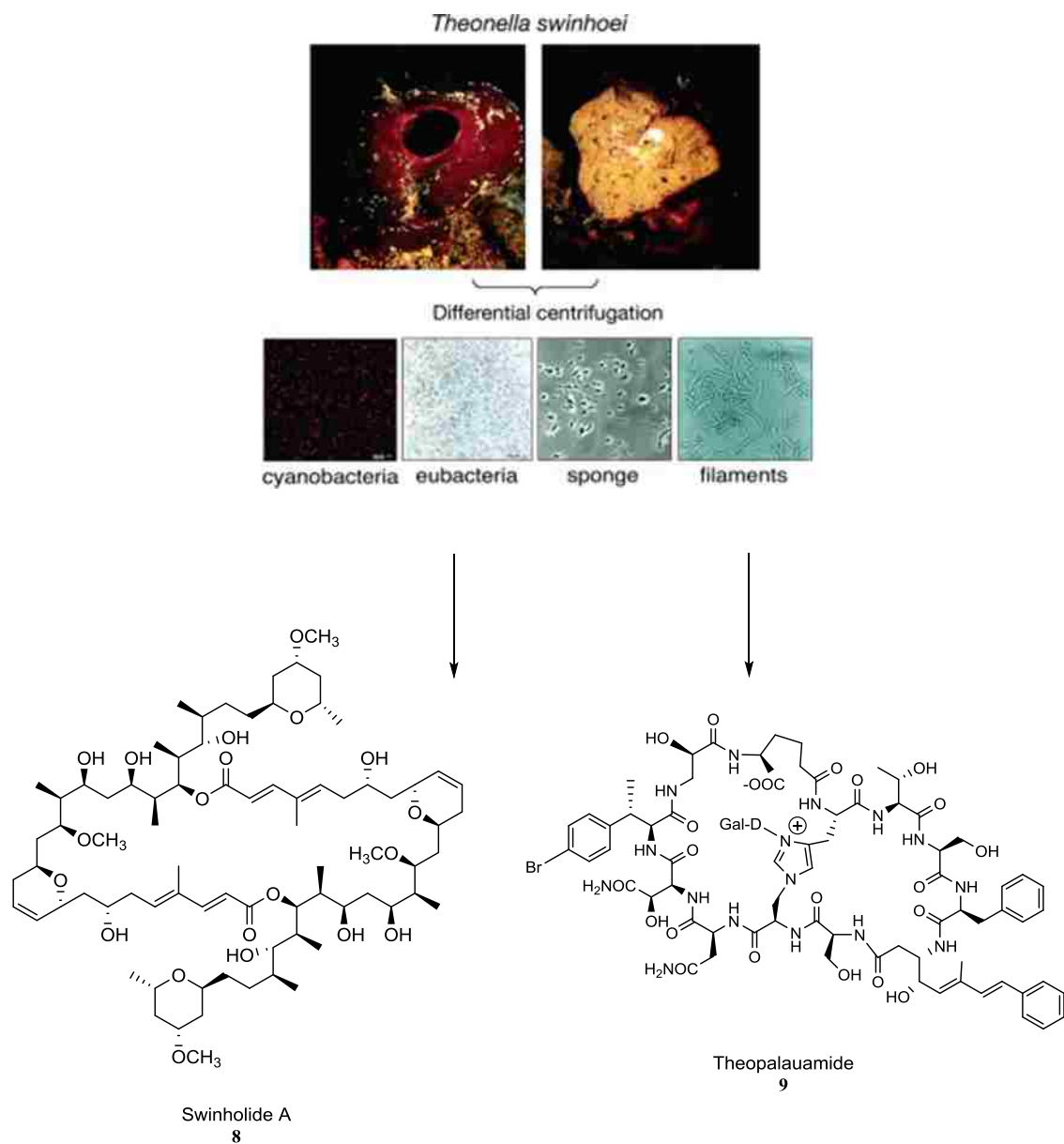


Figure 1.3 – Swinholide A and Theopalauamide Derived from Purified Cell Types of *T. Swinhoei*. Copyright 1998, John Wiley and Sons, reprinted with permission (p. 240).

The theonellamides (TNMs) A-F are bicyclic dodecapeptides isolated from marine sponges of the genus *Theonella*.^{6,7} These compounds closely resemble theonegramide **11** (Figure 1.4) and theopalauamide **9**, two glycopeptides isolated by Faulkner and coworkers.^{8,9}

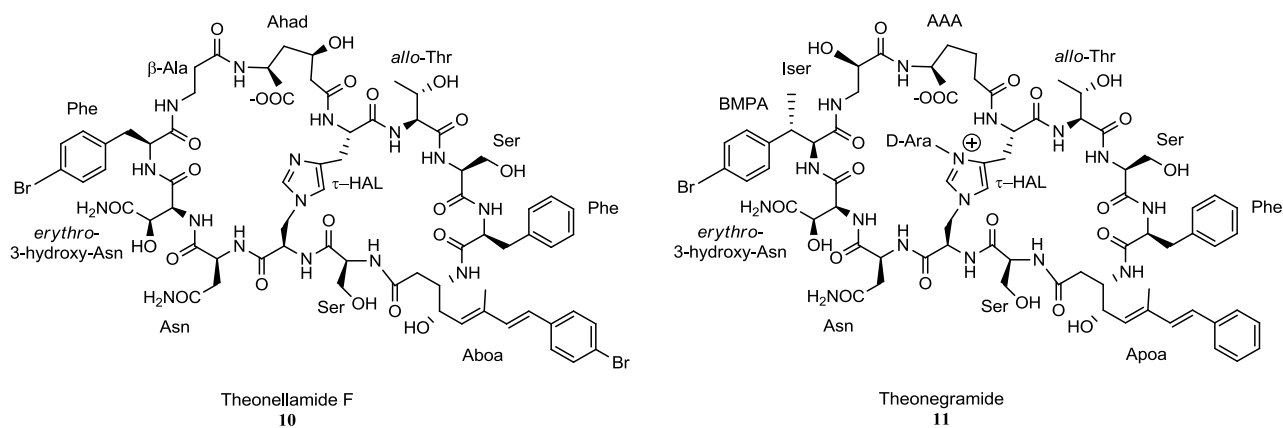
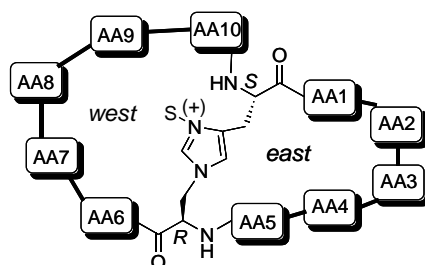


Figure 1.4 – Chemical Structures of TNM F and Theonegramide

From Table 1.1, it can be seen that there are some features common to all family members: *allo*-threonine, serine and phenylalanine in positions AA1-AA3 respectively; serine, asparagine and *erythro*- β -hydroxyasparagine in positions AA5-AA7 respectively. All compounds contain (5*E*,7*E*)-3-amino-4-hydroxy-6-methyl-8-phenyl-5,7-octadienoic acid (Apoa) or its 4'-brominated derivative (Aboa) in position AA4 (Figure 1.5). Other structural variations include β -methylation and 4'-bromination of AA8, hydroxylation of AA9, and deoxygenation at AA10 relative to TNM F. All members are characterized by a bridging τ -histidinoalanine (τ -HAL) residue. The major structural variation is that some congeners contain a sugar, covalently linked to the π -nitrogen of the τ -HAL residue. Specifically, β -D-galactose is present in TNMs A, E and theopalauamide whereas β -arabinose is present in TNM D and theonegramide.

Table 1.1 – Amino Acid Composition of TNMs A-F (**10** and **12-16**), Theonegramide (**11**) and Theopalauamide (**9**). Copyright 2007, Elsevier, reprinted with permission (p. 241).



(Table 1.1 continued)

Amino acid	Theonellamide congener							
	A	B	C	D	E	F	Theonegramide	Theopalauamide
	12	13	14	15	16	10	11	9
AA1					<i>allo</i> -Threonine			
AA2					Serine			
AA3					Phenylalanine			
AA4	Apoa	Apoa	Aboa	Aboa	Aboa	Aboa	Apoa	Apoa
AA5					Serine			
AA6					Asparagine			
AA7					(2 <i>S</i> ,3 <i>R</i>)-3-Hydroxyasparagine			
AA8	BMPA	BMPA	Phe	BPA	BPA	BPA	BMPA	BMPA
AA9	Iser	β -Ala	β -Ala	β -Ala	β -Ala	β -Ala	Iser	Iser
AA10	Ahad	Ahad	Ahad	Ahad	Ahad	Ahad	AAA	AAA
S (sugar)	β -D-Gal			β -L-Ara	β -D-Gal		β -D-Ara	β -D-Gal

Abbreviations: AAA = α -amino adipic acid; Aboa = (5*E*, 7*E*)-3-amino-4-hydroxy-6-methyl-8-*p*-bromophenyl-5,7-octadienoic acid; Ahad = α -amino- γ -hydroxyadipic acid; Apoa = (5*E*, 7*E*)-3-amino-4-hydroxy-6-methyl-8-phenyl-5,7-octadienoic acid; Ara = arabinose; BMPA = β -methyl-*p*-bromophenylalanine; BPA = *p*-bromophenylalanine; Gal = galactose; Iser = isoserine.

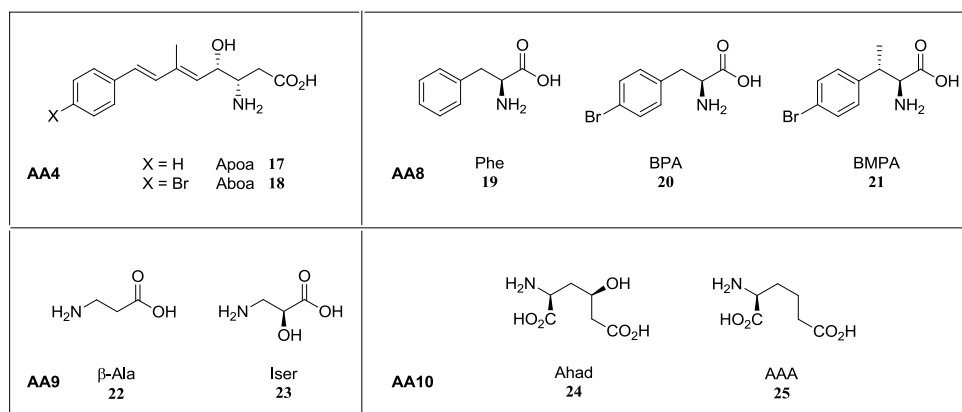


Figure 1.5 – Structures of Varying Amino Acids for the Theonellamides and Related Compounds

The stereochemistry of the β -arabinose residue deserves further comment. Notice that the configuration of the β -galactose unit was determined to be D using chiral GC analysis by both the Fusetani and Faulkner groups for their respective natural products. For the β -arabinose residue, Faulkner hydrolyzed theonegramide using 4 N HCl (70 °C for 12 hours) and the hydrolysate was derivatized with pentafluoropropionic anhydride to produce a compound identical to that obtained from D-arabinose as detected by chiral GC-MS.⁸ For the monosaccharide derived from theonegramide, Fusetani used

methanolysis (10% HCl:MeOH, 100 °C, 1 hour) and treated the intermediate with trifluoroacetic anhydride (100 °C, 10 minutes) to form a derivative of L-arabinose that was detected by chiral GC analysis.⁷ The authors commented on the very acid labile nature of this sugar residue. We believe β -L-arabinose is more likely because the -OH topology in its pyranose form is the same as that in D-galactose (Figure 1.6).

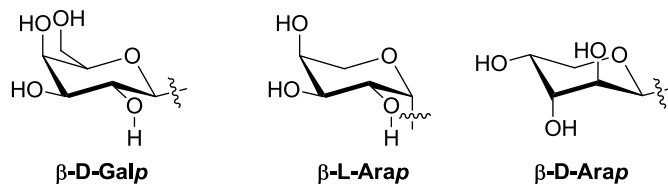


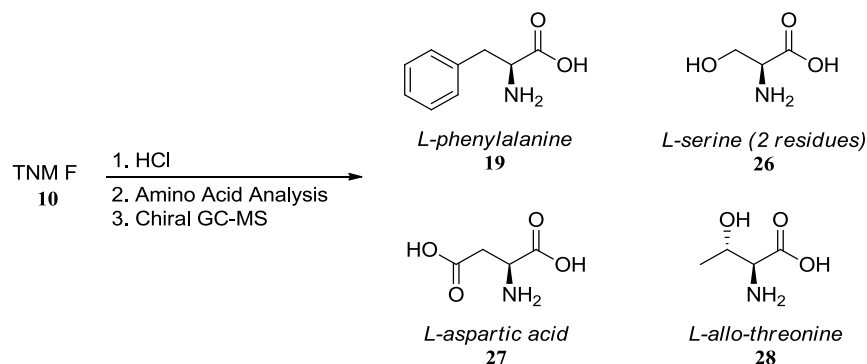
Figure 1.6 - β -L-Arabinose and β -D-Arabinose in their Pyranose Forms Compared to D-Galactose

Theonellamide F was the first congener isolated and was shown to be an antifungal and cytotoxic agent. Theonellamides A-F showed moderate toxicities against P388 leukemia cells with IC₅₀ values of 5.0, 1.7, 2.5, 1.7, 0.9, and 2.7 μ g/ml respectively.^{6,7} Glycosylation seems to have little effect on the cytotoxicity of the theonellamides. In addition, congener F was toxic to L1210 leukemia cells with an IC₅₀ value of 3.2 μ g/mL.⁶ Theonellamide F inhibited fungal growth of *Candida*, *Trichophyton*, and *Aspergillus* species.

1.2 Structure Determination of Selected Amino Acids of TNM F⁶

Theonellamide F showed a multiplet in the FAB mass spectrum with an intensity ratio of 1:2:1.6 for peaks at m/z 1649, 1651, 1653. When bromine is present in a compound, the $M + 2$ ion peak becomes very significant. The fact that bromine is comprised of two isotopes (⁷⁹Br and ⁸¹Br) in a nearly 1:1 ratio for singularly brominated compounds suggests that TNM F contains two bromine atoms. The compound displayed UV maxima at 283 nm, 294 nm, and 315 nm. Treatment of TNM F with acid generated a number of ninhydrin active spots on TLC.

Each ninhydrin-active spot represents a discrete amino acid and the structure elucidation of each AA will be presented in the order shown in Table 1.1 with some exceptions: the elucidation of Aboa (AA4), which will be covered towards the end of the section and the elucidation of Ahad (AA10) and τ -HAL, which will be the subject of other dissertations in the Taylor Group. Some of the individual amino acids were readily identified from the acid hydrolysate and assigned the L-configuration by chiral GC-MS: *allo*-Thr, Ser, Phe, Ser, and Asp (Scheme 1.1).

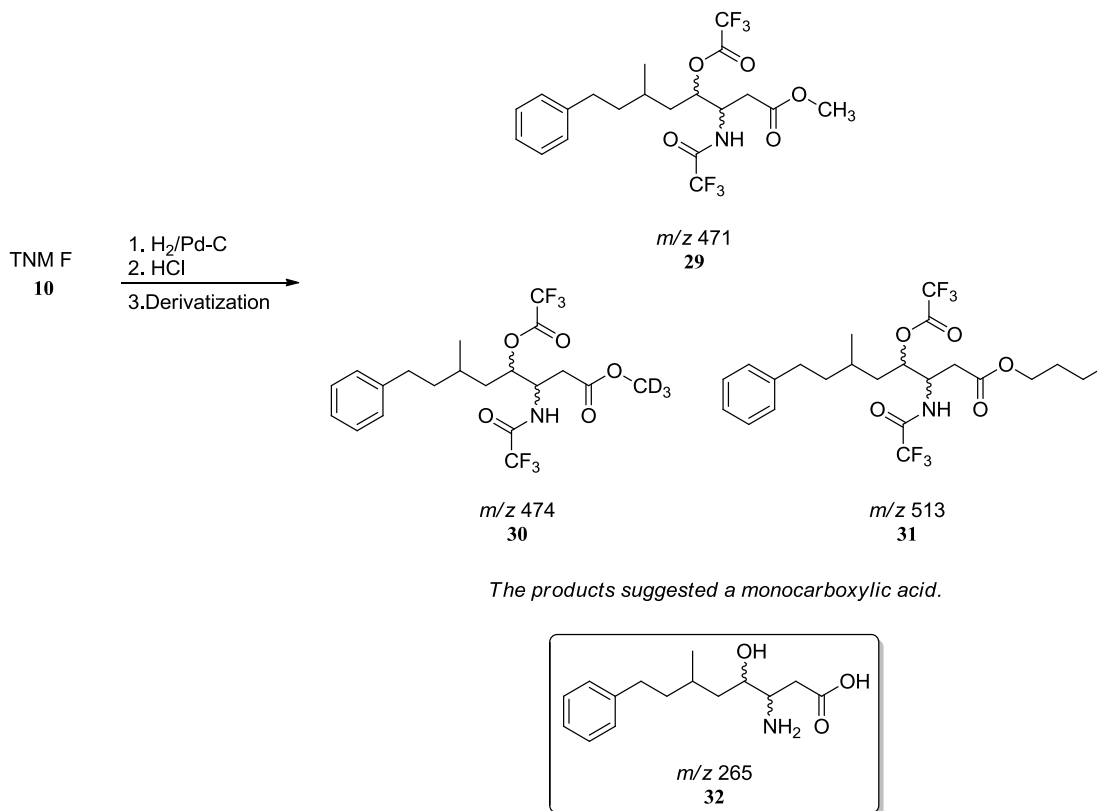


Scheme 1.1 – Amino Acids of TNM F Assigned the *L*-Configuration by Chiral GC-MS

For the nonstandard amino acids, identification first required separation of the hydrolysis products by ion-exchange chromatography. ^1H NMR, ^{13}C NMR, ninhydrin stain color (greenish-gray), and FAB-MS (MH^+ ion peak at m/z 150) data provided evidence that AA7 gave rise to β -hydroxyaspartic acid on degradation. Literature optical rotation values for all four stereoisomers led to assignment of the (2*S*, 3*R*) stereochemistry for 3-hydroxyaspartic acid. GC-MS analysis helped establish the presence of an isomer of bromophenylalanine. *Para*-disubstitution of a benzene ring was deduced from the ^1H NMR spectrum. At this point, comparison with authentic material revealed *L*-*p*-bromophenylalanine. Furthermore, when TNM F was reacted with $\text{H}_2/\text{Pd-C}$ and hydrolyzed, two residues of *L*-Phe were obtained, supporting the assignment of AA8 as bromo-Phe.

The acid-labile nature of the chromophoric AA4 (321/323 molecular ion indicative of one bromine atom) of TNM F was stabilized by hydrogenation. The hydrogenated product was subjected to

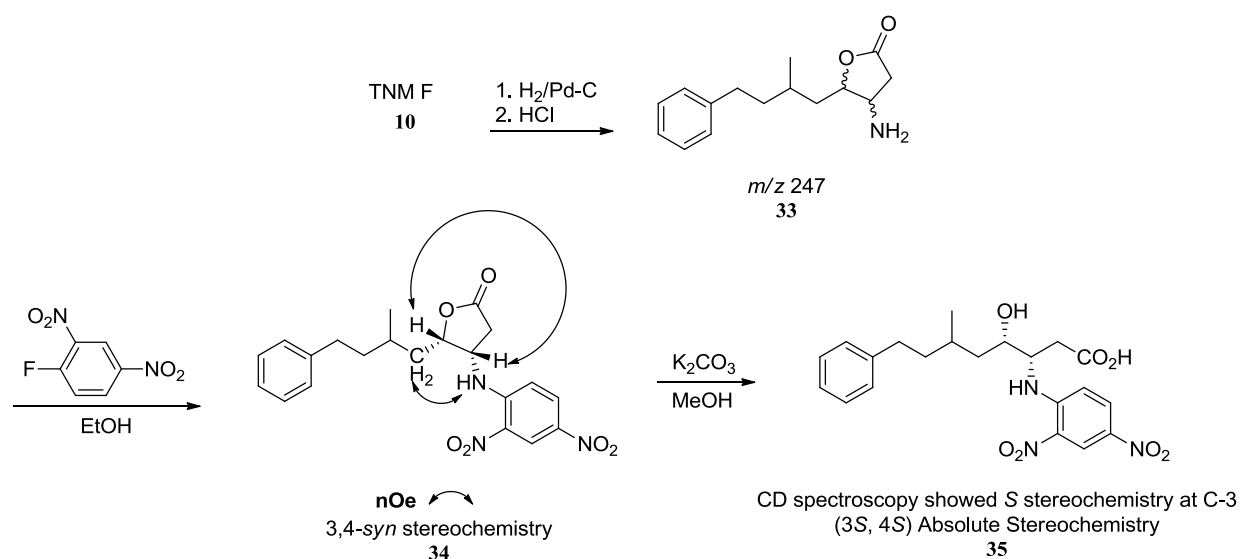
acid hydrolysis and then modified to its trifluoroacetamide (TFA) methyl ester derivative **29** (Scheme 1.2). Two additional ester derivatives, **30** and **31**, were generated to give products with M^+ peaks at m/z 474 and 513. This suggested that the amino acid has one carboxylic acid functional group. The fragmentation pattern in the EI-MS of $[471 - CF_3CO_2]$, $[471 - CF_3CONH]$, and $[471 - CF_3CONH - CF_3CO_2]$ indicated that the hydrogenated amino acid **32** has a molecular weight of 265.



Scheme 1.2 - Aboa Structure Elucidation: Functional Group Determination

A UV-active lactone (M^+ at m/z 247) was isolated from the organic layer after acid hydrolysis of the hydrogenated TNM F (Scheme 1.3). The authors were able to assign a crude structure for lactone **33**, however, preparation of the 2,4-DNP derivative **34** was key to solving stereochemical issues. $^1H-^1H$ NOE correlations between H-3 and H-4 of **34** proved 3,4-*syn* stereochemistry. Nagai and coworkers developed a reliable method for resolving the absolute configuration of α - and β -amino acids.^{10,11} CD spectroscopy of carboxylic acid **35** (obtained from base hydrolysis of **34**) was used to determine the

absolute configuration of C-3. The sign of the Cotton effect near 400 nm correlated to the absolute configuration at the β -carbon atom. The CD spectrum for carboxylic acid **35** showed negative values at 340 and 285 nm and a positive value at 410 nm. Thus, C-3 was assigned with (*S*) stereochemistry and **35** had (*3S,4S*) absolute configuration.



Scheme 1.3 - Aboa Structure Elucidation: Absolute Stereochemistry Assignment

Acid hydrolysis of TNM F led to degradation products of the chromophore, which were assigned using NMR spectroscopy (ROESY, TOCSY, HMBC, and HMQC). ROESY correlations showed protons of a *para*-disubstituted benzene ring linked to protons of an (*E*)-alkene. The (*E*)-olefin protons were connected to an olefinic methyl group and an olefinic proton. Strong COSY cross peaks between the protons shown in Figure 1.7 indicated (*E, E*) geometry. The TOCSY spectrum provided the remaining structural unit [-CH(OH)CH(NH)CH₂CO-] while HMQC and HMBC spectra supported the (*3S, 4S, 5E, 7E*)-3-amino-8-(4-bromophenyl)-4-hydroxy-6-methyl-5,7-octadienoic acid (Aboa) assignment. The identity of the remaining amino acid was β -Ala, as determined in conjunction with the standard amino acids.

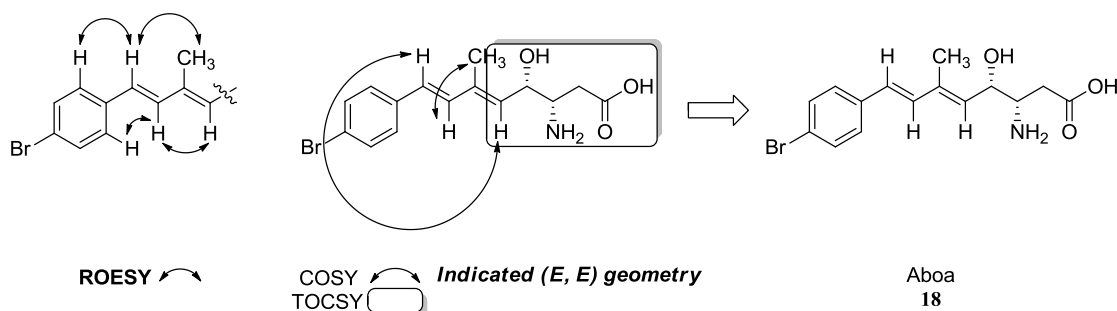


Figure 1.7 - Aboa Structure Elucidation: NMR Data Correlations for Bond Connectivity

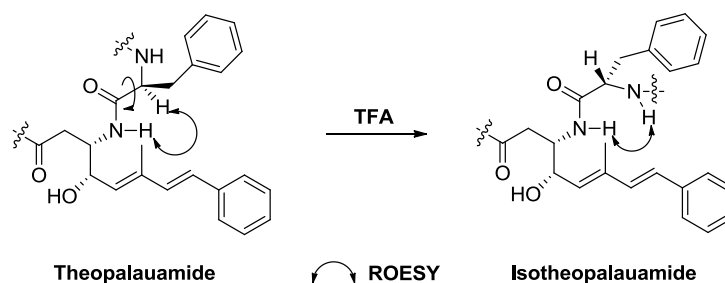
1.3 The Relationship between Isotheopalauamide and Theopalauamide⁹

One of the more puzzling features concerning the isolation of theopalauamide was the presence of a minor peptide, isotheopalauamide. Theopalauamide, as mentioned previously, is found only in the interior of the sponge (eubacteria). The isolation protocol included extracting a lyophilized sample of *T. swinhoei* with a variety of organic and aqueous solvents. The acetonitrile/water extract provided the peptides which were purified using reversed-phase HPLC to secure both isotheopalauamide and theopalauamide. It was during the purification step that theopalauamide was being partially converted to isotheopalauamide via acid-catalyzed isomerization.

Both isomers have identical IR and UV spectra in addition to the same molecular formula and primary structures. The ^1H and ^{13}C NMR data, however, are different. Analysis of the ROESY spectrum of theopalauamide showed a correlation between the NH proton of Apoa and the α -proton of Phe (Scheme 1.4). A correlation between the two NH protons of the Phe and Apoa residues was observed in the isomeric isotheopalauamide. The α -protons of the Phe and Apoa amino acids showed no correlations in isotheopalauamide which implies that the amide bond geometry is *trans*.

^1H NMR chemical shift differences in exchangeable proton signals with temperature indicate the degree of intramolecular hydrogen bonding. The spectra, acquired from 25 to 40 °C in 5 °C increments, showed that the NH protons on both the Apoa and Phe residues were more strongly hydrogen bonded in

isothopalauamide than in theopalauamide, consistent with the ROESY data. Other differences (NH-CH α coupling constants for Phe and Apoa) are not large enough to indicate a change in the geometry about these bonds. Therefore, isothopalauamide and theopalauamide were proposed to be conformational isomers differing in the dihedral angle about the C-1-C-2 bond in Phe.



Scheme 1.4 – Important ROESY Correlations for Both Conformational Isomers

1.4 Early Biological Studies

TNM F was isolated by Matsunaga and co-workers and identified as a cytotoxic and antifungal peptide. The reported biological activities of TNM F and other related compounds were similar and can be deemed modest. The earliest studies were all conducted by Wada, Matsunaga, Fusetani, and Watabe.¹²⁻¹⁴ One study explored the effects of TNM F on 3Y1 rat embryonic fibroblasts while a second investigation screened for theonellamide-binding proteins present in rabbit liver.

The researchers reported that TNM F was capable of inducing very large (>30 μm in diameter) vacuole formation in 3Y1 rat embryonic fibroblasts (Figure 1.8).^{13,14} At concentrations of 6 μM of TNM F for 24 hours, many cells generated large vacuoles but cell morphology was not affected. At higher concentrations of TNM F (18 μM for 120 hours), formation of many more vacuoles that were even larger occurred in addition to morphologic changes (retraction of lamellipodia). Monensin, a Na⁺ ionophore traditionally used to disturb Golgi apparatus, induced vacuoles that were smaller (<15 μm in diameter) and fewer in number than those generated by TNM F. It was also noted that, compared to TNM F, monensin displayed a stronger toxicity. Although not the subject of this study, a cell's change in

morphology can give insight about the mode of action of a drug. The ability of TNM F to induce large vacuoles with low fatality in fibroblasts suggests potential as a molecular probe for studies on intracellular membrane structures.

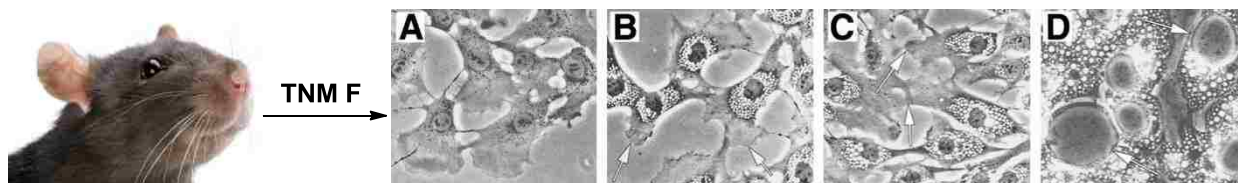
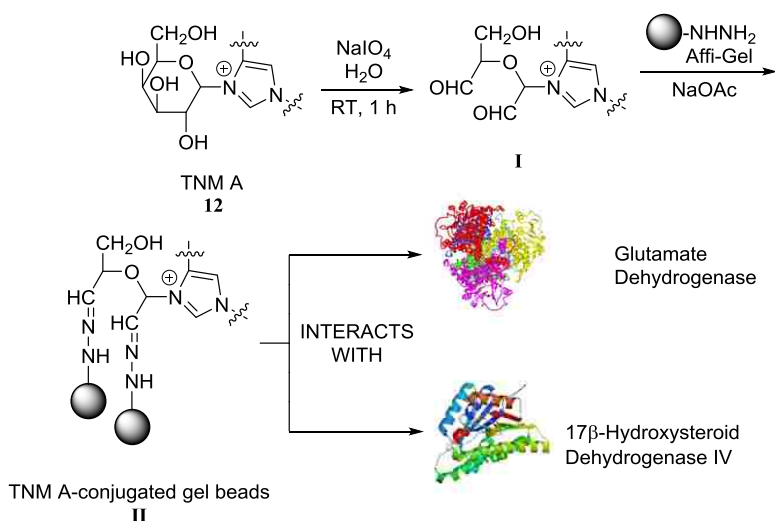


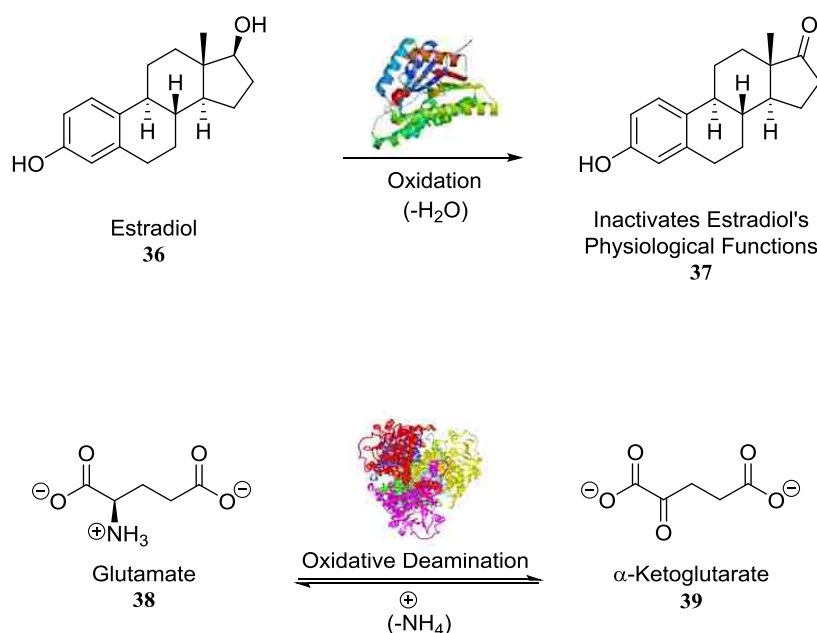
Figure 1.8 – Theonellamides Induced Vacuole Formation in Rat Embryonic 3Y1 Fibroblasts. Treatment with no TNM (A), 2 μM TNM F for 24 hours (B), 4 μM TNM A for 24 hours (C), 10 μM TNM A for 72 hours (D). Copyright 2002, Springer, reprinted with permission (p. 243).

The same researchers also immobilized TNM A on affinity gel beads and screened for theonellamide-binding proteins present in rabbit liver (Scheme 1.5).¹² Sodium periodate oxidation of TNM A formed two aldehyde units from the β -D-galactose residue. The compound **I** was then reacted with hydrazine-containing Affi-Gel beads to give TNM A-conjugated gel beads **II**. Rabbit liver tissue extracts were reacted with the TNM A-conjugated gel beads for two hours and two major proteins were found to bind to the beads. These proteins were identified as glutamate dehydrogenase (55-kDa) and 17 β -hydroxysteroid dehydrogenase IV (80-kDa).



Scheme 1.5 – Preparation of TNM A-Conjugated Gel Beads and the Two Proteins Bound on Subsequent Reaction with Rabbit Liver Tissue Extracts

17 β -Hydroxysteroid dehydrogenase IV oxidizes estradiol to inactivate its physiological functions (Scheme 1.6). Glutamate dehydrogenase reversibly catalyzes glutamate to α -ketoglutarate. Amination of α -ketoglutarate with glutamate dehydrogenase was triggered by TNM F. Theonellamide F did not, however, have any effect on the deamination of glutamate with the enzyme.



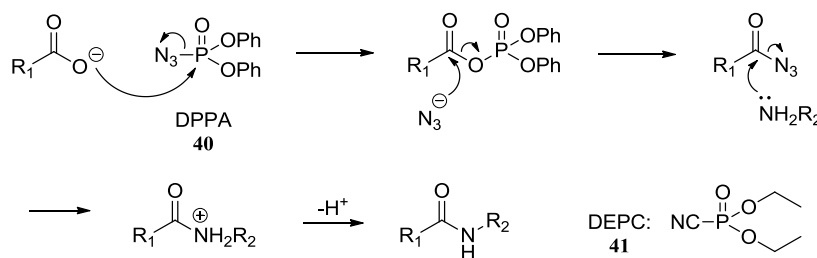
Scheme 1.6 – Biological Functions of 17 β -Hydroxysteroid Dehydrogenase IV and Glutamate Dehydrogenase

1.5 Synthetic Studies of TNM F by Shioiri and co-workers

It has been nearly 20 years since the last reported efforts towards the chemical synthesis of TNM F by Tohdo, Hamada and Shioiri.^{15,16} It is difficult to infer the rationale for their synthetic endeavors because their work was consistently reported in communication format. Their publications were characterized by a lack of discussion of strategy and experimental detail. Although both macrocyclic rings were formed individually, the ultimate goal of bicycle construction was never realized. Other congeners of TNM F have not been the subject of any synthetic studies.

1.5.1 Synthesis of the Southern Hemisphere* of TNM F

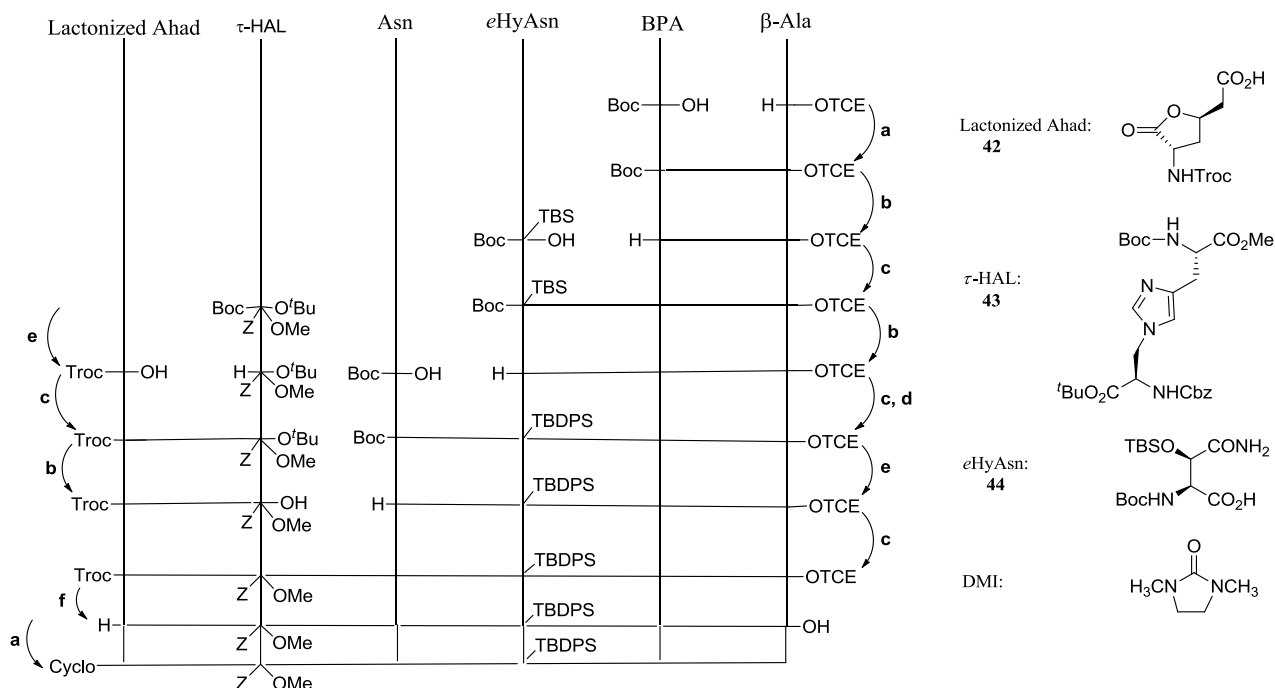
In 1994, Shioiri and coworkers reported the synthesis of the southern hemisphere of TNM F (Scheme 1.8).¹⁵ A linear heptapeptide was prepared to perform the cyclization between the β -Alanine and Ahad (γ -lactone form) units. The linear heptapeptide was generated from condensation of tripeptide and tetrapeptide fragments with diphenyl phosphorazidate (DPPA, **40**) or diethyl phosphorocyanidate (DEPC, **41**) being the coupling reagents of choice. The use of DPPA and DEPC is not surprising since it was Shioiri who introduced the reagents 40 years ago.¹⁷⁻¹⁹ As a reagent for amide bond formation, DEPC is similar to DPPA. For the assembly of linear peptides, DEPC is preferred for its slightly greater reactivity and lower rate of epimerization.¹⁸ The reaction mechanism of peptide ligation using DPPA is shown in Scheme 1.7.



Scheme 1.7 – DPPA (DEPC) Reaction Mechanism

The C-terminal Asn-*e*HyAsn-BPA- β -Ala tetrapeptide was assembled in a stepwise fashion in the C \rightarrow N direction with coupling yields in the range of 74-97%. The N-terminal tripeptide fragment was prepared in high yield by DEPC coupling of the τ -HAL dipeptide with a *N* α -Troc-lactone acid. The [4 + 3] peptide condensation proceeded in good yield (56%) of the linear heptapeptide while cyclization with DPPA produced the macrolactam in only 21% yield. Details of the synthetic work are shown in Scheme 1.8.

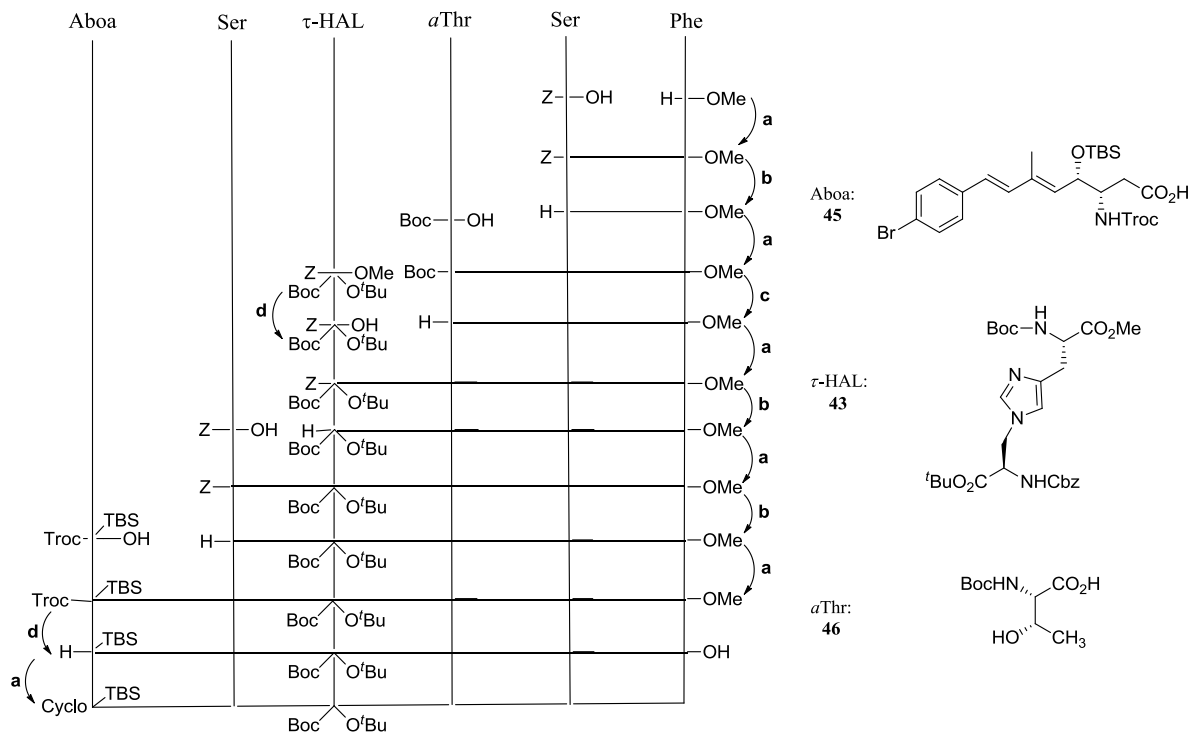
*They drew the molecule rotated 90° relative to representations in this dissertation. Thus, their references to northern and southern hemispheres correlate with our western and eastern hemispheres respectively.



Scheme 1.8 Synthesis of the Southern Hemisphere of TNM F. Reagents: a. DPPA, Et₃N, DMF; b. 4N-HCl-dioxane; c. DEPC, ^tPr₂NEt, DMF; d. TBDPSCl, imidazole, DMF; e. TMSOTf, CH₂Cl₂, 0 °C; f. LiOH, DMI-H₂O, 0 °C. [DMI = 1,3-dimethyl-2-imidazolidinone]

1.5.2 Synthesis of the Northern Hemisphere of TNM F

A subsequent communication in 1994 outlined Shioiri and coworkers' synthesis of the northern hemisphere of TNM F.¹⁶ This was accomplished by cyclizing the linear heptapeptide H-Aboa-Ser- τ -HAL-*a*Thr-Ser-Phe-OH using DPPA. In fact, all coupling reactions associated with this ring used DPPA exclusively. Furthermore, the synthesis was completed without protection of the hydroxyl groups of the Ser and *a*Thr residues. The completely linear, stepwise approach started from the C-terminal H-Phe-OMe residue and afforded the linear heptapeptide with typical coupling yields of 54-83% (Scheme 1.9). The cyclization produced the northern hemisphere of TNM F in 24% yield.



Scheme 1.9 Synthesis of the Northern Hemisphere of TNM F. Reagents: a. DPPA, Et₃N, DMF; b. H₂/Pd-C; c. HCl-MeOH; d. LiOH, dioxane-H₂O.

1.6 Recent Biological Studies

Linking natural products and small bioactive molecules to their molecular targets is a major goal of chemical biology.²⁰⁻²⁷ There is a need to identify the cellular targets and mode of action (MOA) of new compounds quickly and accurately.²⁰⁻²² The combination of chemical biology and functional genomics methodologies and reagents provides a dynamic way of achieving this goal.^{23,24} Chemical-genomics looks to recognize functional relationships between chemical compounds and specific genes through complete analysis of all genes in a genome. To this end, a common approach is to genetically alter each gene and assess the resulting mutants for a phenotypic response in the presence of a bioactive molecule (a in Figure 1.9).

In yeast, *Saccharomyces cerevisiae*, ~6000 potential genes have been characterized by the genome sequencing project. As each gene has been deleted, ~1000 essential genes and ~5000 viable

In addition, two natural product extracts (prior to purification of the bioactive compound) acquired from different organisms and various locations showed very similar chemical-genetic profiles (correlation coefficient = 0.892). Upon purification, the bioactive components were identified as the highly dissimilar structures stichloroside and theopalauamide (a in Figure 1.10). These results suggest that the two compounds have a common mode of action. To lend additional support to this theory, stichloroside-resistant mutants were isolated and then tested for theopalauamide resistance. Four strains were isolated as resistant to extract 00-192, which was confirmed to be resistant to its active compound (stichloroside). For each of the four strains, the mutants fell into two complementation groups (00-192-RA and 00-192-RB). As predicted by chemical-genetic profiling, all four strains displayed resistance to theopalauamide (b in Figure 1.10). It seems that chemical-genetic profiling can be applied to compounds that impair yeast growth as well as to natural product extracts.

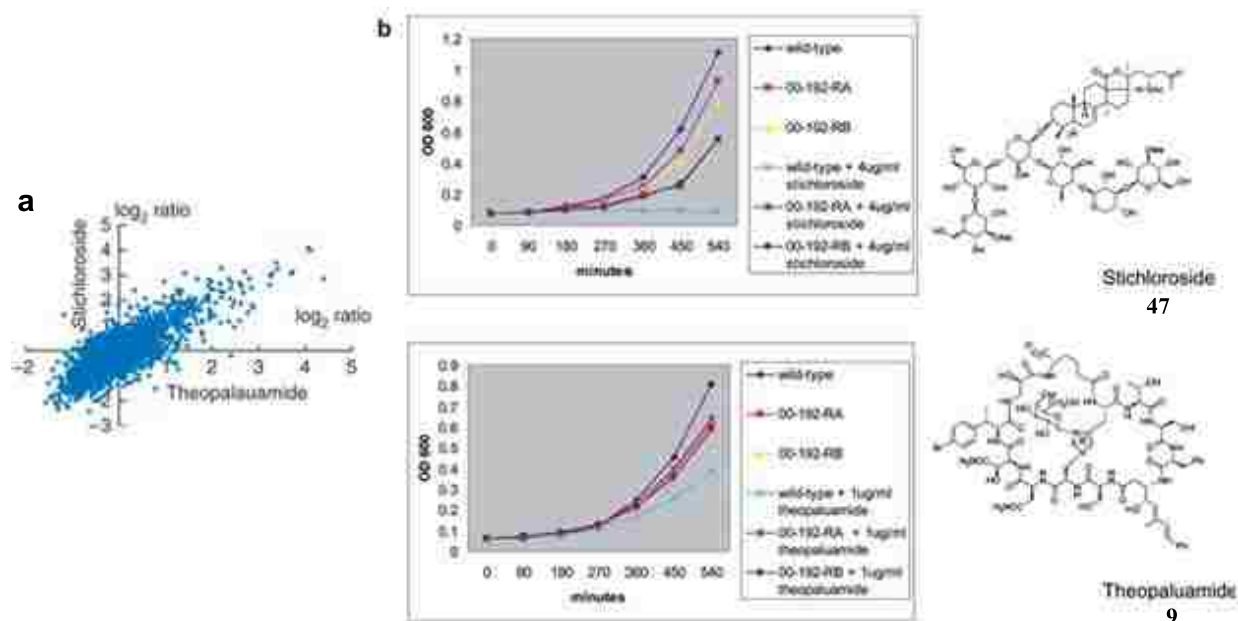


Figure 1.10 – Recent TNM Biological Studies, Part 1. (a) Theopalauamide and stichloroside chemical-genetic profiles correlation plot (correlation coefficient = 0.892). (b) Cross-resistance of extract 00-192 resistant strains 00-192-RA and 00-192-RB to 4 μg/mL stichloroside and 1 μg/mL theopalauamide. Copyright 2009, Nature Publishing Group, reprinted with permission (p. 248). Copyright 2006, Elsevier, reprinted with permission (p. 246).

Ho and co-workers developed a yeast chemical-genomic approach for identifying drug-resistant mutations in yeast.²¹ A molecular barcoded yeast open reading frame (MoBY-ORF) library was constructed to clone wild-type versions of mutant drug-resistant genes by complementation using a minimal amount of bioactive compound. Cloning by complementation with the MoBY-ORF library is a portable assay that can be carried out with any *S. cerevisiae* strain.

The MoBY-ORF complementation assay identified an enzyme involved in ergosterol biosynthesis, mevalonate pyrophosphate decarboxylase (MVD1) (Figure 1.11). To test whether theopalauamide targets a product of the MVD1 pathway, the theopalauamide-resistant (*theo*^R) mutant was found to be partially resistant to amphotericin B (a compound that bind sterols). Additional experiments proved that other deletion mutants, *erg3*Δ and *erg2*Δ, involved in ergosterol biosynthesis were resistant to theopalauamide as well.

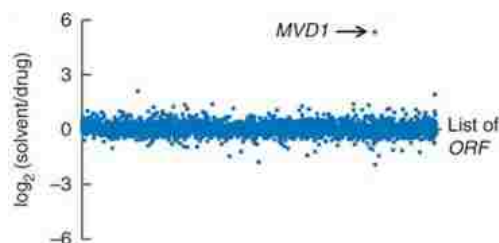


Figure 1.11 - Recent TNM Biological Studies, Part 2. *Theo*^R mutant barcode depletion plot (grown in a medium containing 2 μg/mL theopalauamide). The most depleted ORF was MVD1. Copyright 2009, Nature Publishing Group, reprinted with permission (p. 248).

To indirectly determine whether stichloroside and theopalauamide bind to ergosterol, ergosterol was added to environments containing toxic amounts of these compounds (a in Figure 1.12). The effects of exogenous ergosterol on the toxicity of amphotericin B and ketoconazole provided controls for this experiment. Cells could be rescued by treatment with exogenous ergosterol indicating that theopalauamide, stichloroside, and amphotericin B interact physically with ergosterol (no effect on ketoconazole's toxicity). This interaction was further showcased by assessing fluorescent marker (calcein) release from phosphatidylcholine liposomes containing different amounts of ergosterol (b in

Figure 1.12). Theopalauamide (10 $\mu\text{g}/\text{mL}$) had no effect on liposomes containing no ergosterol but had maximum leakage ($\sim 30\%$) of liposomes containing 20% ergosterol. Theonellamide A was also found to bind to ergosterol in *S. cerevisiae* using fluorescently labeled TNM A in an *in vitro* lipid-binding assay (c in Figure 1.12). In addition, the *theo*^R strain was resistant to TNM A. The saponin and polyene classes are the most common group of sterol-binding compounds. All the evidence presented suggests that the TNMs and theopalauamide represent a novel class of sterol-binding compound.

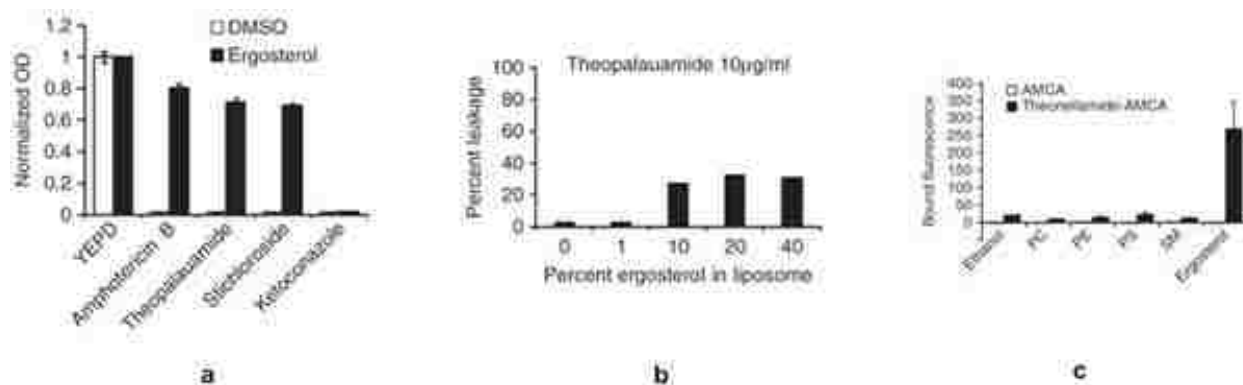


Figure 1.12 - Recent TNM Biological Studies, Part 3. (a) The toxicity of theopalauamide, stichloroside, and amphotericin B is rescued by ergosterol. Wild type cells (growth after 16 h at 30 °C) in the presence of ergosterol and other compounds. (b) Theopalauamide permeabilizes liposomes containing ergosterol. Leakage of calcein from liposomes containing ergosterol after exposure to theopalauamide. (c) *In vitro* binding of fluorescently labeled TNM A (theonellamide-AMCA) to ergosterol. [YEPD = yeast extract peptone dextrose; PC = phosphatidylcholine; PE = phosphatidylethanol; PS = phosphatidylserine; SM = sphingomyelin]. Copyright 2009, Nature Publishing Group, reprinted with permission (p. 248).

Yoshida *et al.* used a yeast chemical biology method to identify the target and MOA of the TNMs.²² Using fission yeast *Schizosaccharomyces pombe* as a model, a chemical-genomic profile of TNM F was generated. *S. pombe* is a eukaryotic model that differs from *S. cerevisiae* in cell cycle organization and centromere complexity. The overexpression strains were exposed individually to TNM F and a compendium of 10 reference compounds with known targets at various concentrations. Strains showing a significantly altered sensitivity compared to the control strain were selected. Two-dimensional clustering analysis of Gene Ontology (GO) terms associated with the genes that alter drug sensitivity found a link between TNM and 1,3- β -D-glucan synthesis (a in Figure 1.13). Of 32 TNM F hit genes, 12 genes were in common with FK463 (a clinical drug that inhibits 1,3- β -D-glucan synthesis), suggesting

that both compounds are functionally related. Cell morphology was compared after exposure to TNM F and FK463. FK463 compromised cell wall integrity in fungi and induced cell lysis (b in Figure 1.13) whereas TNM F treated cells showed no signs of cell lysis. In fact, TNM F seemed to reverse the effects of FK463 by promoting 1,3- β -D-glucan synthesis (c in Figure 1.13). The pathway to 1,3- β -D-glucan synthesis with TNM F treatment is the activation of Bgs1 by Rho1 (regulatory subunit, GTPase).

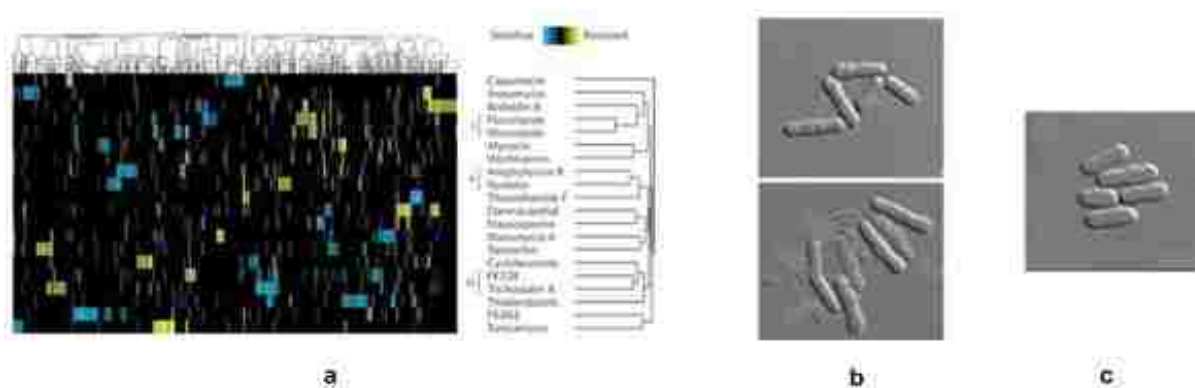


Figure 1.13 – Recent TNM Biological Studies, Part 4. (a) 2-D hierarchical clustering analysis of 20 compound profiles. Y-axis shows compounds with similar chemical-genomic profiles. X-axis plots 575 ORFs based on the degree of resistance (yellow) and hypersensitivity (blue). (b) FK463 induced cell lysis. WT cells treated with (bottom) or without (top) FK463. (c) Counteraction of FK463 induced cell lysis by TNM F. Copyright 2010, Nature Publishing Group, reprinted with permission (p. 249).

A fluorescently labeled TNM A derivative was used to perform subcellular localization studies. Using plasma membrane lipid components, a binding assay showed that the TNM A derivative recognizes ergosterol, cholesterol, cholestanol, and 5 α -cholest-7-en-3 β -ol (a in Figure 1.14). More specifically, TNMs bind to 3 β -hydroxysterols (a class of lipid molecules, rather than a protein). The binding of TNM F to exert its effects on a cell wall requires both proper membrane organization and an environment rich in ergosterol. Mutations in the ergosterol biosynthetic pathway can attenuate sensitivity to antibiotics in yeast. Ergosterol mutants caused by deletion or lack of certain enzymes (erg31 and erg32, erg2) displayed high tolerance to TNM F and a decreased ability of the cells to bind TNM F (b in Figure 1.14). Drug sensitivity was well correlated with *in vivo* TNM binding of the membrane. Deletion of other enzymes (erg5, Δ ts1/erg4), however, conferred slight resistance to TNM F.

A consequence of TNM binding the sterol-rich membrane was the loss of membrane integrity (reducing cell viability). Calcein (fluorescent dye) was added to *S. pombe* cells that had been treated with TNM F for 9 hours. Entry of calcein over the plasma membrane was observed with TNM F treatment, suggesting that the membrane integrity of cells cannot be retained in the presence of TNM F (c in Figure 1.14). Additionally, the dye exclusion assay showed that TNM F disrupted the integrity of the plasma membrane in a concentration and time dependent manner. The MOA of TNM F is different from that of polyene antibiotics because the phenotypic changes induced by these two families of antifungals are different. A typical change of yeast cells after polyene antibiotics treatment is the expansion of vacuoles. The vacuoles of TNM F-treated cells became marginally fragmented. In agreement with Ho and co-workers, Yoshida *et al.* found that the TNMs represent a new class of sterol-binding agents.

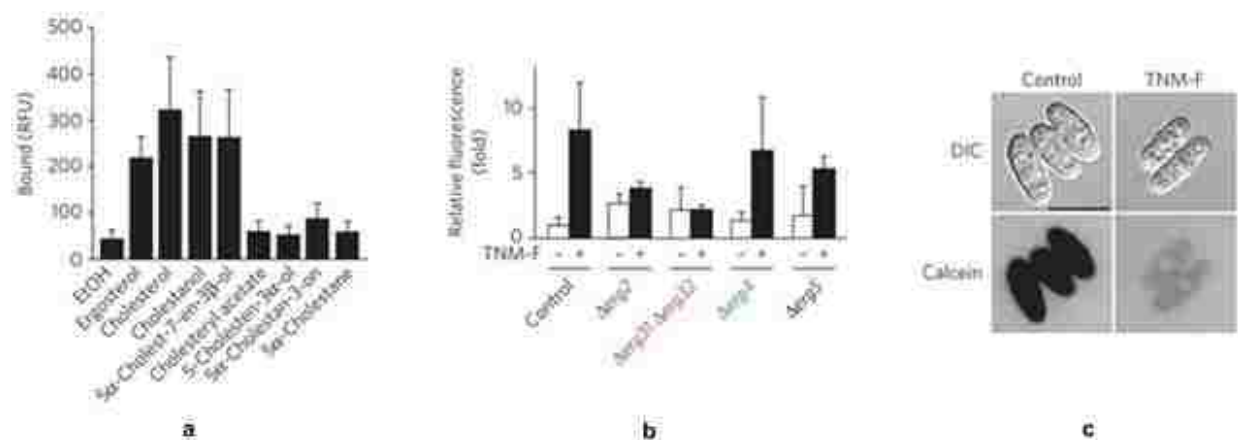


Figure 1.14 – Recent TNM Biological Studies, Part 5. (a) *In-vitro* binding of TNM-BF to various sterols. (b) Different *erg* mutants were treated with TNM F and the amount of abnormal cell wall synthesis revealed using calcofluor white staining (fluorescence intensity shown). (c) Testing plasma membrane integrity using calcein in a dye exclusion assay. Entry of calcein over the plasma membrane was induced by TNM F. No calcein diffusion occurred in the absence of TNM F. Copyright 2010, Nature Publishing Group, reprinted with permission (p. 249).

Through the efforts of the Boone and Yoshida groups, yeast chemical-genomics approaches have been shown to be effective for elucidating cellular targets and MOAs.²⁰⁻²² Boone's studies made use of the budding yeast *S. cerevisiae* whereas Yoshida's investigations utilized the fission yeast *S. pombe*. The key result from Boone's work revealed that a mutation in MVD1, encoding an enzyme involved in

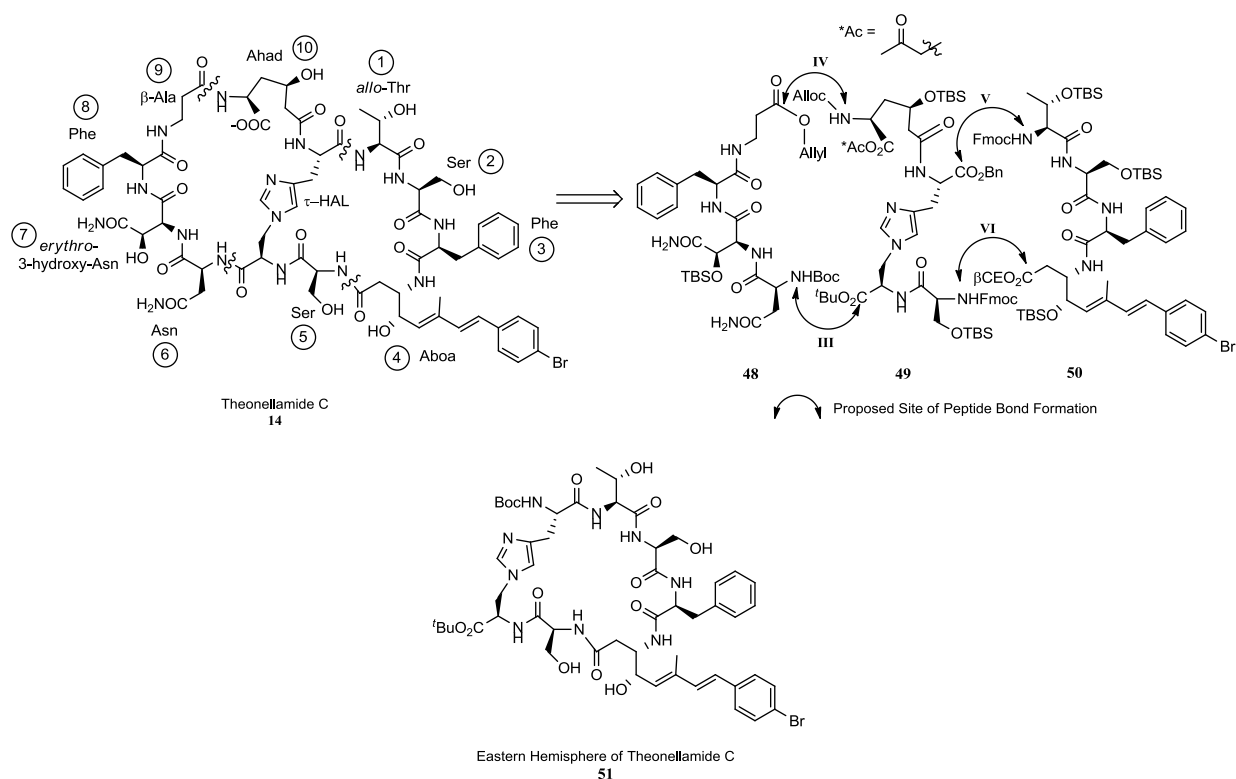
ergosterol biosynthesis was shown to be resistant to theopalauamide in *S. cerevisiae*, suggesting a link between the drug target and ergosterol biosynthesis. The Yoshida investigations took advantage of a chemical-genomic screen for the genes that alter TNM sensitivity when overexpressed and demonstrated that TNM specifically binds to a class of lipid molecules (3 β -hydroxysterols) in the fission yeast. The idea that ergosterol, the major sterol in fungi, is the target of TNM in fission yeast is supported by the compound's physical interaction with 3 β -hydroxysterols and several lines of genetic and biochemical evidence (mutants defective in ergosterol biosynthesis). While both groups answered some fundamental questions and came to the same conclusion (TNMs define a new class of sterol-binding compound), many questions remain. There is a need to perform structure-activity relationship studies to find the minimum chemical structure essential for TNM's biological activity. Also, upon TNM binding of the sterol-rich membrane, the processes leading to subsequent membrane damage are of interest.

1.7 Goals of the Current Work

Theonella swinhoei produces a limited quantity of the TNMs that have restricted investigations into their biology. From 15 kilograms of sponge, Fusetani and co-workers isolated: TNM A (200 mg), B (19 mg), C (32 mg), D (14 mg), E (30 mg), and F (500 mg). It stands to reason that biological studies have focused primarily on TNMs A and F. Despite considerable synthetic effort to produce TNM F by the Shioiri group in the early 1990s, a total synthesis of a TNM has yet to be reported. An efficient chemical synthesis of these compounds offers benefits such as an alternative to cultivation from natural sources and new ideas about their biological role.

The main goal is to synthesize TNM C and our approach is depicted in Scheme 1.10. The major disconnections are between residues 4 and 5 (Aboa/Ser), residues 9 and 10 (β -Ala/Ahad), and τ -HAL with their remaining amino acid partners *allo*-Thr and Asn. This would lead to the H-Asn-*e*HyAsn-Phe- β -Ala-OH tetrapeptide and the H-*allo*-Thr-Ser-Phe-Aboa-OH tetrapeptide associated with the “western” and “eastern” hemispheres respectively of TNM C. The western ring should be constructed first to allow late

stage incorporation of the sensitive diene of Aboa. Of the eleven amino acids required to generate TNM C, four are not commercially available; Aboa (4), *e*HyAsn (7), Ahad (10), and τ -HAL. The work in this dissertation focused on the synthesis of the *e*HyAsn-Phe dipeptide, the Aboa residue and our efforts toward the eastern hemisphere of TNM C.



Scheme 1.10 – Major Disconnections for TNM C

1.8 References

1. Wright, A. E.: The Lithistida: important sources of compounds useful in biomedical research. *Curr. Opin. Biotechnol.* **2010**, *21*, 801-807.
2. Winder, P. L.; Pomponi, S. A.; Wright, A. E.: Natural products from the Lithistida: a review of the literature since 2000. *Mar. Drugs.* **2011**, *9*, 2643-2682.
3. Bewley, C. A.; Faulkner, D. J.: Lithistid sponges: star performers or hosts to the stars. *Angew. Chem. Int. Ed.* **1998**, *37*, 2162-2178.

4. Bewley, C. A.; Holland, N. D.; Faulkner, D. J.: Two classes of metabolites from *Theonella swinhoei* are localized in distinct populations of bacterial symbionts. *Experientia*. **1996**, *52*, 716-722.
5. Piel, J.; Hui, D.; Wen, G.; Butzke, D.; Platzer, M.; Fusetani, N.; Matsunaga, S.: Antitumor polyketide biosynthesis by an uncultivated bacterial symbiont of the marine sponge *Theonella swinhoei*. *Proc. Natl. Acad. Sci. USA*. **2004**, *101*, 16222-16227.
6. Matsunaga, S.; Fusetani, N.; Hashimoto, K.; Walchli, M.: Theonellamide F. A novel antifungal bicyclic peptide from a marine sponge *Theonella* sp. *J. Am. Chem. Soc.* **1989**, *111*, 2582-2588.
7. Matsunaga, S.; Fusetani, N.: Theonellamides A-E, cytotoxic bicyclic peptides, from a marine sponge *Theonella* sp. *J. Org. Chem.* **1995**, *60*, 1177-1181.
8. Bewley, C. A.; Faulkner, D. J.: Theonegramide, an antifungal glycopeptide from the Philippine Lithistid sponge *Theonella swinhoei*. *J. Org. Chem.* **1994**, *59*, 4849-4852.
9. Schmidt, E. W.; Bewley, C. A.; Faulkner, D. J.: Theopalauamide, a bicyclic glycopeptide from filamentous bacterial symbionts of the Lithistid sponge *Theonella swinhoei* from Palau and Mozambique. *J. Org. Chem.* **1998**, *63*, 1254-1258.
10. Nagai, U.; Kawai, M.; Yamada, T.; Kuwata, S.; Watanabe, H.: A method for determining absolute configuration of β -amino acids by CD spectra of their DNP derivatives. *Tetrahedron Lett.* **1981**, *22*, 653-654.
11. Kawai, M.; Nagai, U.; Katsumi, M.; Tanaka, A.: CD spectra of DNP derivatives of aromatic α -amino acids and related compounds. DNP-aromatic rule as a method for determining absolute configuration of chiral amines of RCH(NH₂)XAr type. *Tetrahedron*. **1978**, *34*, 3435-3444.
12. Wada, S.; Matsunaga, S.; Fusetani, N.; Watabe, S.: Interaction of cytotoxic bicyclic peptides, theonellamides A and F, with glutamate dehydrogenase and 17 β -hydroxysteroid dehydrogenase IV. *Mar. Biotechnol.* **2000**, *2*, 285-292.
13. Wada, S.; Matsunaga, S.; Fusetani, N.; Watabe, S.: Theonellamide F, a bicyclic peptide marine toxin, induces formation of vacuoles in 3Y1 rat embryonic fibroblast. *Mar. Biotechnol.* **1999**, *1*, 337-341.
14. Wada, S.; Kantha, S. S.; Yamashita, T.; Matsunaga, S.; Fusetani, N.; Watabe, S.: Accumulation of H⁺ in vacuoles induced by a marine peptide toxin, theonellamide F, in rat embryonic 3Y1 fibroblasts. *Mar. Biotechnol.* **2002**, *4*, 571-582.
15. Tohdo, K.; Hamada, Y.; Shioiri, T.: Synthesis of the southern hemisphere of theonellamide F, a bicyclic dodecapeptide of marine origin. *Synlett*. **1994**, *4*, 247-249.
16. Tohdo, K.; Hamada, Y.; Shioiri, T.: Synthesis of the northern hemisphere of theonellamide F, a bicyclic dodecapeptide of marine origin. *Synlett*. **1994**, *4*, 250.

17. Shioiri, T.; Ninomiya, K.; Yamada, S.: Diphenylphosphoryl azide. New convenient reagent for a modified Curtius reaction and for peptide synthesis. *J. Am. Chem. Soc.* **1972**, *94*, 6203-6205.
18. Yamada, S.; Kasai, Y.; Shioiri, T.: Diethylphosphoryl cyanide. A new reagent for the synthesis of amides. *Tetrahedron Lett.* **1973**, 1595-1598.
19. Shioiri, T.: Diphenyl phosphorazidate (DPPA) - more than three decades later. *TCIMAIL.* **2007**, *134*, 2-19.
20. Parsons, A. B.; Lopez, A.; Givoni, I. E.; Williams, D. E.; Gray, C. A.; Porter, J.; Chua, G.; Sopko, R.; Brost, R. L.; Ho, C. H.; Wang, J.; Ketela, T.; Brenner, C.; Brill, J. A.; Fernandez, G. E.; Lorenz, T. C.; Payne, G. S.; Ishihara, S.; Ohya, Y.; Andrews, B.; Hughes, T. R.; Frey, B. J.; Graham, T. R.; Andersen, R. J.; Boone, C.: Exploring the mode-of-action of bioactive compounds by chemical-genetic profiling in yeast. *Cell.* **2006**, *126*, 611-625.
21. Ho, C. H.; Magtanong, L.; Barker, S. L.; Gresham, D.; Nishimura, S.; Natarajan, P.; Koh, J. L. Y.; Porter, J.; Gray, C. A.; Andersen, R. J.; Giaever, G.; Nislow, C.; Andrews, B.; Botstein, D.; Graham, T. R.; Yoshida, M.; Boone, C.: A molecular barcoded yeast ORF library enables mode-of-action analysis of bioactive compounds. *Nat. Biotechnol.* **2009**, *27*, 369-377.
22. Nishimura, S.; Arita, Y.; Honda, M.; Iwamoto, K.; Matsuyama, A.; Shirai, A.; Kawasaki, H.; Kakeya, H.; Kobayashi, T.; Matsunaga, S.; Yoshida, M.: Marine antifungal theonellamides target 3 β -hydroxysterol to activate Rho1 signaling. *Nat. Chem. Biol.* **2010**, *6*, 519-526.
23. Andrusiak, K.; Piotrowski, J. S.; Boone, C.: Chemical-genomic profiling: systematic analysis of the cellular targets of bioactive molecules. *Bioorg. Med. Chem.* **2012**, *20*, 1952-1960.
24. Ho, C. H.; Piotrowski, J.; Dixon, S. J.; Baryshnikova, A.; Costanzo, M.; Boone, C.: Combining functional genomics and chemical biology to identify targets of bioactive compounds. *Curr. Opin. Chem. Biol.* **2011**, *15*, 66-78.
25. Tashiro, E.; Imoto, M.: Target identification of bioactive compounds. *Bioorg. Med. Chem.* **2012**, *20*, 1910-1921.
26. Wierzba, K.; Muroi, M.; Osada, H.: Proteomics accelerating the identification of the target molecule of bioactive small molecules. *Curr. Opin. Chem. Biol.* **2011**, *15*, 57-65.
27. Chan, J. N. Y.; Nislow, C.; Emili, A.: Recent advances and method development for drug target identification. *Trends Pharmacol. Sci.* **2010**, *31*, 82-88.

CHAPTER 2: ASYMMETRIC SYNTHESIS OF *ERYTHRO*- β -HYDROXYASPARAGINE (EHYASN)

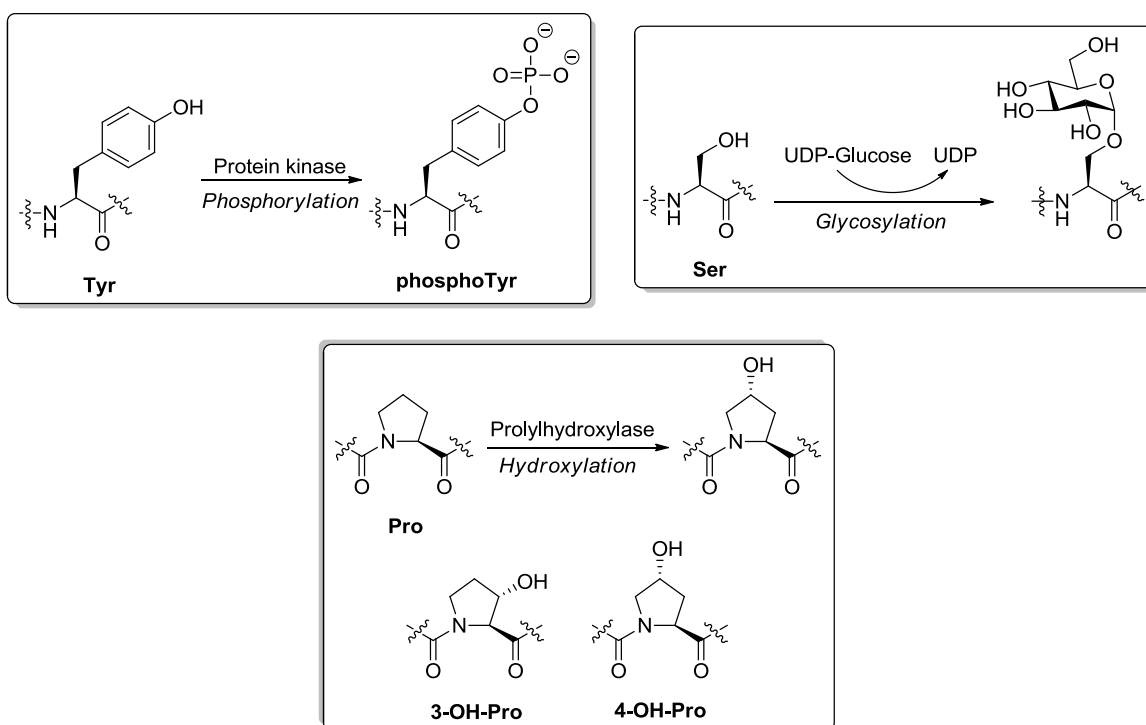
2.1 Proteinogenic vs Nonproteinogenic Amino Acids

The 20 amino acids that are coded for by the standard genetic code and that are found in proteins are referred to as proteinogenic amino acids (Figure 2.1). These amino acids can only be incorporated into proteins through translation. Human beings must acquire 9 of the 20 amino acids from their diet (essential), the other 11 are readily synthesized.¹

<p>52</p> <p>E Glu Glutamic Acid</p>	<p>1-Letter AA Code 3-Letter AA Code Chemical Name</p>					<p>53</p> <p>R Arg Arginine</p>
<p>27</p> <p>D Asp Aspartic Acid</p>	<p>26</p> <p>S Ser Serine</p>	<p>54</p> <p>Y Tyr Tyrosine</p>	<p>55</p> <p>Q Gln Glutamine</p>	<p>56</p> <p>M Met Methionine</p>	<p>57</p> <p>A Ala Alanine</p>	<p>58</p> <p>H His Histidine</p>
<p>59</p> <p>T Thr Threonine</p>	<p>60</p> <p>N Asn Asparagine</p>	<p>61</p> <p>C Cys Cystine</p>	<p>62</p> <p>G Gly Glycine</p>	<p>63</p> <p>L Leu Leucine</p>	<p>19</p> <p>F Phe Phenylalanine</p>	<p>64</p> <p>K Lys Lysine</p>
<p>65</p> <p>P Pro Proline</p>	<p>66</p> <p>I Ile Isoleucine</p>	<p>67</p> <p>W Trp Tryptophan</p>	<p>68</p> <p>V Val Valine</p>	<p>Acidic Basic Nonpolar (hydrophobic) Polar, uncharged</p>		

Figure 2.1 – The Standard Amino Acids

Nonproteinogenic amino acids are those not coded for by the standard genetic code. Enzymatic modifications (post-translational modification, PTM) of amino acid residues in proteins or peptides give rise to a variety of nonproteinogenic amino acids.² These reactions involve polar amino acid residues and Scheme 2.1 illustrates a subset of PTMs, covalent modifications of individual amino acid residues at one site. Asparagine and serine residues can be glycosylated while tyrosine, threonine and serine side chains are often phosphorylated. Disulfide bonds arise from oxidative crosslinking of the thiol groups of two cysteine residues.



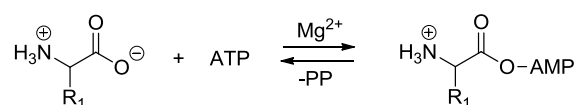
Scheme 2.1 – Some Examples of PTM: Specific Covalent Modifications

2.2 Nonribosomal Peptide Synthesis

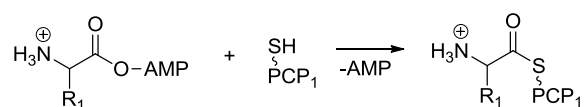
There is an abundance of nonproteinogenic amino acids used in nature for the production of nonribosomal peptides. Nonribosomal peptides are constructed by nonribosomal peptide synthetases (NRPSs), multi-enzyme complexes with modular organization.^{3,4} A module is a portion of the NRPS peptide chain that ultimately incorporates individual amino acids into the final structure. Domains,

subsets of the module, are units that catalyze each step of nonribosomal peptide synthesis. Every NRPS module contains at least three domains for peptide backbone synthesis. These include the adenylation- (A)-domain for substrate recognition and activation, the peptidyl carrier protein (PCP) for transport to catalytic centers, and the condensation-(C)-domain for formation of the peptide bond (Scheme 2.2).⁴ The selection of amino acids for nonribosomal peptide synthesis and their activation as aminoacyl adenylates is determined by A-domains. The amino acid is then moved to the cofactor of the transport unit, which allows amino acids and intermediates to move from one catalytic center to another. Peptide bond formation in nonribosomal biosynthesis, by action of the C-domain, is the result of reaction between a nucleophilic aminoacyl-S-4'PP-PCPs and an electrophilic peptidyl-S-4'PP-PCP component. The importance of this reaction is highlighted by the presence of C-domains in nearly all NRPS elongation module.

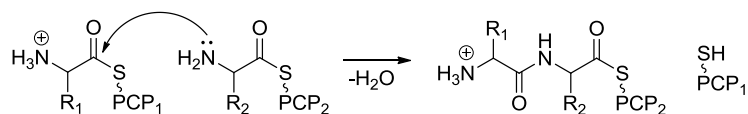
A-Domain



PCP-Domain



C-Domain



Scheme 2.2 – Roles of 3 Primary Domains in a NRPS Module

The intriguing biological profiles of nonribosomal peptides such as the TNMs make them appealing targets for total synthesis. As mentioned previously, they were isolated from the marine sponge *Theonella swinhoei*, produced specifically by the filamentous bacteria (symbiotic microorganism). Also,

the structure of TNM C was discussed in §1.1 and we alluded to the fact that four of the 11 amino acid residues are nonproteinogenic. Two of them, β -hydroxyasparagine and Aboa, warrant further discussion as they are the focus of this dissertation.

2.3 Identification and Occurrence of HyAsn in Nature

The nonproteinogenic amino acid β -hydroxy-L-asparagine was first identified as a normal component in human urine by Tominaga *et al.* in 1963.⁵ The isolation of the amino acid made use of classical techniques such as desalting and fractionation followed by recrystallization of the concentrate from 80% ethanol. Two hundred liters of urine provided 116 milligrams of crystalline β -hydroxyasparagine.

Okai and Izumiya synthesized the *erythro* (2*S*,3*R*) **70** and *threo* (2*S*,3*S*) **71** diastereomers, both of which will be highlighted in the next section.⁶ In an attempt to assign the configuration of the urine-derived hydroxyasparagine, synthetic diastereomers were compared to an authentic sample using chromatography and optical rotation data. The data collectively suggested that the natural product was the *erythro* diastereomer. Both isomers, in addition to β -hydroxyaspartic acid **69** (Figure 2.2), have been the subject of several enantioselective syntheses.

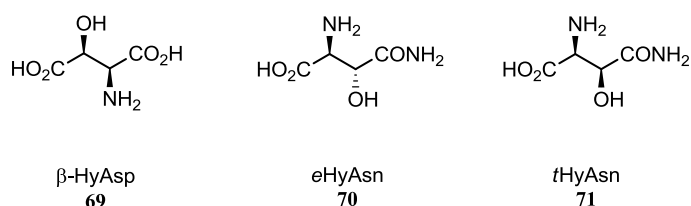


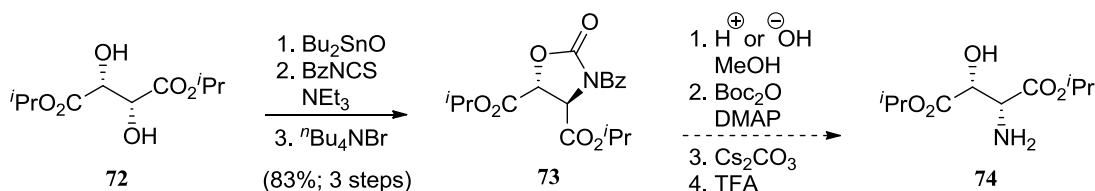
Figure 2.2 – Structures of β -Hydroxyaspartic Acid, *e*HyAsn and *t*HyAsn

Epidermal growth factor (EGF) precursor is present in human secretions and fluids. This integral membrane protein (160-170 kDa) was purified using monoclonal antibodies to target EGF module 7 and verified to have an *N*-terminal sequence, SAPNHWSXPE.⁷⁻⁹ Epidermal growth factor precursor modules 2, 7 and 8 contain the sequence for post-translational modification (hydroxylation at C- β) of asparagine

residues. *eHyAsn* was discovered in the acid hydrolysates of the precursor. For every unit of EGF precursor, there is 2.4 units of *eHyAsn*.

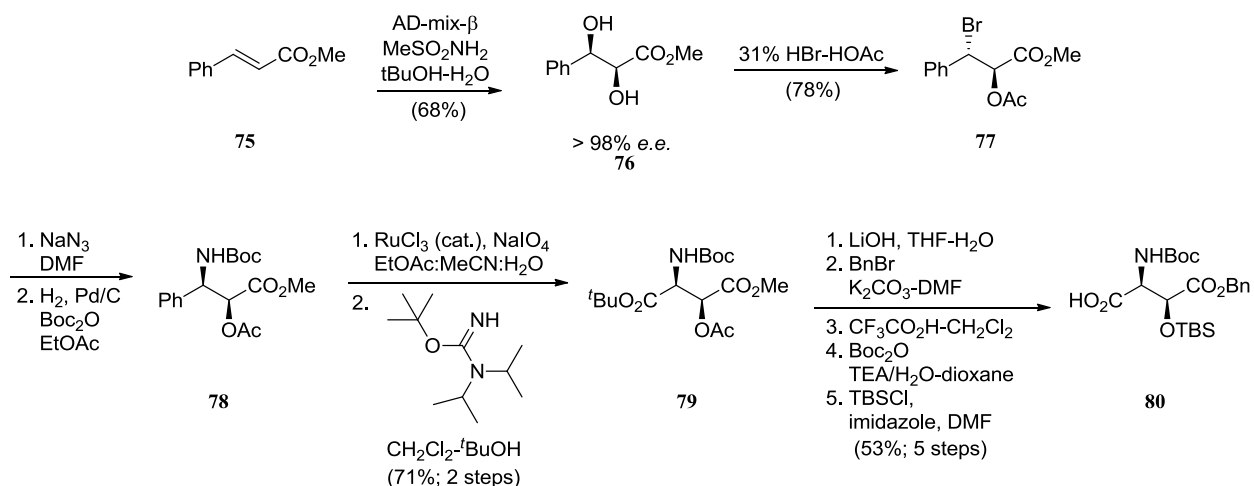
2.4 Previous Syntheses of 3-Hydroxyaspartic Acid

Cho and Ko introduced cyclic iminocarbonates as intermediates *en route* to *syn*-amino alcohols.¹⁰ The starting *syn*-diol **72** was activated as a tin acetal and then an isothiocyanate was added immediately (Scheme 2.3). Without isolation of the intermediate, tetra-*n*-butylammonium bromide was added to the reaction mixture to give *N*-benzoyloxazdidin-2-one **73** in good yield. The product, obtained from a one pot reaction, can be manipulated to give amino alcohol **74**. Specifically, acid or base treatment in alcoholic media cleaves the benzoyl group followed by removal of the cyclic carbamate group in 3 steps. This includes *N*-Boc protection, basic removal of the carbamate ring and Boc deprotection.



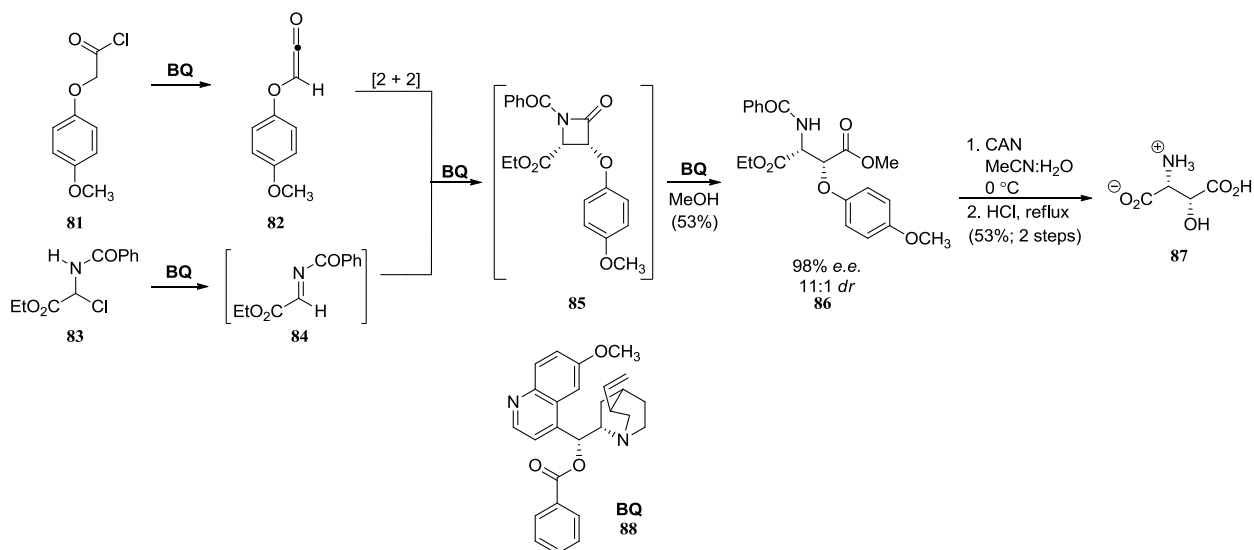
Scheme 2.3 – Cho and Ko's¹⁰ Cyclic Iminocarbonate Intermediate for a Projected 3-Hydroxyaspartic Acid Synthesis

Shioiri and co-workers generated *L-threo*- β -hydroxyaspartic acid in protected form *en route* to alterobactin A.¹¹ The synthesis started with the SAD reaction of α,β -unsaturated methyl ester **75** using AD-mix- β to produce a *syn*-diol **76** which upon the reaction with HBr-HOAc underwent inversion at C- β and protection at α -OH (Scheme 2.4). Azide inversion at C- β accompanied by reduction and protection of the resulting amino group as its Boc carbamate formed **78**. Oxidative cleavage of the phenyl group in **78** followed by protection of the carboxyl group as its *tert*-butyl ester afforded **79**. A series of deprotections and reprotections according to Scheme 2.4 secured target compound **80**.



Scheme 2.4 – Shioiri and Co-workers¹¹ *L-threo*- β -Hydroxyaspartic Acid Synthesis *En Route* to Alterobactin A

Lectka *et al.* reported the use of a chiral nucleophilic catalyst, benzoylquinine (BQ, **88**) to make β -substituted aspartic acid precursors in four operations, one pot.¹² The initial acid chloride **81** goes through catalytic dehydrohalogenation to form a ketene **82** which reacts with an *N*-acyl imine **84** that was generated by dehydrohalogenation of an α -chloroamine **83** to trigger a catalyzed [2 + 2] cycloaddition to form an intermediate β -lactam **85** (Scheme 2.5). Nucleophilic ring opening using alcohols provides a substrate that was transformed to β -hydroxyaspartic acid **87** in two additional steps.

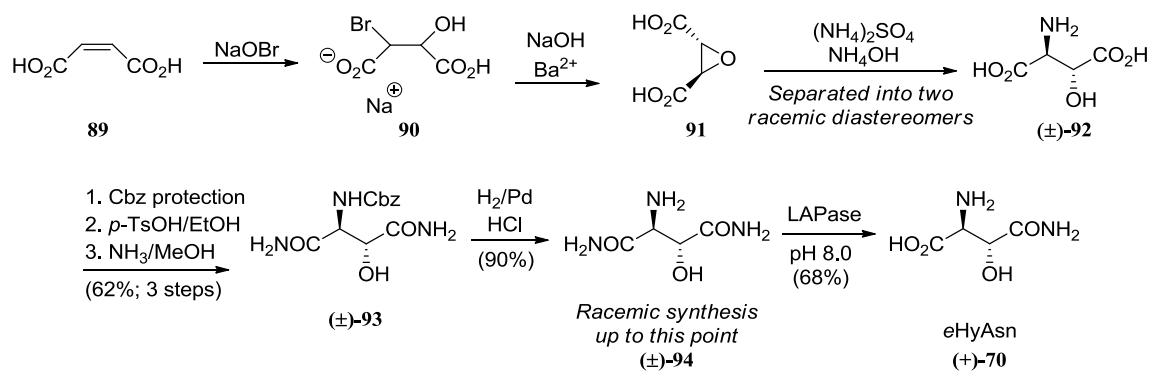


Scheme 2.5 – Lectka *et al.*¹² BQ Catalyzed Synthesis of β -Substituted Aspartic Acid Precursors

2.5 Previous Syntheses of β -Hydroxy-L-asparagine

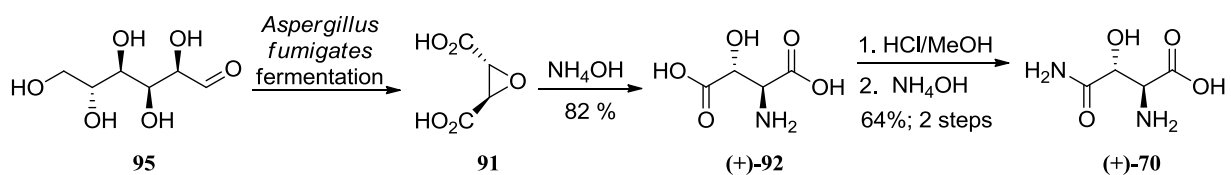
2.5.1 Previous Syntheses of *Erythro*- β -Hydroxyasparagine

Okai and Izumiya started with olefin **89** and the addition of sodium hypobromite formed **90** (Scheme 2.6).^{6,13} This in turn reacted with NaOH to produce *trans*-epoxy diacid **91** which was ammonolyzed to give (2*S*,3*R*)-2-amino-3-hydroxysuccinic acid (\pm)-**92** after separation. The authors further elaborated (\pm)-**92** by first protecting the amino group as its Cbz derivative. Tonic acid in ethanol converted both carboxylic acid groups to their ethyl ester counterparts that were subsequently ammonolyzed to give diamide (\pm)-**93**. Hydrogenolysis of the Cbz group from compound (\pm)-**93** generated the free amine. The stage was now set for regioselective hydrolysis of *eHyAsp* diamide using leucine aminopeptidase (LAPase).



Scheme 2.6 - Okai and Izumiya's^{6,13} Synthesis of *eHyAsn* Using an Enzyme-Catalyzed Reaction

Sendai and co-workers started with (-)-*trans*-epoxysuccinic acid, a product of glucose fermentation by *Aspergillus fumigates* (Scheme 2.7).¹⁴ The oxirane **91** was ammonolyzed to give *erythro*- β -hydroxy-*L*-aspartic acid (+)-**92** and then converted regioselectively to its methyl ester at the β -CO₂H. The selectivity observed is probably due to preferential hydrogen bonding of the protonated amine group to the β -CO₂H. Ammonium hydroxide introduced the primary amide (+)-**70** by ammonolysis of the aforementioned methyl ester. This approach was adopted by Tohdo *et al.* to produce a building block for their attempted synthesis of TNM F.^{15,16}



Scheme 2.7 - Sendai and Co-workers¹⁴ Synthesis of *e*HyAsn Using an Enzyme-Catalyzed Reaction

2.5.2 Previous Syntheses of *Threo*- β -Hydroxyasparagine

Threo- β -hydroxy-L-asparagine (*t*HyAsn) features in lysobactin **96** and ramoplanin A1 **97**, lipoglycopeptides that show promise against vancomycin-resistant bacteria (Figure 2.3). Due to the importance of these antibiotics, the synthesis of *t*HyAsn has drawn the attention of the Lectka,¹⁷ VanNieuwenhze,¹⁸ and Boger^{19,20} groups.

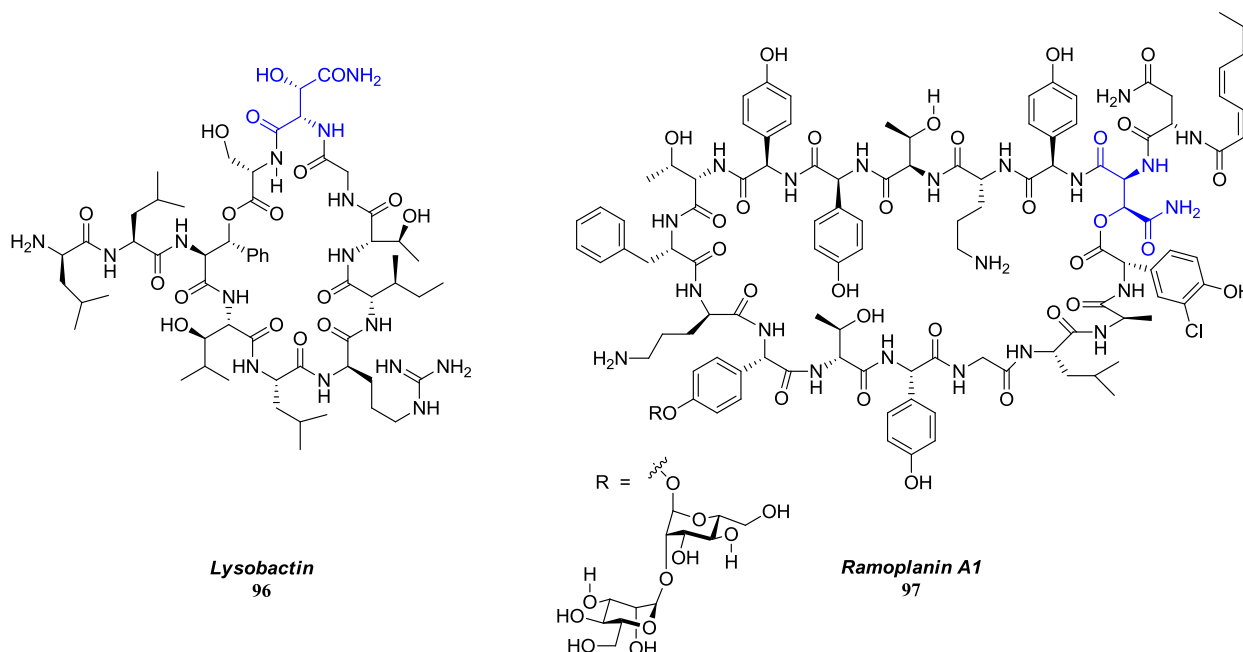
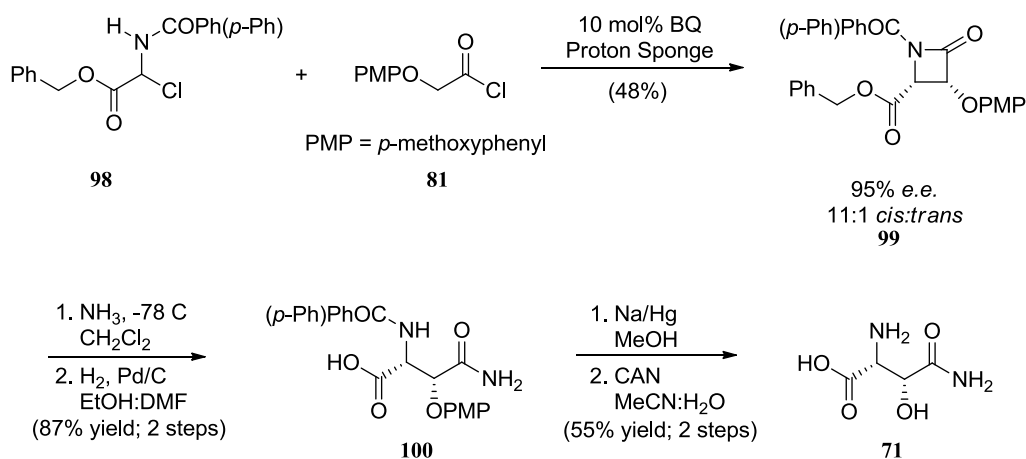


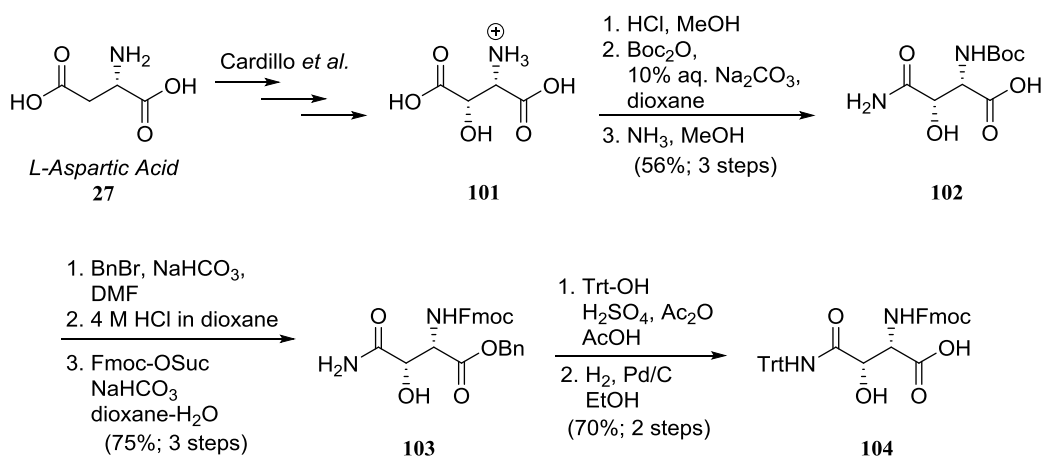
Figure 2.3 – Lysobactin and Ramoplanin A1

Lectka and co-workers applied the same benzoylquinine (BQ) catalyst methodology described in §2.4 to synthesize *t*HyAsn for the cyclic peptide, lysobactin.¹⁷ As shown in Scheme 2.8, benzyl ester **98** reacted with acyl chloride **81** under BQ catalyzed conditions to produce β -lactam **99** with good stereoselectivity. Ring opening of **99** using ammonia followed by hydrogenolysis led to carboxylic acid **100**. Removal of the biphenyl protecting group followed by CAN-mediated deprotection of the remaining aromatic protecting group generated final product **71** in short order.



Scheme 2.8 – Lectka and Co-workers¹⁷ BQ Catalyzed Synthesis of *t*HyAsn

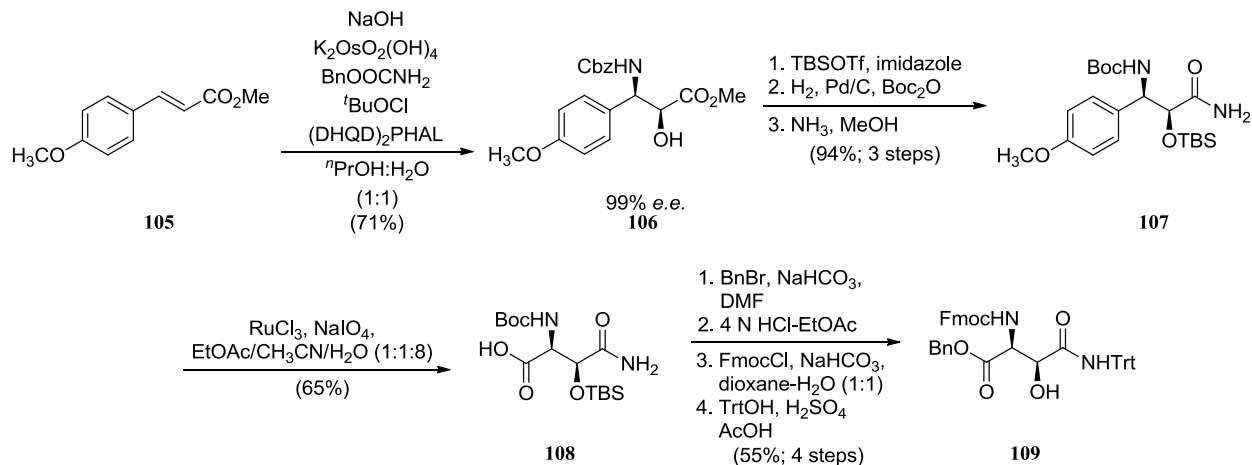
VanNieuwenhze *et al.*¹⁸ began with the stereoselective synthesis of *L-threo*- β -hydroxyaspartic acid from *L*-aspartic acid **27** as prescribed by Cardillo *et al.*²¹ Regioselective protection of the C- β carboxyl group as its methyl ester followed by Boc-protection of the amino group and aminolysis of the aforementioned methyl ester provided **102** (Scheme 2.9). The remaining carboxyl group was protected as its benzyl ester and at this point, additional protecting group manipulations would give a building block suitable for incorporation into lysobactin. Deprotection of the Boc group using HCl/dioxane followed by re-protection of the amino group as its Fmoc carbamate generated **103**. Lastly, protection of amide in compound **103** with a trityl group and hydrogenolysis of the benzyl ester afforded the target compound **104**.



Scheme 2.9 – VanNieuwenhze *et al.*¹⁸ Synthesis of *t*HyAsn

Boger and co-worker's approach to *t*HyAsn is different from the majority of the syntheses presented previously in that it begins from a nonchiral building block.^{19,20} Instead of enzyme-catalyzed reactions, or relying on the chiral pool, the stereochemistry is introduced by a stereoselective reaction. Initially reported in 2000,¹⁹ and with improvements in 2003,²⁰ the researchers described an elegant route to the *t*HyAsn diastereomer. Their approach capitalized on the use of cinnamate esters as excellent substrates for the Sharpless aminohydroxylation (SAH) reaction and the use of an aromatic group as a surrogate for a carboxylic acid.

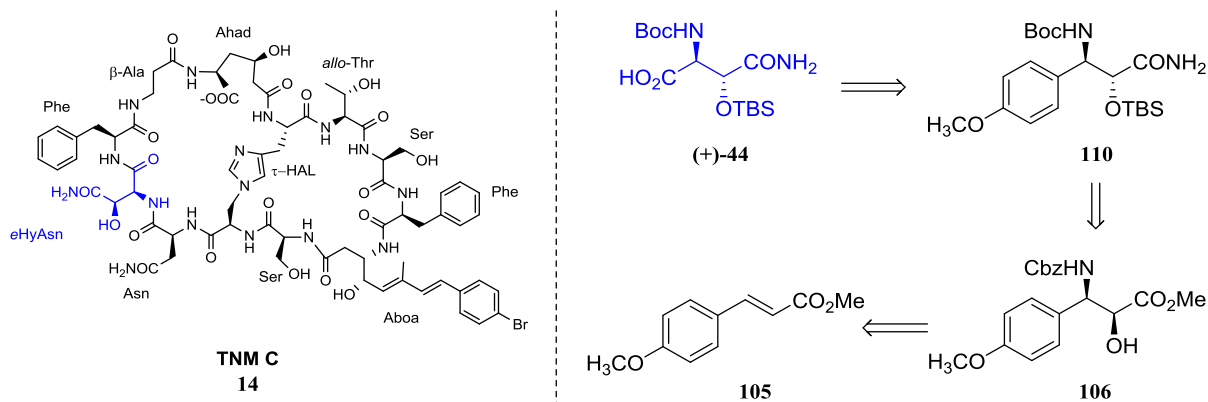
The SAH of α,β -unsaturated methyl ester **105** using the (DHQD)₂PHAL ligand generated β -amino alcohol **106** in good yield and excellent enantioselectivity (Scheme 2.10). Protection of the secondary alcohol as its TBS ether followed by *N*-Cbz/Boc exchange led to an intermediate that was ammonolyzed to provide the side chain primary amide **107**. Oxidative cleavage of the *p*-methoxyphenyl group revealed carboxylic acid **108**. To ensure orthogonality of protecting groups in the target compound, **108** was protected as its benzyl ester followed by single step TBS and Boc protecting group removal. The free amino group was subsequently protected as its Fmoc carbamate while the side chain primary amide was protected with a trityl group.



Scheme 2.10 – Boger and Co-workers^{19,20} Synthesis of *t*HyAsn Using a Stereoselective Reaction

2.6 Retrosynthetic Analysis

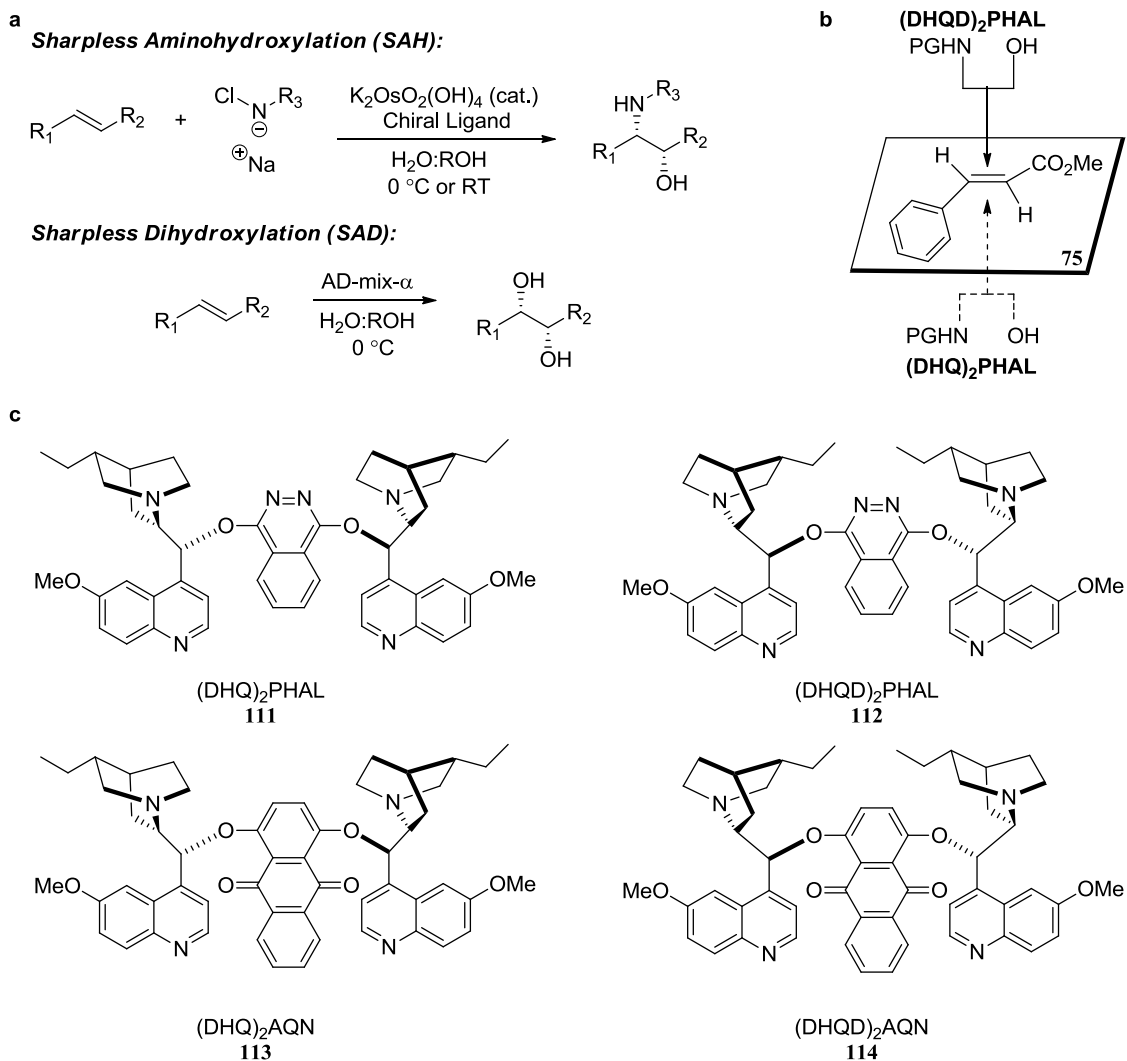
Our approach to *e*HyAsn (+)-**44**²² (Scheme 2.11) made use of several important reactions from Boger's synthesis of *t*HyAsn. The first key step, the SAH reaction would establish *threo* stereochemistry from a *trans* olefin geometry. Mitsunobu inversion at the β -OH would lead to the desired *erythro* configuration and eventual unmasking of the carboxylic acid would rapidly produce a useful building block for TNM synthesis.



Scheme 2.11 - Retrosynthetic Analysis of *e*HyAsn

2.7 The Sharpless Asymmetric Aminohydroxylation

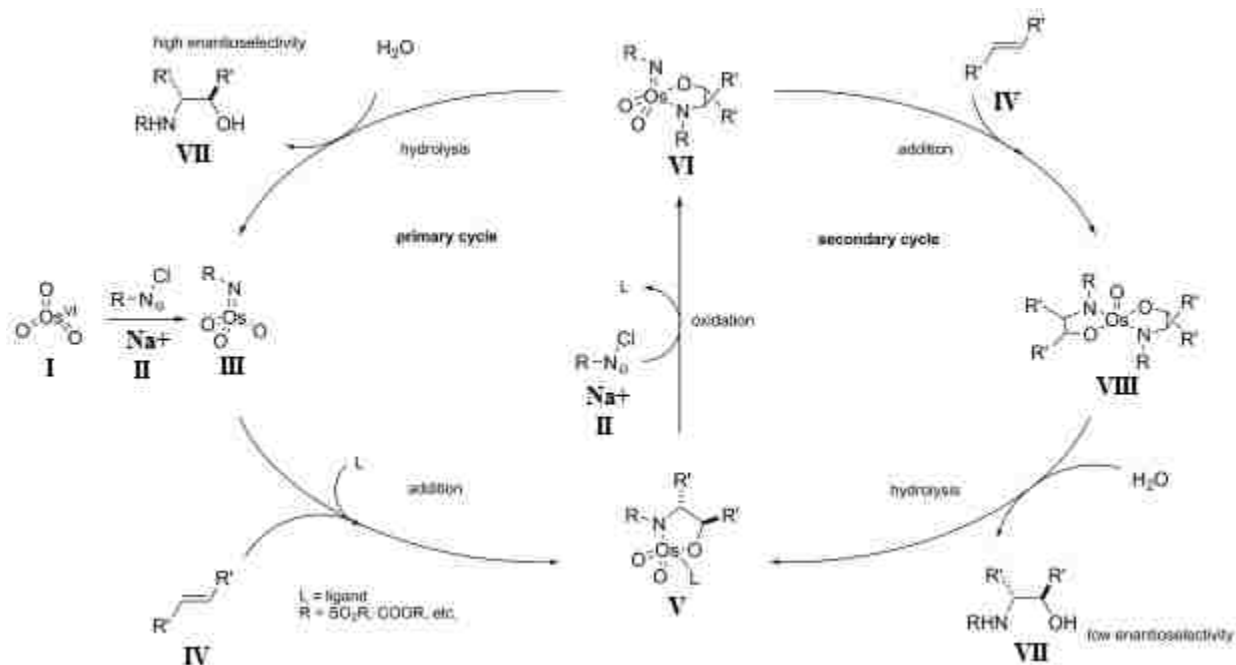
The first key step to our synthesis of *e*HyAsn required the SAH reaction. A recurring theme of this and future chapters is that key steps are prefaced with relevant literature examples and details about mechanism. The SAH, first reported in 1996, is a powerful method for the rapid construction of vicinal amino alcohols from alkenes (a in Scheme 2.12).²³



Scheme 2.12 – Sharpless Chemistry. (a) Comparing Sharpless’s vicinal functionalization reactions: aminohydroxylation vs dihydroxylation. (b) The Sharpless mnemonic device. (c) The Sharpless chiral ligands.

The first nitrogen source used was the chloramine salt of tosylsulfonamide, but numerous other sources of nitrogen have been developed to provide more useful amine derivatives.²⁴ Unlike the Sharpless asymmetric dihydroxylation (SAD) reaction and its commercially available reagents (AD-mix- α and AD-mix- β), the presence of a variable nitrogen source requires that the reagents for the SAH reaction must be mixed fresh. Like the SAD reaction, however, the mnemonic (b in Scheme 2.12) used to predict the enantiofacial selectivity that results in addition to one face of the alkene can be utilized for the SAH reaction (since it employs the same alkaloid-derived ligands **111-114**, c in Scheme 2.12).

The reaction occurs via two simultaneous catalytic cycles, each competing to form products with different selectivities (Scheme 2.13).^{24,25} The primary cycle starts with the oxidation of the Os^{VI} species **I** by the alkali metal salt of the nitrogen source **II** to give the osmium^{VIII} trioxoimido species **III**. This intermediate adds with *syn*-stereoselectivity to the alkene **IV** to generate the Os^{VI} azaglycolate complex **V**. The chiral ligand influences several aspects of this reaction including acceleration of the rate of reaction, regioselectivity during the addition, and induction of enantioselectivity.

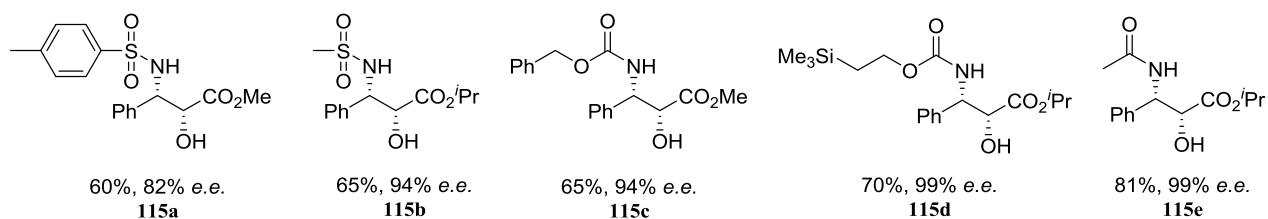


Scheme 2.13 - Reaction Mechanism for the Sharpless Aminohydroxylation Reaction. Copyright 2010, John Wiley and Sons, reprinted with permission (p. 250).

The exact mode of addition for the crucial bond forming step (**III** + **IV** → **V**) has been an area of considerable debate. An early computational study and a more recent one by Munz and Strassner lends weight to the [3 + 2] cycloaddition for this process.²⁶⁻²⁹ The authors report that Sharpless' proposed [2 + 2] cycloadditions are kinetically and thermodynamically disfavored by more than 25 kcal mol⁻¹. Also, a ligand-induced reaction-rate acceleration of 2.7 kcal mol⁻¹ s⁻¹ was calculated for the cycloaddition step of the [3 + 2] addition.

Oxidation of **V** by the nitrogen oxidizing agent gives Os^{VIII} azaglycolate **VI**. Hydrolysis of **VI** provides amino alcohol **VII** and the osmium species **III** is ready for another catalytic cycle. Conversely, **VI** may enter the second cycle and add to another olefin molecule to give the *bis*(azaglycolate) complex **VIII**. Fokin and co-workers proposed that the five-coordinate disposition of **VI** generates enough electron density at the metal center to allow the reaction to proceed without an external ligand.^{30,31} As a consequence, addition products from this second catalytic cycle are obtained with low regio- and enantioselectivity. Hydrolysis of **VIII** regenerates **V**, which completes the secondary cycle. Both hydrolysis steps are the turnover-determining steps in either catalytic cycle. Suppression of the secondary cycle relies on the effective hydrolysis of **VI**, which in turn can be accomplished by conducting the reaction in alcohol-H₂O mixtures.

It was noted early on that cinnamates are among the best substrates for the SAH reaction (Scheme 2.14).³² The mnemonic correctly predicts that use of (DHQ)₂PHAL produces regioisomer **115a-e** as the major product.



Scheme 2.14 - Aminohydroxylation of Cinnamates Using (DHQ)₂PHAL

Early work by Janda and co-workers utilized a substrate-based approach for control of regioselectivity.³³ They proposed a catalytically active complex **IX** (Figure 2.4) analogous to that proposed by Corey for the SAD reaction. The OsO₃NX species is coordinated to the nitrogen of the quinuclidine ring in a distorted trigonal bipyramid geometry. With the two nitrogen ligands occupying axial positions, the regioselectivity is determined by how an alkene binds to the catalyst.

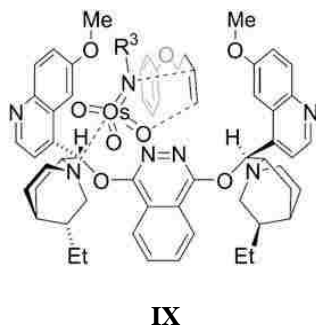
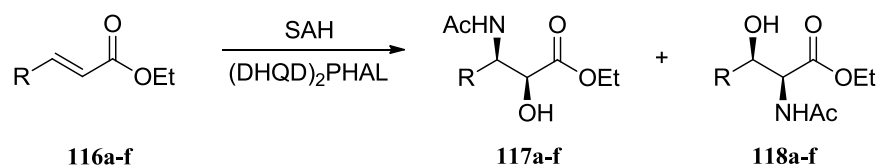


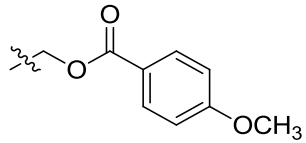
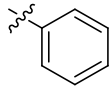
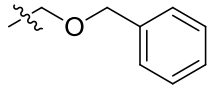
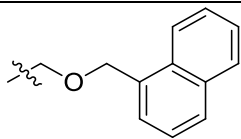
Figure 2.4 - Janda and Co-Workers³³ Proposed a Catalytically Active Complex for the SAH Reaction. Copyright 2009, Elsevier, reprinted with permission (p. 251).

The α,β -unsaturated compounds (similar to the cinnamates) used by the researchers examined the influence of steric and ligand-substrate interactions. Experimental results showed the preferential addition of nitrogen to the β -carbon atom and the oxygen to the α -carbon atom (Table 2.1) relative to the ester functional group. Also, entries 3 and 4 displayed excellent regioselectivity and enantioselectivity while entries 5 and 6 exhibited lowered regioselectivity. It seems that ligand-substrate interactions influence both regioselectivity and enantioselectivity.

Table 2.1 - A Substrate Based Approach for Control of Regioselectivity by Janda and Co-Workers

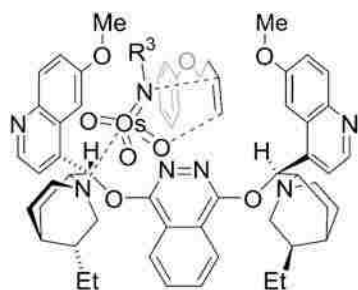


(Table 2.1 continued)

Entry	R	Regioselectivity (117a-f:118a-f)	ee [%]	Yield [%]
1	H	15.2:1	NR	NR
2	CH ₃	1.4:1	NR	NR
3		>20.0:1	>95	79
4		>20.0:1	>95	65
5		2.4:1	NR	51
6		4.3:1	NR	53

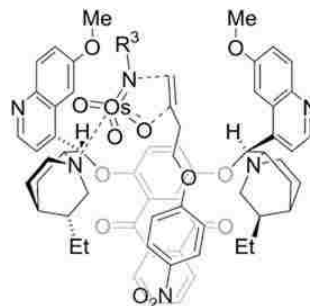
NR = Not Reported

A report by Sharpless *et al.* noted that the regioselectivity observed with the PHAL ligands can be reversed by changing to the AQN ligands.³⁴ Inspired by Sharpless's work, McLeod and co-workers carried out theoretical studies of ligand-osmium binding geometry and also conducted experimental investigations of the SAH reaction on several ester substrates to better understand ligand-substrate control of regioselectivity.³⁵ The B3LYP/6-31G* calculations support the proposition of Janda *et al.* that the mechanism involves a complex with apical nitrogen ligands in a distorted trigonal bipyramidal geometry (Scheme 2.15). This lowest energy configuration has implications on regioselectivity in the SAH reaction. Specifically, changes in regioselectivity result from changes in substrate-catalyst orientation.



IX

Reactions Employing PHAL Ligands



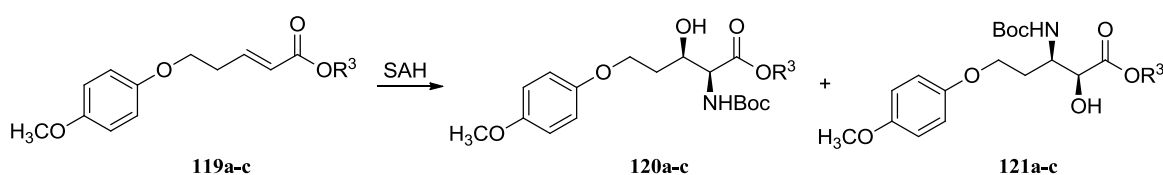
X

Reactions Employing AQN Ligands

Scheme 2.15 – The Catalytically Active Complexes as Supported by B3LYP/6-31G* Calculations. Copyright 2009, Elsevier, reprinted with permission (p. 251).

To test this hypothesis, a range of similarly substituted esters **119a-c** were synthesized and the outcomes of the SAH reactions are presented in Table 2.2.³⁵ Chemical yields for the PHAL-catalyzed reactions were consistently higher than the AQN-catalyzed reactions. An increase in the bulk of the ester substituent (R^3) has little effect on the selectivity of the PHAL reaction. For the PHAL ligands, stabilizing aromatic-aromatic interactions of the aryl ether with the methoxyquinoline rings of the catalyst led to regioselective formation of the β -amino product. The increasing size of the ester (Me \rightarrow t Bu) should have little influence on stereoselectivity of the reaction since it resides on an open region of the catalyst over the phthalazine spacer. The AQN reaction on the same series of ester substituents led to a reversal in regioselectivity. However, increasing the size of the ester led to deterioration of selectivity. To see why this is so, Scheme 2.15 shows the subtle differences. The AQN catalyst features an aromatic spacer region that is elongated compared to its PHAL counterpart. This leads directly to an increase in steric crowding. The α -amino product, as favored by the AQN ligand, relies on interaction of the aryl ether with the AQN aromatic spacer. This mode of binding is evident with the loss of stereoselectivity for the favored product as the ester substituent increases in size.

Table 2.2 - McLeod and Co-Workers' Investigation on Factors Affecting Regioselectivity Using Similarly Substituted Esters

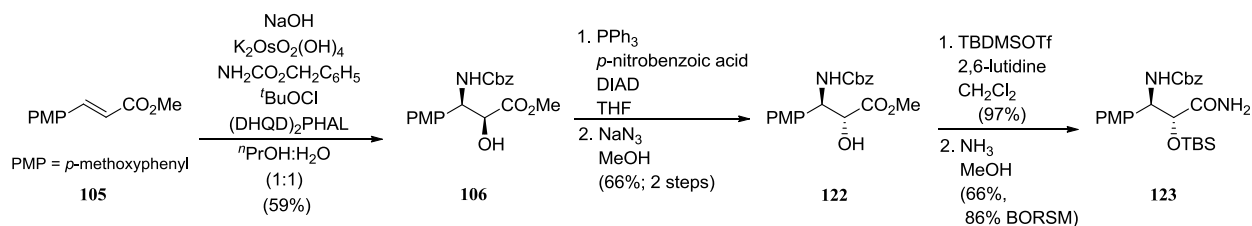


Entry	Substrate	R ³	Alkaloid	PHAL α:β(120:121)	PHAL % <i>ee</i> (121)	AQN α:β(120:121)	AQN % <i>ee</i> (120)
1	119a	CH ₃	DHQD	1:20	96	5:1	89
2	119a	CH ₃	DHQ	1:20	97	5:1	68
3	119b	ⁿ Bu	DHQD	ND	ND	2:1	87
4	119b	ⁿ Bu	DHQ	1:9	99	ND	ND
5	119c	^t Bu	DHQ	1:6	96	1.2:1	51

ND = Not Determined

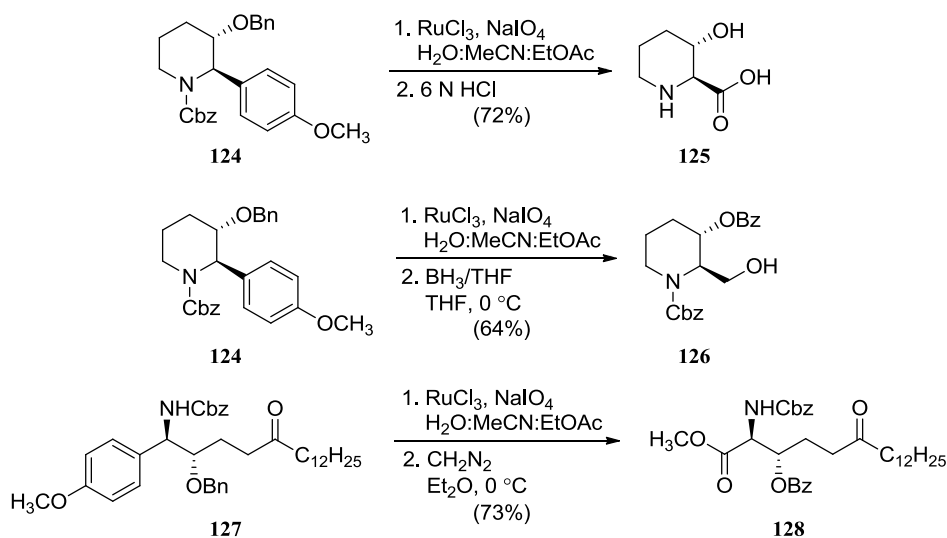
2.8 Synthesis of *e*HyAsn

On this background, we began as previously reported, the SAH reaction of cinnamate **105** gave a good yield of Cbz-protected amino alcohol **106** (Scheme 2.16).^{19,20,22} The authors reported an enantiomeric excess of 99% and an optical rotation value, $[\alpha]^{23.0}_D -5.3$ (*c* 0.94, CHCl₃), for **106**. The **106** produced in our hands was characterized and proved identical in both respects. We then conducted a Mitsunobu reaction with *p*-nitrobenzoate as the nucleophile, resulting in inversion of configuration at the center undergoing substitution. The *p*-nitrobenzoate ester was cleaved by azidolysis³⁶ to give **122**. The secondary alcohol was protected as its TBS ether and the methyl ester converted to the side chain primary amide, giving compound **123**.



Scheme 2.16 – Part 1 of *eHyAsn* Synthesis

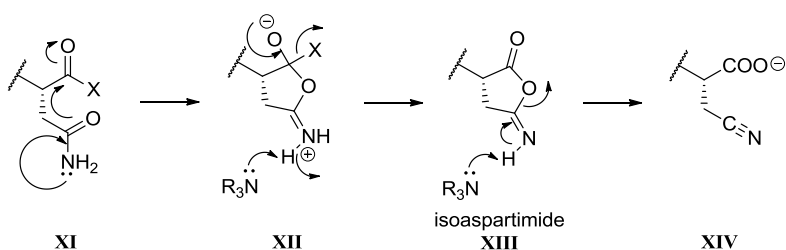
Reports by Jung and co-workers have shown that oxidative cleavage of a *p*-methoxyphenyl aromatic ring can occur selectively in the presence of a benzyl carbamate (Scheme 2.17).^{37,38}



Scheme 2.17 – Precedents for Oxidative Cleavage of the PMP Group in the Presence of Cbz

We tried to unmask the α -COOH from compound **123** but were unsuccessful. To avoid competitive degradation between the PMP and Cbz aromatic rings, we resorted to switching carbamate protecting groups. Specifically, single step *N*-Cbz/Boc exchange was accomplished in 98% yield (Scheme 2.18). The oxidative degradation of compound **110** was initially conducted on a small scale but the yield was not synthetically useful. When the reaction was conducted on a reasonable scale (600 mg or more) with a mechanical stirrer, however, the yield improved dramatically. Also, careful control of pH during workup and exhaustive extraction of the aqueous layer are critical. The isolated yield of crude

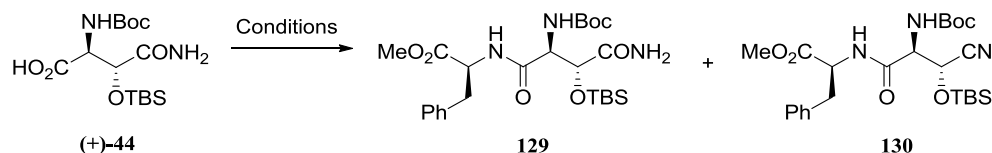
The main concern with Asn residues is that upon carboxyl activation, unprotected side chain carboxamido groups **XI** are known to undergo isoaspartimide formation **XIII** followed by dehydration to give β -cyanoalanine derivatives **XIV** (Scheme 2.20).³⁹⁻⁴¹ This was, in fact, a major side product isolated on coupling Phe to *e*HyAsn with BOP/DIPEA (Table 2.3, Entry 1). König and Geiger⁴² demonstrated in 1970 that the most effective conditions to suppress this side reaction, involve a carbodiimide-mediated coupling with addition of one equivalent of hydroxybenzotriazole (HOBt) in the reaction mixture.^{43,44} The role of this additive is to serve as a superior proton donor relative to the NH of the isoaspartimide. Thus, formation of the BtO⁻ (benzotriazoloxo) anion occurs in preference to dehydration to generate a nitrile. The 1-hydroxybenzotriazole ester is the active species in solution and it undergoes aminolysis at a rate of about 10³-fold faster than the ester formed from NHS.



Scheme 2.20 – Side Reaction of Unprotected Asn Residues: β -Cyanoalanine Derivative Formation. Copyright 2009, Elsevier, reprinted with permission (p. 253).

The crude acid (+)-**44** was subjected directly to the peptide coupling reaction. The addition of HOBt was beneficial to the reaction as the ratio of desired dipeptide to undesired nitrile increased (Entry 2). Switching coupling reagent (BOP \rightarrow EDC) and base (diisopropylethylamine \rightarrow triethylamine) led to formation of **129**, albeit in modest yield (Entry 4). *N*-[3-(dimethylamino)propyl]-*N'*-ethylcarbodiimide can be used in place of DCC as this reagent and its corresponding urea by-product is soluble in aqueous solvents and can be removed in the workup. Under optimized conditions (EDC/HOBt/THF), the isolated yield of dipeptide **129** is 68%. We have found conditions to form a dipeptide, and demonstrated that this can be done without protection of the side-chain amide functionality.

Table 2.3 - *e*HyAsn-Phe Dipeptide Formation: Optimization Study

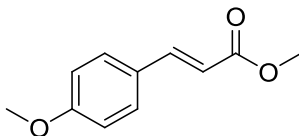


Entry	Additive	Base	Coupling Reagent	Solvent	Yield 129 (%)	Yield 130 (%)
1	-	<i>i</i> Pr ₂ NEt	BOP	CH ₃ CN	27	17
2	HOBt	<i>i</i> Pr ₂ NEt	BOP	CH ₃ CN	36	12
3	-	<i>i</i> Pr ₂ NEt	DPPA	CH ₃ CN	24	0
4	HOBt	NEt ₃	EDC	CH ₂ Cl ₂	43	0
5	HOBt	NEt ₃	EDC	CH ₃ CN	60	0
6	HOBt	NEt ₃	EDC	THF	68	0

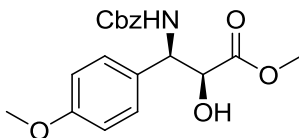
2.10 Experimental Section

General methods: all reactions were performed under a dry nitrogen atmosphere unless otherwise noted. Reagents were obtained from commercial sources and used directly; exceptions are noted. Diisopropylethylamine and triethylamine were dried and distilled from CaH₂ and stored over KOH pellets. Ethanol and methanol were distilled from Mg turnings and stored over 4Å molecular sieves. Flash chromatography was performed using flash silica gel (32-63 μ) from Dynamic Adsorbents Inc. Reactions were followed by TLC on precoated silica plates (200 μm, F-254 from Dynamic Adsorbents Inc.). The compounds were visualized by UV fluorescence or by staining with phosphomolybic acid, ninhydrin or KMnO₄ stains. NMR spectra were recorded on Bruker DPX-250 or AV-400-liquid spectrometers. Proton NMR data is reported in ppm downfield from TMS as an internal standard. High resolution mass spectra were recorded using either time-of-flight or electrospray ionization.

2.10.1 Experimental Procedures

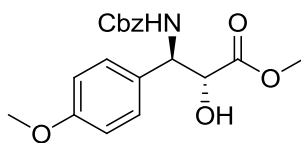


(*E*)-Methyl 3-(4-methoxyphenyl)acrylate (**105**). Boron trifluoride diethyl etherate (14.10 mL, 15.93 g, 112.2 mmol, 1.0 equiv.) was added dropwise to a solution of (*E*)-3-(4-methoxyphenyl)acrylic acid (20.00 g, 112.2 mmol, 1.0 equiv.) in anhydrous methanol (50 mL) under N₂. The resulting solution was heated under reflux for 13 h and cooled to room temperature. Aqueous Na₂CO₃ (5%, 300 mL) was added and the mixture stirred for 30 min. The crystalline precipitate was collected by filtration, washed with H₂O, and dried to afford a colorless solid (20.62 g, 96%). mp 86-88 °C (lit. mp 85-87 °C); *R*_f 0.26 (5:1 Hex-EtOAc); ¹H NMR (CDCl₃, 400 MHz) δ 3.79 (s, 3H), 3.83 (s, 3H), 6.31 (d, *J* = 16.0 Hz, 1H), 6.90 (d, *J* = 8.8 Hz, 2H), 7.47 (d, *J* = 8.8 Hz, 2H), 7.65 (d, *J* = 16.0 Hz, 1H); ¹³C NMR (CDCl₃, 100 MHz) δ 51.5, 55.3, 114.3 [2C], 115.3, 127.1, 129.7 [2C], 144.5, 161.4, 167.7; HRMS (ESI) calcd for C₁₁H₁₃O₃ (M+H)⁺ 193.0859, obsd 193.0856.

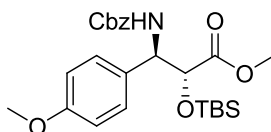


(2*S*,3*R*)-Methyl 3-(benzyloxycarbonylamino)-2-hydroxy-3-(4-methoxyphenyl)propanoate (**106**). Benzyl carbamate (9.05 g, 60.0 mmol, 2.30 equiv.) was dissolved in *n*-PrOH (70 mL). A solution of NaOH (2.44 g, 61.0 mmol, 2.35 equiv.) in H₂O (110 mL) was added and the resulting solution stirred for 10 min. Freshly prepared *tert*-butyl hypochlorite (6.90 mL, 6.62 g, 61.0 mmol, 2.35 equiv.) was added dropwise and the resulting solution stirred for an additional 10 min. (DHQD)₂PHAL (0.83 g, 1.3 mmol, 5 mol %) in *n*-PrOH (40 mL) was added and the reaction vessel immersed in a water bath at ambient temperature and stirred for 5 min. (*E*)-Methyl 3-(4-methoxyphenyl)acrylate **105** (5.0 g, 26.0 mmol, 1.0 equiv.) was added, followed immediately by K₂OsO₂(OH)₄ (0.38 g, 1.0 mmol, 4 mol %). The reaction

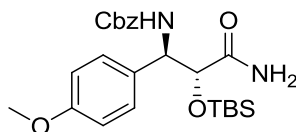
mixture was stirred for 2 h at 0 °C. The pale yellow slurry was filtered, and the solid washed with ice cold EtOH-H₂O (1:1, 15 mL), and dried to afford **106** as a colorless solid (5.44 g, 58%). *R_f* 0.32 (1:1 Hex-EtOAc); $[\alpha]^{26.5}_{\text{D}}$ -5.2 (*c* 1.0, CHCl₃) Lit, $[\alpha]^{23}_{\text{D}}$ -5.3 (*c* 0.94, CHCl₃); ¹H NMR (CDCl₃, 400 MHz) δ 3.24 (s, 1H), 3.78 (s, 6H), 4.43 (s, 1H), 5.02-5.09 (m, 2H), 5.20 (d, *J* = 9.4 Hz, 1H), 5.67 (d, *J* = 9.4 Hz, 1H), 6.86 (d, *J* = 8.6 Hz, 2H), 7.25-7.32 (m, 7H); ¹³C NMR (CDCl₃, 100 MHz) δ 53.0, 55.2, 56.0, 66.9, 73.5, 114.0, 127.9, 128.0, 128.1, 128.4, 131.0, 136.2, 155.6, 159.2, 173.2; HRMS (ESI) calcd for C₁₉H₂₀NO₆(M-H)⁺ 358.1296, obsd 358.1299.



(2*R*,3*R*)-Methyl-3-(benzyloxycarbonylamino)-2-hydroxy-3-(4-methoxyphenyl)propanoate (**122**). *p*-Nitrobenzoic acid (3.94 g, 23.6 mmol, 2.2 equiv.) was added to a solution of (2*S*,3*R*)-methyl 3-(benzyloxycarbonylamino)-2-hydroxy-3-(4-methoxyphenyl)propanoate **106** (3.86 g, 10.7 mmol, 1.0 equiv.) in dry THF (130 mL). Triphenylphosphine (6.19 g, 23.6 mmol, 2.2 equiv.) was added, then the mixture cooled to 0 °C under N₂. Diisopropyl azodicarboxylate (4.65 mL, 4.77 g, 23.6 mmol, 2.2 equiv.) was slowly added via syringe. Upon completion of the addition, the ice bath was removed and the contents stirred at room temperature for 2 d. The reaction mixture was concentrated and the residue dissolved in anhydrous MeOH (130 mL). Sodium azide (3.49 g, 53.6 mmol, 5.0 equiv.) was added and the mixture heated at 45 °C for 3.5 d. The solvent was removed under reduced pressure and the product isolated from the residue by flash chromatography (Hex-EtOAc, 3:1) to give a pale yellow solid (2.56 g, 66%). *R_f* 0.32 (1:1 Hex-EtOAc); $[\alpha]^{25.0}_{\text{D}}$ -20.8 (*c* 0.8, CHCl₃); ¹H NMR (CDCl₃, 400 MHz) δ 2.92 (d, *J* = 6.5 Hz, 1H), 3.69 (s, 3H), 3.77 (s, 3H), 4.59 (dd, *J* = 6.5, 3.3 Hz, 1H), 5.05 (d, *J* = 12.2 Hz, 1H), 5.11 (d, *J* = 12.2 Hz, 1H), 5.10-5.13 (m, 1H), 5.83 (d, *J* = 8.6 Hz, 1H), 6.82 (d, *J* = 8.5 Hz, 2H), 7.17 (d, *J* = 8.5 Hz, 2H), 7.34 (m, 5H); ¹³C NMR (CDCl₃, 100 MHz) δ 52.4, 55.1, 56.4, 66.8, 73.1, 113.8, 128.1, 128.3, 128.4, 128.6, 136.2, 155.5, 159.3, 172.1; HRMS (ESI) calcd for C₁₉H₂₀NO₆(M-H)⁺ 358.1296, obsd 358.1295.

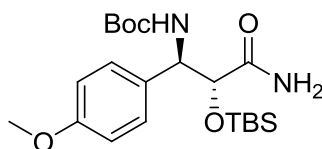


(2*R*,3*R*)-Methyl-3-(benzyloxycarbonylamino)-2-(*tert*-butyldimethylsilyloxy)-3-(4-methoxyphenyl)propanoate (**123 Precursor**). 2,6-Lutidine (190 μ L, 180 mg, 1.67 mmol, 3.0 equiv.) was added dropwise to a solution of (2*R*,3*R*)-methyl 3-(benzyloxycarbonylamino)-2-hydroxy-3-(4-methoxyphenyl)propanoate **122** (200 mg, 0.56 mmol, 1.0 equiv.) in dry CH_2Cl_2 (2.23 mL). The mixture was stirred for 10 min before dropwise addition of TBDMSOTf (150 μ L, 180 mg, 0.67 mmol, 1.2 equiv.). The resulting solution was stirred for 3 h at room temperature, at which point another portion of TBDMSOTf (150 μ L, 180 mg, 0.67 mmol, 1.2 equiv.) was added and the mixture stirred for 17 h at room temperature. The mixture was diluted with ethyl acetate (25 mL) and concentrated in vacuo. Flash chromatography on silica gel (Hex-EtOAc, 2:1) afforded the TBS ether as a clear oil (255 mg, 97%). R_f 0.24 (4:1 Hex-EtOAc); ^1H NMR (CDCl_3 , 400 MHz) δ 0.02 (s, 3H), 0.05 (s, 3H), 0.91 (s, 9H), 3.55 (s, 3H), 3.76 (s, 3H), 4.60 (d, $J = 4.0$ Hz, 1H), 5.05-5.13 (m, 3H), 5.52 (d, $J = 8.2$ Hz, 1H), 6.81 (d, $J = 8.7$ Hz, 2H), 7.24 (d, $J = 8.1$ Hz, 2H), 7.33 (m, 5H); ^{13}C NMR (CDCl_3 , 100 MHz) δ -5.5, -5.2, 18.2, 25.7, 51.7, 55.2, 57.0, 66.8, 74.3, 113.7, 128.1, 128.5, 128.9, 129.6, 136.4, 155.5, 159.3, 171.3; HRMS (ESI, m/z) calcd for $\text{C}_{25}\text{H}_{36}\text{NO}_6\text{Si}$ (MH) $^+$ 474.2306, obsd 474.2298.

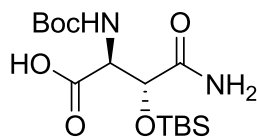


Benzyl-(1*R*,2*R*)-3-amino-2-(*tert*-butyldimethylsilyloxy)-1-(4-methoxyphenyl)-3-oxopropyl-carbamate (**123**). Ammonia gas was bubbled through a solution of (2*R*,3*R*)-methyl 3-(benzyloxycarbonylamino)-2-(*tert*-butyldimethylsilyloxy)-3-(4-methoxyphenyl)propanoate (2.20 g, 4.65 mmol) in dry MeOH (23 mL) at 0 $^\circ\text{C}$. The reaction vessel was stoppered and the mixture stirred for 7 d at room temperature. The solution was cooled to 0 $^\circ\text{C}$ and resaturated with ammonia gas. The reaction

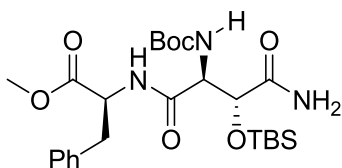
vessel was stoppered and the mixture stirred for 7 d at room temperature. The solvent was removed under reduced pressure. Flash chromatography (Hex-EtOAc, 3:1) led to recovery of the methyl ester (440 mg, 20%) and isolation of the primary amide **123** as a colorless foam (1.40 g, 66%). R_f 0.29 (1:1 Hex-EtOAc); $[\alpha]_D^{26.5} +2.2$ (c 1.0, CHCl_3); $^1\text{H NMR}$ (CDCl_3 , 400 MHz) δ -0.01 (s, 3H), 0.02 (s, 3H), 0.92 (s, 9H), 3.78 (s, 3H), 4.44 (d, $J = 3.7$ Hz, 1H), 4.97 (m, 1H), 5.05-5.11 (m, 2H), 5.37 (s, 1H), 5.45 (d, $J = 6.5$ Hz, 1H), 5.99 (s, 1H), 6.83 (d, $J = 8.7$ Hz, 2H), 7.23 (d, $J = 8.2$ Hz, 2H), 7.33 (m, 5H); $^{13}\text{C NMR}$ (CDCl_3 , 100 MHz) δ -5.5, -5.4, 18.0, 25.7, 55.2, 57.6, 66.8, 75.9, 113.6, 128.0, 128.1, 128.4, 129.1, 129.7, 136.4, 155.2, 159.3, 173.8; HRMS (ESI, m/z) calcd for $\text{C}_{24}\text{H}_{35}\text{N}_2\text{O}_5\text{Si}$ (MH) $^+$ 459.2309, obsd 459.2313.



Tert-butyl-(1*R*,2*R*)-3-amino-2-(*tert*-butyldimethylsilyloxy)-1-(4-methoxyphenyl)-3-oxopropylcarbamate (**110**). A solution of benzyl (1*R*,2*R*)-3-amino-2-(*tert*-butyldimethylsilyloxy)-1-(4-methoxyphenyl)-3-oxopropylcarbamate **123** (117 mg, 0.25 mmol) and Boc_2O (61 mg, 0.28 mmol) in CH_3OH (5 mL) was treated with 10% Pd-C (5 mg). The resulting black suspension was stirred under H_2 (1 atm) at 25 °C overnight. The catalyst was removed by filtration through Celite, and the filtrate was concentrated. Flash chromatography (Hex-EtOAc, 2:1) provided **110** as a colorless foam (107 mg, 99%): $^1\text{H NMR}$ (CDCl_3 , 400 MHz) δ 0.05 (s, 6H), 0.94 (s, 9H), 1.41 (s, 9H), 3.78 (s, 3H), 4.43 (s, 1H), 4.92 (app s, 1H), 5.18 (app s, 1H), 5.71 (s, 1H), 5.97 (s, 1H), 6.82 (d, $J = 8.4$ Hz, 2H), 7.22 (d, $J = 8.4$ Hz, 2H); $^{13}\text{C NMR}$ (CDCl_3 , 100 MHz) δ -5.5, -5.3, 18.0, 25.7, 28.3, 55.1, 57.1, 76.0, 79.6, 113.5, 129.1, 129.8, 154.6, 159.1, 174.0.



(2*S*,3*R*)-4-Amino-2-(*tert*-butoxycarbonylamino)-3-(*tert*-butyldimethylsilyloxy)-4-oxobutanoic acid ((+)-**44**). Sodium periodate (5.504 g, 26 mmol, 18.1 equiv.) in H₂O (128 mL) was added to a solution of *tert*-butyl (1*R*,2*R*)-3-amino-2-(*tert*-butyldimethylsilyloxy)-1-(4-methoxyphenyl)-3-oxopropylcarbamate **110** (0.604 g, 1.4 mmol, 1.0 equiv.) in EtOAc-CH₃CN (1:1, 32 mL). The resulting solution was mechanically stirred at room temperature for 30 minutes. RuCl₃·3H₂O (60 mg, 0.3 mmol, 20 mol %) was added, followed by NaHCO₃ (0.464 g, 5.5 mmol, 3.9 equiv.). The reaction mixture was stirred mechanically at room temperature overnight. The yellow solution was diluted with sat'd aqueous NaHCO₃ (240 mL) and extracted with CH₂Cl₂ (160 mL). The organic layer was washed with sat'd aqueous NaHCO₃ (240 mL) again. The combined aqueous layers were acidified with 10% aqueous HCl to pH 2.5 at 0 °C and extracted with EtOAc (6 x 300 mL). The combined organic layers were dried over MgSO₄, filtered and concentrated to give (+)-**44** as a brown foam (0.414 g, 80%). *R*_f 0.64 (6:4:1 CHCl₃-MeOH-H₂O); [α]^{24.0}_D +51.1 (*c* 1.0, MeOH) Lit¹⁵, [α]^{24.0}_D +40.9 (*c* 1.0, MeOH); ¹H NMR (CD₃OD, 400 MHz) δ 0.15 (s, 3H), 0.16 (s, 3H), 0.94 (s, 9H), 1.45 (s, 9H), 3.83 (s, 1H), 4.57 (d, *J* = 9.7 Hz, 1H), ¹³C NMR (CD₃OD, 100 MHz) δ -5.1, -4.9, 19.0, 26.2, 28.7, 58.7, 75.3, 81.0, 157.1, 171.7, 175.9; HRMS (ESI) calcd for C₁₅H₃₁N₂O₆Si (M+H)⁺ 363.1945, obsd 363.1955.

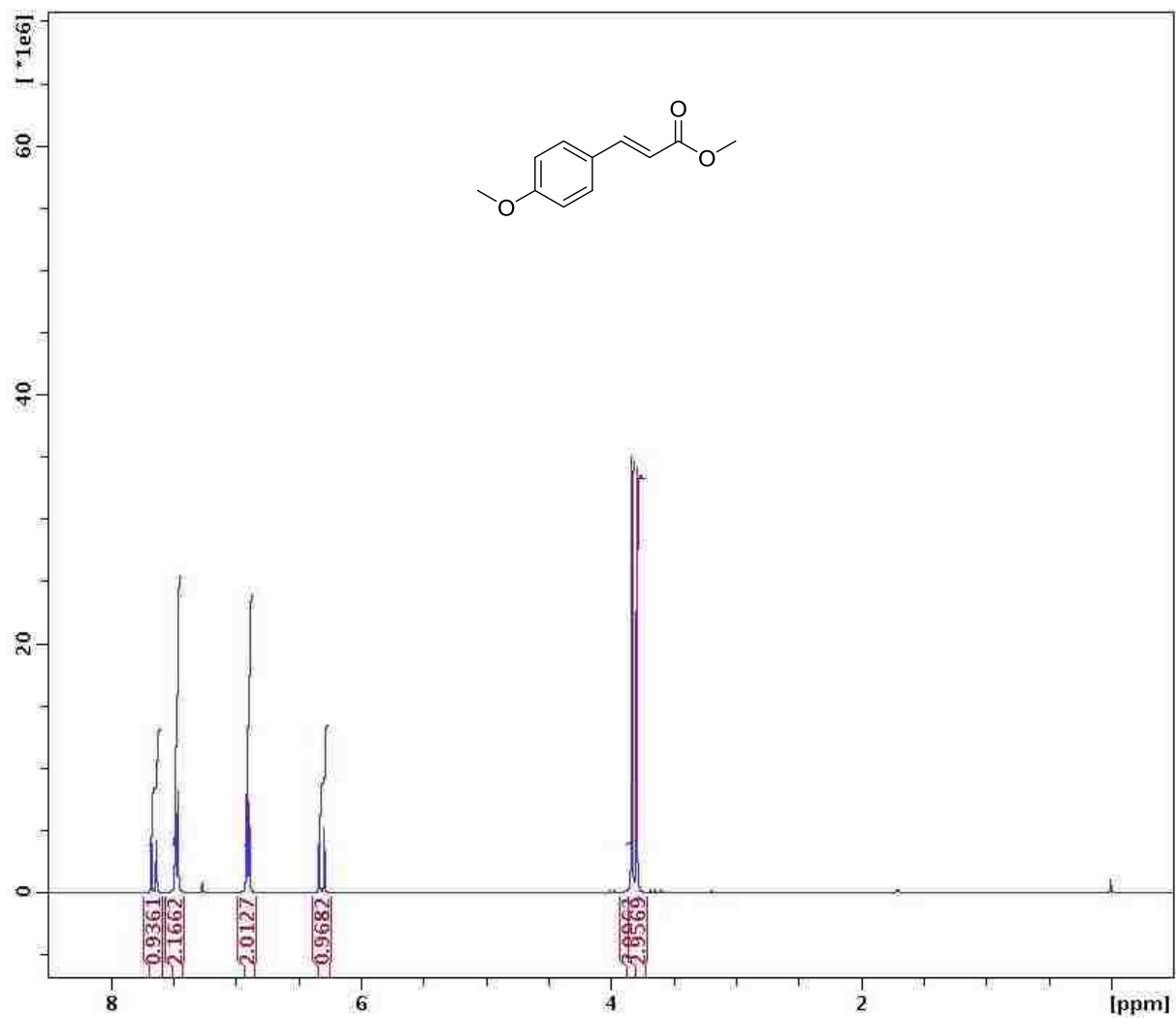


(*S*)-Methyl 2-((2*S*,3*R*)-4-amino-2-(*tert*-butoxycarbonylamino)-3-(*tert*-butyldimethylsilyloxy)-4-oxobutanamido)-3-phenylpropanoate (**129**). (2*S*,3*R*)-4-Amino-2-(*tert*-butoxycarbonylamino)-3-(*tert*-butyldimethylsilyloxy)-4-oxobutanoic acid (+)-**44** (266 mg, 0.7 mmol, 1.0 equiv.) was dissolved in anhydrous THF (15 mL) and the resulting solution cooled to 0 °C. *L*-Phenylalanine methyl ester hydrochloride (158 mg, 0.7 mmol, 1.0 equiv.) was added and the solution stirred at 0 °C for 15 min. Triethylamine (204 μL, 149 mg, 1.5 mmol, 2.0 equiv.) was added and the solution stirred at 0 °C for 10 min. 1-(3-Dimethylamino-propyl)-3-ethyl-carbodiimide hydrochloride (148 mg, 0.8 mmol, 1.05 equiv.)

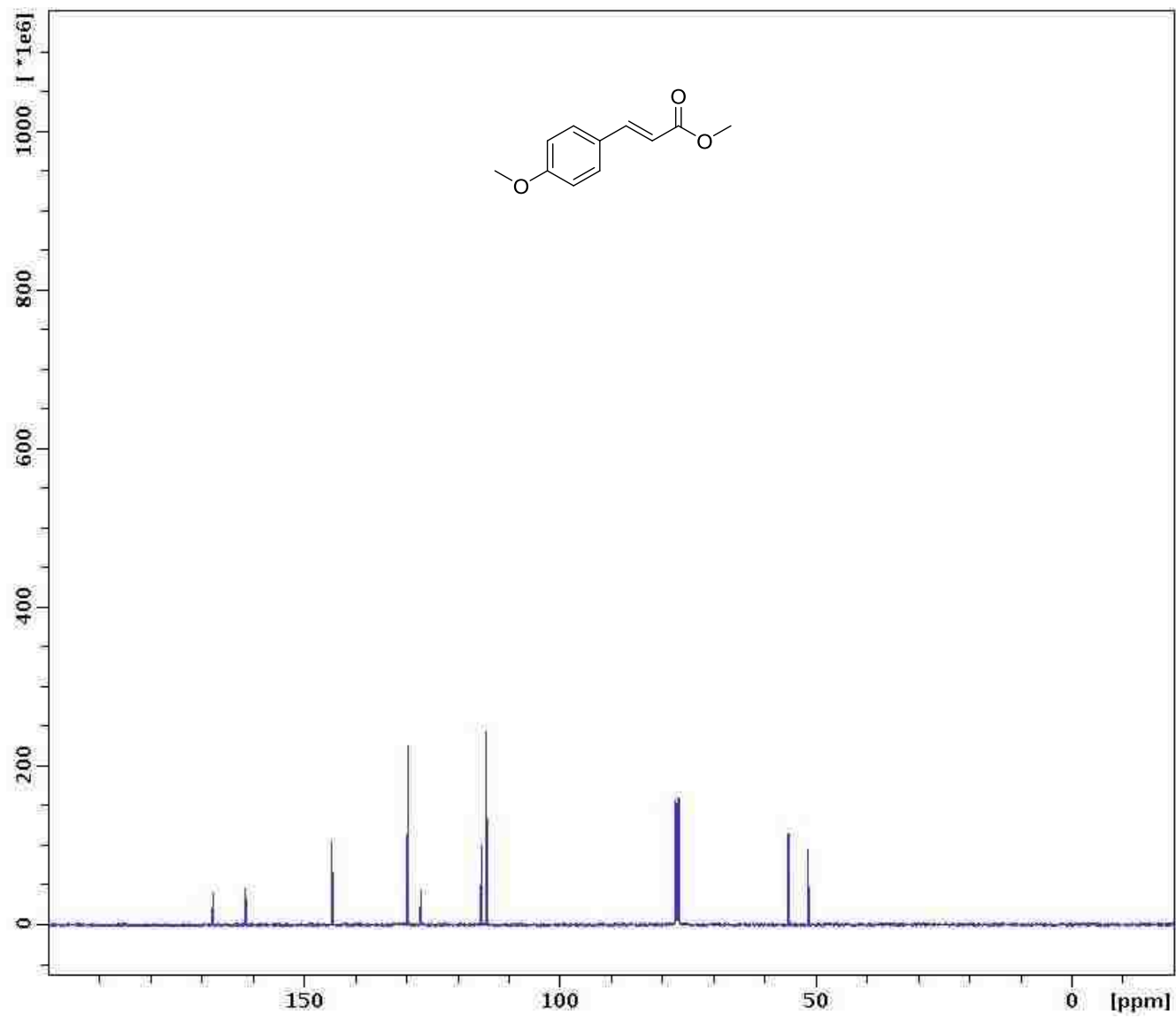
was added, followed by HOBt (149 mg, 1.1 mmol, 1.5 equiv.) at 0 °C. The reaction mixture was allowed to stir for 20 min at 0 °C and then warmed to room temperature and stirred overnight. The solvent was removed and the product isolated **129** from the residue by flash chromatography (Hex-EtOAc 4:1 → Hex-EtOAc 1:1) to give a colorless foam (262 mg, 68%). R_f 0.33 (1:1 Hex-EtOAc); $[\alpha]_D^{25.0} +48.6$ (c 1.0, CHCl₃); ¹H NMR (CDCl₃, 400 MHz) δ 0.10 (s, 3H), 0.13 (s, 3H), 0.90 (s, 9H), 1.44 (s, 9H), 3.08 (d, J = 5.4 Hz, 2H), 3.65 (s, 3H), 4.60-4.70 (m, 2H), 4.80 (d, J = 6.5 Hz, 1H), 5.44 (s, 1H), 5.98 (s, 1H), 6.54 (s, 1H), 6.60 (d, J = 7.4 Hz, 1H), 7.12-7.30 (m, 5H); ¹³C NMR (CDCl₃, 100 MHz) δ -5.3, -5.1, 18.0, 25.6, 28.3, 37.8, 52.2, 53.5, 57.4, 74.0, 80.1, 127.1, 128.6, 129.3, 135.7, 154.9, 167.5, 171.4, 174.3; HRMS (ESI) calcd for C₂₅H₄₀N₃O₇Si (M-H)⁺ 522.2641, obsd 522.2654.

2.10.2 Spectra

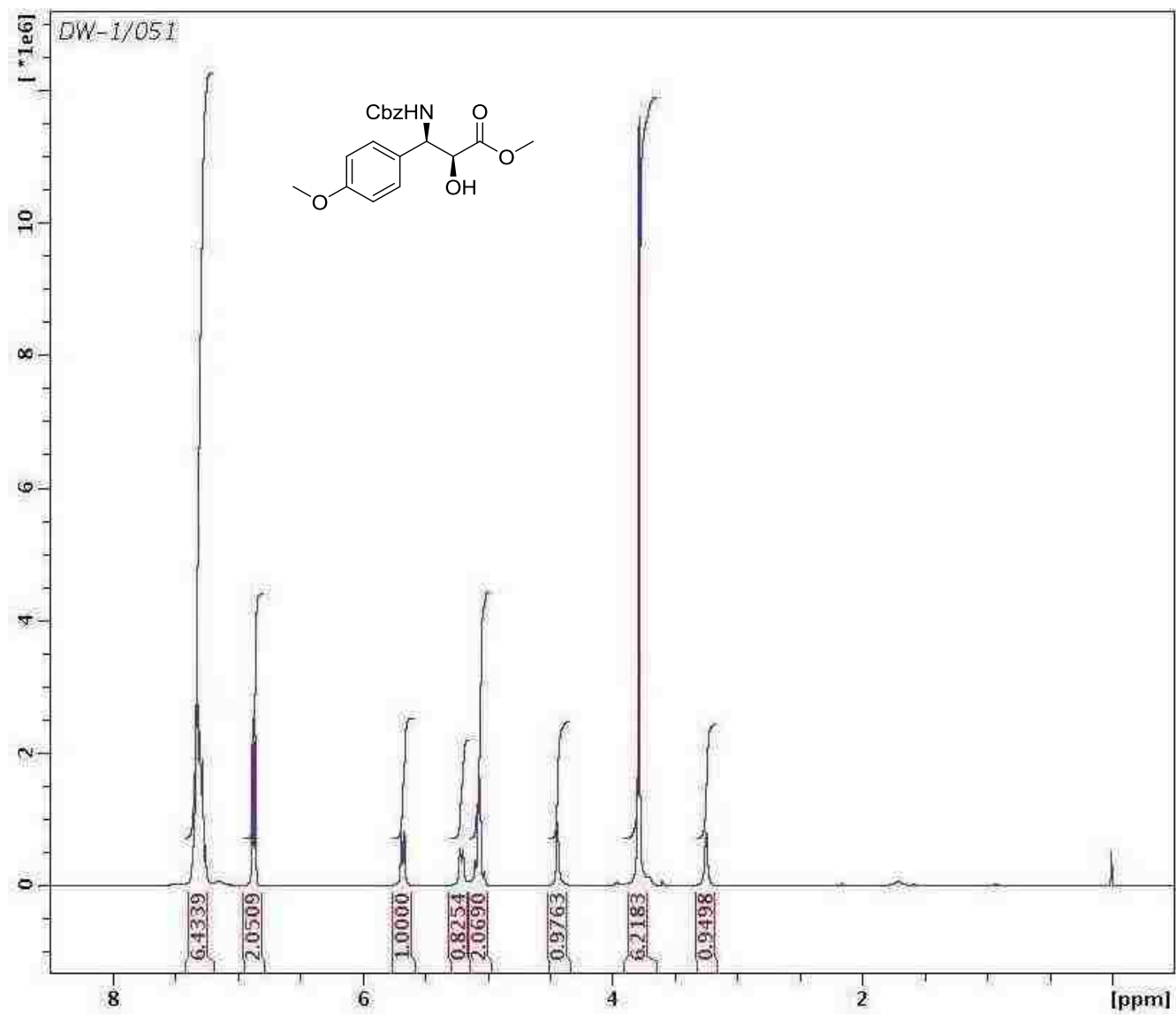
Compound **105** - ^1H NMR in CDCl_3 at 400 MHz



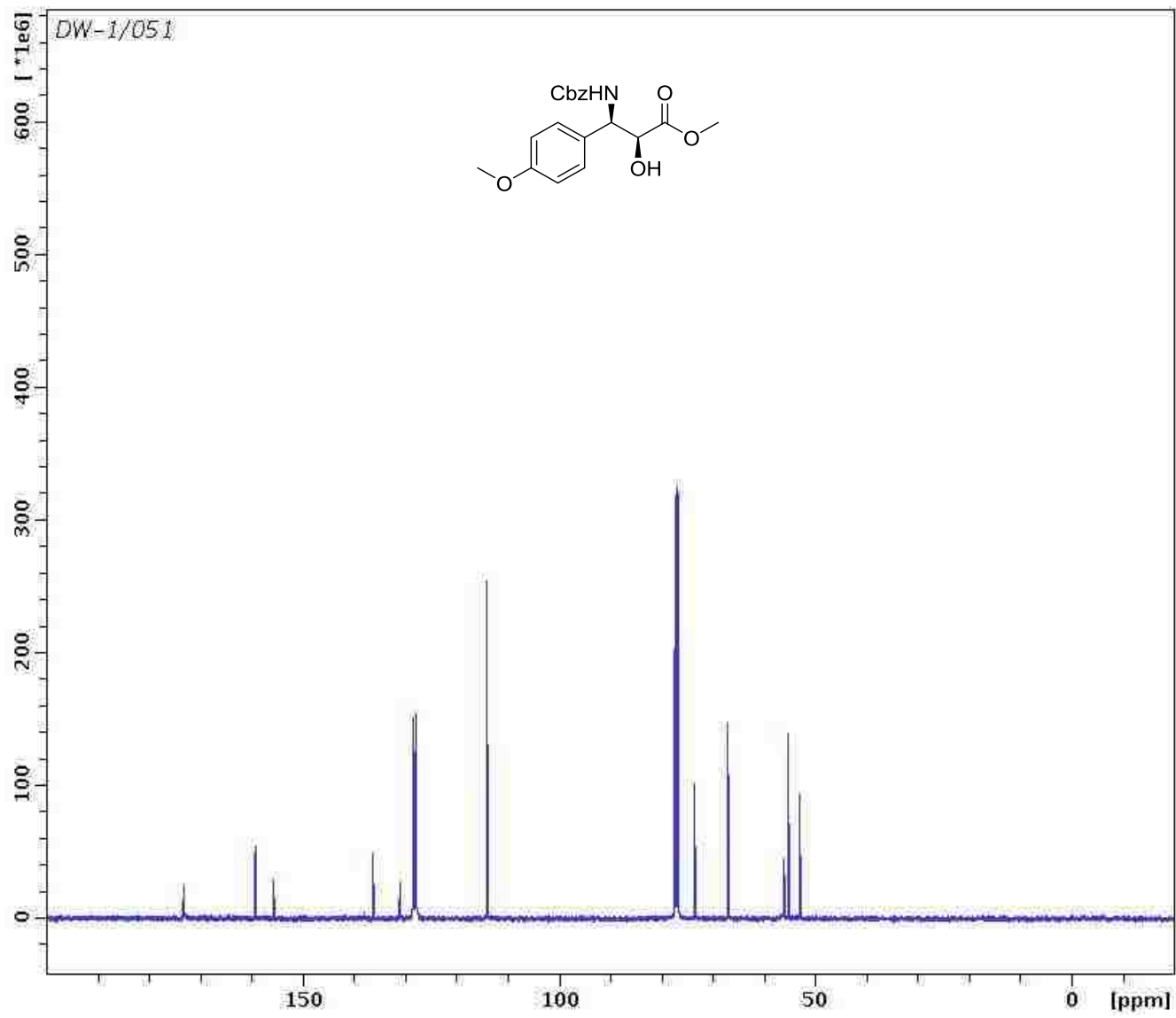
Compound **105** – ^{13}C NMR in CDCl_3 at 100 MHz



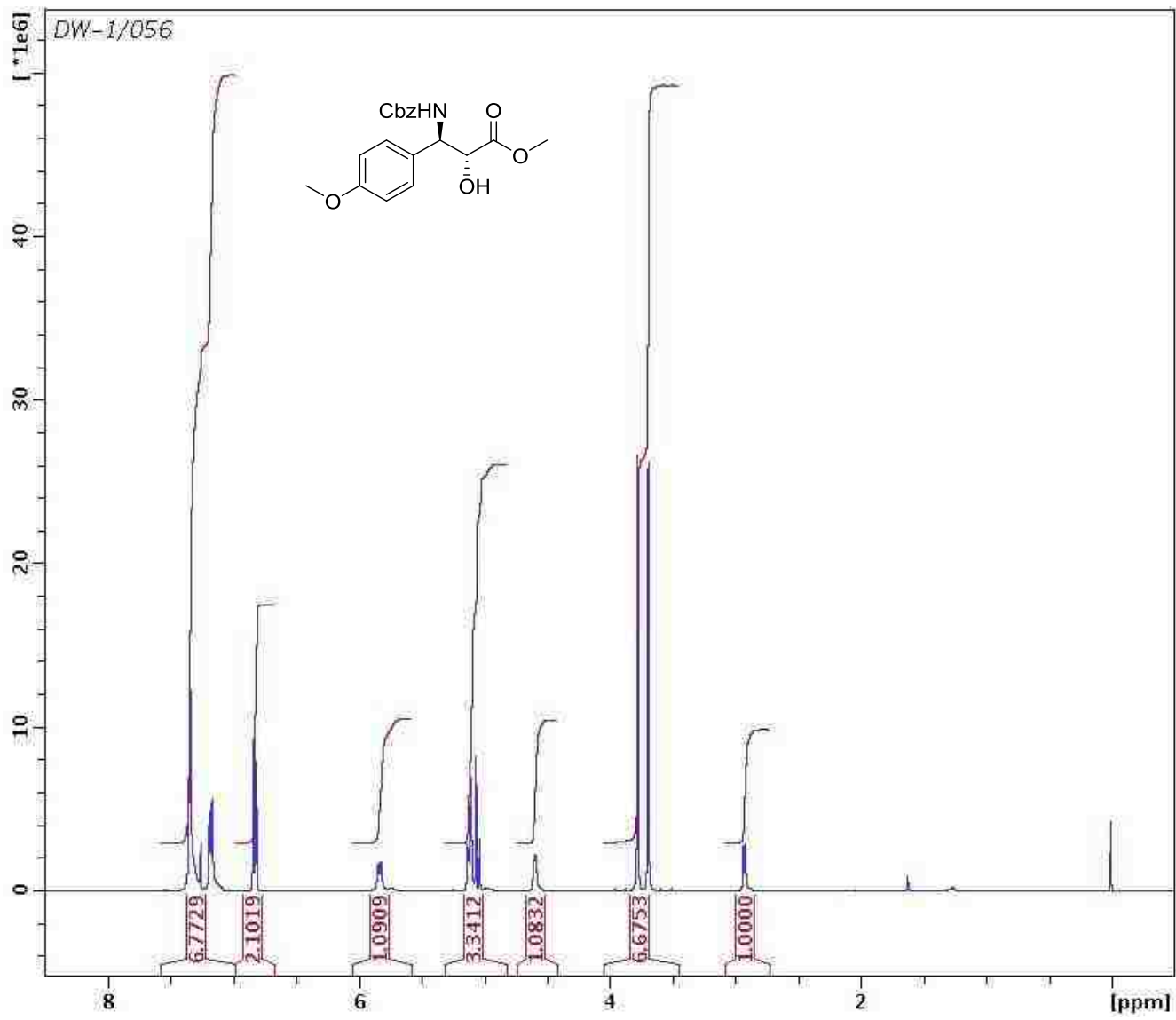
Compound **106** - ^1H NMR in CDCl_3 at 400 MHz



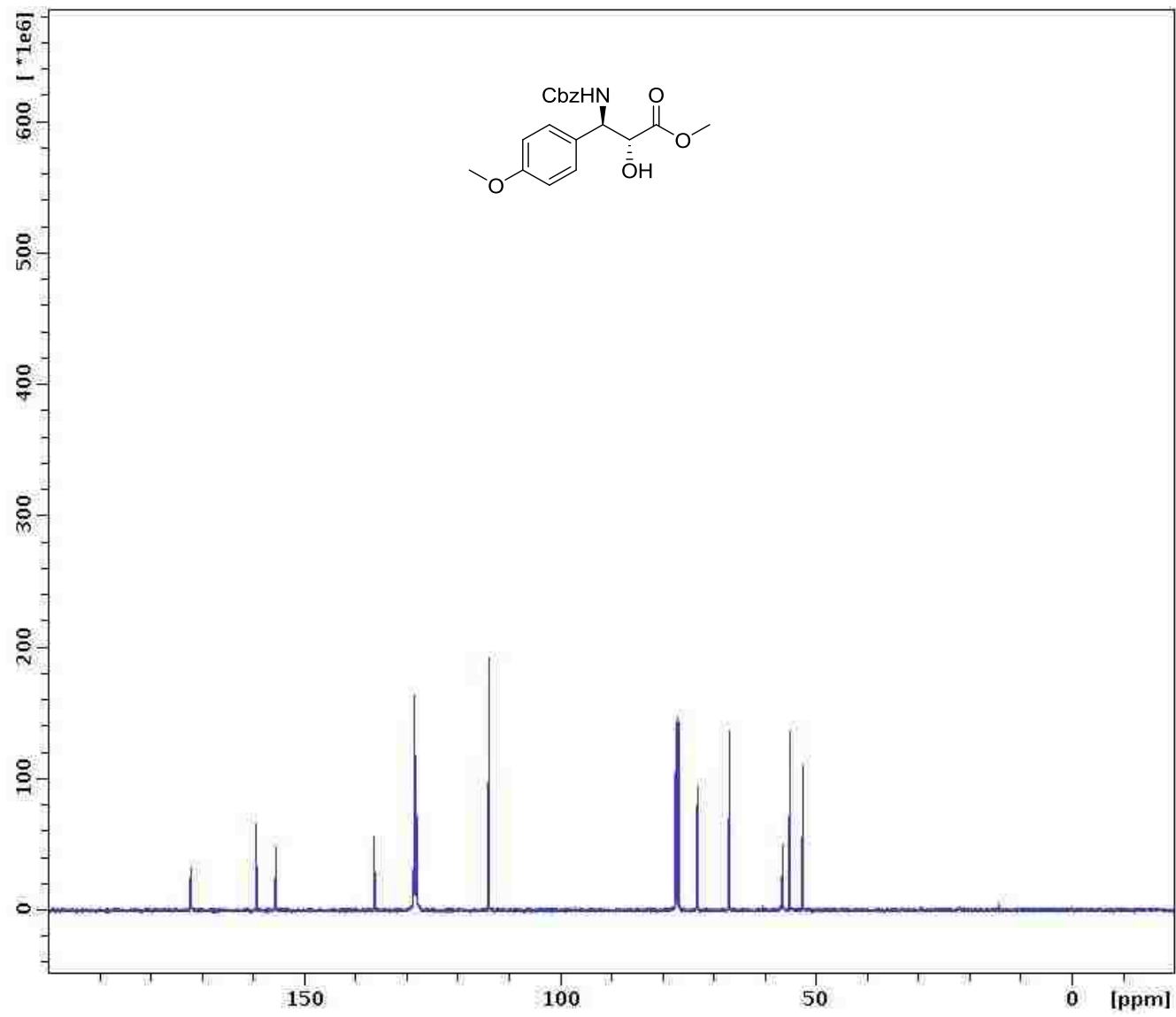
Compound **106** – ^{13}C NMR in CDCl_3 at 100 MHz



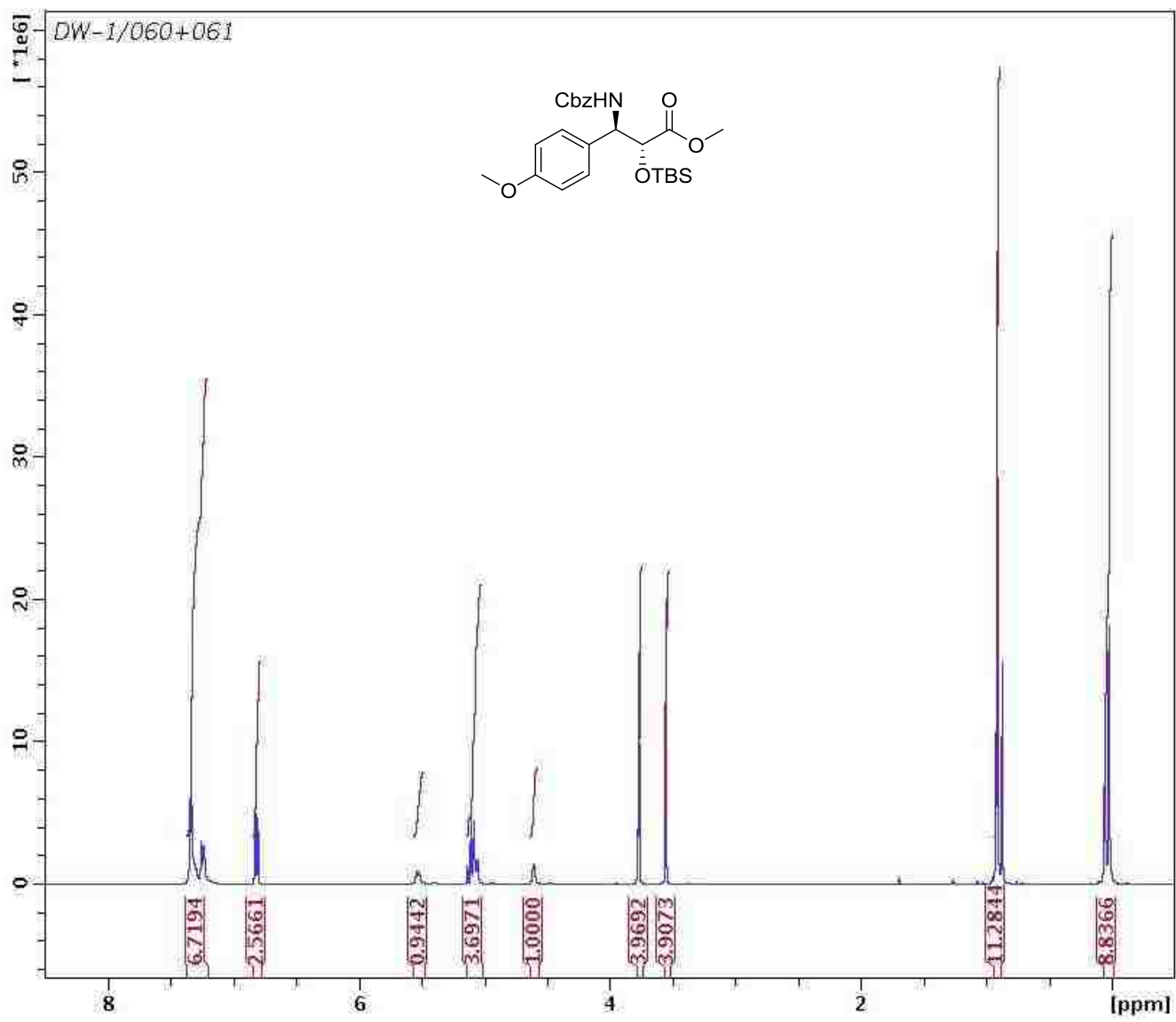
Compound **122** - ^1H NMR in CDCl_3 at 400 MHz



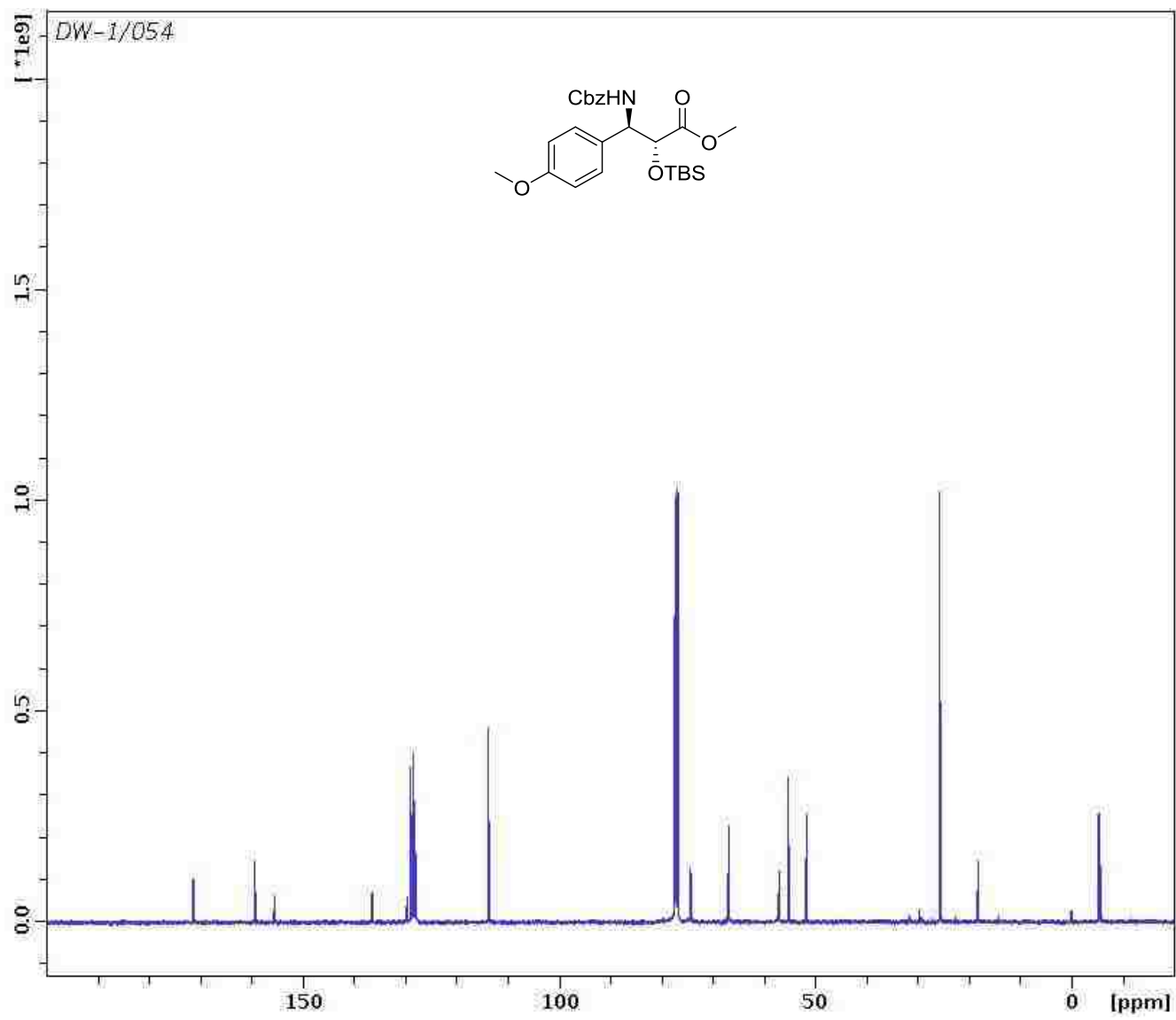
Compound **122** – ^{13}C NMR in CDCl_3 at 100 MHz



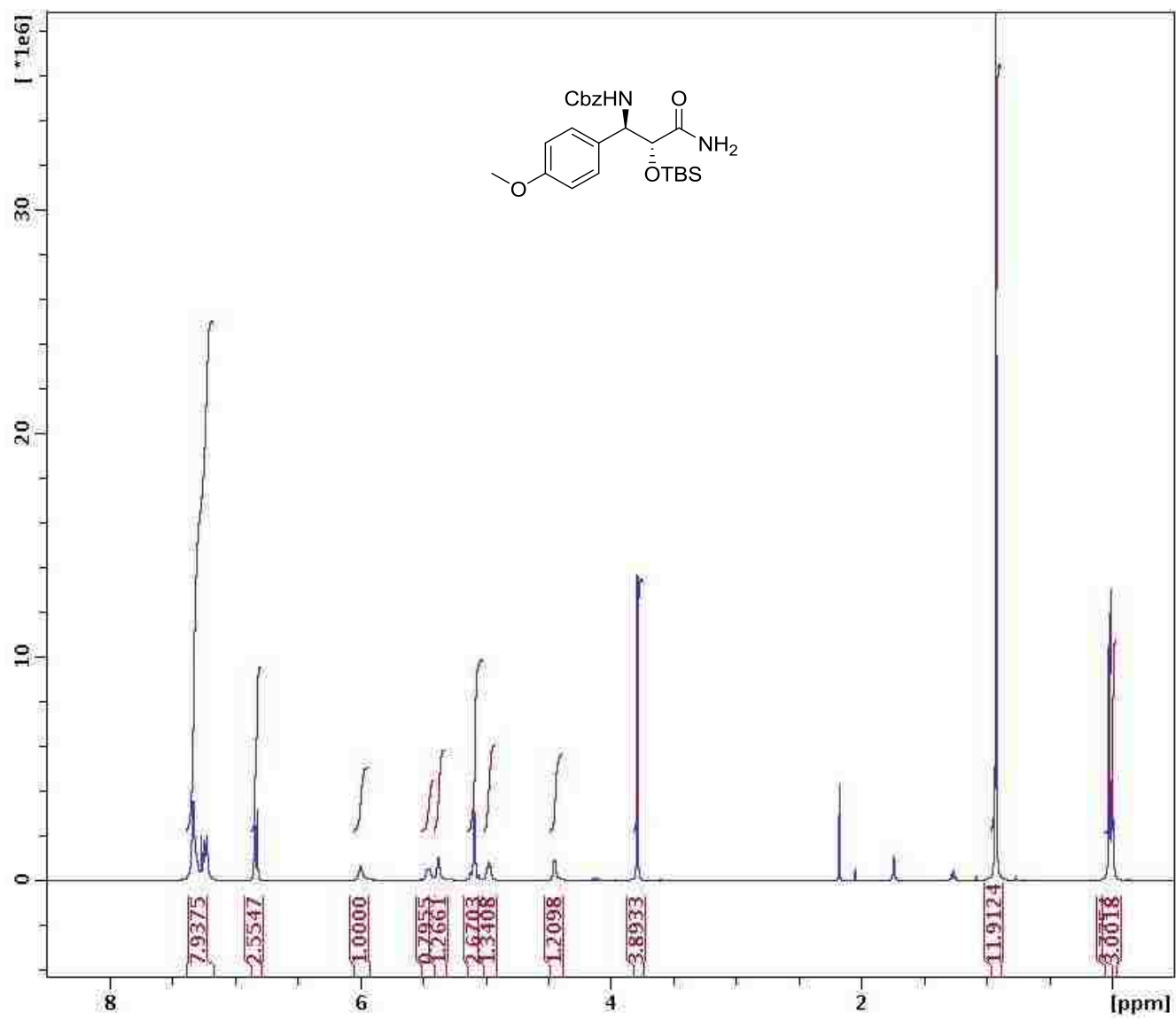
Compound **123 Precursor** - ^1H NMR in CDCl_3 at 400 MHz



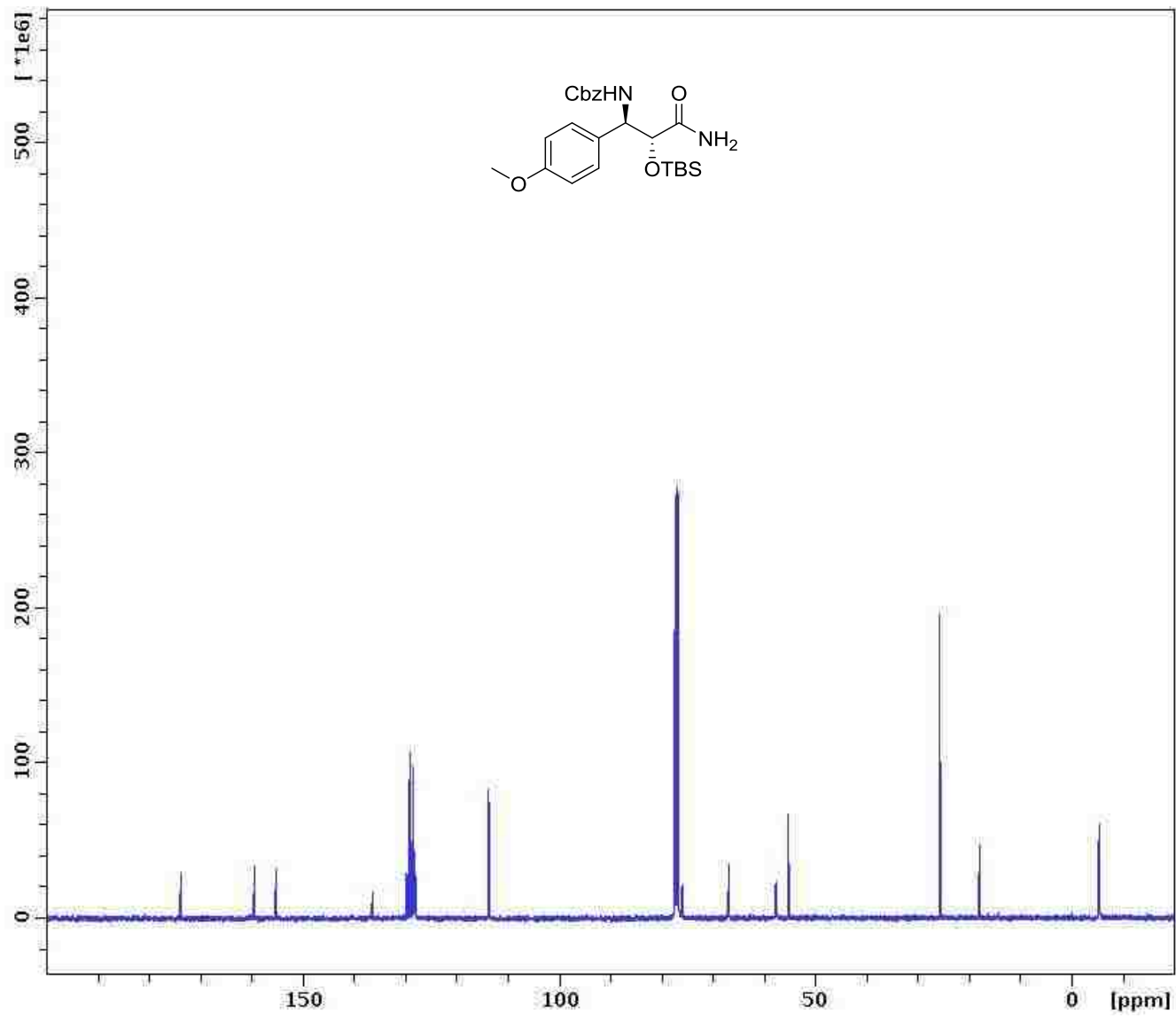
Compound **123 Precursor** – ^{13}C NMR in CDCl_3 at 100 MHz



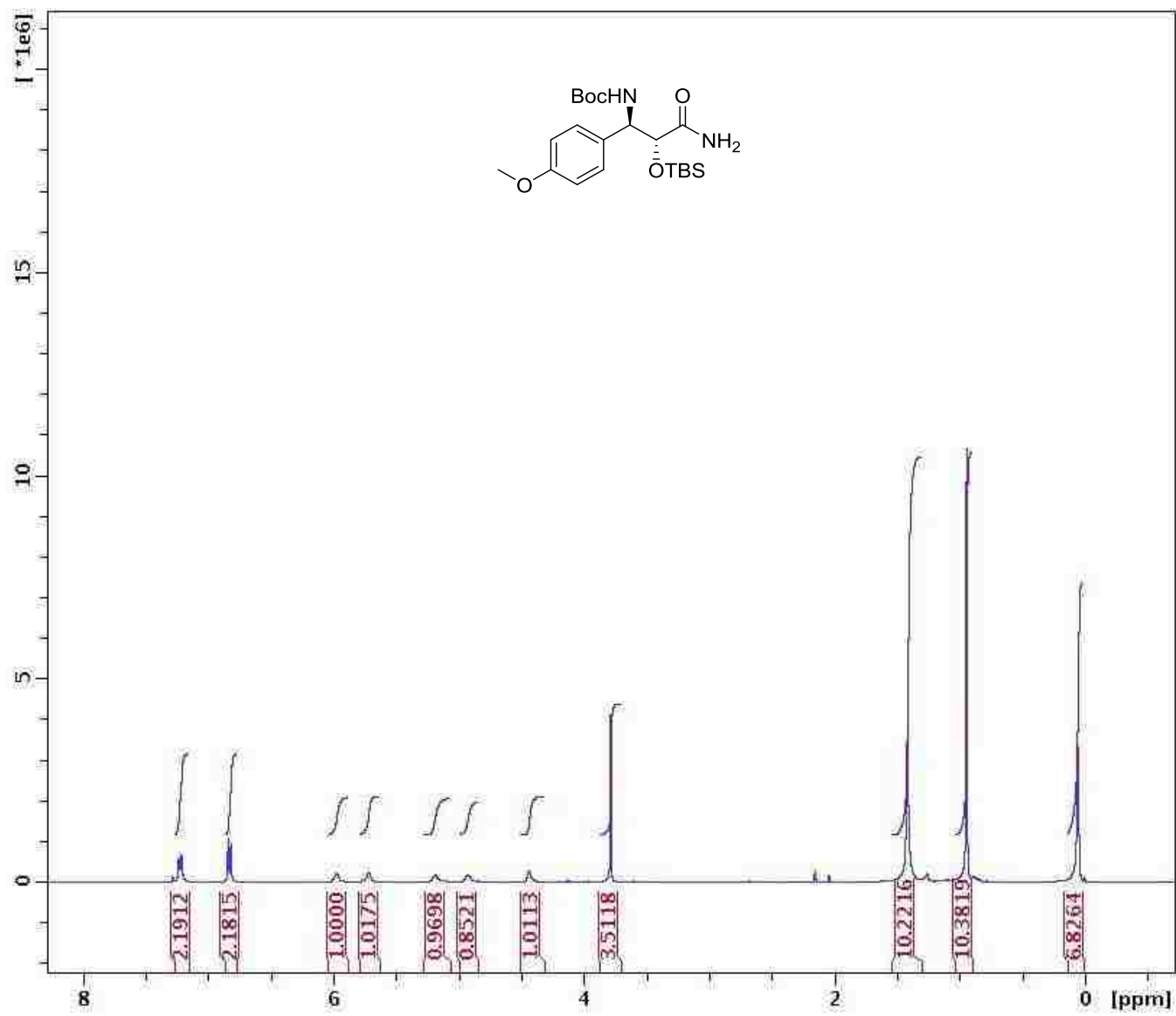
Compound **123** – ^1H NMR in CDCl_3 at 400 MHz



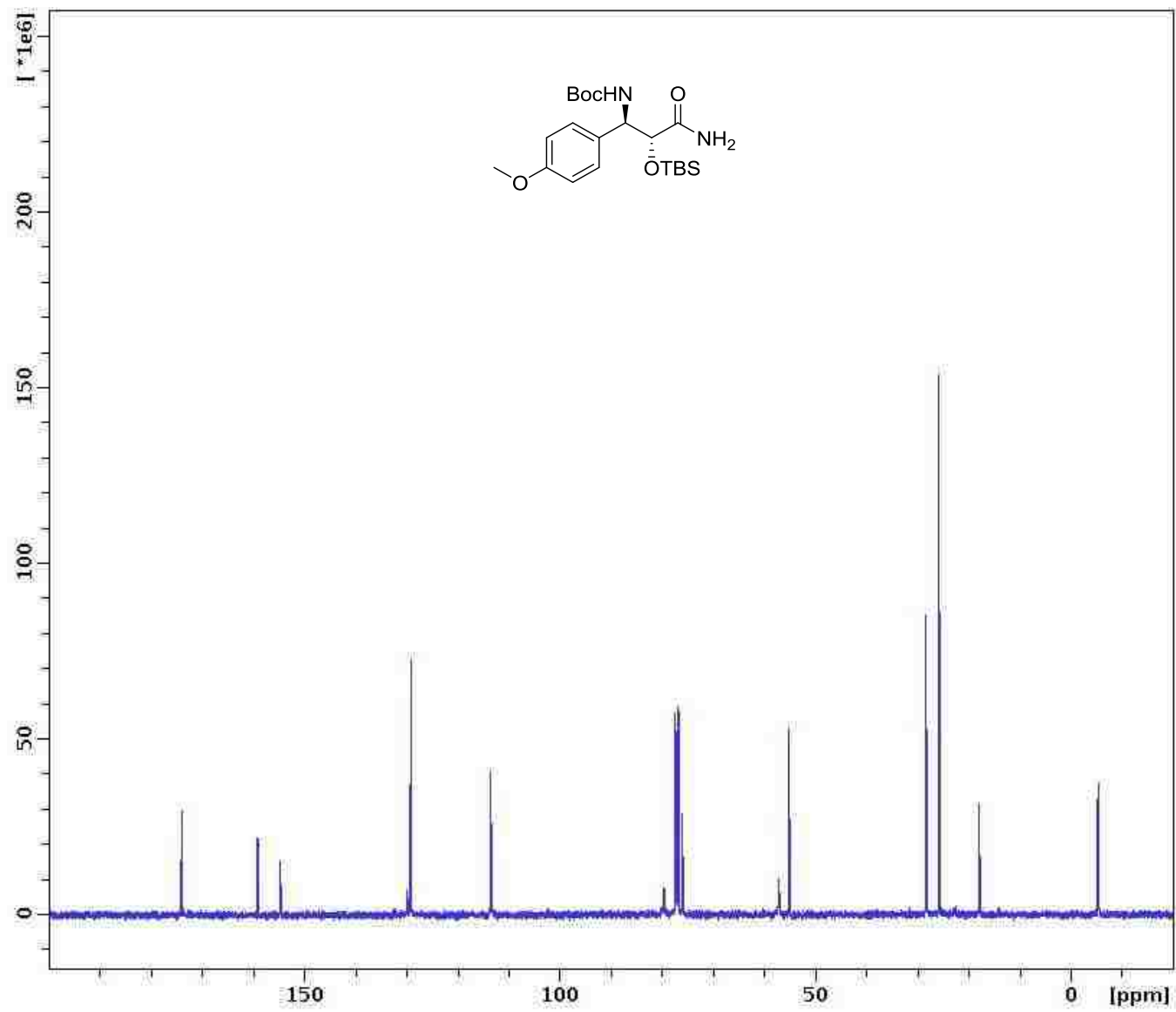
Compound **123** – ^{13}C NMR in CDCl_3 at 100 MHz



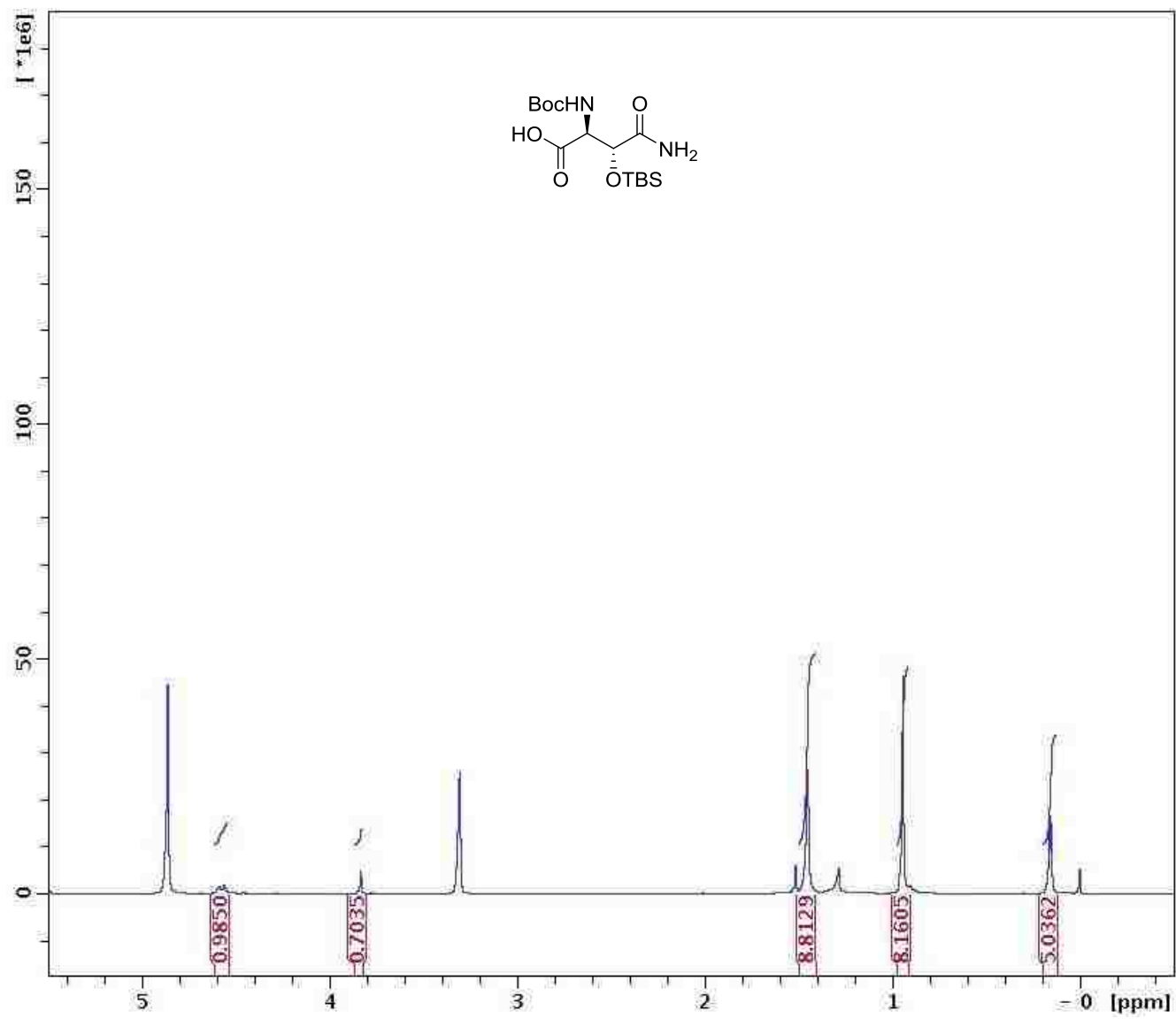
Compound **110** – ^1H NMR in CDCl_3 at 400 MHz



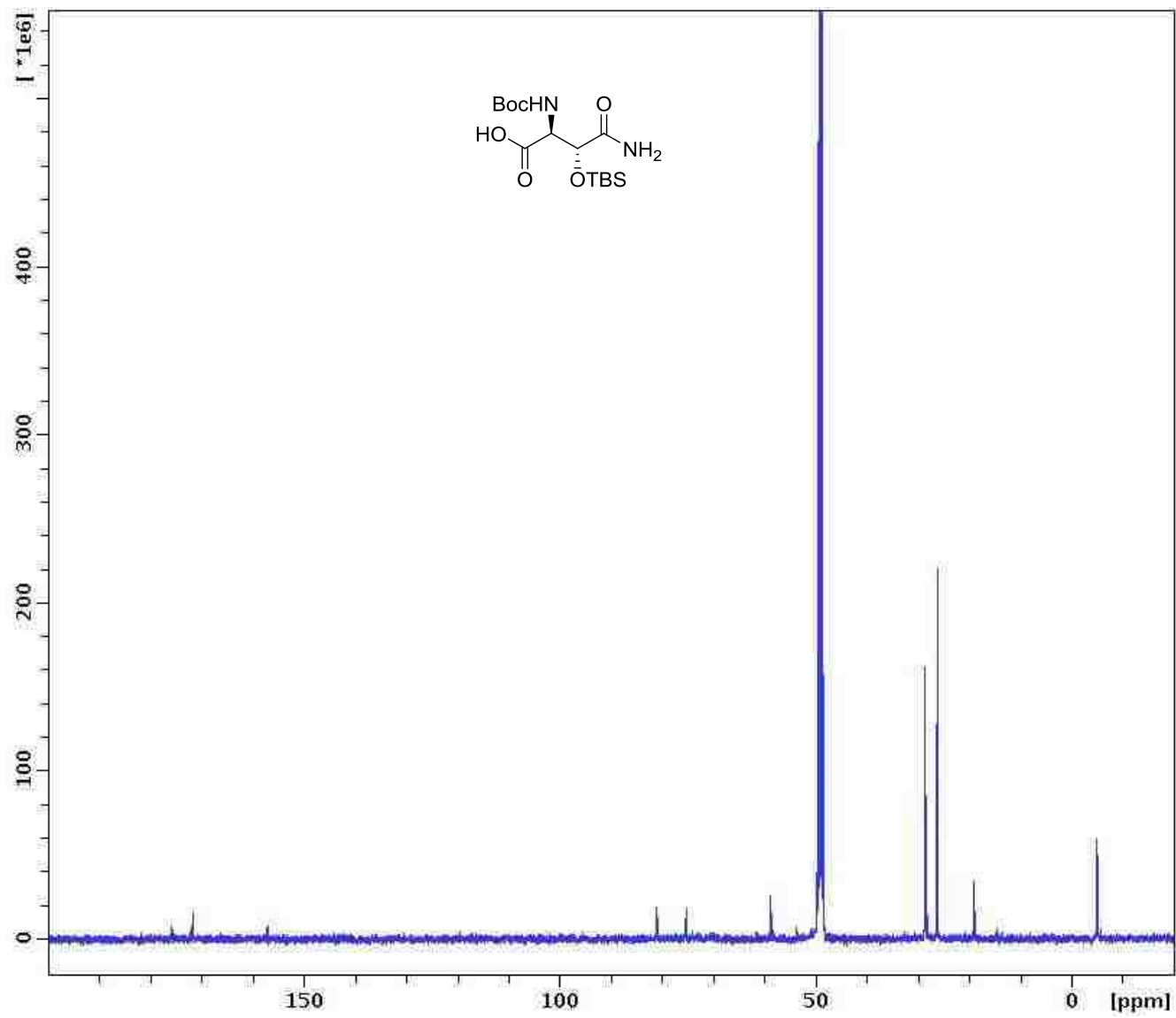
Compound **110** – ^{13}C NMR in CDCl_3 at 100 MHz



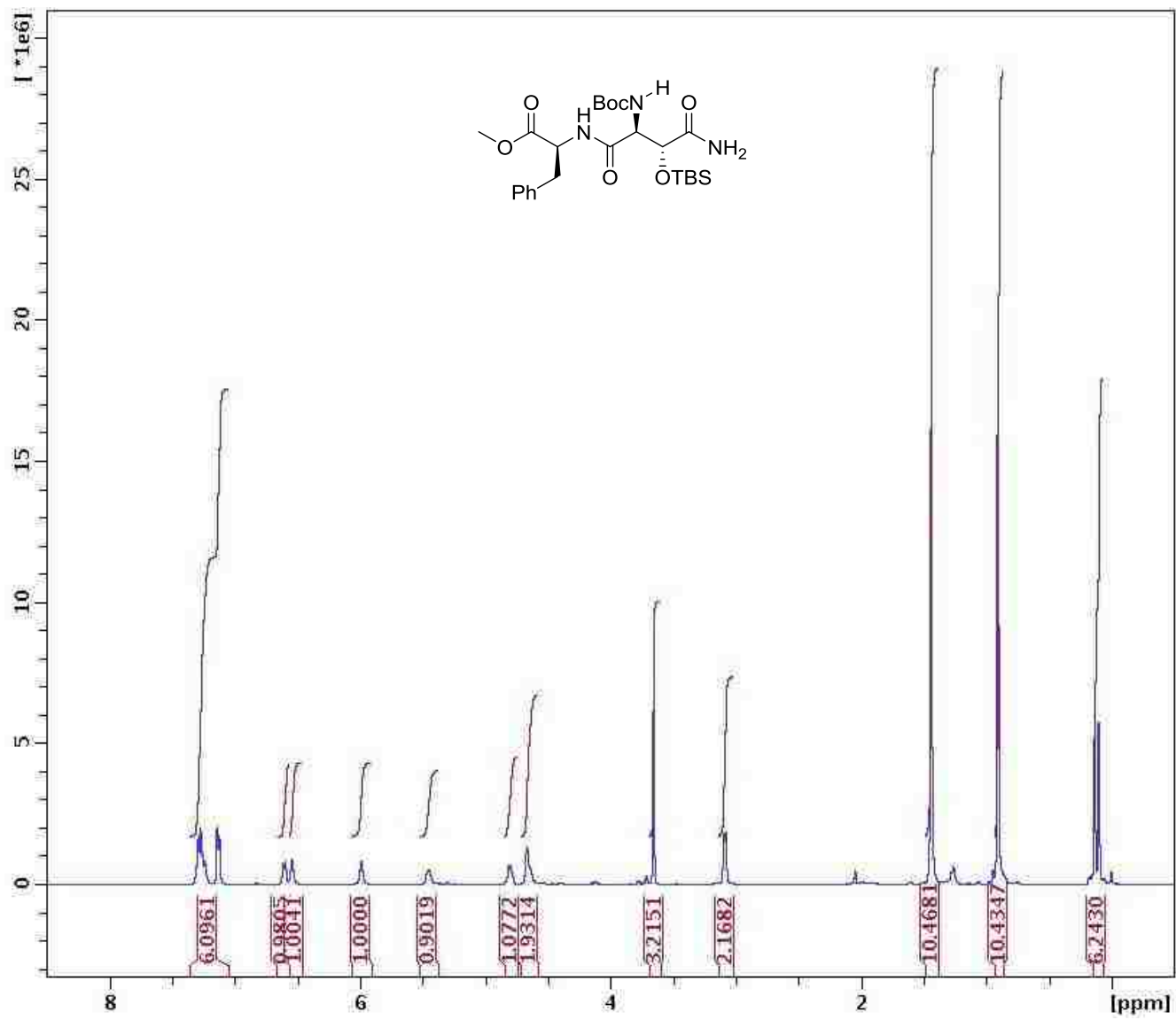
Compound (+)-44 – ^1H NMR in CD_3OD at 400 MHz



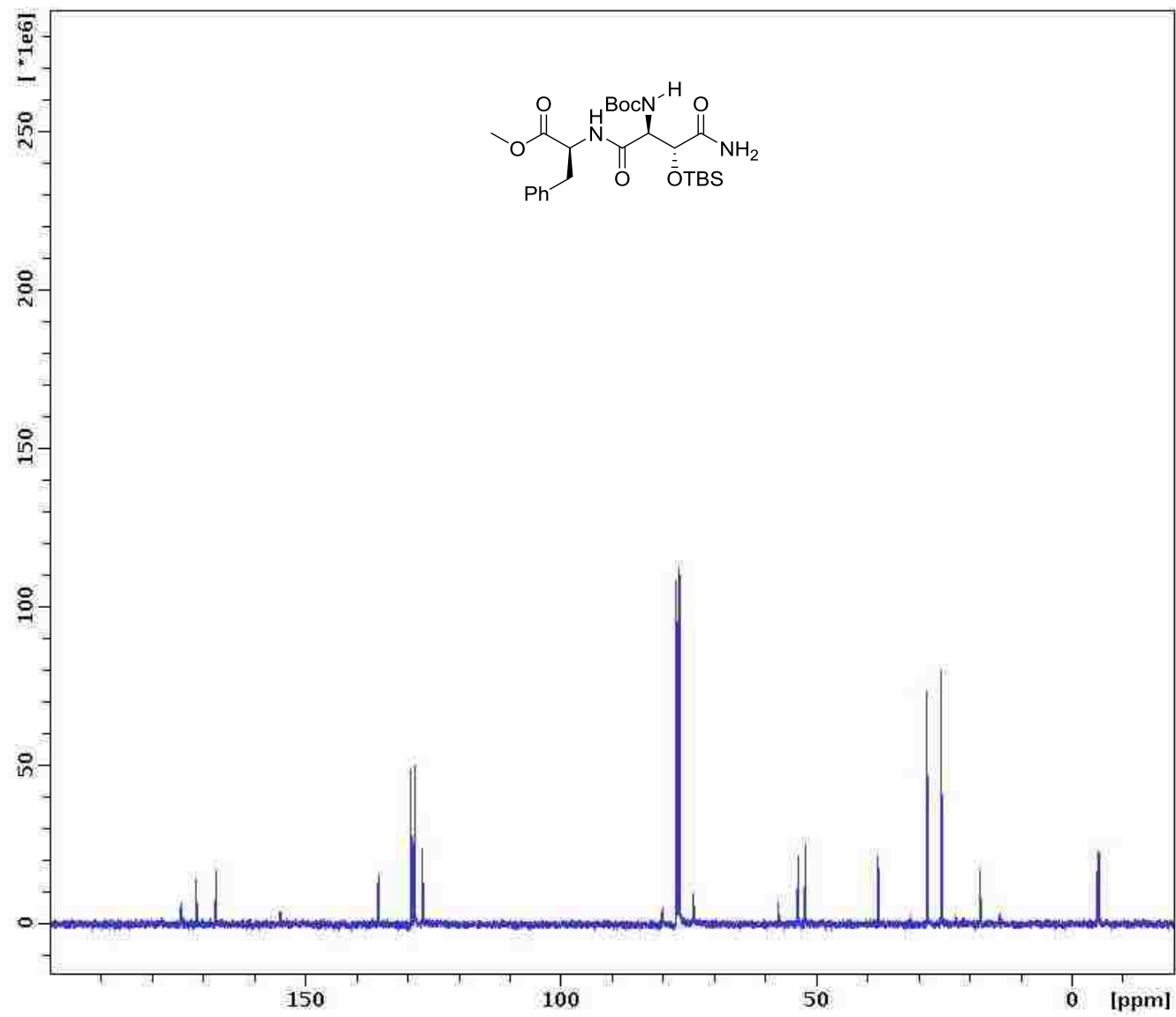
Compound (+)-**44** – ^{13}C NMR in CD_3OD at 100 MHz



Compound **129** - ^1H NMR in CDCl_3 at 400 MHz



Compound **129** – ^{13}C NMR in CDCl_3 at 100 MHz



2.11 References

1. Ambrogelly, A.; Palioura, S.; Soll, D.: Natural expansion of the genetic code. *Nat. Chem. Biol.* **2007**, *3*, 29-35.
2. Walsh, C. T.; Garneau-Tsodikova, S.; Gatto, G. J.: Protein posttranslational modifications: the chemistry of proteome diversifications. *Angew. Chem. Int. Ed.* **2005**, *44*, 7342-7372.
3. Ducho, C.: Convergence leads to success: total synthesis of the complex nonribosomal peptide polytheonamide B. *Angew. Chem. Int. Ed.* **2010**, *49*, 5034-5036.
4. Schwarzer, D.; Finking, R.; Marahiel, M. A.: Nonribosomal peptides: from genes to products. *Nat. Prod. Rep.* **2003**, *20*, 275-287.
5. Tominaga, F.; Hiwaki, C.; Maekawa, T.; Yoshida, H.: The occurrence of β -hydroxyasparagine in normal human urine. *J. Biochem.* **1963**, *53*, 227-230.
6. Okai, H.; Izumiya, N.: Resolution of amino acids. IX. Studies on the preparation of β -hydroxyasparagines and configuration of natural hydroxyasparagine. *Bull. Chem. Soc. Jpn.* **1969**, *42*, 3550-3555.
7. Stenflo, J.; Lundwall, A.; Dahlback, B.: β -Hydroxyasparagine in domains homologous to the epidermal growth factor precursor in vitamin K-dependent protein S. *Proc. Natl. Acad. Sci. USA.* **1987**, *84*, 368-372.
8. Valcarce, C.; Bjork, I.; Stenflo, J.: The epidermal growth factor precursor-a calcium-binding, β -hydroxyasparagine containing modular protein present on the surface of platelets. *Eur. J. Biochem.* **1999**, *260*, 200-207.
9. Przysiecki, C. T.; Stagers, J. E.; Ramjit, H. G.; Musson, D. G.; Stern, A. M.; Bennett, C. D.; Friedman, P. A.: Occurrence of β -hydroxylated asparagine residues in non-vitamin K-dependent proteins containing epidermal growth factor-like domains. *Proc. Natl. Acad. Sci. USA.* **1987**, *84*, 7856-7860.
10. Cho, G. Y.; Ko, S. Y.: Expanding synthetic utilities of asymmetric dihydroxylation reaction: conversion of *syn*-diols to *syn*-aminoalcohols. *J. Org. Chem.* **1999**, *64*, 8745-8747.
11. Deng, J.; Hamada, Y.; Shioiri, T.: Total synthesis of alterobactin A, a super siderophore from an open-ocean bacterium. *J. Am. Chem. Soc.* **1995**, *117*, 7824-7825.
12. Dudding, T.; Hafez, A. M.; Taggi, A. E.; Wagerle, T. R.; Lectka, T.: A catalyst that plays multiple roles: asymmetric synthesis of β -substituted aspartic acid derivatives through a four-stage, one-pot procedure. *Org. Lett.* **2002**, *4*, 387-390.

13. Okai, H.; Imamura, N.; Izumiya, N.: Resolution of amino acids. VIII. The preparation of the four optical isomers of β -hydroxyaspartic acid. *Bull. Chem. Soc. Jpn.* **1967**, *40*, 2154-2159.
14. Sendai, M.; Hashiguchi, S.; Tomimoto, M.; Kishimoto, S.; Matsuo, T.; Ochiai, M.: Synthesis of carumonam (AMA-1080) and a related compound starting from (2*R*,3*R*)-epoxysuccinic acid. *Chem. Pharm. Bull.* **1985**, *33*, 3798-3810.
15. Tohdo, K.; Hamada, Y.; Shioiri, T.: Synthetic studies of theonellamide F. *Pept. Chem.* **1992**, 7-12.
16. Tohdo, K.; Hamada, Y.; Shioiri, T.: Synthesis of the southern hemisphere of theonellamide F, a bicyclic dodecapeptide of marine origin. *Synlett.* **1994**, *4*, 247-249.
17. Hafez, A. M.; Dudding, T.; Wagerle, T. R.; Shah, M. H.; Taggi, A. E.; Lectka, T.: A multistage, one-pot procedure mediated by a single catalyst: a new approach to the catalytic asymmetric synthesis of β -amino acids. *J. Org. Chem.* **2003**, *68*, 5819-5825.
18. Guzman-Martinez, A.; VanNieuwenhze, M. S.: An operationally simple and efficient synthesis of orthogonally protected L-threo- β -hydroxyasparagine. *Synlett.* **2007**, 1513-1516.
19. Boger, D. L.; Lee, R. J.; Bounaud, P. Y.; Meier, P.: Asymmetric synthesis of orthogonally protected L-threo- β -hydroxyasparagine. *J. Org. Chem.* **2000**, *65*, 6770-6772.
20. Jiang, W.; Wanner, J.; Lee, R. J.; Bounaud, P. Y.; Boger, D. L.: Total synthesis of the ramoplanin A2 and ramoplanose aglycon. *J. Am. Chem. Soc.* **2003**, *125*, 1877-1887.
21. Cardillo, G.; Gentilucci, L.; Tolomelli, A.; Tomasini, C.: A practical method for the synthesis of β -amino α -hydroxy acids. Synthesis of enantiomerically pure hydroxyaspartic acid and isoserine. *Synlett.* **1999**, 1727-1730.
22. Wong, D.; Taylor, C. M.: Asymmetric synthesis of erythro- β -hydroxyasparagine. *Tetrahedron Lett.* **2009**, *50*, 1273-1275.
23. Li, G.; Chang, H. T.; Sharpless, K. B.: Catalytic asymmetric aminohydroxylation (AA) of olefins. *Angew. Chem. Int. Ed. Engl.* **1996**, *35*, 451-454.
24. Bodkin, J. A.; McLeod, M. D.: The Sharpless asymmetric aminohydroxylation. *J. Chem. Soc., Perkin Trans. 1.* **2002**, 2733-2746.
25. Rudolph, J.; Sennhenn, P. C.; Vlaar, C. P.; Sharpless, K. B.: Smaller substituents on nitrogen facilitate the osmium-catalyzed asymmetric aminohydroxylation. *Angew. Chem. Int. Ed. Engl.* **1996**, *35*, 2810-2813.
26. Deubel, D. V.; Frenking, G.: [3+2] versus [2+2] addition of metal oxides across C=C bonds. Reconciliation of experiment and theory. *Acc. Chem. Res.* **2003**, *36*, 645-651.

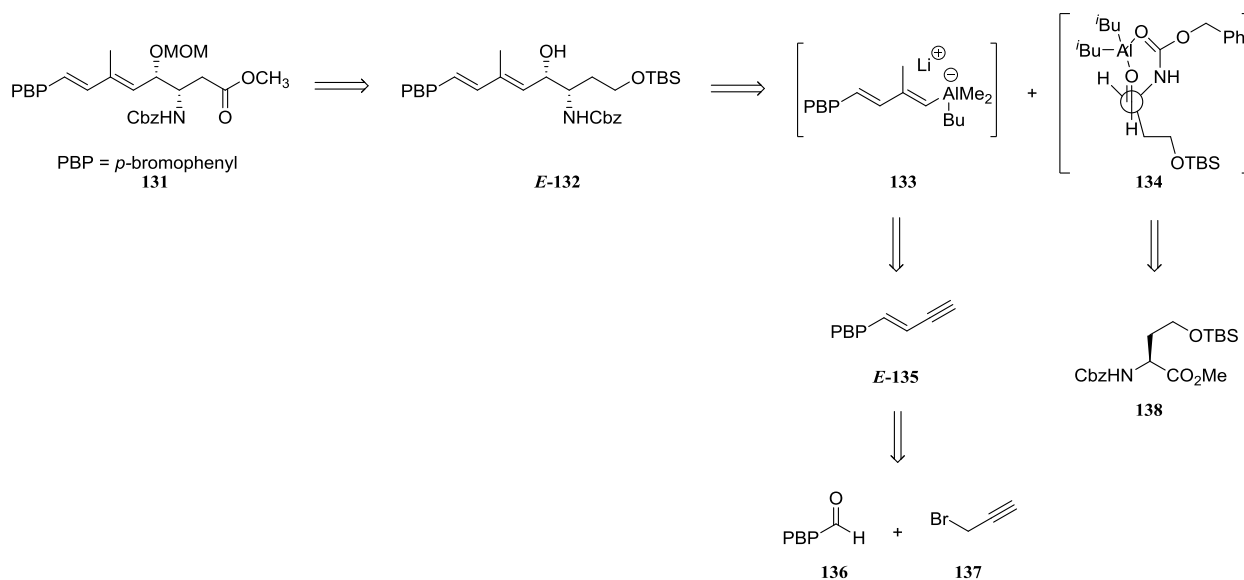
27. Corey, E. J.; Noe, M. C.; Grogan, M. J.: Experimental test of the [3+2]- and [2+2]-cycloaddition pathways for the bis-cinchona alkaloid-OsO₄ catalyzed dihydroxylation of olefins by means of C-12/C-13 kinetic isotope effects. *Tetrahedron Lett.* **1996**, *37*, 4899-4902.
28. DelMonte, A. J.; Haller, J.; Houk, K. N.; Sharpless, K. B.; Singleton, D. A.; Strassner, T.; Thomas, A. A.: Experimental and theoretical kinetic isotope effects for asymmetric dihydroxylation. Evidence supporting a rate-limiting “(3+2)” cycloaddition. *J. Am. Chem. Soc.* **1997**, *119*, 9907-9908.
29. Munz, D.; Strassner, T.: Mechanism and regioselectivity of the osmium-catalyzed aminohydroxylation of olefins. *J. Org. Chem.* **2010**, *75*, 1491-1497.
30. Andersson, M. A.; Epple, R.; Fokin, V. V.; Sharpless, K. B.: A new approach to osmium-catalyzed asymmetric dihydroxylation and aminohydroxylation of olefins. *Angew. Chem. Int. Ed.* **2002**, *41*, 472-475.
31. Wu, P.; Hilgraf, R.; Fokin, V. V.: Osmium-catalyzed olefin dihydroxylation and aminohydroxylation in the second catalytic cycle. *Adv. Synth. Catal.* **2006**, *348*, 1079-1085.
32. O'Brien, P.: Sharpless asymmetric aminohydroxylation: scope, limitations, and use in synthesis. *Angew. Chem. Int. Ed.* **1999**, *38*, 326-329.
33. Han, H.; Cho, C. W.; Janda, K. D.: A substrate-based methodology that allows the regioselective control of the catalytic aminohydroxylation reaction. *Chem. Eur. J.* **1999**, *5*, 1565-1569.
34. Tao, B.; Schlingloff, G.; Sharpless, K. B.: Reversal of regioselection in the asymmetric aminohydroxylation of cinnamates. *Tetrahedron Lett.* **1998**, *39*, 2507-2510.
35. Bodkin, J. A.; Bacskey, G. B.; McLeod, M. D.: The Sharpless asymmetric aminohydroxylation reaction: optimising ligand/substrate control of regioselectivity for the synthesis of 3- and 4-aminosugars. *Org. Biomol. Chem.* **2008**, *6*, 2544-2553.
36. Gomez-Vidal, J. A.; Forrester, M. T.; Silverman, R. B.: Mild and selective sodium azide mediated cleavage of *p*-nitrobenzoic esters. *Org. Lett.* **2001**, *3*, 2477-2479.
37. Kim, I. S.; Ji, Y. J.; Jung, Y. H.: An efficient stereoselective synthesis of (2*S*,3*S*)-3-hydroxypipelicolic acid using chlorosulfonyl isocyanate. *Tetrahedron Lett.* **2006**, *47*, 7289-7293.
38. Kim, I. S.; Ryu, C. B.; Li, Q. R.; Zee, O. P.; Jung, Y. H.: An efficient stereoselective synthesis of (+)-deoxoprosophylline. *Tetrahedron Lett.* **2007**, *48*, 6258-6261.
39. Gish, D. T.; Katsoyannis, P. G.; Hess, G. P.; Stedman, R. J.: Unexpected formation of anhydro compounds in the synthesis of asparaginy and glutaminy peptides. *J. Am. Chem. Soc.* **1956**, *78*, 5954.
40. Ressler, C.: Formation of α,γ -diaminobutyric acid from asparagine-containing peptides. *J. Am. Chem. Soc.* **1956**, *78*, 5956-5957.

41. Stammer, C.: The synthesis of two peptides containing methylene-L-asparagine. *J. Org. Chem.* **1961**, *26*, 2556–2560.
42. König, W.; Geiger, R.: A new method for synthesis of peptides-activation of carboxyl group with dicyclohexylcarbodiimide using 1-hydroxybenzotriazoles as additives. *Chem. Ber.* **1970**, *103*, 788-798.
43. Mojsov, S.; Mitchell, A. R.; Merrifield, R. B.: A quantitative evaluation of methods for coupling asparagine. *J. Org. Chem.* **1980**, *45*, 555–560.
44. Gausepohl, H.; Kraft, M.; Frank, R. W.: Asparagine coupling in fmoc solid-phase peptide-synthesis. *Int. J. Pept. Protein Res.* **1989**, *34*, 287–294.

CHAPTER 3: EARLY APPROACHES TO THE SYNTHESIS OF ABOA

3.1 Previous Synthesis of Aboa by Tohdo *et al*¹

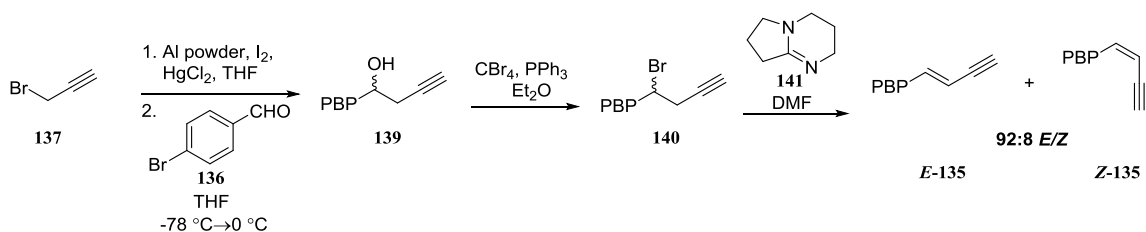
Tohdo *et al.* reported a regio- and stereoselective synthesis of Aboa in protected form in 1992. The key step in this synthesis, as highlighted in Scheme 3.1, involved stereoselective addition of the ate complex **133** to the complexed aldehyde **134**.



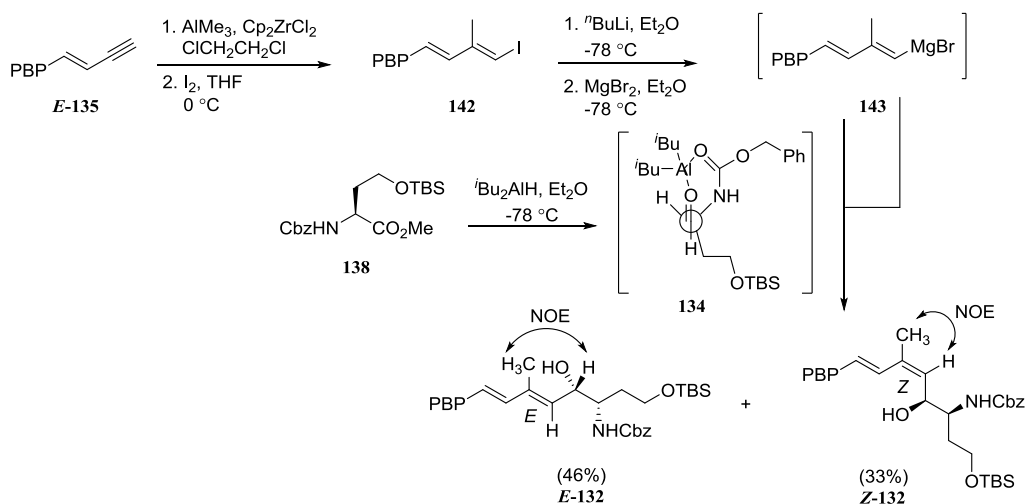
Scheme 3.1 - Tohdo *et al.*¹ Retrosynthesis of Aboa

The synthesis started with the activation of propargyl bromide **137** and its addition to *p*-bromobenzaldehyde **136** to give a benzylic alcohol intermediate **139** (Scheme 3.2). The hydroxyl group was converted to a bromide via the Appel reaction and subsequent dehydrohalogenation with 1,5-diazabicyclo[4.3.0]non-5-ene (DBN) generated a 92:8 mixture of (*E*)- and (*Z*)-enyne (*E*-**135** and *Z*-**135** respectively). Two nucleophiles were formed *in situ* from *E*-**135** (Approaches 1 and 2). The first nucleophile was generated by carbometalation of *E*-**135** with $\text{AlMe}_3/\text{Cp}_2\text{ZrCl}_2$. The resulting aluminum species reacted with iodine to produce **142**, which was subsequently converted to Grignard reagent **143**

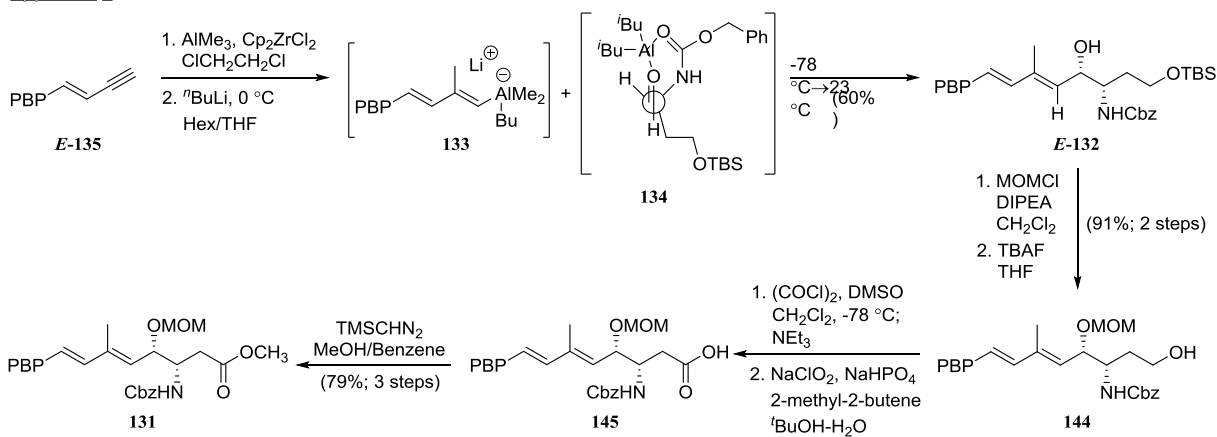
using *n*-BuLi/MgBr₂. The key step, reaction between Grignard reagent **143** and aluminum complex **134** (from homoserine derivative **138**) formed the (*E*)- and (*Z*)-dienes **132** in 46% and 33% yields, respectively. Nuclear Overhauser effect (nOe) experiments on each isomer clearly established *E* and *Z* geometry respectively.



Approach 1



Approach 2

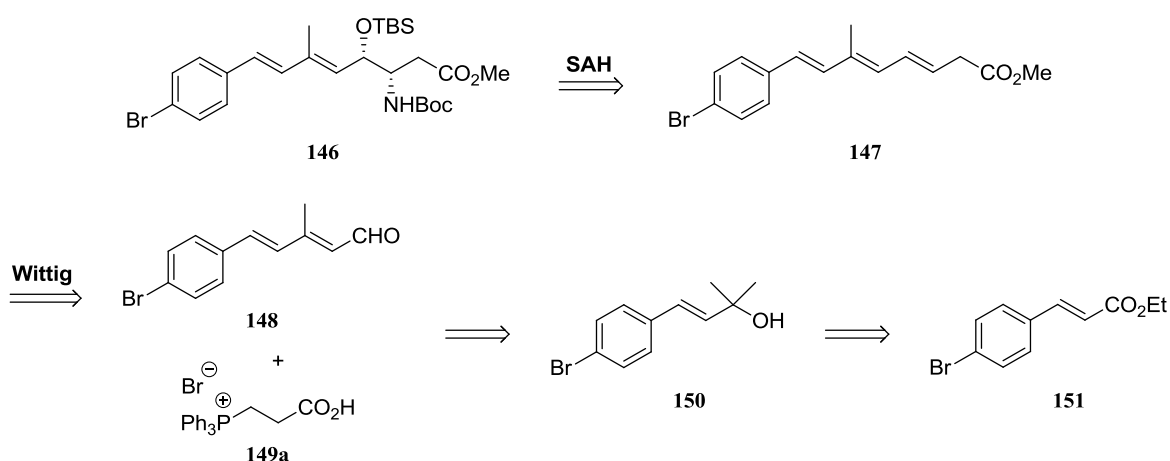


Scheme 3.2 – Synthesis of Aboa by Tohdo *et al.*¹

An improvement in the selectivity of the coupling reaction came from the use of a different nucleophile (Approach 2). Addition of $\text{AlMe}_3/\text{Cp}_2\text{ZrCl}_2/n\text{-BuLi}$ to **E-135** led to formation of ate complex **133**, which was reacted in turn, with **134** to produce the (*E*-**132**)-diene exclusively. With the framework of Aboa secured, additional functional group modifications led to a protected form of the fragment. The secondary alcohol of **E-132** was protected using MOMCl/DIPEA and the primary alcohol **144** was revealed using TBAF. The full oxidation of **144** required two steps: Swern conditions to give the aldehyde and Pinnick oxidation to afford the carboxylic acid **145**. $\text{TMSCHN}_2/\text{MeOH}$ effectively generated the methyl ester derivative **131**.

3.2 A Challenging Application of the Sharpless Aminohydroxylation Reaction

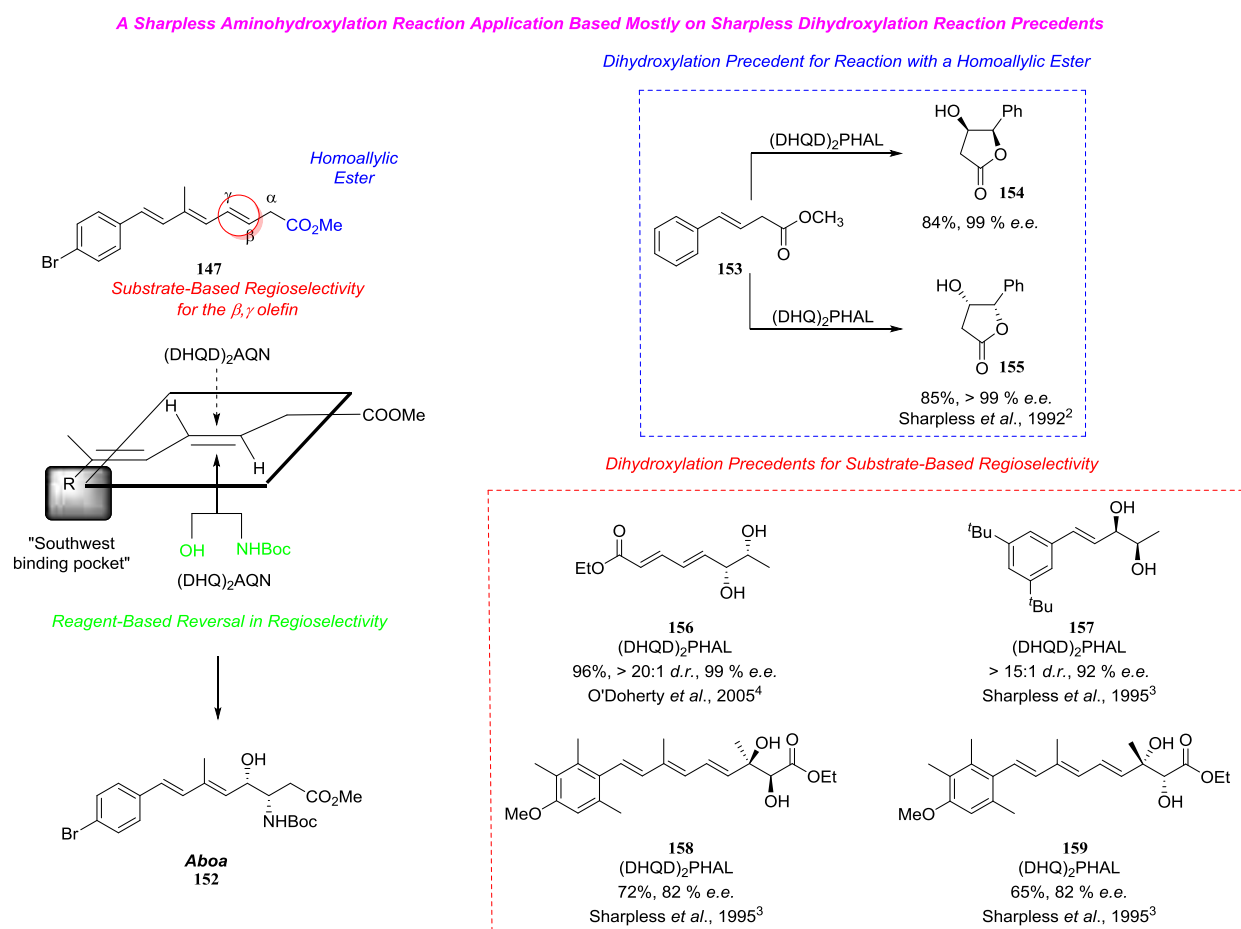
Our original approach to the synthesis of Aboa relied again on Sharpless' aminohydroxylation (SAH) chemistry (Scheme 3.3). Retrosynthetically, the target compound can be accessed via a regioselective and stereoselective SAH reaction of triene **147**. Compound **147** can be generated from a Wittig reaction between phosphonium ylide **149a** and aldehyde **148**. The synthesis of aldehyde **148** starts with double Grignard addition of MeMgI to α,β -unsaturated ester **151** followed by a Vilsmeier-type reaction (POCl_3/DMF) of the resulting allylic alcohol **150**.



Scheme 3.3 – The Original Retrosynthetic Analysis

There are three nontrivial issues (Scheme 3.4) that make this application of the SAH reaction more challenging than that utilized in the *e*HyAsn substrate (Chapter 2).

1. The ester is homoallylic rather than allylic. Homoallylic esters have been *dihydroxylated* in high yield and high *ee* (blue in Scheme 3.4).²
2. The oxidation needs to be regioselective for the β,γ -olefin of the substrate. Scheme 3.4 (red) illustrates that where multiple double bonds are present in a substrate, the Sharpless asymmetric *dihydroxylation* (SAD) occurs in a sense that minimizes disruption to conjugation.^{3,4} If this trend holds for the SAH reaction, it should work in our favor leading to functionalization of the β,γ -olefin of ester **147**.



Scheme 3.4 – Challenges in the Aminohydroxylation Reaction of **147** (Left) with Selected Dihydroxylation Reaction Precedents (Right)

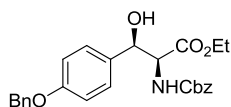
3. A reversal in regioselectivity is required in the sense that the amino group is closer to the electron-withdrawing group than the hydroxyl group is (green in Scheme 3.4). Recall, Sharpless and co-workers determined that use of the AQN ligand core in the SAH reaction of cinnamates reverses the regiochemical outcome of the previously known PHAL ligand system.⁵

3.3 The Regioreversed Sharpless Aminohydroxylation Reaction

The greatest limitation to the widespread application of the SAH reaction continues to be regioselectivity. The factors responsible for regioselectivity using cinnamate-type reaction substrates have been investigated by McLeod and co-workers.⁶ Recall that the opposite regioselectivity provided using the AQN and PHAL ligands is a consequence of a change in substrate orientation with respect to the catalyst (§2.7). The catalyst contains two ligand-binding domains that undergo attractive interactions with the substrates. Other substrate classes have not been subjected to such detailed investigations.

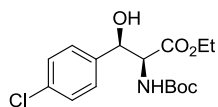
Publications citing the seminal work of Sharpless and co-workers⁵ have reported mixed results.⁷⁻
²⁰ Some of the examples that have worked reasonably well are highlighted in Figure 3.1 and generally fall into three categories: cinnamates **160-166**,⁷⁻¹⁴ β -(3-indolyl)acrylates **167-170**,¹⁵⁻¹⁸ and aliphatic substrates **171-172**.^{19,20} Some common features to all categories include the α,β -unsaturated ester containing a 1,2-*trans*-disubstituted olefin. While both cinnamate and β -(3-indolyl)acrylate reactions employ methyl/ethyl ester derivatives, they differ in the identity of the other substituent. Cinnamate reactions, by definition, consist of a phenyl group while β -(3-indolyl)acrylate reactions comprise of a indole group (cyclomarin analogs). The latter have been popular targets since the cyclic antibiotic heptapeptides, cyclomarins A-D, were recently found to target a protein in *Mycobacterium tuberculosis* (*Mtb*).²¹ The natural product binds the regulatory subunit ClpC of the Clp complex in *Mtb* resulting in enhanced proteolysis and cell death. Much of the initial work regarding the regioreversed SAH reaction falls into the aliphatic category.

Cinnamate-Derived Products



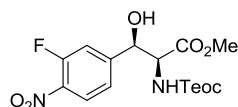
160

Cbz-NH₂, (DHQD)₂AQN
45%, 87 % e.e.
Nicolaou *et al.*, 1998¹⁴



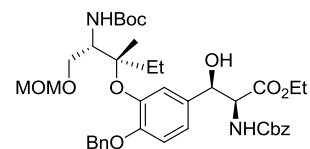
161

Boc-NH₂, (DHQD)₂AQN
48%, 95 % e.e.
Pearson *et al.*, 2001¹²



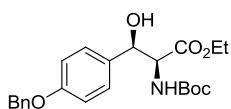
162

Teoc-NH₂, (DHQD)₂AQN
50%, 89 % e.e.
Joullié *et al.*, 2001¹³



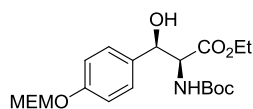
163

Cbz-NH₂, (DHQD)₂AQN
58%, 5:1 Regioselectivity, 91 % d.s.
Joullié *et al.*, 2002¹¹



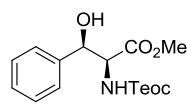
164

Cbz-NH₂, (DHQD)₂AQN
40-45%, >100:1 *syn/anti*, 89 % e.e.
After H₂, Pd/C, (Boc)₂O
Tao *et al.*, 2003¹⁰



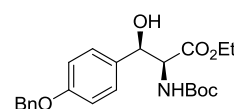
165

Boc-NH₂, (DHQD)₂AQN
85%, 7:1 Regioselectivity, 89 % e.e.
Konno *et al.*, 2007⁸



166

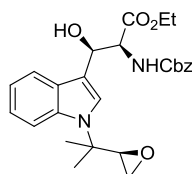
Teoc-NH₂, (DHQD)₂AQN
60%, > 98 % e.e.
Guzman-Martinez *et al.*, 2007⁹



164

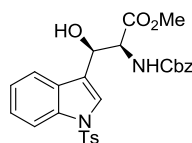
Boc-NH₂, (DHQD)₂AQN
45%, 92 % e.e.
Dethe *et al.*, 2011⁷

β-(3-Indolyl)acrylate-Derived Products



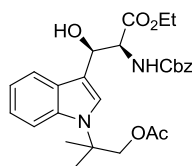
167

Cbz-NH₂, (DHQD)₂AQN
36%, 95:5 *d.r.*
Sugiyama *et al.*, 2002¹⁸



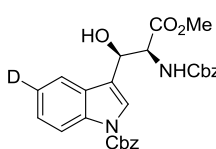
168

Cbz-NH₂, (DHQD)₂AQN
69%, 10:1 Regioselectivity, > 99 % e.e.
Feldman *et al.*, 2004¹⁷



169

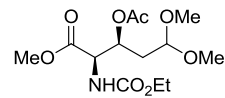
Cbz-NH₂, (DHQD)₂AQN
44%, 86 % e.e.
Wen *et al.*, 2004¹⁶



170

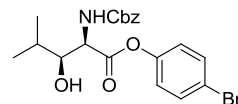
Cbz-NH₂, (DHQD)₂AQN
45%, 78 % e.e.
Koketsu *et al.*, 2006¹⁵

Products from Aliphatic Olefins



171

EtOCO-NH₂, (DHQ)₂AQN
57%, 11:1 Regioselectivity, 89 % e.e.
After Ac₂O, NEt₃, DMAP
Davey *et al.*, 2000¹⁹



172

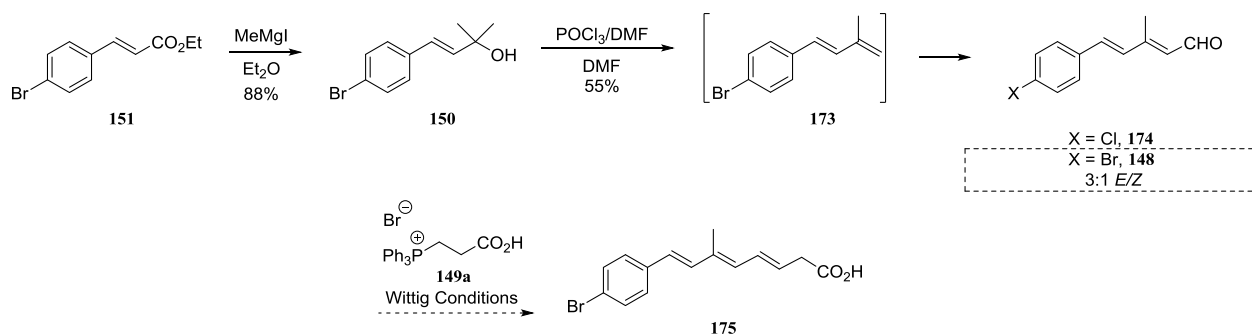
Cbz-NH₂, (DHQ)₂AQN
60%, 7:1 Regioselectivity, 87 % e.e.
Panek *et al.*, 1999²⁰

Figure 3.1 – Representative Products of the Regioreversed SAH

According to Figure 3.1, all three reaction classes provided the desired products in moderate yields with high regio- and enantioselectivities. Although a wide range of nitrogen protecting groups²² is available for this reaction (sulfonamides, carbamates, amides, etc), the examples presented all utilize popular carbamates. A variety of aromatic substituents are well tolerated by the regioreversed SAH reaction.⁶ Substrates containing electron-rich (**160**, **163**, **164** and **165**) and electron-deficient (**161** and **162**) substituents gave comparable results. When utilized in target-oriented synthesis, the SAH reaction is typically employed in the early stages (**160**, **161**, **164**, **166**, **168** and **169**). The advanced intermediate **163** *en route* to ustiloxin D by Joullié and co-workers¹¹ represents the most complex example. The near exclusive use of the (DHQD)₂AQN ligand system in recent years is also noteworthy. In spite of the results of the regioreversed SAH in Figure 3.1, many challenges remain before the SAH reaction gains the popularity of its predecessors (SAD and SAE) and can be reliably implemented in synthesis.

3.4 Attempted Synthesis of Triene **175**, an Aboa Precursor

Our synthesis of aldehyde **148** (Scheme 3.5) relied upon the work of Reddy and Rao, who reported the formation of the analogous 4'-chlorinated aldehyde **174** in 86% yield, over two steps.²³ As reported, double addition of methyl magnesium iodide to (*E*)-ethyl 3-(4-bromophenyl)acrylate afforded tertiary alcohol **150** in high yield.



Scheme 3.5 – Attempted Synthesis of **175**

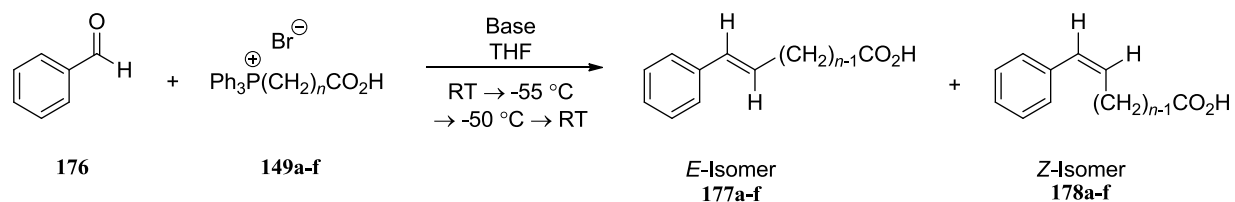
The second step, conducted under Vilsmeier conditions, was problematic in our hands. We isolated intermediate diene **173**, signaling that the first step in this reaction involves dehydration of the tertiary alcohol. We believe that two equivalents of the Vilsmeier reagent are required: one to effect the dehydration and the second to formylate. Integration of the –CHO peaks (^1H NMR) of the crude reaction mixture indicated a 3:1 mixture of *E/Z* isomers. These diastereomers are separable by careful flash chromatography.

The spectral data (^1H NMR and ^{13}C NMR) for the *E*-isomer was in excellent agreement with the phenyl analog of aldehyde **148** as put forth by the Helquist and Wojtkielewicz research groups.^{24,25} This included the –CHO peak in the ^1H NMR at 10.17 ppm with a coupling constant of 8.0 Hz and the corresponding peak in the ^{13}C NMR at 191.1 ppm. Time spent optimizing this reaction was prolonged due to two contributing factors. First, there was confusion about reaction stoichiometry as Reddy and Rao recommended 1.3 equivalents of Vilsmeier reagent with respect to the starting alcohol.²³ We proved that the first equivalent of Vilsmeier reagent only completes the dehydration sequence (formation of **173**) while a second equivalent is required to introduce the aldehyde. Compounding this confusion, we became aware that the purity of POCl_3 from Sigma-Aldrich had been questionable during this time. Retroactively, it was impossible to estimate the content of active POCl_3 participating in the early reactions and obtain a reproducible, moderate yield. With 2.5 equivalents of good POCl_3 , we were able to isolate *E*-aldehyde **148** in 40% yield.

Next, we required triene **175** via a Wittig reaction between aldehyde **148** and phosphonium salt **149a** (commercially available). (2-Carboxyethyl)triphenylphosphonium bromide and related carboxy ylides, varying only in methylene chain length, were reacted with benzaldehyde in the presence of a series of HMDS bases (Li^+ , K^+ and Na^+) by Maryanoff *et al.* to examine trends in *E/Z* stereoselectivity (Table 3.1).²⁶ Carboxy ylides of short chain length (up to four methylene units **149a-c**) used in conjunction with benzaldehyde and $\text{LiN}(\text{SiMe}_3)_2$ (2.1 equivalents) generated products with 9:1 *E/Z* selectivity. The same reaction conditions applied to carboxy ylides with longer methylene chain lengths (**149e-f**) resulted in

reduced *E*-stereoselectivity to the point where the *Z*-isomer was favored. Also, at longer chain lengths, reactions with the K^+ cation led to the most dramatic decrease in *E*-stereoselectivity whereas the lithium counterion gave the best results in terms of *E*-stereoselectivity. Curiously, no yield was reported for the reaction utilizing **149a** specifically. Our attempts to conduct the Wittig reaction between **176** and **149a** under the Maryanoff conditions resulted in decomposition and no isolable products.

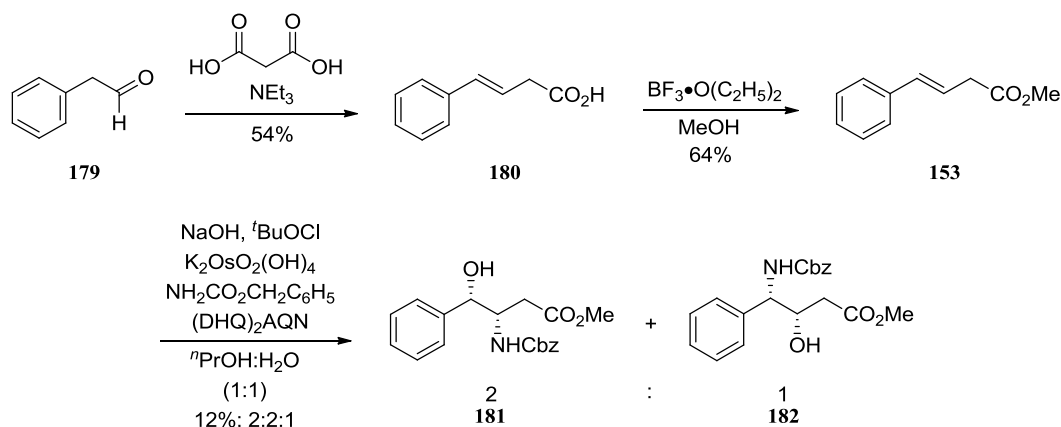
Table 3.1 – Wittig Reaction Between Benzaldehyde and Carboxy Ylides Varying in Methylene Chain Length to Examine Trends in *E/Z* Stereoselectivity as Performed by Maryanoff *et al.*²⁶



Entry	<i>n</i>	Base	<i>E/Z</i> Ratio	Isolated Yield, %
1	2	LiHMDS	90:10	-
2	3	LiHMDS	93:7	61
3	4	LiHMDS	87:13	74
4	4	NaHMDS	79:21	65
5	4	KHMDS	69:31	44
6	6	LiHMDS	69:31	48
7	7	LiHMDS	37:63	28
8	10	LiHMDS	40:60	-

3.5 A Model System for the Regioreversed SAH

Model studies for the SAH reaction were conducted on β,γ -unsaturated methyl ester **153** (Scheme 3.6). This model system removed the substrate-based regioselectivity issue while maintaining the homoallylic ester functionality. Compound **153** was readily synthesized in two steps from commercially available phenylacetaldehyde. Malonic acid and phenylacetaldehyde (**179**) underwent the Linstead modification of the Knoevenagel condensation^{27,28} to produce β,γ -unsaturated acid **180**. Formation of the methyl ester was accomplished using boron trifluoride diethyl etherate in methanol.²⁹ Experiments for the key reaction were carried out under standard carbamate conditions (3 equivalents of benzyl carbamate/NaOH/^tBuOCl) using the (DHQ)₂AQN ligand.⁵ We isolated two compounds from the product mixture by normal phase silica HPLC. They were identified as desired product **181** and regioisomer **182** in a 2:1 ratio with a combined yield of 12%. Enantiomeric purities were not determined.



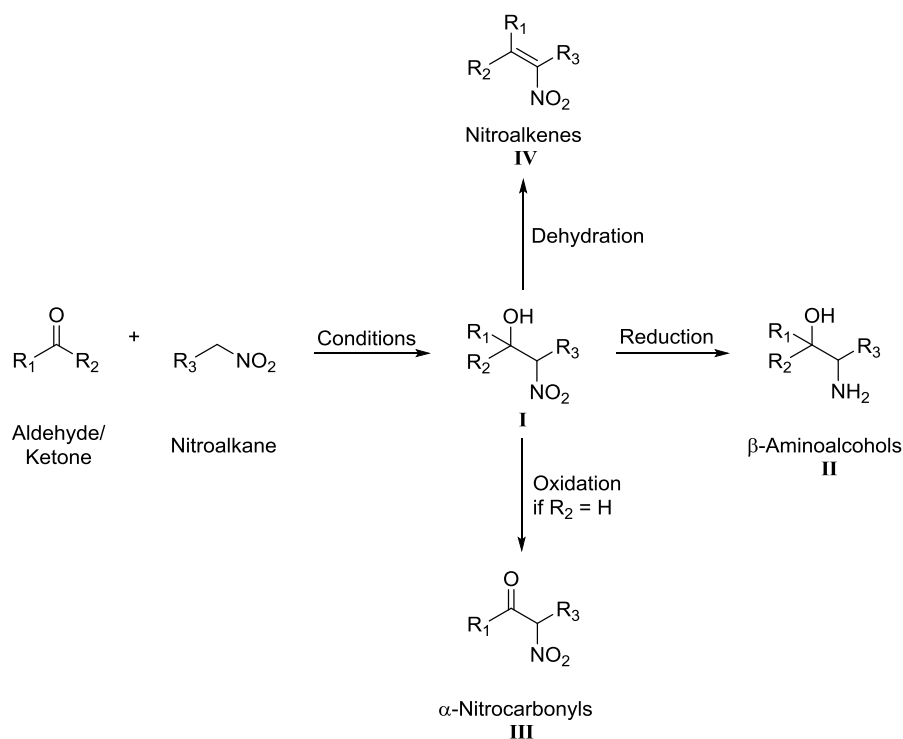
Scheme 3.6 - Application of the Regioreversed SAH on a Model Compound

We decided to abandon the regioreversed SAH route to Aboa for several reasons. Firstly, there was our inability to synthesize **175** from a seemingly trivial Wittig reaction between **148** and **149a**. The model system SAH reaction did not produce synthetically useful amounts of desired amino alcohol and its lactone counterpart. It was not clear how much this reaction could be optimized. Typical chemical yields

for much simpler regioreversed SAH reactions are between 45%-55% with varying levels of enantioselectivity.

3.6 The Nitroaldol Reaction

While attending a presentation on recent advances in the nitroaldol reaction by Shibasaki,³⁰ it dawned on us that aldehyde **148** could possibly be used in an nitroaldol reaction to access a precursor to Aboa. The nitroaldol reaction, which enables the formation of β -nitroalcohols **I** has been known for over a century.³¹⁻³³ Additional transformations involving the newly generated β -nitro derivatives such as reduction, oxidation and dehydration leads to β -aminoalcohols **II**, α -nitrocarbonyls **III** and nitroalkenes **IV**, useful moieties in organic synthesis (Scheme 3.7).

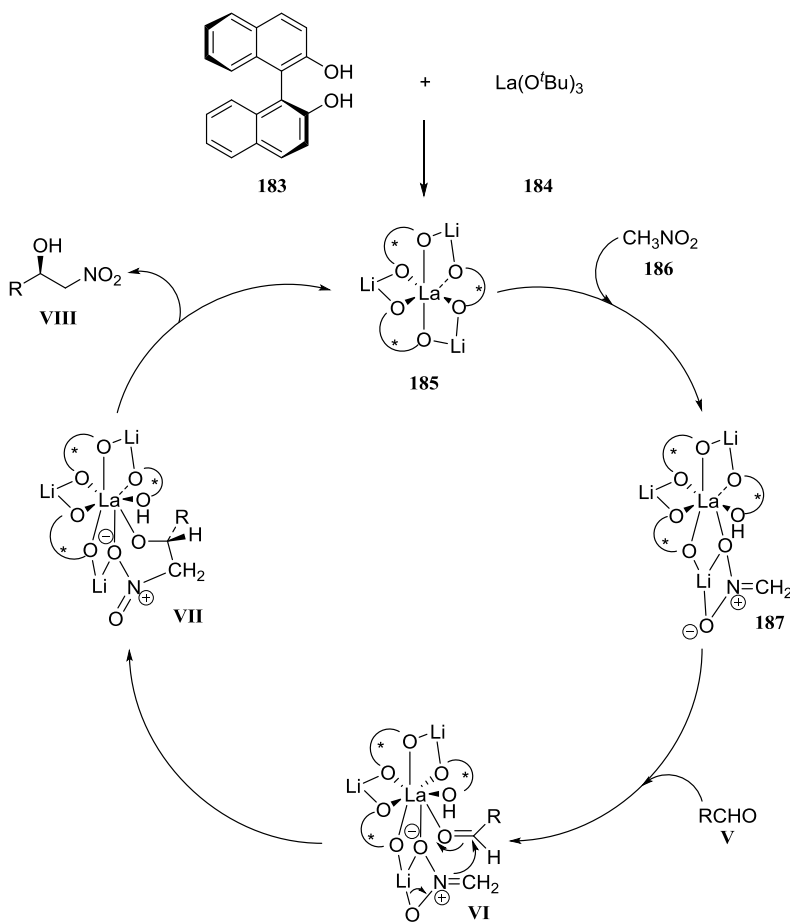


Scheme 3.7 – Nitroaldol Reaction Products are Precursors to Useful Moieties in Organic Synthesis

Nitroaldol reactions are promoted/catalyzed by a wide range of conditions. Some of these conditions include quaternary ammonium salts, organic bases and inorganic bases in solvent and

solventless protocols.³⁴⁻³⁶ The conditions utilized depend on the existing functionality and substrate solubility.

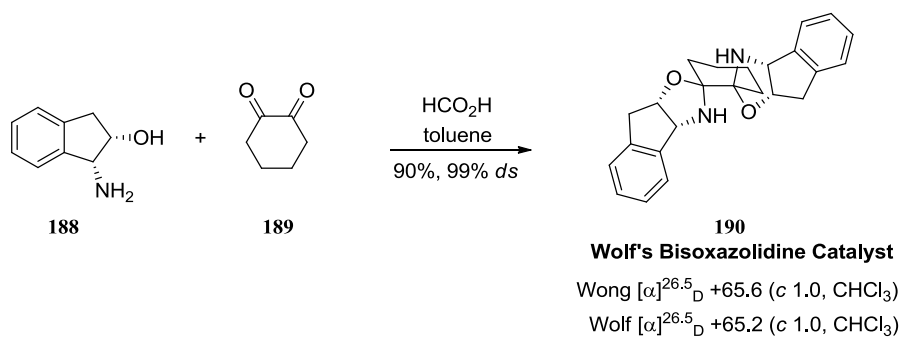
The first asymmetric nitroaldol reaction, reported by Shibasaki *et al.* in 1992, employed a chiral catalyst generated from (*S*)-(-)-binaphthol **183** and La(O^{*t*}Bu)₃ **184**.³⁷ The use of aliphatic aldehydes in conjunction with the asymmetric catalyst/nitromethane/THF generated (*R*)-nitroalcohols with good enantioselectivity (73-90% *ee*). The mechanistic details are not fully understood but an aryloxide oxygen of the chiral catalyst **185** deprotonates nitromethane **186** to form the lithium nitronate **187** (Scheme 3.8).³⁸ Aldehyde **V** coordination to the lanthanide center activates it toward attack by the nitronate. The alkoxide intermediate is then protonated to produce the alcohol product **VIII** and regenerate the catalyst **185**.



Scheme 3.8 – Walsh and Kowzlowski's Proposed Mechanism³⁸ for Shibasaki's Li₃(THF)_{*n*}(BINOLate)₃La(OH)₂ Catalyzed Nitroaldol Reaction. Copyright 2008, University Science Books, reprinted with permission (p. 255).

3.7 Wolf's Asymmetric Nitroaldol Reaction

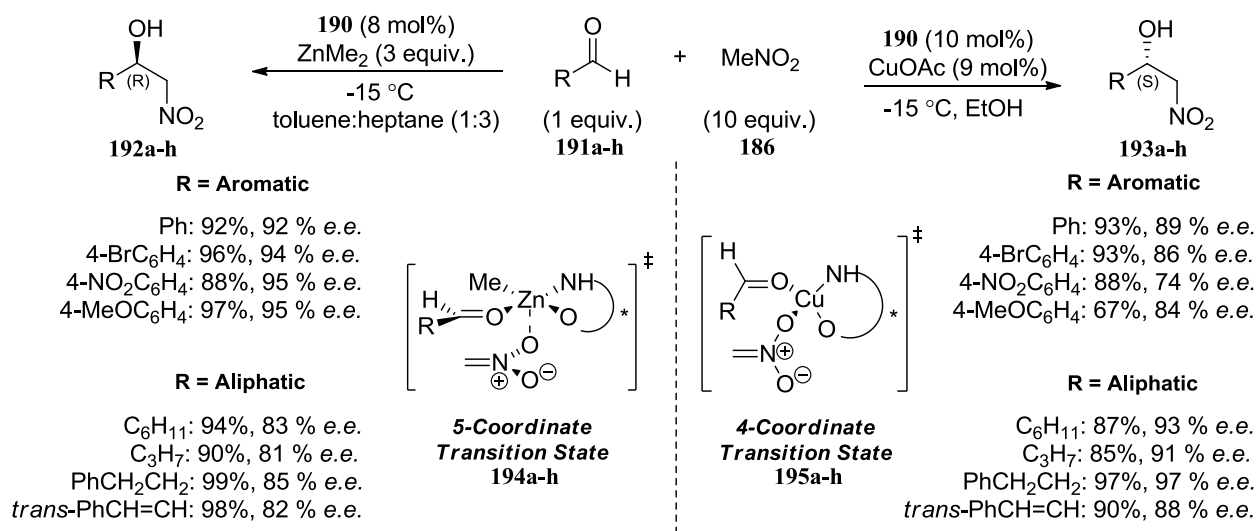
Shibasaki's chiral catalyst is based on BINOL, a C_2 -symmetric ligand. The development of asymmetric catalysts derived from C_2 -symmetric bisoxazolidines is still in its infancy. Wolf and co-workers reported the first chiral bisoxazolidine catalyst **190** from acid-promoted reaction of (1*R*,2*S*)-*cis*-1-amino-2-indanol with 1,2-cyclohexanedione in 2006 (Scheme 3.9).³⁹ The bisoxazolidine **190**, acquired in 90% yield and excellent diastereoselectivity (99% *ds*), was reported to catalyze the asymmetric nitroaldol reaction of aliphatic and aromatic aldehydes in 2008 (*vide infra*).⁴⁰ The (*S,S*)-*N,O*-"diketal" has an average separation of 2.35 Å between the oxygen and nitrogen atoms as determined by crystallographic analysis. This rigid ligand structure facilitates bidentate coordination to metal ions and organometallic compounds. Currently, this chiral catalyst is available from Strem Chemicals Inc. (catalog number 07-0488, \$80 for 250 mg). In addition to asymmetric nitroaldol reactions, application of **190** has been demonstrated in dimethylzinc-mediated enantioselective alkynylation of aldehydes,³⁹ alkylation of aldehydes with $ZnMe_2/ZnEt_2$ ⁴¹ and asymmetric Friedel-Crafts and Reformatsky⁴² reactions.



Scheme 3.9 – Synthesis and Physical Characteristics of Wolf's Bisoxazolidine Catalyst

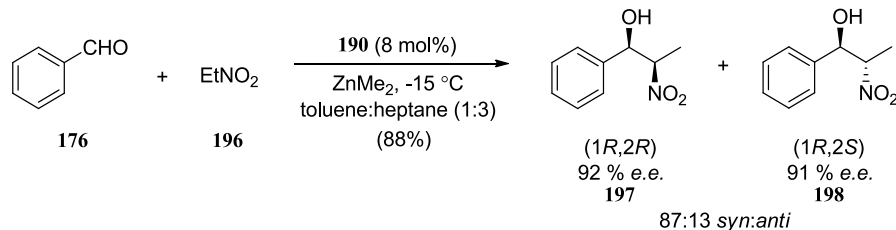
Bisoxazolidine **190**, used in concert with $ZnMe_2$ or $CuOAc$ generates β -hydroxy-nitroalkanes in high yields and *ee*'s from a wide range of aldehydes in asymmetric nitroaldol reactions (Scheme 3.10).^{40,43,44} The complex formed between catalyst **190** and $ZnMe_2$ facilitates deprotonation of nitromethane which then reacts with aromatic/aliphatic aldehydes to produce (*R*)-nitro alcohols **192a-h** in up to 99% yield and 95% *ee*.⁴⁰ The same ligand used with catalytic $CuOAc$ in ethanol led to nitro alcohol

products, again in high yields and *ee*'s but with opposite asymmetric induction, *viz.* the (*S*)-enantiomer **193a-h**.⁴³ Reversing the enantioselectivity of a catalytic reaction while employing the same source of chirality has been previously achieved.⁴⁵ Mechanistically, Wolf *et al.* ascribed this observation to a difference in coordination number of the catalytically active zinc (II) and copper (I) complexes (Scheme 3.10).^{40,43} The combination of **190** and ZnMe₂ in the nitroaldol reaction generates a 5-coordinate transition state **194a-h** that bears the nitronate anion, the aldehyde substrate and the bisoxazolidine ligand. With CuOAc, however, attachment of the aldehyde substrate produces a 4-coordinate transition state **195a-h** favoring *Re*-face attack. The enantioselective C-C bond formation via the respective transition states leads to release of the aldol product and regeneration of the bisoxazolidine-derived ZnMe₂ or CuOAc complex.



Scheme 3.10 - Wolf's Nitroaldol Reaction Generates: (*R*)-Nitro Alcohols with **190**/ZnMe₂⁴⁰
 (*S*)-Nitro Alcohols with **190**/CuOAc⁴³

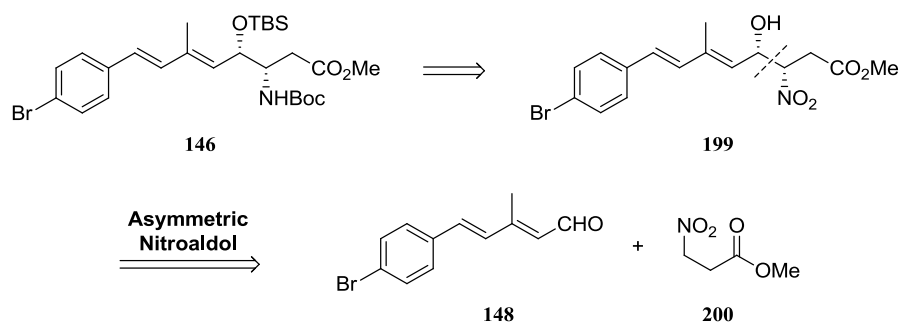
The even more interesting and pertinent result, however, was the reaction between benzaldehyde and nitroethane favoring formation of the *syn* diastereomer **197** in 88% yield (92% *ee* and 74% *de*, Scheme 3.11). Remarkably, both diastereomers were generated with high enantiopurity.



Scheme 3.11 - Wolf's Nitroaldol Reaction Between Benzaldehyde and Nitroethane: Preferential Formation of the *Syn* Diastereomer⁴⁰

3.8 The Second Approach for the Synthesis of Aboa: Application of Wolf's Nitroaldol Reaction

The second approach to the synthesis of Aboa featured Wolf's version of the asymmetric nitroaldol reaction. As can be seen in Scheme 3.12, utilizing aldehyde **148** from the SAH route would make this approach similarly concise. Commercially available 3-nitropropionic acid could be readily esterified, generating both components required to explore this approach. The asymmetric nitroaldol reaction, conducted under Wolf conditions, potentially provides direct access to the carbon framework and stereochemical requirements of Aboa. Reduction of the nitro group in **199** followed by TBS protection of the hydroxyl functionality and Boc-protection would complete the synthesis of Aboa.



Scheme 3.12 – The Second Retrosynthetic Analysis

3.9 A Model System for Wolf's Nitroaldol Reaction

Wolf's bisoxazolidine catalyst **190** was a prerequisite to our foray into Wolf's nitroaldol chemistry. To this end and according to Wolf *et al.*, (1*R*,2*S*)-*cis*-1-amino-2-indanol/1,2-

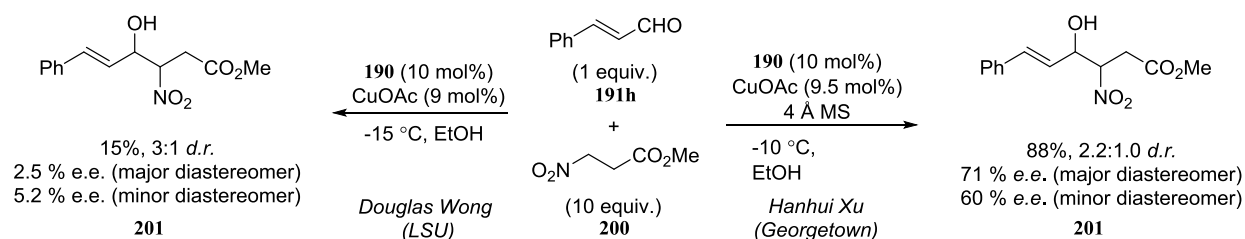
cyclohexanedione/catalytic formic acid was refluxed in toluene using a Dean-Stark trap (Scheme 3.9).³⁹ Toluene removal provided a crude residue that was purified by recrystallization (three times from CH₂Cl₂/MeCN) to form the chiral catalyst as a colorless powder. The catalyst **190**, synthesized in our hands at LSU, was identical in all respects to data put forth by Wolf and co-workers (¹H NMR, ¹³C NMR and $[\alpha]_D^{26.5}$).

Recall that the vicinal amino alcohol moiety in Aboa has an (*S,S*) configuration. This stereochemistry dictated the use of Wolf's copper-catalyzed nitroaldol reaction. Our first goal was to replicate the literature reaction between *trans*-cinnamaldehyde and nitromethane under Wolf conditions (**190**/CuOAc) that generated the (*S*)-nitro alcohol in 90% yield.⁴³ In our hands, the reaction gave the same product in 57% yield. Our chemical yield was noticeably lower for reasons that did not become known to us until much later.

We next set out to look at generation of the nitro component for the key nitroaldol reaction and its reaction with *trans*-cinnamaldehyde (model system). This was logically the next step, keeping the aldehyde component constant while increasing the nitro component complexity. The model system closely resembles an important feature of Aboa, an aldehyde group conjugated to an aromatic ring.

Methyl 3-nitropropanoate **200** was synthesized in 86% yield from 3-nitropropionic acid, TMSCl and 2,2-dimethoxypropane.⁴⁶ The model system reaction proceeded in poor chemical yield (15%) with 3:1 diastereoselectivity (Scheme 3.13). The separation of the diastereomeric products and their purification was complicated by the presence of excess methyl 3-nitropropanoate. Each diastereomer was obtained pure by normal phase silica HPLC but it was never determined whether the major diastereomer was the *syn* or *anti* diastereomer. The enantiopurity of each diastereomer was determined on a Chiralcel OD-H column. The major (less polar) diastereomer had an *e.e.* of 2.5% and the minor (more polar) diastereomer had an *e.e.* of 5.2%. The same reaction was also performed by Hanhui Xu (Professor Wolf's graduate student) at Georgetown University. The chemical yield of **201** was good (88%) but the

diastereoselectivity was poor (2.2:1). The product mixture was sent to us at LSU and each diastereomer was obtained pure by normal phase silica HPLC. Again, it was never determined whether the major diastereomer was the *syn* or *anti* diastereomer. The major (less polar) diastereomer had an *e.e.* of 71% and the minor (more polar) diastereomer had an *e.e.* of 60%.



Scheme 3.13 – Nitroaldol Reaction Between *Trans*-Cinnamaldehyde and Methyl 3-Nitropropanoate Under Wolf Conditions

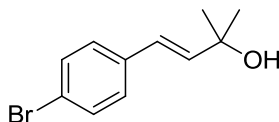
At the conclusion of these nitroaldol reactions and Carol Taylor’s visit to Georgetown University, we became aware that our handling of the chiral catalyst just prior to performing the nitroaldol reaction was a point of difference. Wolf’s group lyophilized the catalyst three times and upon addition of CuOAc/EtOH produced a blue/black solution. In our hands, no such precautions were taken and addition of CuOAc/EtOH generated a blue/green mixture. The residual moisture resulted in a lower bisoxazolidine catalyst content and therefore, a reduced chemical yield for both of our reactions.

The strict exclusion of moisture is critical for ensuring reproducible yields and enantioselectivities, a point not gleaned from publications.^{40,43} We adhered to the reported procedure prescribed by Wolf *et al.* and in doing so, bypassed the catalyst lyophilization and incorporation of 4 Å molecular sieves steps.⁴³ On the basis of the results described in §3.8, we decided not to pursue the nitroaldol route further. For the purposes of chemical synthesis, the levels of diastereo- and enantioselectivity were not acceptable.

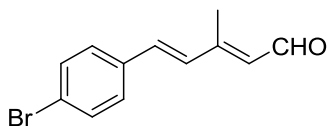
3.10 Experimental Section

General methods: as detailed in Chapter 2

3.10.1 Experimental Procedures

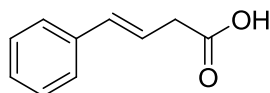


(*E*)-4-(4-bromophenyl)-2-methylbut-3-en-2-ol (**150**). A solution of methylmagnesium iodide in dry diethyl ether (3.0 *M*, 7.82 mL, 23.5 mmol, 1.4 equiv.) was added dropwise to a solution of ethyl *trans*-4-bromocinnamate (4.2 g, 16.5 mmol, 1.0 equiv.) in dry diethyl ether (30 mL) at 0 °C. The resulting solution was stirred under N₂ at 0 °C for 45 min, warmed to rt and stirred for an additional 18 h. The reaction mixture was heated under reflux for 2 h and cooled to 0 °C. Slow addition of ice-cold H₂O (15 mL), was followed by addition of ice-cold saturated aqueous ammonium chloride (35 mL). The mixture was extracted with ether (3 x 30 mL); the combined extracts were washed with H₂O (30 mL), dried (MgSO₄), filtered, and concentrated. The residue (3.48 g, 88 %) was used without further purification. *R*_f 0.18 (5:1 hexanes-EtOAc). ¹H NMR (400 MHz, CDCl₃) δ 1.41 (s, 3H), 1.42 (s, 3H), 1.61 (s, 1H), 6.34 (dd, *J* = 16.1, 0.7 Hz, 1H), 6.53 (d, *J* = 16.1 Hz, 1H), 7.24 (d, *J* = 8.2 Hz, 2H), 7.42 (d, *J* = 8.2 Hz, 2H); ¹³C NMR (100 MHz, CDCl₃) δ 29.8, 71.0, 121.1, 125.3, 127.9, 131.6, 135.9, 138.2. HRMS (ESI-TOF) calcd for C₁₁H₁₂Br (M-H₂O)⁺ 223.0122, obsd 223.0126.

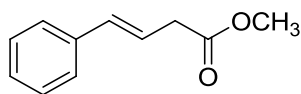


(*2E,4E*)-5-(4-bromophenyl)-3-methylpenta-2,4-dienal (**148**). The Vilsmeier reagent was prepared according to the following procedure: POCl₃ (190 μL, 318 mg, 2.1 mmol, 2.5 equiv.) was added dropwise over 45 min to a cooled solution of dry DMF (175 μL). A solution of (*E*)-4-(4-bromophenyl)-2-

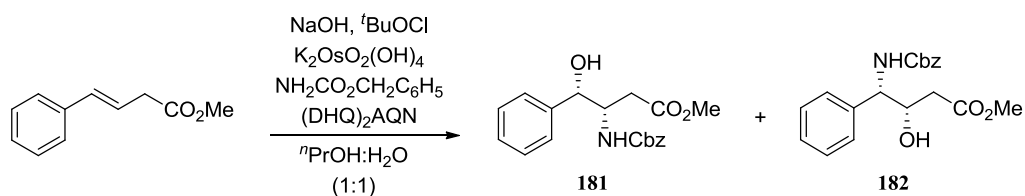
methylbut-3-en-2-ol (200 mg, 0.83 mmol, 1.0 equiv.) in dry DMF (395 μ L) was cooled to 0 $^{\circ}$ C. The Vilsmeier reagent was added dropwise over 1 h at 0 $^{\circ}$ C to the solution of tertiary alcohol. The reaction mixture was gradually heated to 80 $^{\circ}$ C over 45 min and kept at that temperature for 3 h. A solution of sodium acetate (2 g) in H₂O (5 mL) was added dropwise over 1 h at 0 $^{\circ}$ C. The solution was heated to 80 $^{\circ}$ C and stirred for 30 min. The solution was extracted with EtOAc (4 x 20 mL). The combined organic layers were washed with brine (100 mL), dried over MgSO₄, filtered, and concentrated. Flash chromatography (Hex-EtOAc, 7:1) provided **148** as a yellow solid (83 mg, 40%). R_f 0.43 (7:1 hexanes-EtOAc). ¹H NMR (CDCl₃, 400 MHz) δ 2.38 (s, 3H), 6.09 (d, J = 8.0 Hz, 1H), 6.88 (d, J = 16.1 Hz, 1H), 7.00 (d, J = 16.1 Hz, 1H), 7.36 (d, J = 8.4 Hz, 2H), 7.50 (d, J = 8.4 Hz, 2H), 10.17 (d, J = 8.0 Hz, 1H); ¹³C NMR (CDCl₃, 100 MHz) δ 13.1, 123.2, 128.7, 130.4, 132.0, 132.1, 134.2, 134.9, 153.6, 191.0. HRMS (ESI-TOF) calcd for C₁₂H₁₂BrO (M+H)⁺ 251.0066, obsd 251.0062.



(*E*)-4-phenylbut-3-enoic acid (**180**). Dry triethylamine (10.0 mL, 0.07 mol, 1.7 equiv.) was added dropwise to a solution of malonic acid (10.82 g, 0.10 mol, 2.5 equiv.) in phenylacetaldehyde (4.65 mL, 5.0 g, 0.04 mol, 1.0 equiv.). The reaction mixture was heated under reflux until the evolution of CO₂ ceased (4 h) and cooled to room temperature. The resulting solution was partitioned between ether (100 mL) and ice-cold 2 *M* HCl (50 mL). The organic layer was washed with 5 % NaOH (50 mL) and the aqueous layer extracted with ether (100 mL). The aqueous layer was acidified with 2 *M* HCl (50 mL) and extracted with ether (160 mL). The organic layer was washed with brine (100 mL), dried (MgSO₄), filtered, and concentrated. The residue (3.63 g, 71 %) was used without further purification. ¹H NMR (400 MHz, CDCl₃) δ 3.29 (dd, J = 7.1, 1.2 Hz, 2H), 6.28 (dt, J = 15.9, 7.1 Hz, 1H), 6.51 (d, J = 15.9 Hz, 1H), 7.22-7.39 (m, 5H); ¹³C NMR (100 MHz, CDCl₃) δ 38.0, 120.8, 126.3, 127.7, 128.5, 134.0, 136.6, 177.9.



(*E*)-methyl 4-phenylbut-3-enoate (**153**). Boron trifluoride diethyl etherate (1.51 mL, 1.71 g, 12.0 mmol, 1.0 equiv.) was added dropwise to a solution of (*E*)-4-phenylbut-3-enoic acid (1.95 g, 12.0 mmol, 1.0 equiv.) in anhydrous methanol (16.0 mL). The resulting solution was heated under reflux for 18.5 h and cooled to room temperature. Aqueous Na₂CO₃ (5%, 50 mL) was added and the mixture stirred for 30 min. The mixture was partitioned between H₂O (50 mL) and ether (250 mL). The organic layer was dried (MgSO₄), filtered, and concentrated. The residue was purified by flash column chromatography, eluting with 8:1 hexanes-EtOAc, to afford a yellow oil (1.35 g, 65 %). *R*_f 0.31 (8:1 hexanes-EtOAc). ¹H NMR (400 MHz, CDCl₃) δ 3.25 (dd, *J* = 7.1, 1.4 Hz, 2H), 3.71 (s, 3H), 6.30 (dt, *J* = 15.9, 7.1 Hz, 1H), 6.49 (d, *J* = 15.9 Hz, 1H), 7.20-7.39 (m, 5H); ¹³C NMR (100 MHz, CDCl₃) δ 38.2, 51.9, 121.6, 126.2, 127.5, 128.5, 133.4, 136.7, 172.0. HRMS (ESI-TOF) calcd for C₁₁H₁₃O₂ (M+H)⁺ 177.0910, obsd 177.0917.



Regioreversed SAH Reaction Using (*E*)-methyl 4-phenylbut-3-enoate. A solution of NaOH (170 mg, 4.25 mmol, 3.0 equiv.) in H₂O (5.4 mL) was added to a solution of benzyl carbamate (643 mg, 4.25 mmol, 3.0 equiv.) dissolved in *n*-PrOH (3.4 mL) and the resulting solution stirred for 10 min. Freshly prepared *tert*-butyl hypochlorite⁴⁷ (481 μL, 462 mg, 4.25 mmol, 3.0 equiv.) was added dropwise and the resulting solution stirred for an additional 10 min. (DHQ)₂AQN (61 mg, 0.07 mmol, 5 mol %) in *n*-PrOH (2.0 mL) was added and the reaction vessel immersed in a water bath at ambient temperature and stirred for 5 min. (*E*)-methyl 4-phenylbut-3-enoate (250 mg, 1.42 mmol, 1.0 equiv.) was added, followed immediately by K₂OsO₂(OH)₄ (26 mg, 0.07 mmol, 5 mol %). The reaction mixture was stirred for 2 h at

rt and quenched with NaHSO₃ (710 mg, 6.82 mmol, 4.8 equiv.). Ethyl acetate (10 mL) was added and the layers were separated. The aqueous layer was extracted with EtOAc (3 x 10 mL). The combined organic layers were washed with H₂O (10 mL) and brine (10 mL), dried with MgSO₄, filtered and concentrated. The residue was subjected to flash chromatography (5:1 Hex-EtOAc → 1:1 Hex-EtOAc) to provide a mixture of two compounds that were separated via normal phase HPLC (Figure 3.2).

The following chromatogram is from a typical preparative run.

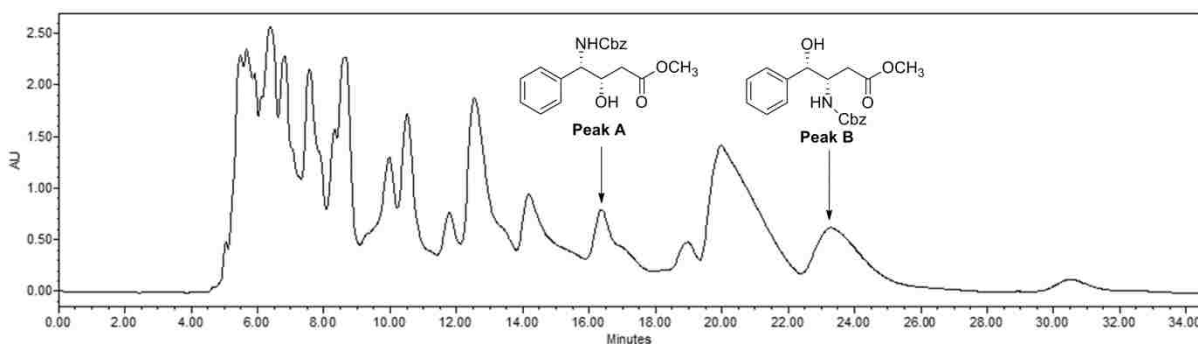
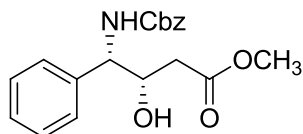


Figure 3.2: HPLC Chromatogram of Sharpless Aminohydroxylation Reaction After Flash Chromatography. Econosil Silica (250 mm X 10 mm), Hex/EtOAc = 2:1, flow rate 3.0 mL/min, 300 mg crude product mixture, 20 mg per injection, retention times of importance: 16.37 min and 23.28 min, detection 250 nm

THE REGIOISOMERS ARE PRESENTED IN ORDER OF ELUTION

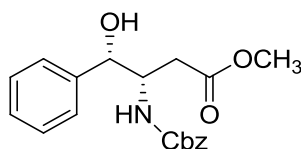
Peak A: (3*S*,4*S*)-methyl 4-(((benzyloxy)carbonyl)amino)-3-hydroxy-4-phenylbutanoate (**182**), undesired regioisomer, total of 11 mg collected, retention time: 16.37 min



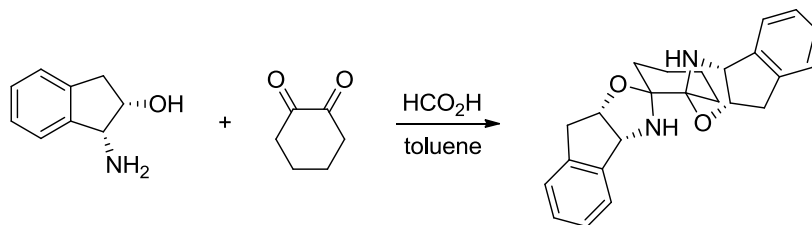
R_f 0.33 (2:1 hexanes-EtOAc). ¹H NMR (CDCl₃, 400 MHz) δ 2.79 (dd, $J = 13.7, 9.0$ Hz, 1H), 2.89 (dd, $J = 13.7, 3.8$ Hz, 1H), 3.75 (s, 3H), 4.34-4.42 (m, 1H), 4.45 (d, $J = 9.4$ Hz, 1H), 5.13-5.22 (m, 2H), 5.63 (d, $J = 9.4$ Hz, 1H), 7.20-7.40 (m, 10H); ¹³C NMR (CDCl₃, 100 MHz) δ 40.3, 52.6, 57.4, 67.3, 72.7,

127.0, 128.1, 128.2, 128.6, 128.8, 129.4, 136.9, 156.7, 171.5. HRMS (ESI-TOF) calcd for $C_{19}H_{21}NNaO_5$ ($M+Na$)⁺ 366.1312, obsd 366.1314.

Peak B: (3*S*,4*S*)-methyl 3-(((benzyloxy)carbonyl)amino)-4-hydroxy-4-phenylbutanoate (**181**), desired regioisomer with spectra contaminated by benzyl carbamate, total of 22 mg collected, retention time: 23.28 min



R_f 0.27 (2:1 hexanes-EtOAc). ¹H NMR ($CDCl_3$, 400 MHz) δ 2.53 (dd, $J = 16.6, 3.4$ Hz, 1H), 2.62 (dd, $J = 16.6, 9.0$ Hz, 1H), 3.20 (br s, 1H), 3.68 (s, 3H), 4.23-4.37 (m, 1H), 4.62-4.74 (m, 1H), 5.01-5.15 (m, 2H), 5.82 (d, $J = 8.4$ Hz, 1H) 7.25-7.36 (m, 10H); ¹³C NMR ($CDCl_3$, 100 MHz) δ 38.5, 51.9, 58.6, 66.9, 70.9, 126.7, 127.7, 128.1, 128.2, 128.5, 128.7, 136.2, 156.3, 172.8. HRMS (ESI-TOF) calcd for $C_{19}H_{22}NO_5$ ($M+H$)⁺ 344.1492, obsd 344.1505.

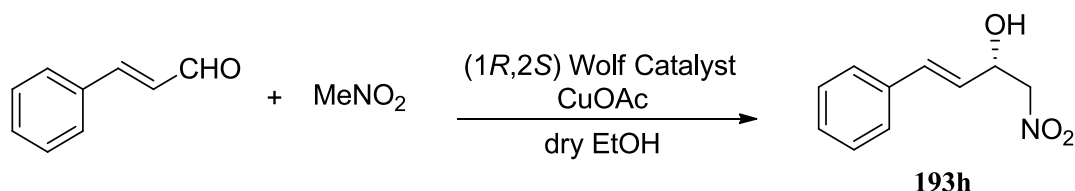


Wolf's Catalyst (**190**). To a stirred solution of (1*R*,2*S*)-*cis*-1-aminoindan-2-ol (2.0 g, 13.4 mmol, 2.06 equiv.) and 1,2-cyclohexanedione (0.73 g, 6.52 mmol, 1.0 equiv.) in toluene (20 mL) was added formic acid (2 drops from a Pasteur pipet). The reaction mixture was refluxed for 2 h using a Dean-Stark trap. After cooling to room temperature, toluene was removed *in vacuo*. Recrystallization of the crude residue using acetonitrile and dichloromethane (3 times) produced the title compound as a colorless powder (0.45 g, 18%) that was collected via vacuum filtration (washing well with acetonitrile). R_f 0.27 and 0.55 (5:1 hexanes-EtOAc). $[\alpha]^{26.5}_D +65.6$ (c 1.0, $CHCl_3$) Lit, $[\alpha]^{26.5}_D +65.2$ (c 1.0, $CHCl_3$); ¹H NMR (400 MHz, $CDCl_3$) δ 0.86 (d, $J = 12.2$ Hz, 2H), 1.25-1.45 (m, 6H), 2.83 (br s, 2H), 3.12 (s, 4H), 4.69-4.74

(m, 2H), 5.00 (d, $J = 5.3$ Hz, 2H), 7.18-7.25 (m, 6H), 7.39-7.43 (m, 2H); ^{13}C NMR (100 MHz, CDCl_3) δ 23.2, 36.4, 38.9, 69.2, 81.1, 101.3, 125.2, 125.3, 127.0, 127.9, 141.0, 143.9. HRMS (ESI-TOF) calcd for $\text{C}_{24}\text{H}_{27}\text{N}_2\text{O}_2$ ($\text{M}+\text{H}$) $^+$ 375.2067, obsd 375.2078.

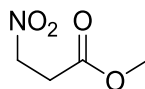
Enantioselective Nitroaldol

Wolf *et al.* report 90% yield under apparently similar reaction conditions.⁴³



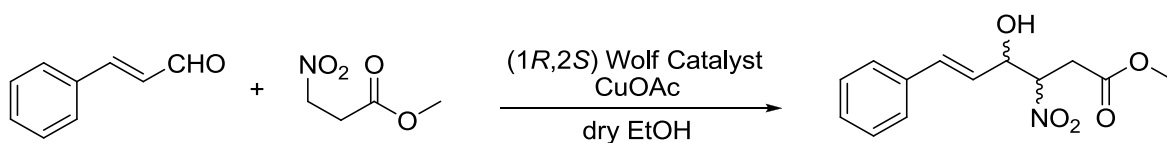
Our highest yielding trial for the reaction between *trans*-cinnamaldehyde and nitromethane:

To a flame-dried flask, the bisoxazolidine ligand (37.0 mg, 0.10 mmol, 10 mol %) and CuOAc (11.0 mg, 0.09 mmol, 9 mol %) were dissolved in dry EtOH (2.4 mL) under N_2 at room temperature. After stirring for 1.5 h, nitromethane (537 μL , 610 mg, 10 mmol, 10 equiv.) was added, and the mixture stirred for an additional 1.5 h. Upon the addition of flame-dried molecular sieves (powder, 4 Å), the solution was cooled to -15 °C and *trans*-cinnamaldehyde (126 μL , 132 mg, 1 mmol, 1 equiv.) was added. The contents were stirred at -15 °C (FTS Multi-Cool Bath with Syltherm XLT cooling fluid) overnight under N_2 . The reaction mixture was gradually warmed to room temperature. The contents were filtered through Celite, washing the filter pad with EtOH. The filtrate was concentrated and the residue subjected to flash chromatography (5:1 Hex/EtOAc) to provide 110 mg (57% yield) of the desired compound. R_f 0.31 (5:1 hexanes-EtOAc). ^1H NMR (CDCl_3 , 400 MHz) δ 2.99 (br, 1H), 4.49 (d, $J = 6.1$ Hz, 2H), 5.02 (qd, $J = 6.1, 1.0$ Hz, 1H), 6.12 (dd, $J = 15.7, 6.3$ Hz, 1H), 6.76 (d, $J = 15.7$ Hz, 1H), 7.27-7.39 (m, 5H); ^{13}C NMR (CDCl_3 , 100 MHz) δ 69.5, 79.8, 125.0, 126.7, 128.4, 128.7, 133.5, 135.5.



Methyl 3-nitropropanoate (**200**). 2,2-Dimethoxypropane (6.72 mL, excess) was added to a stirred solution of 3-nitropropanoic acid (500 mg, 4.20 mmol, 10.0 equiv.) in dry MeOH (1.68 mL). After stirring for 10 min, TMSCl (53 μ L, 45 mg, 0.42 mmol, 1.0 equiv.) was added dropwise. The reaction mixture was stirred at rt for 21 h, concentrated, and applied directly to flash column. Elution with 4:1 Hex/EtOAc \rightarrow 1:1 Hex/EtOAc afforded the title compound as a colorless oil (457 mg, 82%). ^1H NMR (CDCl_3 , 400 MHz) δ 3.00 (t, J = 6.2 Hz, 2H), 3.75 (s, 3H), 4.66 (t, J = 6.2 Hz, 2H); ^{13}C NMR (CDCl_3 , 100 MHz) δ 30.5, 52.1, 69.5, 169.9.

Diastereoselective Nitroaldol



The following reaction was performed at room temperature, 0 $^{\circ}\text{C}$, and -10 $^{\circ}\text{C}$. The following procedure represents the reaction run at 0 $^{\circ}\text{C}$. Only trace amounts of the two products were obtained and they were difficult to separate from each other and the excess of methyl 3-nitropropionate.

To a flame-dried flask, the bisoxazolidine ligand (19.0 mg, 0.05 mmol, 25 mol %) and CuOAc (6.0 mg, 0.05 mmol, 24 mol %) were dissolved in dry EtOH (1.2 mL) under N_2 at room temperature. After stirring for 1.5 h, methyl 3-nitropropionate (276 mg, 2.07 mmol, 10 equiv.) was added, and the mixture stirred for an additional 1.5 h. Upon the addition of flame-dried molecular sieves (powder, 4 \AA), the solution was cooled to 0 $^{\circ}\text{C}$ and *trans*-cinnamaldehyde (26 μL , 27 mg, 0.21 mmol, 1 equiv.) was added. The mixture was stirred at 0 $^{\circ}\text{C}$ (FTS Multi-Cool Bath with Syltherm XLT cooling fluid) overnight under N_2 . The reaction mixture was gradually warmed to room temperature. The contents were filtered through Celite, washing the filter pad with EtOH. The filtrate was concentrated and the residue subjected to flash chromatography (8:1 Hex/EtOAc \rightarrow 1:1 Hex/EtOAc) to provide a mixture of three compounds that were separated via normal phase HPLC (Figure 3.3).

The following chromatogram is from a typical preparative run.

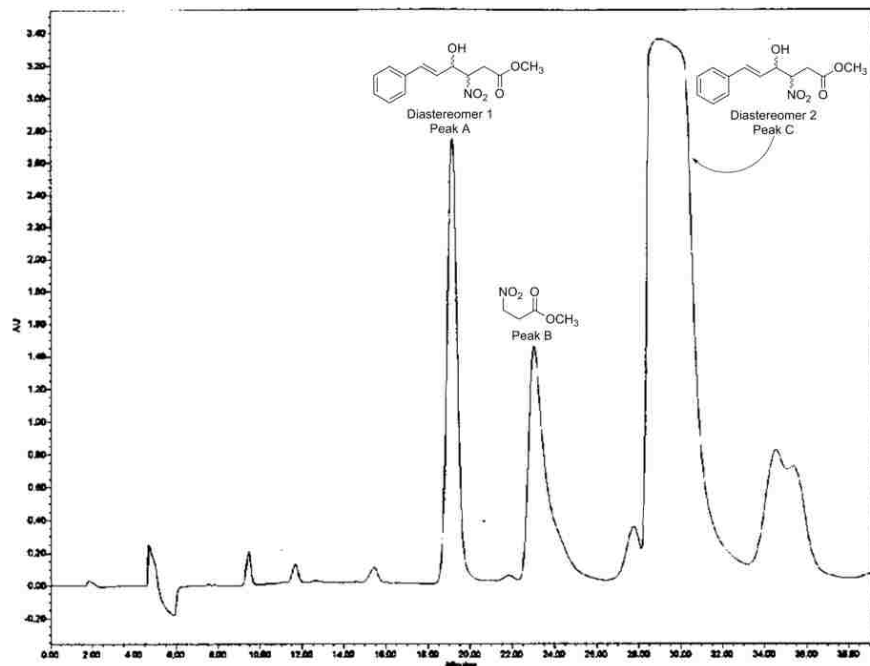
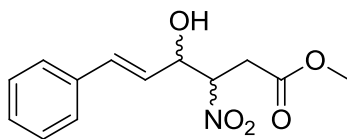


Figure 3.3: HPLC Chromatogram of Nitroaldol Reaction After Flash Chromatography. Econosil Silica (250 mm X 10 mm), Hex/EtOAc = 4:1, flow rate 3.0 mL/min, 2.5 mg injection, retention times of importance: 19.64 min, 23.27 min, 31.01 min, detection 254 nm

THE COMPOUNDS ARE PRESENTED IN ORDER OF ELUTION

The nitro compound absorbs much less at 254 nm than the two products. Thus, despite large amounts, it only gives rise to a small peak.

Peak A: Diastereomer 1 as a mixture of enantiomers, retention time: 19.64 min (Figure 3.4 and 3.5)



201 Diastereomer 1

R_f 0.38 (2:1 Hex/EtOAc). $^1\text{H NMR}$ (CDCl_3 , 400 MHz) δ 2.45 (br, 1H), 2.85 (dd, $J = 17.8, 3.3$ Hz, 1H), 3.29 (dd, $J = 17.8, 9.6$ Hz, 1H), 3.69 (s, 3H), 5.00-5.07 (m, 2H), 6.12 (dd, $J = 15.9, 5.4$ Hz, 1H), 6.79

(d, $J = 15.9$ Hz, 1H), 7.26-7.39 (m, 5H); ^{13}C NMR (CDCl_3 , 100 MHz) δ 31.4, 52.4, 72.6, 86.3, 124.8, 126.7, 128.6, 128.7, 133.7, 135.4, 170.4. HRMS (ESI-TOF) calcd for $\text{C}_{13}\text{H}_{15}\text{NNaO}_5$ ($\text{M}+\text{Na}$) $^+$ 288.0842, obsd 288.0844.

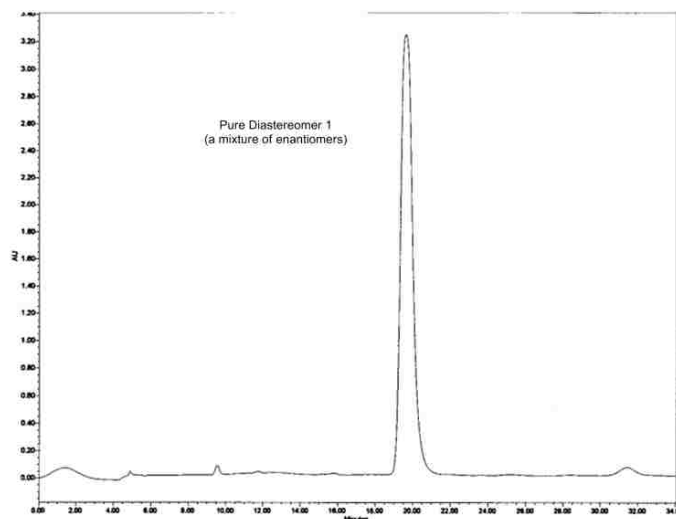


Figure 3.4: HPLC Chromatogram of **201 Diastereomer 1**. Econosil Silica (10 mm X 25 cm), Hex/EtOAc = 4:1, flow rate 3.0 mL/min, 200 μg injection, retention time: 19.64 min, detection 254 nm

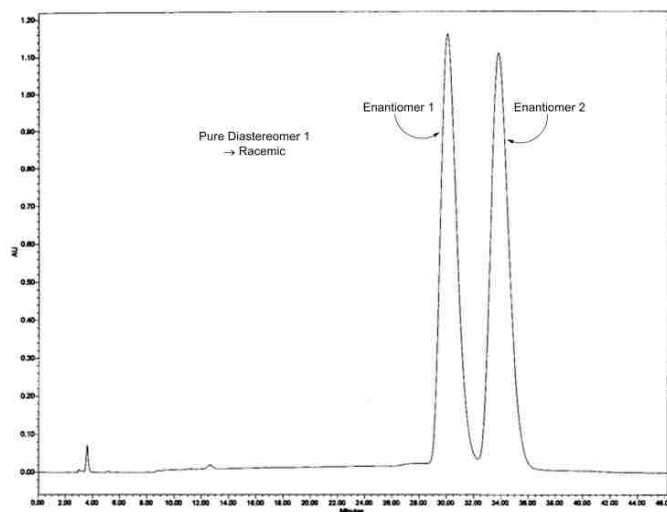


Figure 3.5: Chiral HPLC Chromatogram of **201 Diastereomer 1**. Chiralcel OD-H (0.46 cm X 25 cm), Hex/Isopropanol = 9:1, flow rate 1.0 mL/min, retention time: 30.10, 33.83 min, detection 254 nm

Peak B: recovered methyl 3-nitropropionate, retention time: 23.27 min (Figure 3.6)

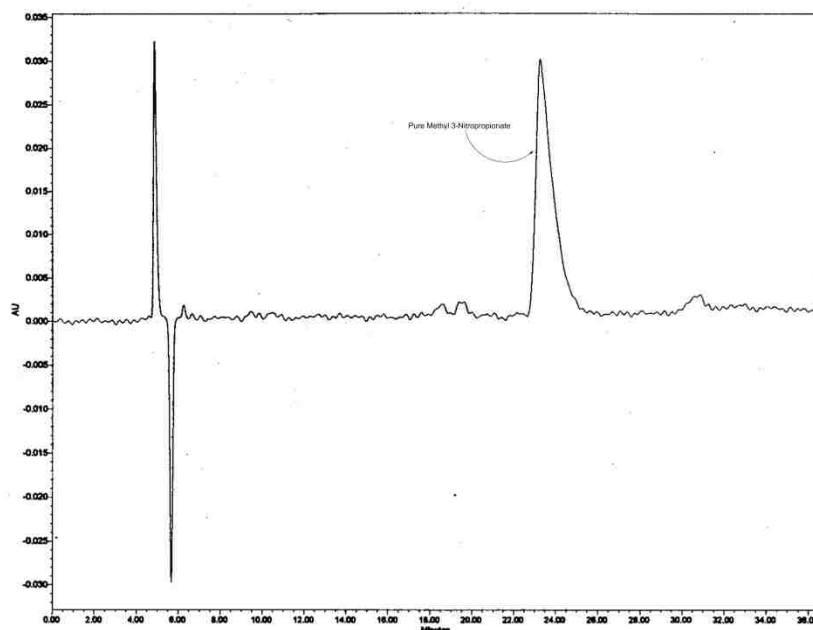
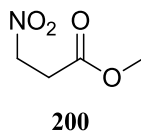
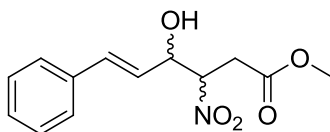


Figure 3.6: HPLC Chromatogram of **200**. Econosil Silica (10 mm X 25 cm), Hex/EtOAc = 4:1, flow rate 3.0 mL/min, 2 mg injection, retention time: 23.27 min, detection 254 nm

^1H and ^{13}C NMR spectra shown above

Peak C: Diastereomer 2 as a mixture of enantiomers, retention time: 31.01 min (Figure 3.7 and 3.8)



201 Diastereomer 2

R_f 0.29 (2:1 Hex/EtOAc). ^1H NMR (CDCl_3 , 400 MHz) δ 2.41 (br, 1H), 2.92 (dd, $J = 17.5, 4.6$ Hz, 1H), 3.17 (dd, $J = 17.5, 9.0$ Hz, 1H), 3.68 (s, 3H), 4.76 (t, $J = 6.7, 1\text{H}$), 5.06 (ddd, $J = 9.0, 6.7, 4.6$ Hz,

1H), 6.11 (dd, $J = 15.9, 7.2$ Hz, 1H), 6.73 (d, $J = 15.9$ Hz, 1H), 7.29-7.39 (m, 5H); ^{13}C NMR (CDCl_3 , 100 MHz) δ 34.0, 52.4, 73.3, 86.6, 124.4, 126.8, 128.8, 135.1, 135.2, 169.5. HRMS (ESI-TOF) calcd for $\text{C}_{13}\text{H}_{15}\text{NNaO}_5$ ($\text{M}+\text{Na}$) $^+$ 288.0842, obsd 288.0838.

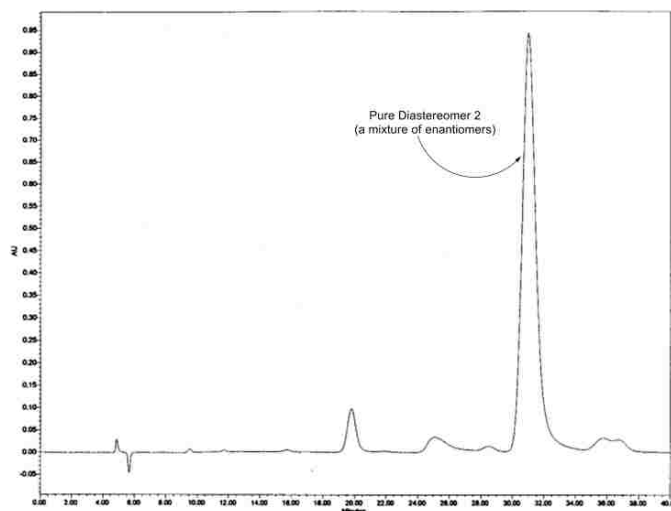


Figure 3.7: HPLC Chromatogram of **201 Diastereomer 2**. Econosil Silica (10 mm X 25 cm), Hex/EtOAc = 4:1, flow rate 3.0 mL/min, 200 μg injection, retention time: 31.01 min, detection 254 nm

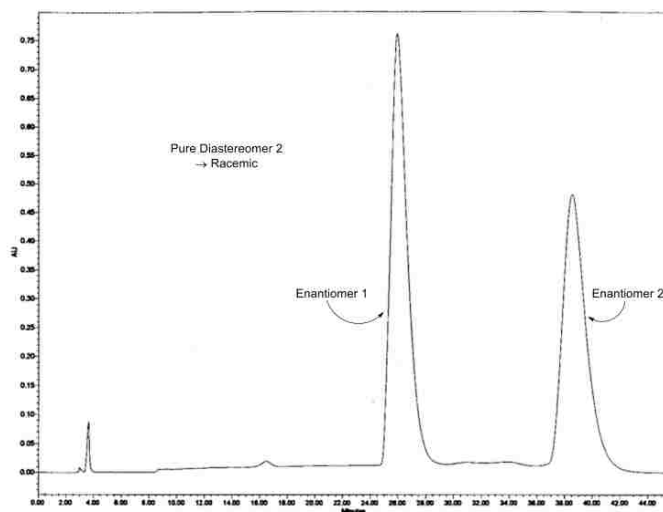
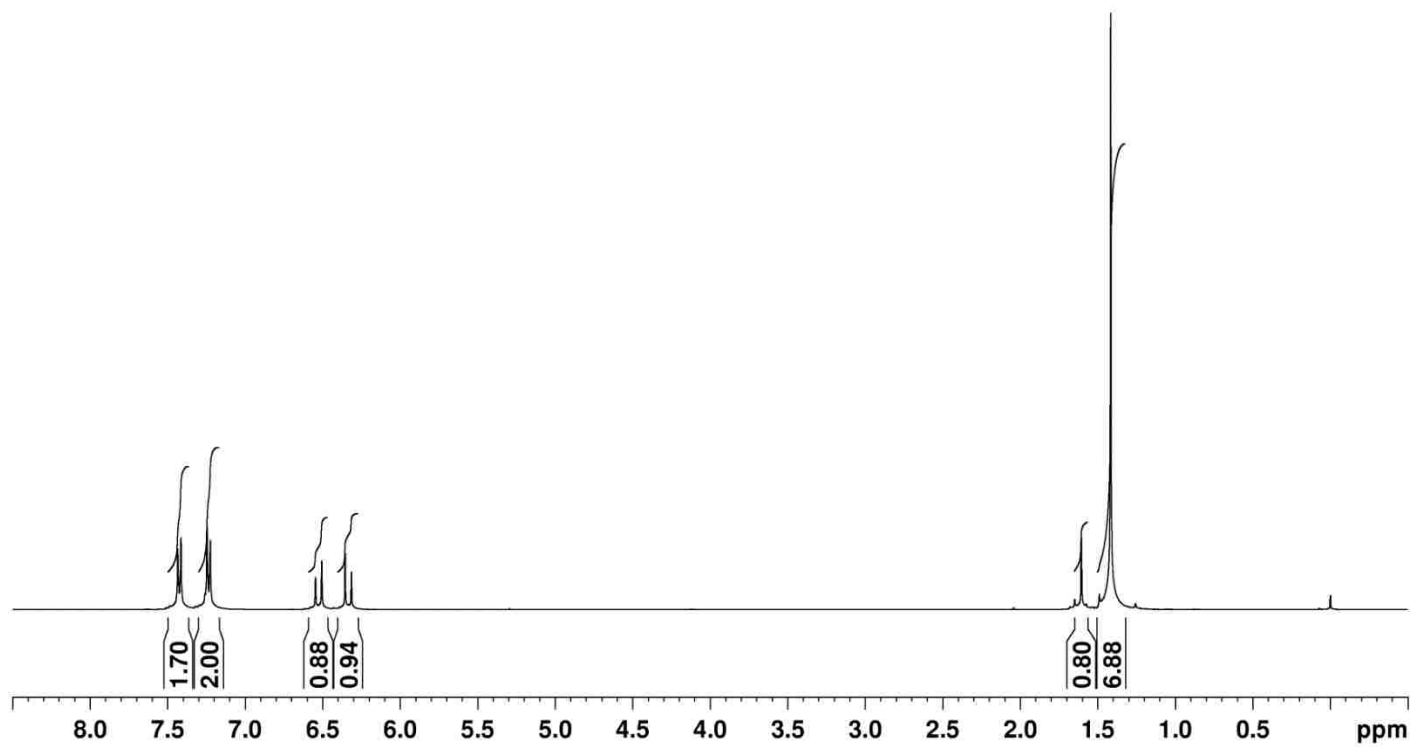
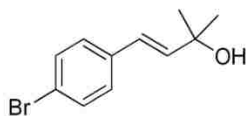


Figure 3.8: HPLC Chromatogram of **201 Diastereomer 2**. Chiralcel OD-H (0.46 cm X 25 cm), Hex/Isopropanol = 9:1, flow rate 1.0 mL/min, retention time: 25.96, 38.53 min, detection 254 nm

3.10.2 Spectra

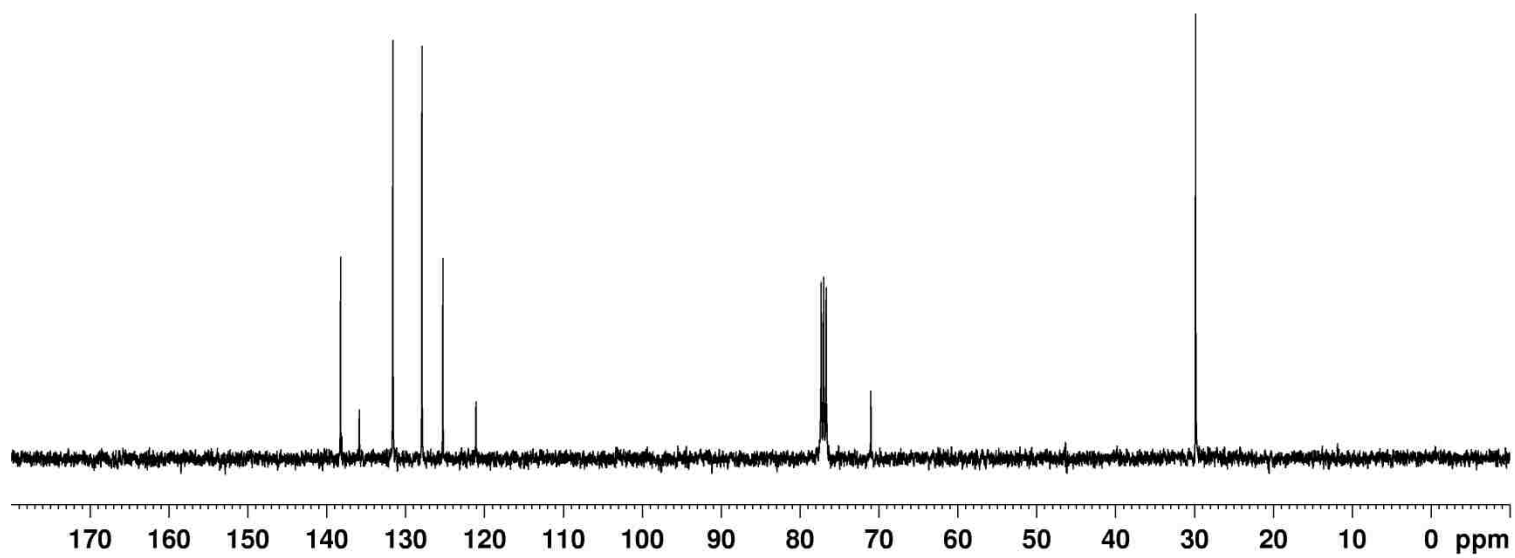
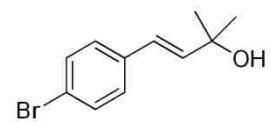
Compound **150** - ^1H NMR spectrum

DW-2-017Part2 in CDCl_3 (400 MHz)



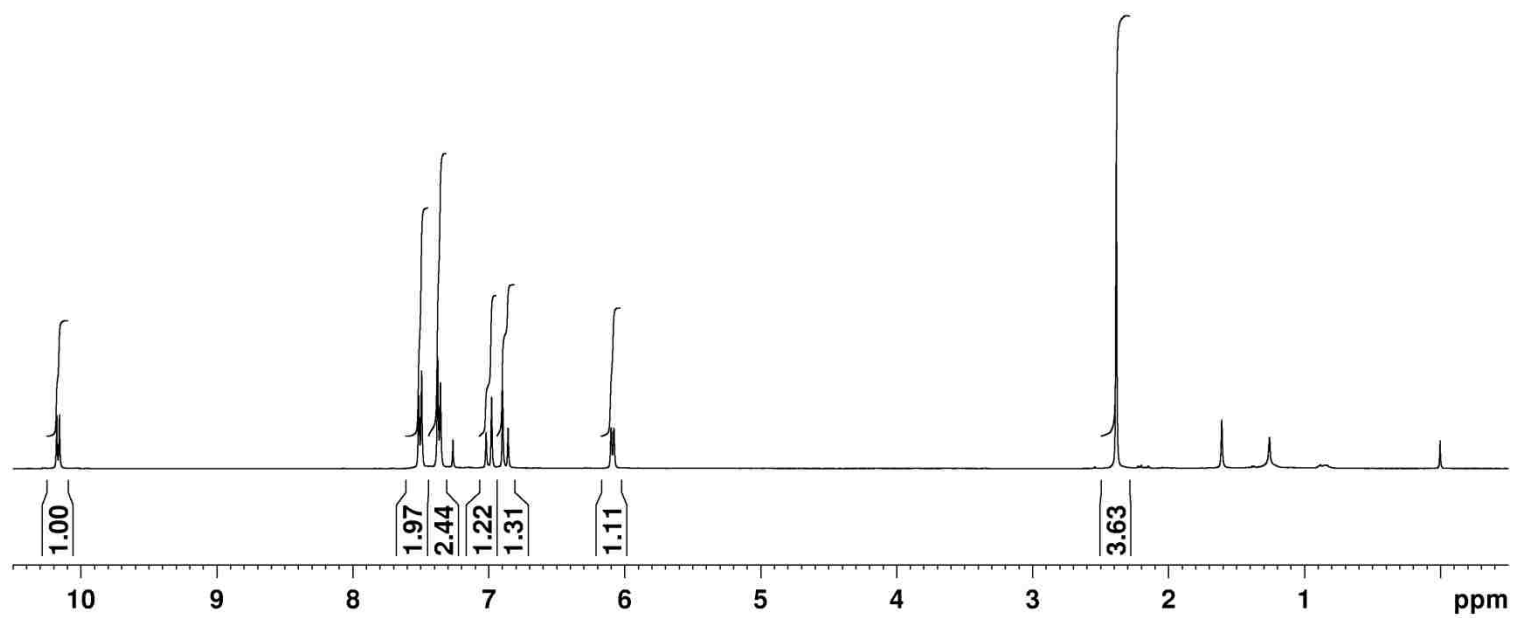
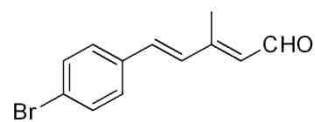
Compound **150** - ^{13}C NMR spectrum

DW-2-017Part2 in CDCl_3 (100 MHz)



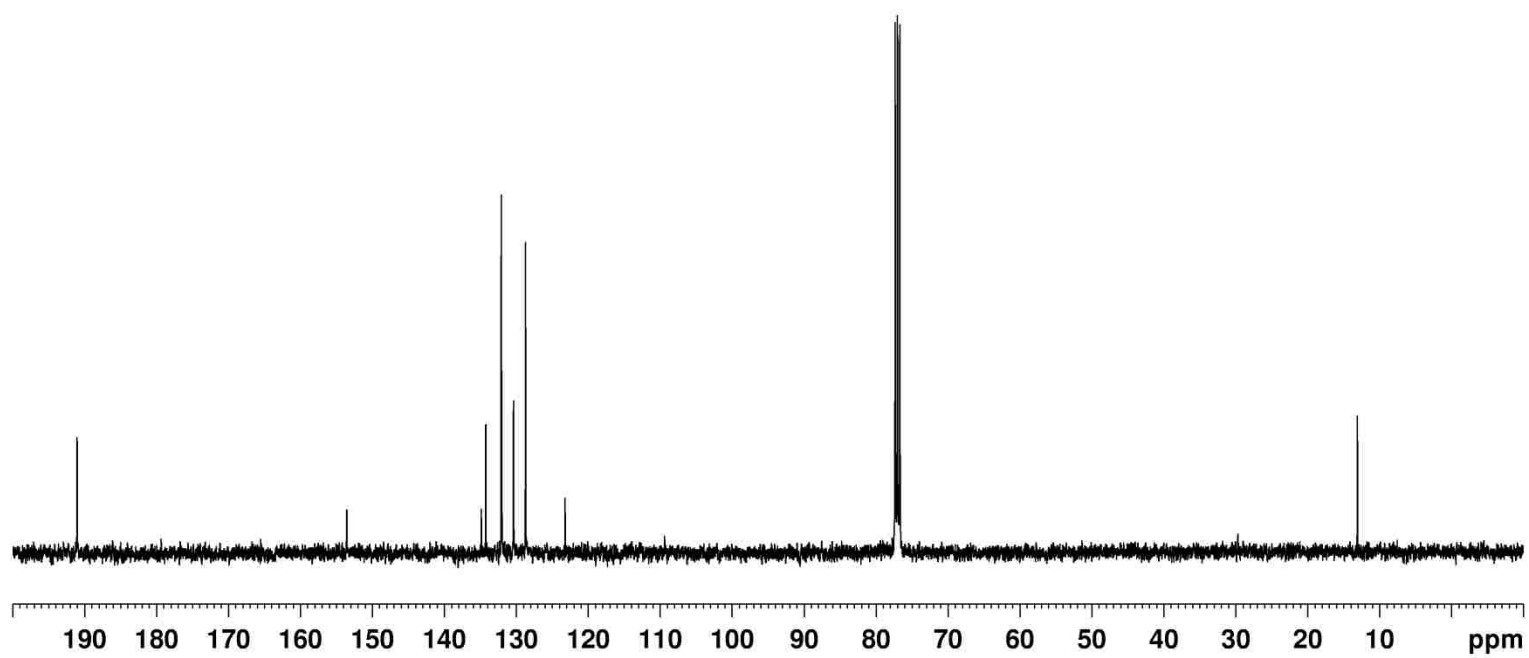
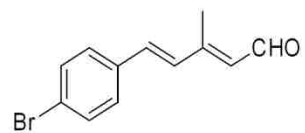
Compound **148** - ^1H NMR spectrum

DW-1-084Bottom in CDCl_3 (400 MHz)



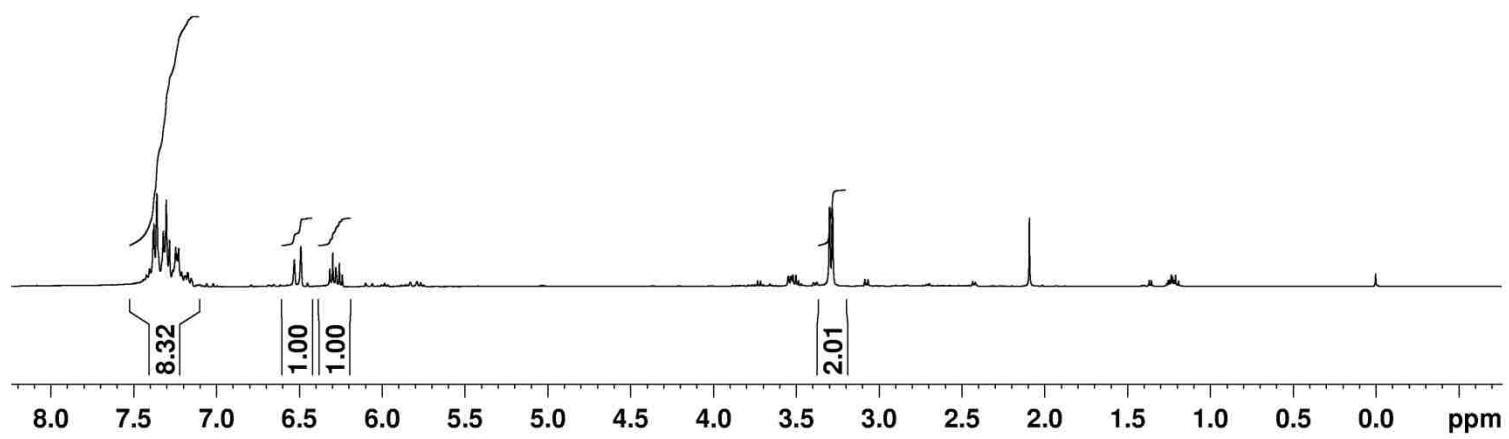
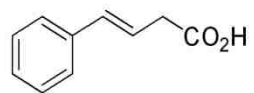
Compound **148** - ^{13}C NMR spectrum

DW-1-084Bottom in CDCl_3 (100 MHz)



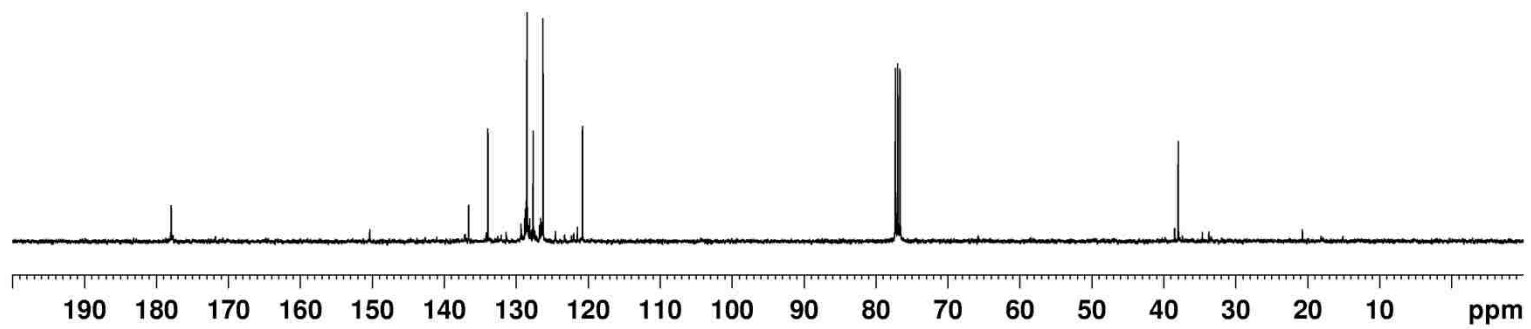
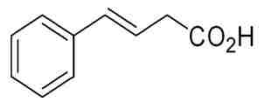
Compound **180** - ^1H NMR spectrum

DW-1-111 in CDCl_3 (400 MHz)



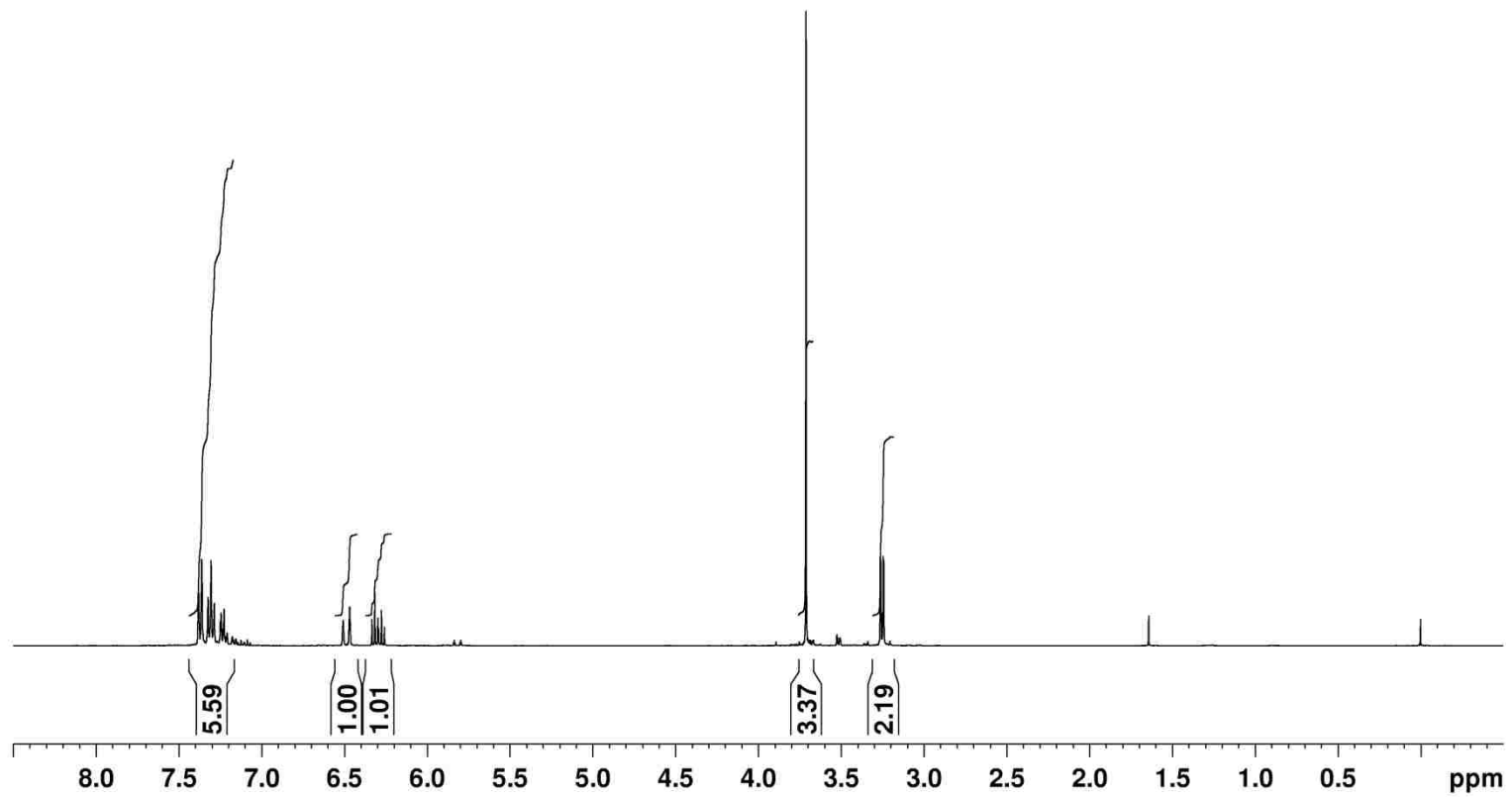
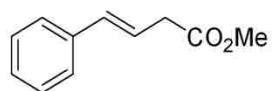
Compound **180** - ^{13}C NMR spectrum

DW-1-111 in CDCl_3 (100 MHz)



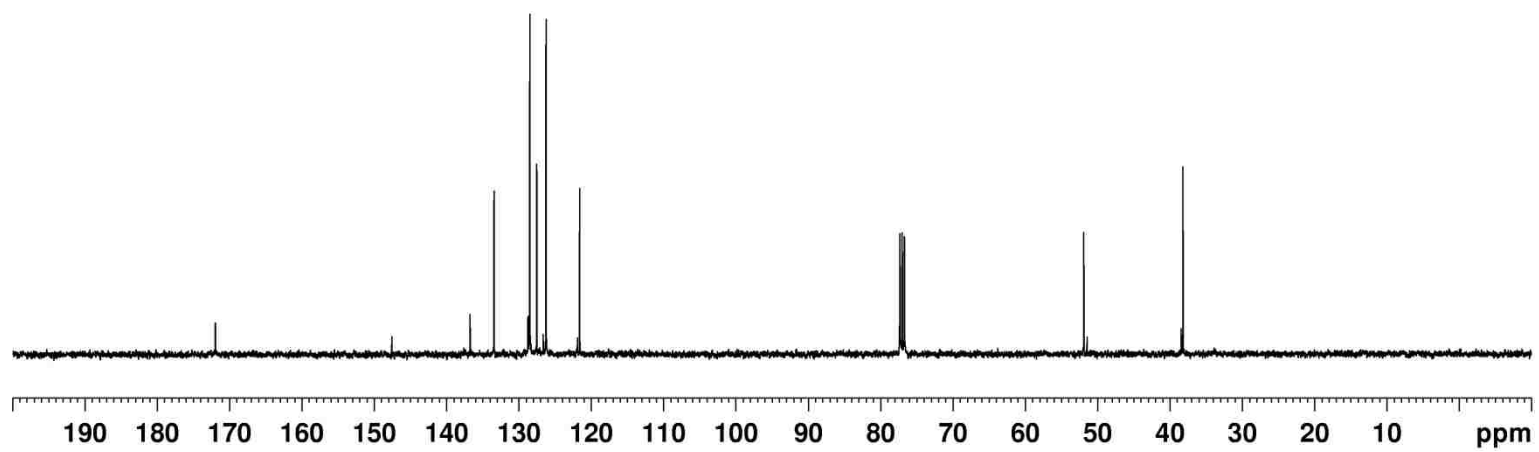
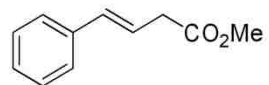
Compound **153** - ^1H NMR spectrum

DW-1-112Part3 in CDCl_3 (400 MHz)



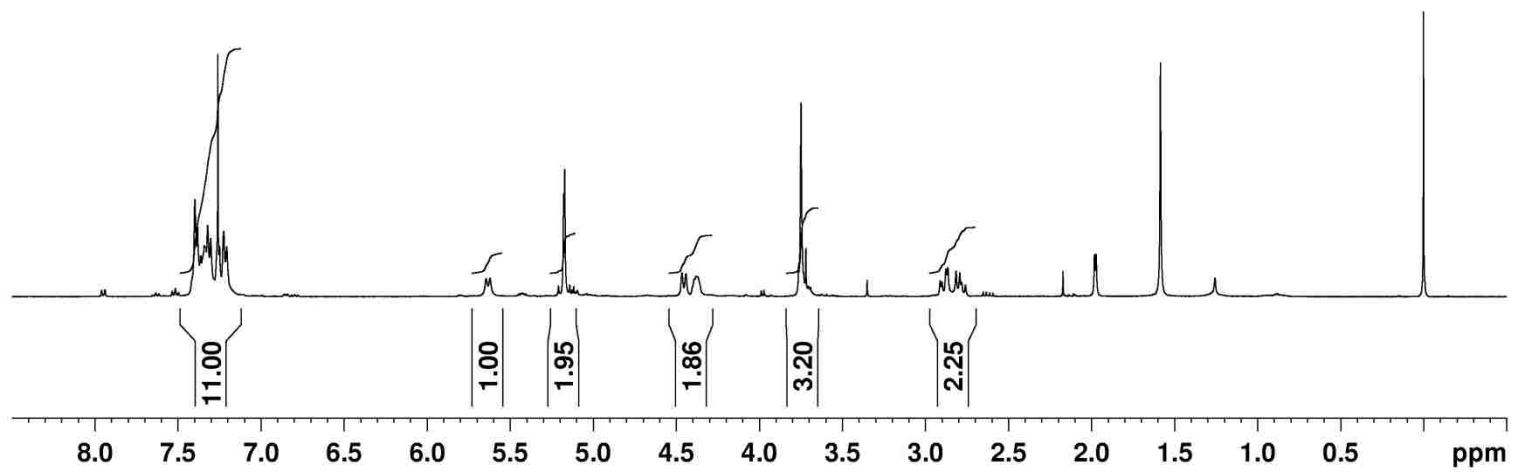
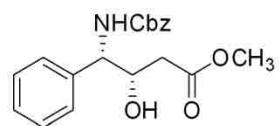
Compound **153** - ^{13}C NMR spectrum

DW-1-112Part3 in CDCl_3 (100 MHz)



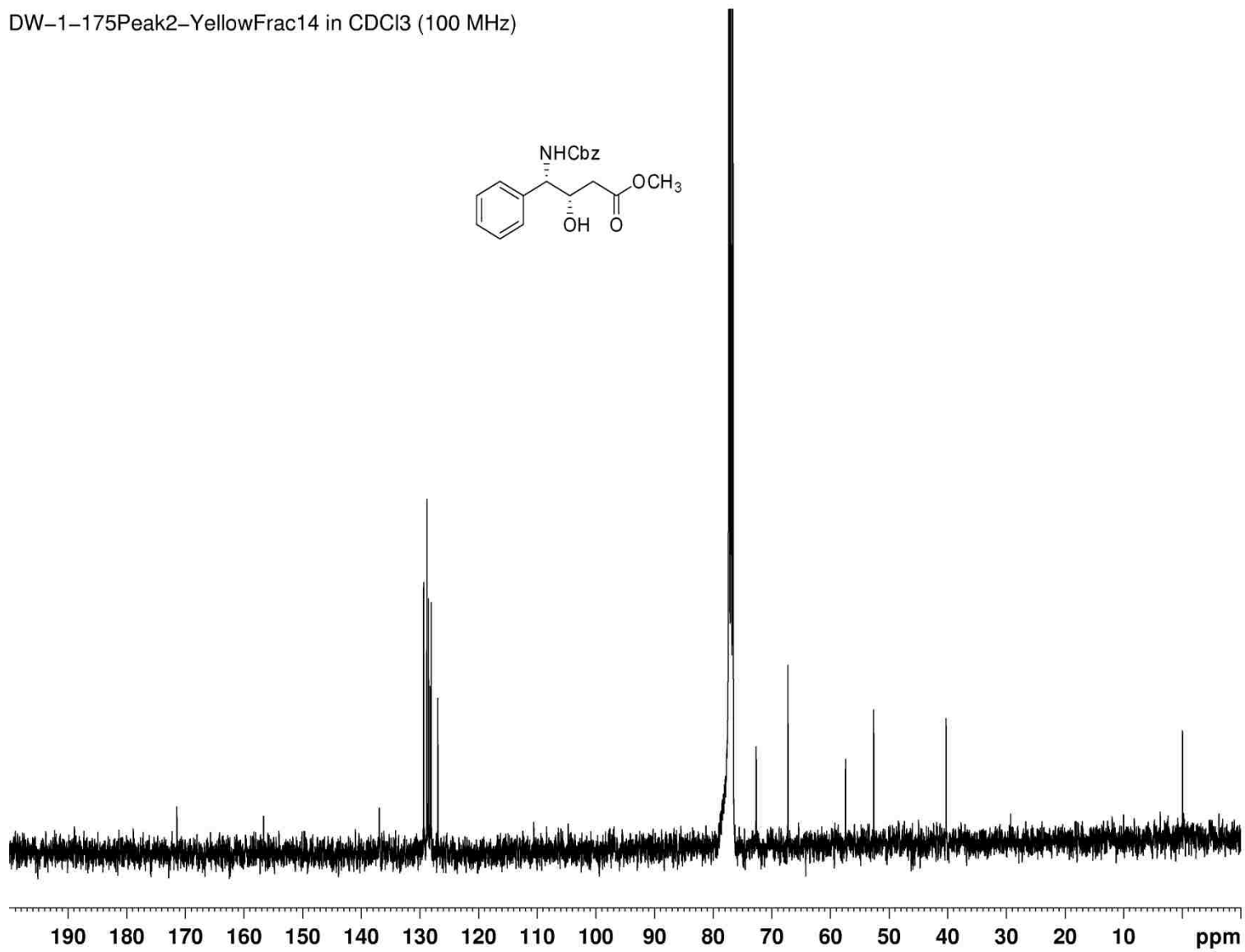
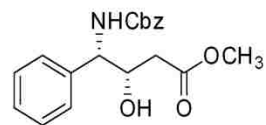
Compound **182** - ^1H NMR spectrum

DW-1-175Peak2 in CDCl₃ (400 MHz)



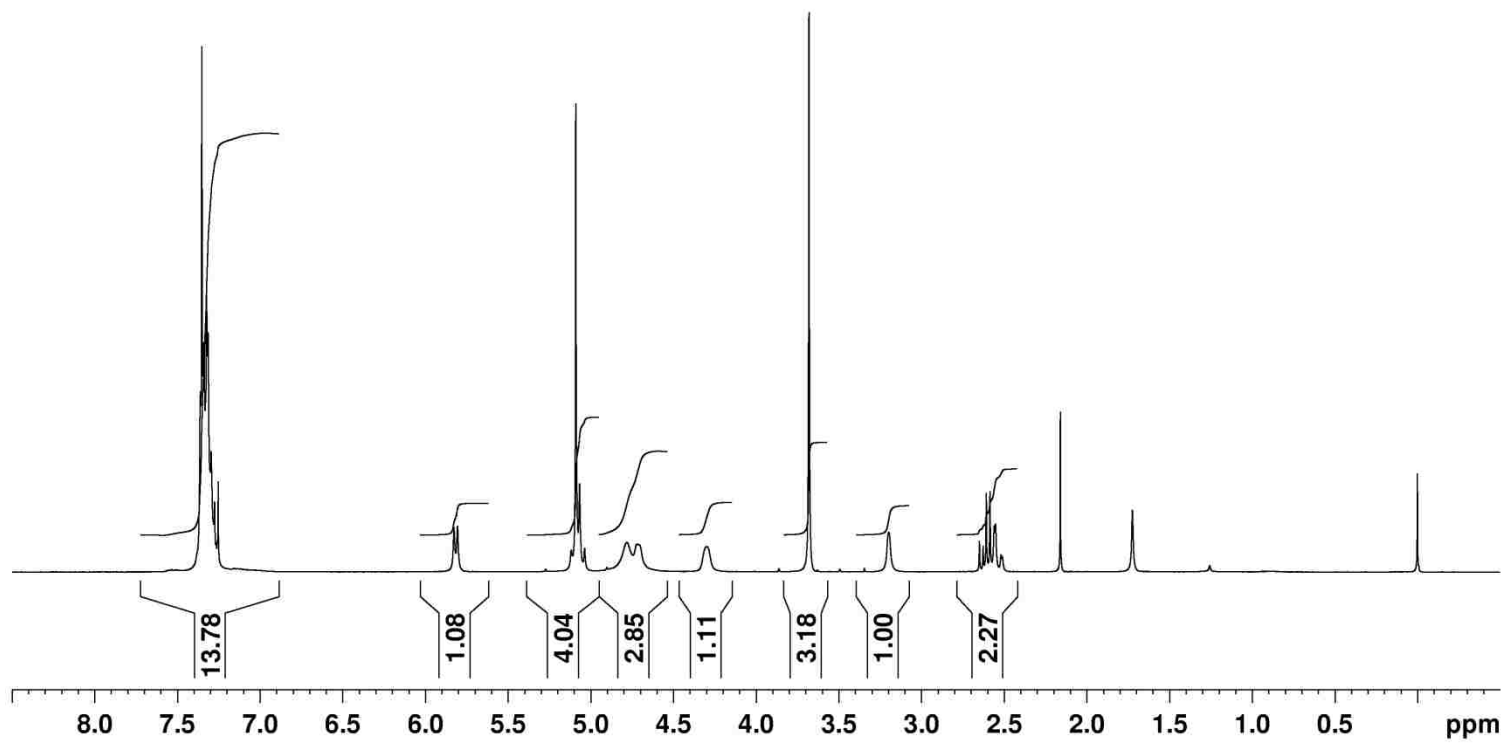
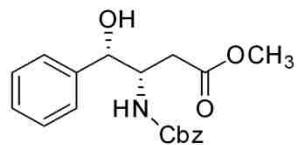
Compound **182** - ^{13}C NMR spectrum

DW-1-175Peak2-YellowFrac14 in CDCl_3 (100 MHz)



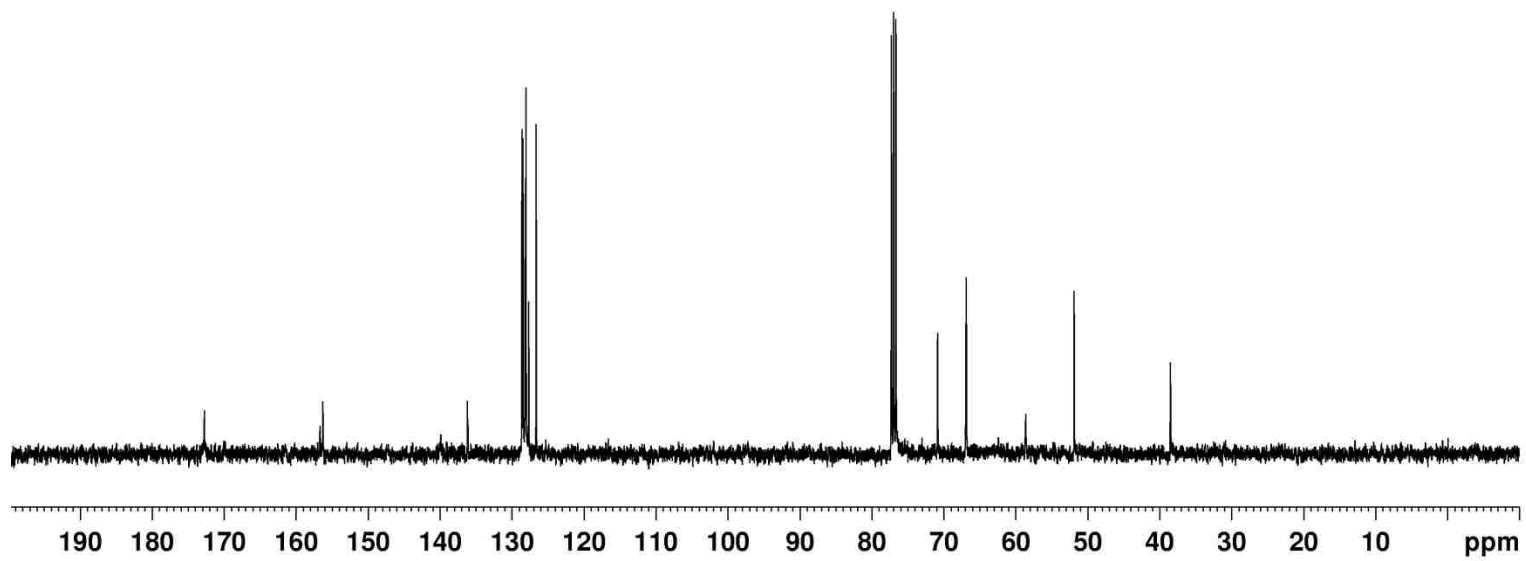
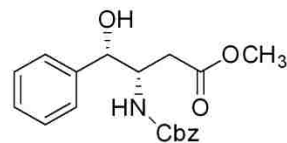
Compound **181** - ^1H NMR spectrum

DW-1-175Peak4 in CDCl_3 (400 MHz)



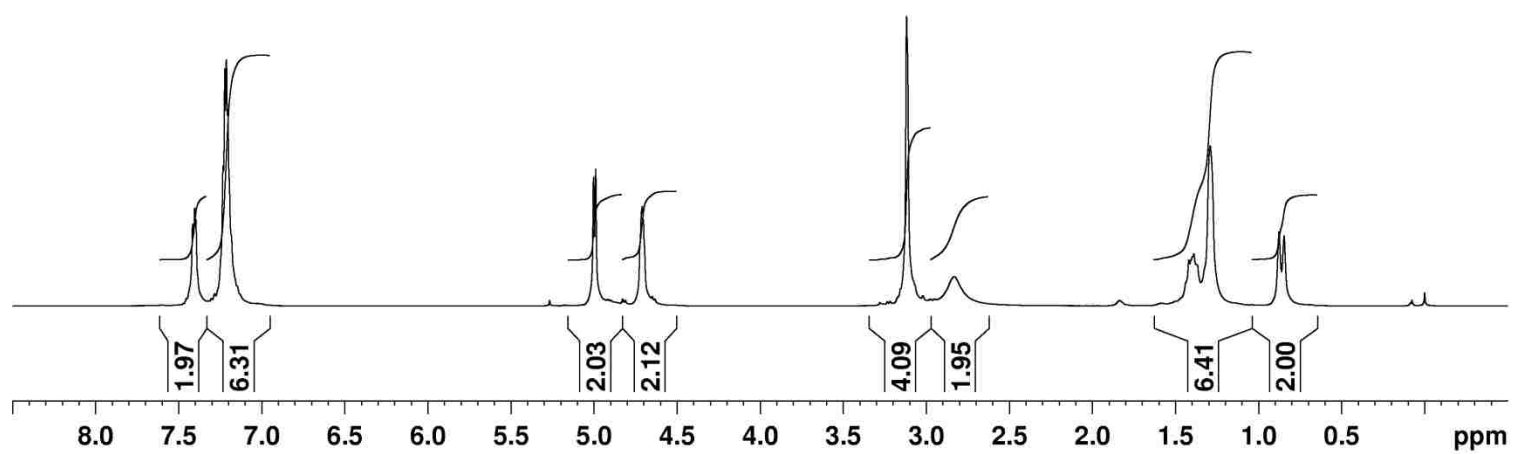
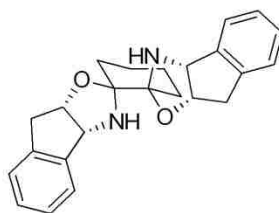
Compound **181** - ^{13}C NMR spectrum

DW-1-175Peak4 in CDCl₃ (100 MHz)



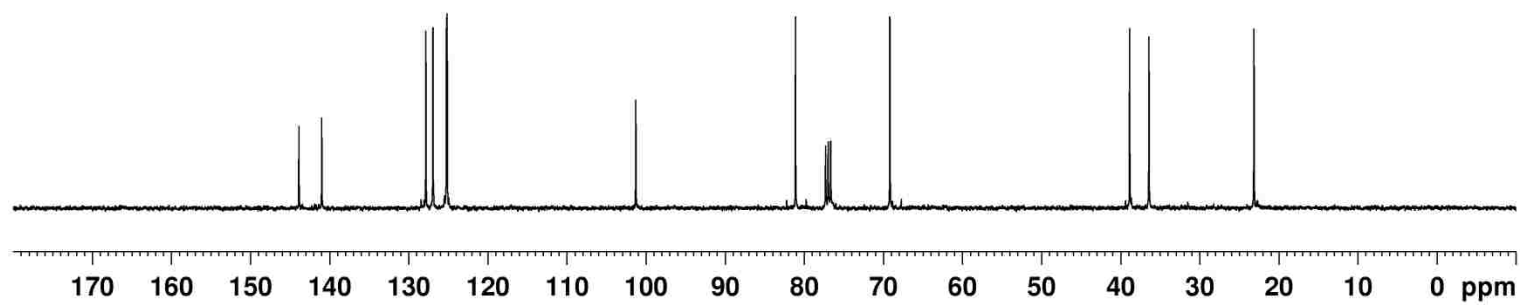
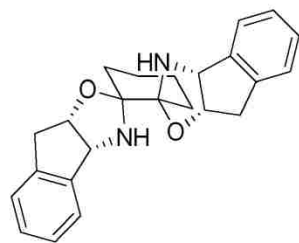
Compound **190** - ^1H NMR spectrum

DW-2-032Part2 in CDCl_3 (400 MHz)



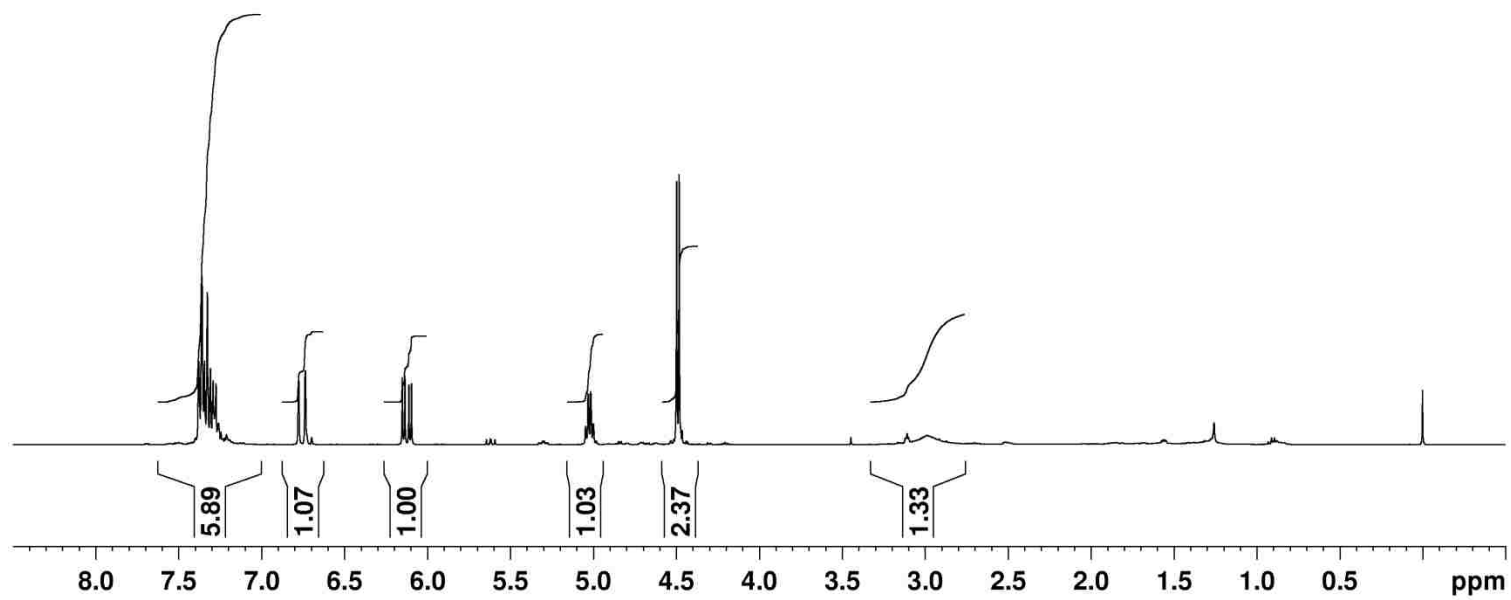
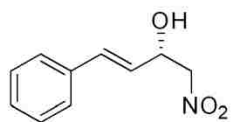
Compound **190** - ^{13}C NMR spectrum

DW-2-032Part2 in CDCl_3 (100 MHz)



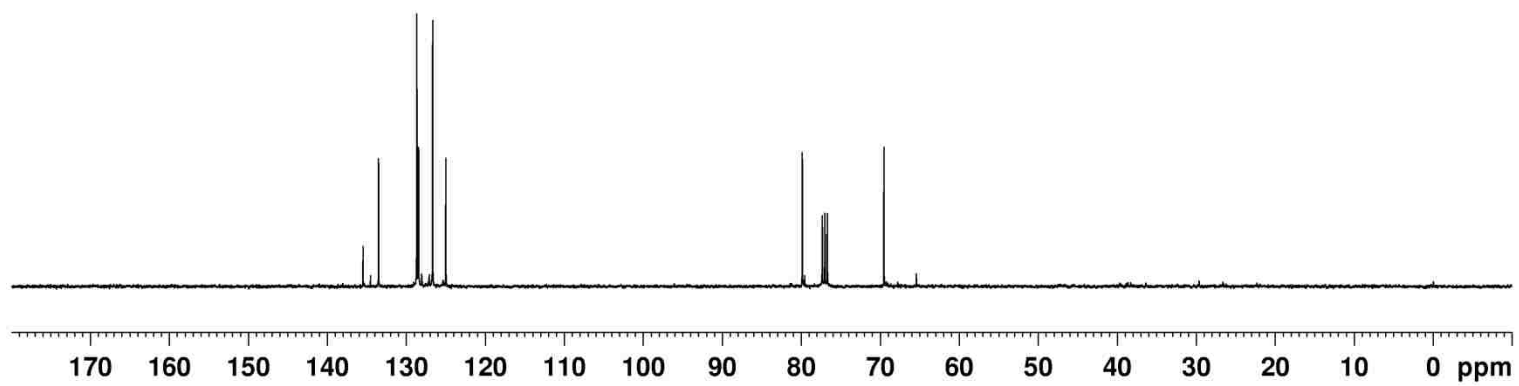
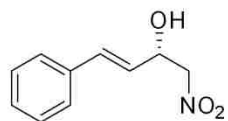
Compound **193h** - ^1H NMR spectrum

DW-2-040 in CDCl_3 (400 MHz)



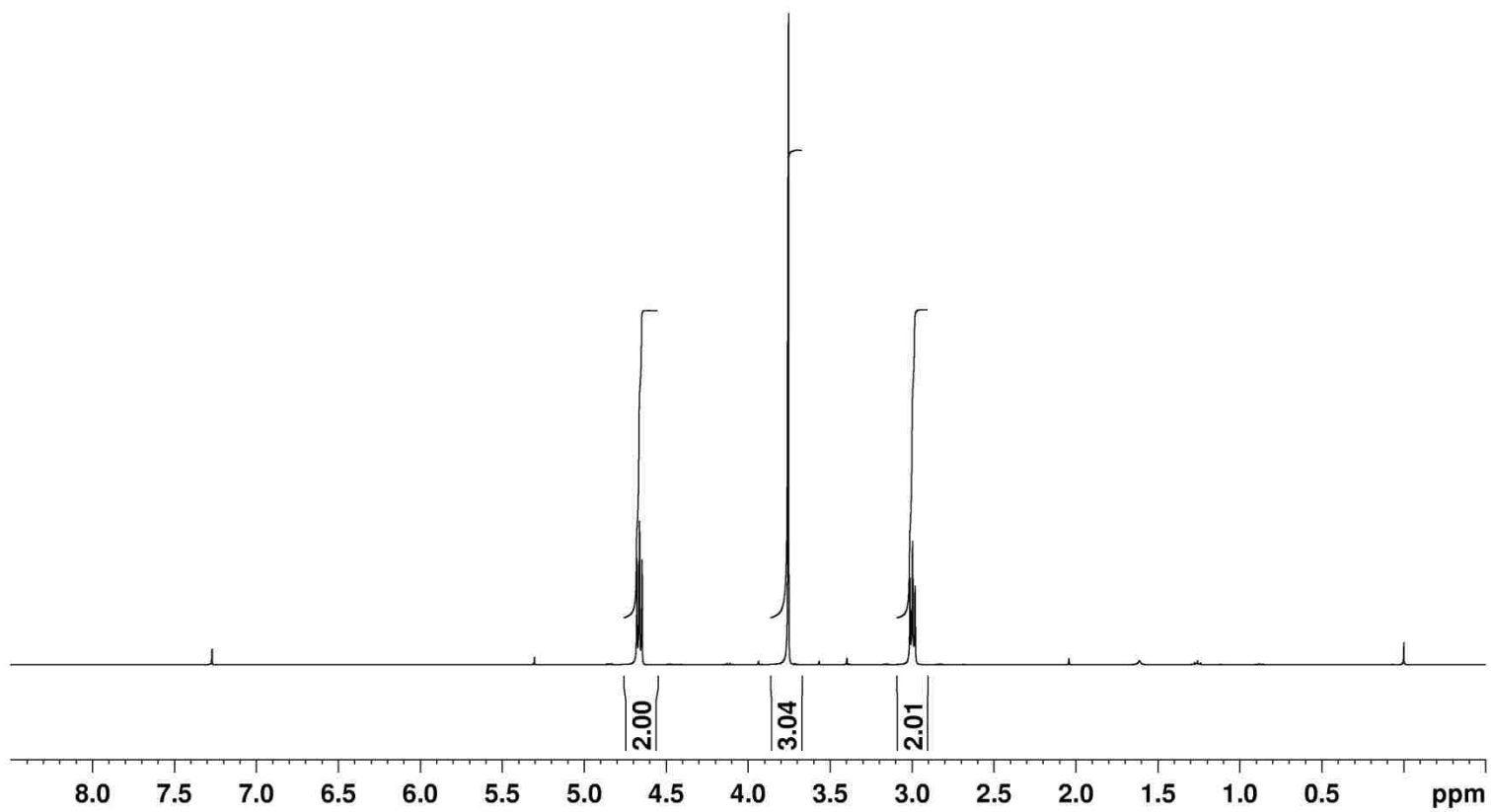
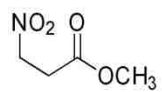
Compound **193h** - ^{13}C NMR spectrum

DW-2-040 in CDCl_3 (100 MHz)



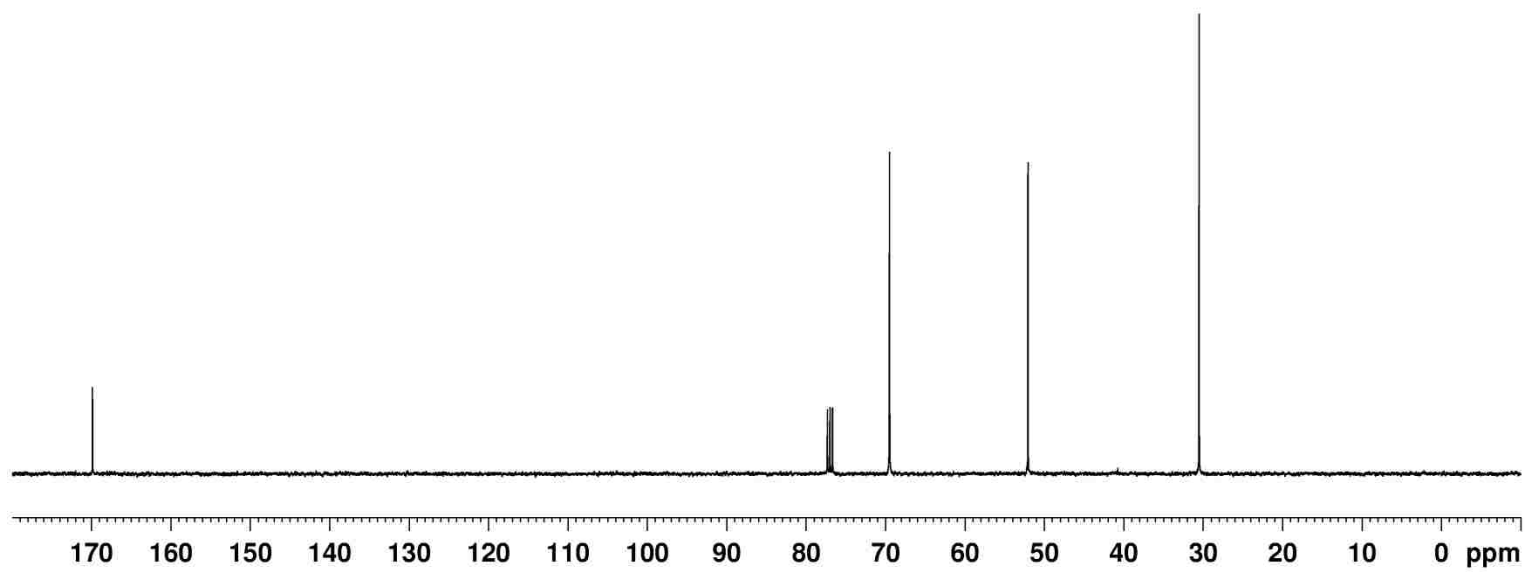
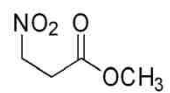
Compound **200** - ^1H NMR spectrum

DW-1-151 in CDCl_3 (400 MHz)



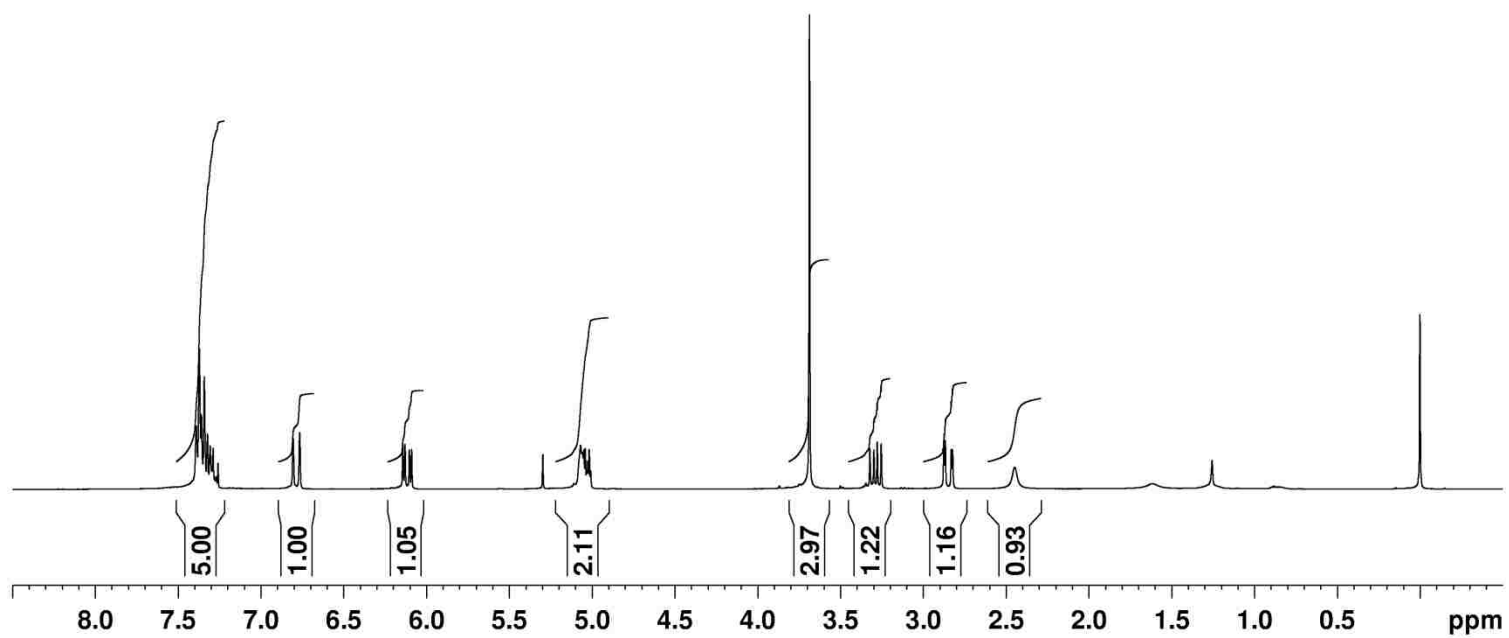
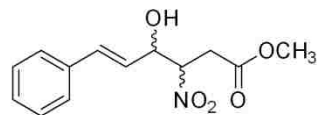
Compound **200** - ^{13}C NMR spectrum

RealNO2Purity in CDCl_3 (100 MHz)



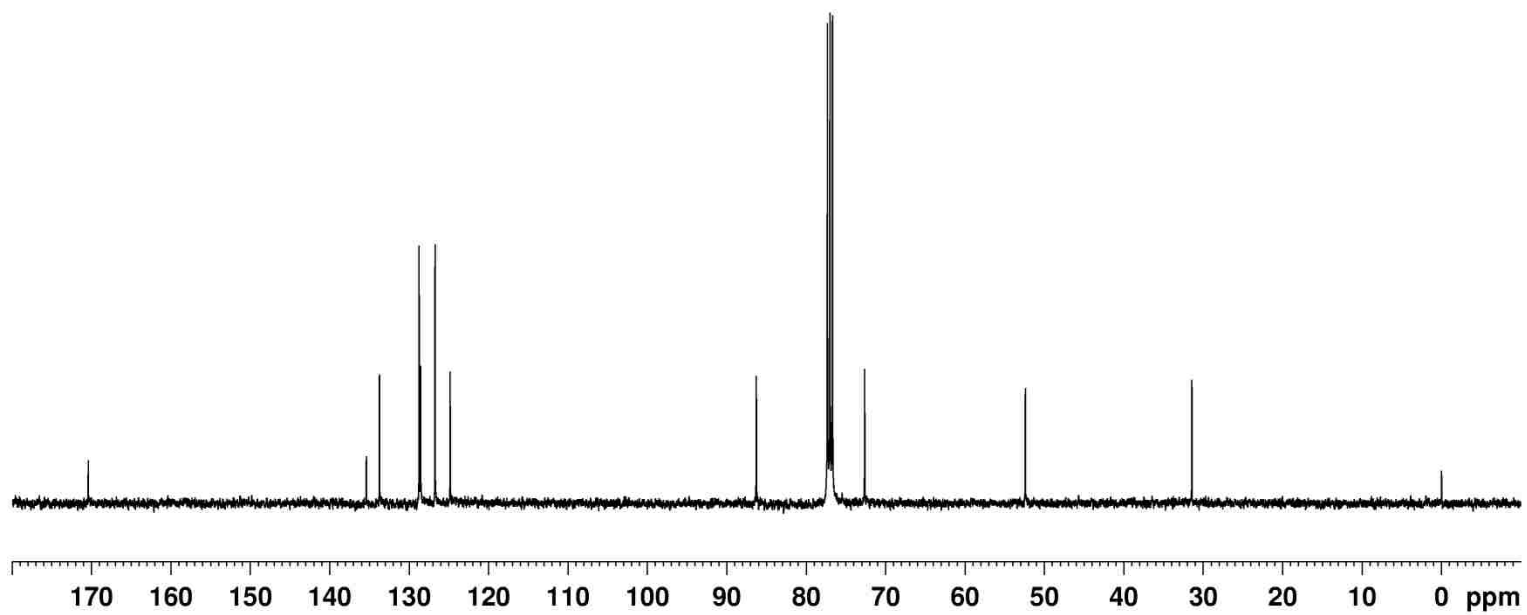
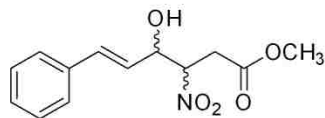
Compound **201 Diastereomer 1** - ^1H NMR spectrum

DW-2-051PureD1EarlierRetentionTime in CDCl_3 (400 MHz)



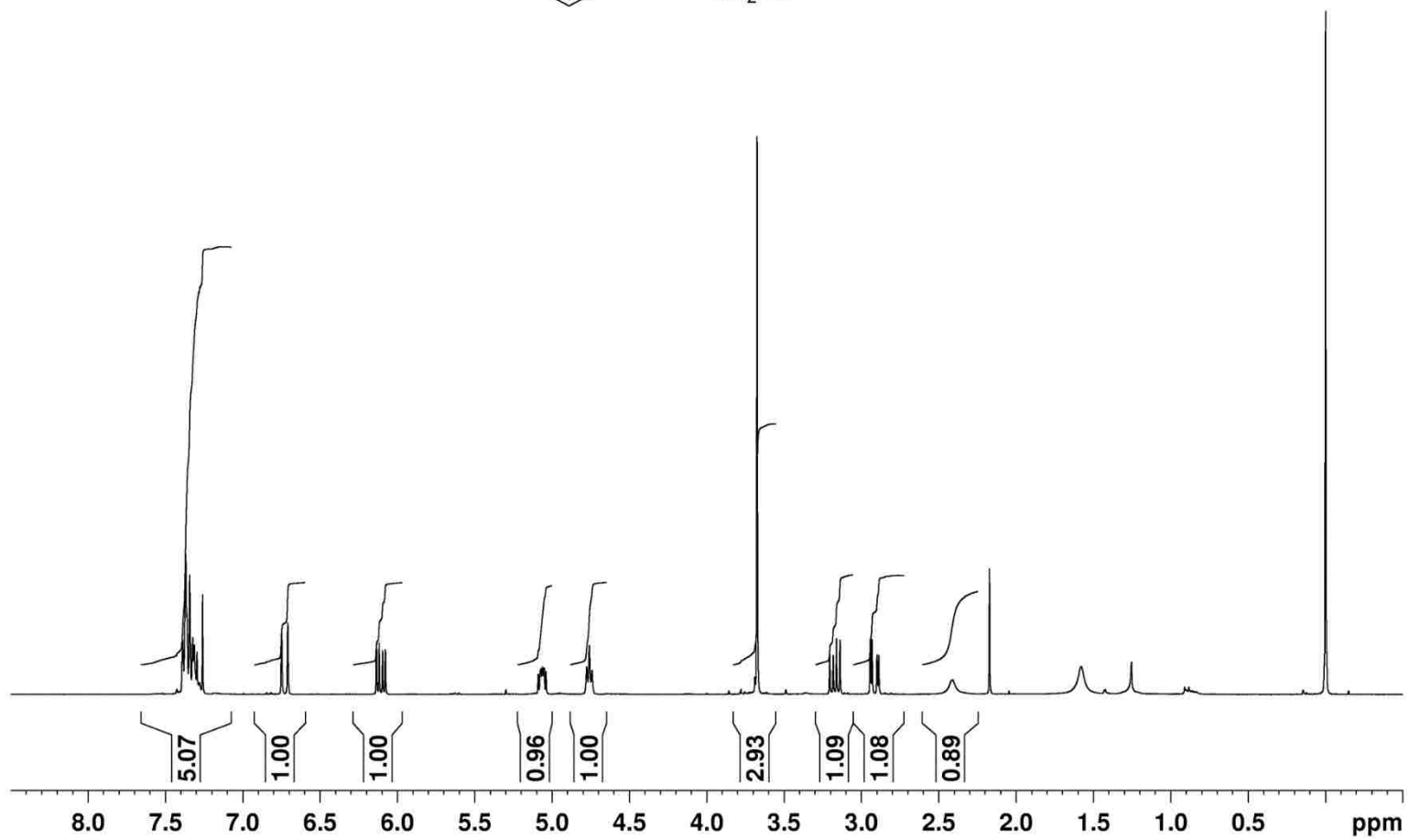
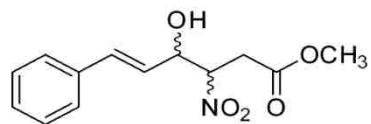
Compound **201 Diastereomer 1** - ^{13}C NMR spectrum

DW-2-051PureD1EarlierRetentionTime in CDCl_3 (100 MHz)



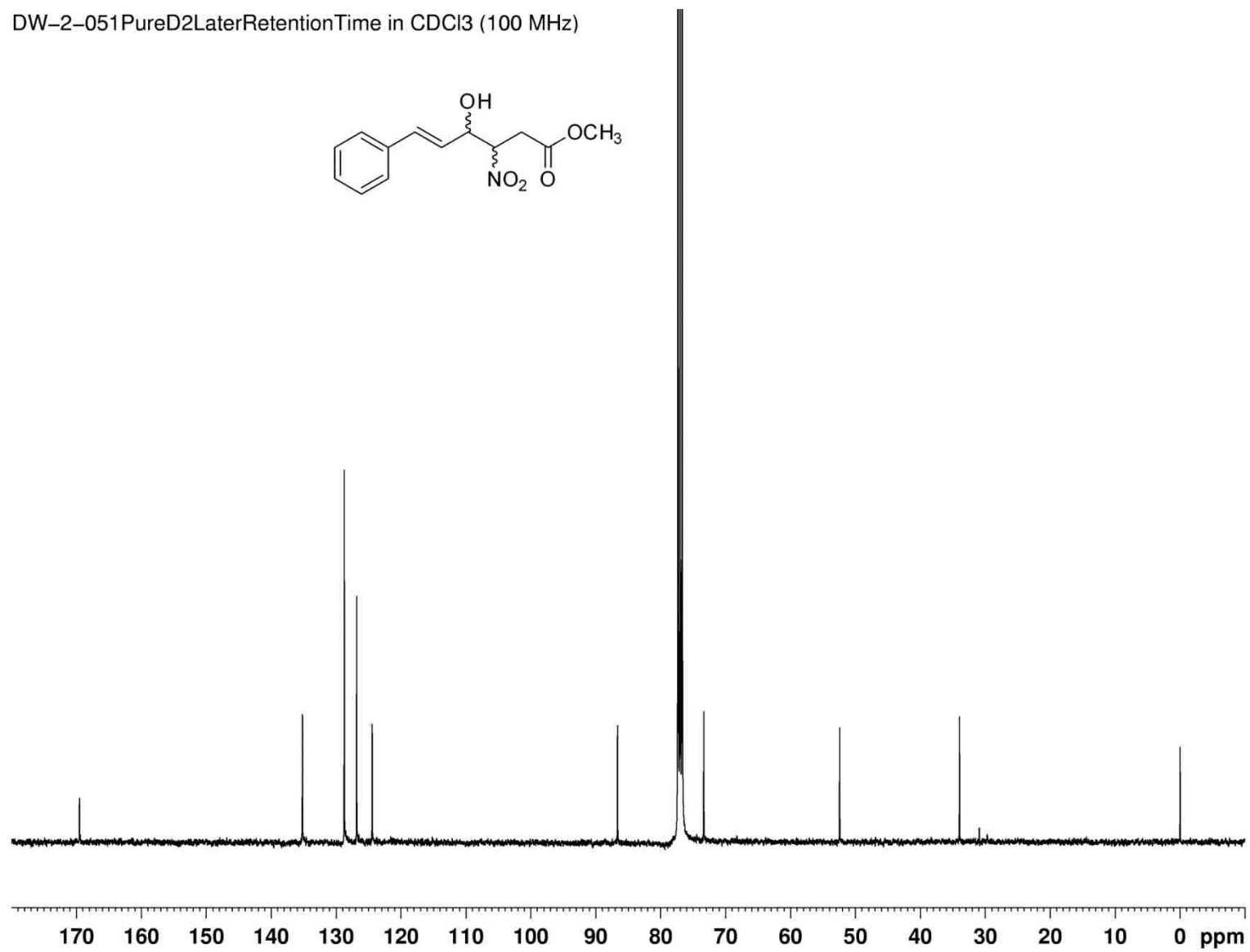
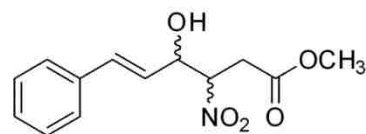
Compound **201 Diastereomer 2** - ^1H NMR spectrum

DW-2-051PureD2LaterRetentionTime in CDCl_3 (400 MHz)



Compound **201 Diastereomer 2** - ^{13}C NMR spectrum

DW-2-051PureD2LaterRetentionTime in CDCl_3 (100 MHz)



3.11 References

1. Tohdo, K.; Hamada, Y.; Shioiri, T.: Theonellamide F synthetic studies. Stereoselective synthesis of (3*S*,4*S*,5*E*,7*E*)-3-amino-8-(4-bromophenyl)-4-hydroxy-6-methyl-5,7-octadienoic acid (aboa). *Tetrahedron Lett.* **1992**, *33*, 2031-2034.
2. Wang, Z. M.; Zhang, X. L.; Sharpless, K. B.; Sinha, S. C.; Sinha-Bagchi, A.; Keinan, E.: A general approach to γ -lactones via osmium catalyzed asymmetric dihydroxylation. Synthesis of (-)- and (+)-muricatacin. *Tetrahedron Lett.* **1992**, *33*, 6407-6410.
3. Becker, H.; Soler, M. A.; Sharpless, K. B.: Selective asymmetric dihydroxylation of polyenes. *Tetrahedron.* **1995**, *51*, 1345-1376.
4. Zhang, Y.; O'Doherty, G. A.: Remote steric effect on the regioselectivity of Sharpless asymmetric dihydroxylation. *Tetrahedron.* **2005**, *61*, 6337-6351.
5. Tao, B.; Schlingloff, G.; Sharpless, K. B.: Reversal of regioselection in the asymmetric aminohydroxylation of cinnamates. *Tetrahedron Lett.* **1998**, *39*, 2507-2510.
6. Bodkin, J. A.; Bacskey, G. B.; McLeod, M. D.: The Sharpless asymmetric aminohydroxylation reaction: optimising ligand/substrate control of regioselectivity for the synthesis of 3- and 4-aminosugars. *Org. Biomol. Chem.* **2008**, *6*, 2544-2553.
7. Dethe, D. H.; Ranjan, A.; Pardeshi, V. H.: Asymmetric first total syntheses and assignment of absolute configuration of oxazin-5, oxazin-6, and preoxazin-7. *Org. Biomol. Chem.* **2011**, *9*, 7990-7992.
8. Konno, H.; Aoyama, S.; Nosaka, K.; Akaji, K.: Stereoselective synthesis of β -methoxytyrosine derivatives for identification of the absolute configuration of callipeltin E. *Synthesis.* **2007**, 3666-3672.
9. Guzman-Martinez, A.; Lamer, R.; VanNieuwenhze, M. S.: Total synthesis of lysobactin. *J. Am. Chem. Soc.* **2007**, *129*, 6017-6021.
10. Tao, J.; Hu, S.; Pacholec, M.; Walsh, C. T.: Synthesis of proposed oxidation-cyclization-methylation intermediates of the coumarin antibiotic biosynthetic pathway. *Org. Lett.* **2003**, *5*, 3233-3236.
11. Cao, B.; Park, H.; Joullié, M. M.: Total synthesis of ustiloxin D. *J. Am. Chem. Soc.* **2002**, *124*, 520-521.
12. Pearson, A. J.; Zigmantas, S.: Synthetic studies on the BCDF ring system of ristocetin A via ruthenium-promoted S_NAr reaction. *Tetrahedron Lett.* **2001**, *42*, 8765-8768.
13. Park, H.; Cao, B.; Joullié, M. M.: Regioselective asymmetric aminohydroxylation approach to a β -hydroxyphenylalanine derivative for the synthesis of ustiloxin D. *J. Org. Chem.* **2001**, *66*, 7223-7226.

14. Nicolaou, K. C.; Natarajan, S.; Li, H.; Jain, N. F.; Hughes, R.; Solomon, M. E.; Ramanjulu, J. M.; Boddy, C. N. C.; Takayanagi, M.: Total synthesis of vancomycin aglycon-part 1: synthesis of amino acids 4-7 and construction of the AB-COD ring skeleton. *Angew. Chem. Int. Ed.* **1998**, *37*, 2708-2714.
15. Koketsu, K.; Oguri, H.; Watanabe, K.; Oikawa, H.: Identification and stereochemical assignment of the β -hydroxytryptophan intermediate in the echinomycin biosynthetic pathway. *Org. Lett.* **2006**, *8*, 4719-4722.
16. Wen, S. J.; Yao, Z. J.: Total synthesis of cyclomarin C. *Org. Lett.* **2004**, *6*, 2721-2724.
17. Feldman, K. S.; Karatjas, A. G.: Extending Pummerer reaction chemistry. Application to the oxidative cyclization of tryptophan derivatives. *Org. Lett.* **2004**, *6*, 2849-2852.
18. Sugiyama, H.; Shioiri, T.; Yokokawa, F.: Syntheses of four unusual amino acids, constituents of cyclomarin A. *Tetrahedron Lett.* **2002**, *43*, 3489-3492.
19. Davey, R. M.; Brimble, M. A.; McLeod, M. D.: Regioselective asymmetric aminohydroxylation of precursors to 2,3,6-trideoxy-3-aminohexoses. *Tetrahedron Lett.* **2000**, *41*, 5141-5145.
20. Panek, J. S.; Masse, C. E.: Total synthesis of (+)-lactacystin. *Angew. Chem. Int. Ed.* **1999**, *38*, 1093-1095.
21. Schmitt, E. K.; Riwanto, M.; Sambandamurthy, V.; Roggo, S.; Miault, C.; Zwingelstein, C.; Krastel, P.; Noble, C.; Beer, D.; Rao, S. P. S.; Au, M.; Niyomrattanakit, P.; Lim, V.; Zheng, J.; Jeffery, D.; Pethe, K.; Camacho, L. R.: The natural product cyclomarin kills *Mycobacterium tuberculosis* by targeting the ClpC1 subunit of the caseinolytic protease. *Angew. Chem. Int. Ed.* **2011**, *50*, 5889-5891.
22. Bodkin, J. A.; McLeod, M. D.: The Sharpless asymmetric aminohydroxylation. *J. Chem. Soc., Perkin Trans. 1.* **2002**, 2733-2746.
23. Reddy, M. P.; Rao, G. S. K.: One step Vilsmeier route to some 5-aryl-3-methyl-2(*E*),4(*E*)-pentadienals and their oxidation to pentadienoic acids. *Synthesis.* **1980**, 815-818.
24. Kann, N.; Rein, T.; Aakermark, B.; Helquist, P.: New functionalized Horner-Wadsworth-Emmons reagents: useful building blocks in the synthesis of polyunsaturated aldehydes. A short synthesis of (\pm)-(*E,E*)-coriolic acid. *J. Org. Chem.* **1990**, *55*, 5312-5323.
25. Maj, J.; Morzycki, J. W.; Rarova, L.; Wasilewski, G.; Wojtkielewicz, A.: A cross-metathesis approach to the synthesis of new etretinate type retinoids, ethyl retinoate and its 9*Z*-isomer. *Tetrahedron Lett.* **2012**, *53*, 5430-5433.
26. Maryanoff, B. E.; Reitz, A. B.; Duhl-Emswiler, B. A.: Stereochemistry of the Wittig reaction. Effect of nucleophilic groups in the phosphonium ylide. *J. Am. Chem. Soc.* **1985**, *107*, 217-226.
27. Ragoussis, N.: Modified Knoevenagel condensations. Synthesis of (*E*)-3-alkenoic acids. *Tetrahedron Lett.* **1987**, *28*, 93-96.

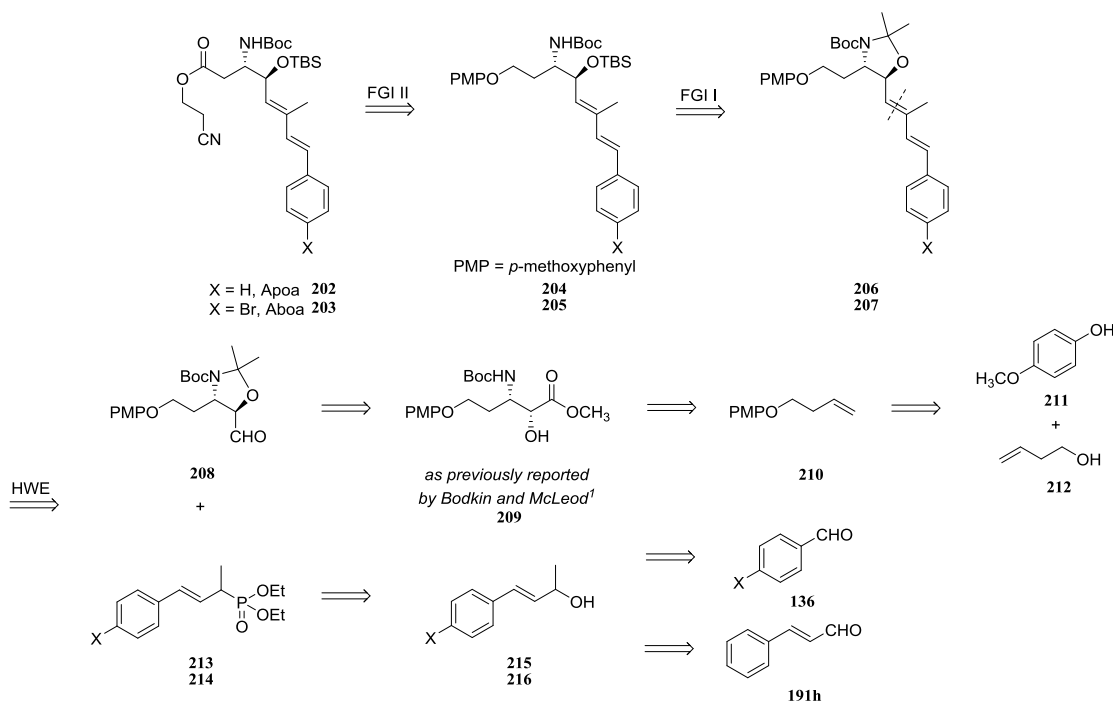
28. Ragoussis, N.; Ragoussis, V.: Improvement on the synthesis of (*E*)-alk-3-enoic acids. *J. Chem. Soc., Perkin Trans. I.* **1998**, 3529-3533.
29. Liegault, B.; Lee, D.; Huestis, M. P.; Stuart, D. R.; Fagnou, K.: Intramolecular Pd (II)-catalyzed oxidative biaryl synthesis under air: reaction development and scope. *J. Org. Chem.* **2008**, *73*, 5022-5028.
30. Shibasaki, M. *Books of Abstracts*, 235th ACS National Meeting, New Orleans, LA, April 6-10, 2008; American Chemical Society: Washington, DC, 2008; ORGN 200.
31. Henry, L. C. R.: *Acad. Sci. Ser. C* **1895**, *120*, 1258-1265.
32. Henry, L.: *Bull. Soc. Chim. Fr.* **1895**, *13*, 999-1004.
33. Luzzio, F. A.: The Henry reaction: recent examples. *Tetrahedron.* **2001**, *57*, 915-945.
34. Simoni, D.; Invidiata, F. P.; Manfredini, S.; Ferroni, R.; Lampronti, I.; Roberti, M.; Pollini, G. P.: Facile synthesis of 2-nitroalkanols by tetramethylguanidine (TMG)-catalyzed addition of primary nitroalkanes to aldehydes and alicyclic ketones. *Tetrahedron Lett.* **1997**, *38*, 2749-2752.
35. Ballini, R.; Bosica, G.; Parrini, M.: Fast nitroaldol reaction using powdered KOH in dry media. *Chem. Lett.* **1999**, 1105-1106.
36. Jenner, G.: Effect of high pressure on Michael and Henry reactions between ketones and nitroalkanes. *New J. Chem.* **1999**, *23*, 525-529.
37. Sasai, H.; Suzuki, T.; Arai, S.; Arai, T.; Shibasaki, M.: Basic character of rare earth metal alkoxides. Utilization in catalytic carbon-carbon bond-forming reactions and catalytic asymmetric nitroaldol reactions. *J. Am. Chem. Soc.* **1992**, *114*, 4418-4420.
38. Walsh, P. J.; Kowzowski, M. C.: *Fundamentals of Asymmetric Catalysis*; University Science Books: California, 2009; p 416-417.
39. Wolf, C.; Liu, S.: Bisoxazolidine-catalyzed enantioselective alkynylation of aldehydes. *J. Am. Chem. Soc.* **2006**, *128*, 10996-10997.
40. Liu, S.; Wolf, C.: Asymmetric nitroaldol reaction catalyzed by a C₂-symmetric bisoxazolidine ligand. *Org. Lett.* **2008**, *10*, 1831-1834.
41. Liu, S.; Wolf, C.: Chiral amplification based on enantioselective dual-phase distribution of a scalemic bisoxazolidine catalyst. *Org. Lett.* **2007**, *9*, 2965-2968.
42. Wolf, C.; Moskowicz, M.: Bisoxazolidine-catalyzed enantioselective Reformatsky reaction. *J. Org. Chem.* **2011**, *76*, 6372-6376.
43. Spangler, K. Y.; Wolf, C.: Asymmetric copper(I)-catalyzed Henry reaction with an aminoindanol-derived bisoxazolidine ligand. *Org. Lett.* **2009**, *11*, 4724-4727.

44. Wolf, C.; Xu, H.: Asymmetric catalysis with chiral oxazolidine ligands. *Chem. Commun.* **2011**, 47, 3339-3350.
45. Kim, H. Y.; Oh, K.: Brucine-derived amino alcohol catalyzed asymmetric Henry reaction: an orthogonal enantioselectivity approach. *Org. Lett.* **2009**, 11, 5682-5685.
46. Rodriguez, A.; Nomen, M.; Spur, B. W.; Godfroid, J. J.: A selective method for the preparation of aliphatic methyl esters in the presence of aromatic carboxylic acids. *Tetrahedron Lett.* **1998**, 39, 8563-8566.
47. Mintz, M.; Walling, C.: *Org. Synth., Coll. Vol. 5*, **1973**, 184.

CHAPTER 4: RECENT APPROACHES TO THE SYNTHESIS OF APOA AND ABOA

4.1 The Third Approach to the Synthesis of Aboa and Apoa

In chapter 3, we described two approaches to Aboa in which the key reactions were an asymmetric aminohydroxylation and a nitroaldol condensation. Our third approach to produce appropriately protected Apoa/Aboa **202/203** included late stage installation of the aromatic conjugated diene fragment via a Horner-Wadsworth Emmons (HWE) reaction (Scheme 4.1). In a forward sense, an HWE reaction followed by two conceptual sets of protecting group manipulations (designated FGI I and II in Scheme 4.1) should provide target compound **202/203**. Specifically, liberation of the vicinal amino-alcohol moiety via oxazolidine deprotection followed by protection of the newly formed secondary alcohol as its TBS ether. The other set of transformations include removal of the *para*-methoxyphenyl ether which reveals a primary alcohol that can be fully oxidized and protected as its β -cyano ethyl ester. The key HWE step was scheduled to maximize convergency, adaptable to the synthesis of the two congeners, Apoa and Aboa.

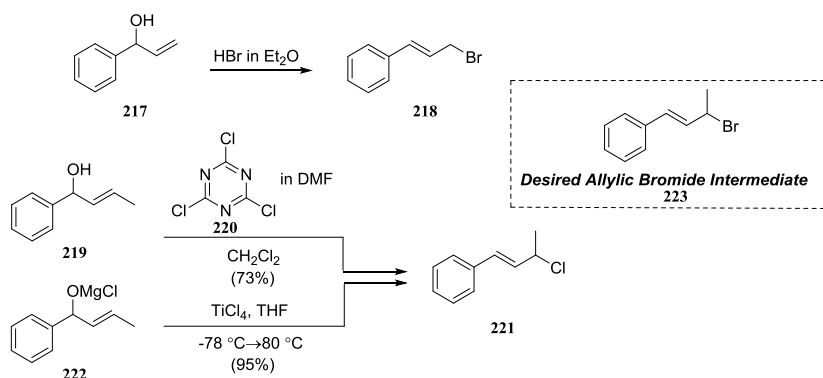


Scheme 4.1 – The Third Retrosynthesis of Aboa and Apoa

The HWE reaction partners are aldehyde **208** and phosphonate ester **213** (Apoa) or **214** (Aboa). Retrosynthetically, aldehyde **208** can be acquired from β -amino alcohol **209**, which in turn can be further simplified to commercially available *p*-methoxyphenol and but-3-en-1-ol as reported previously by Bodkin and McLeod¹. Oxazolidine protection of **209** followed by a methyl ester reduction/oxidation sequence generates **208**. Phosphonate esters **213** and **214** can be derived from their corresponding allylic alcohols leading directly to different starting material for Aboa and Apoa. In a forward sense, Apoa's allylic alcohol intermediate **215** results from Grignard reaction of *trans*-cinnamaldehyde with MeMgBr, whereas Aboa's allylic alcohol intermediate **216** requires Wittig reaction of *p*-bromobenzaldehyde with diethyl (2-oxopropyl)phosphonate followed by carbonyl reduction. The allylic alcohols **215/216** can be converted to their halogenated derivatives followed by an Arbuzov reaction to produce the respective phosphonate esters **213** and **214**.

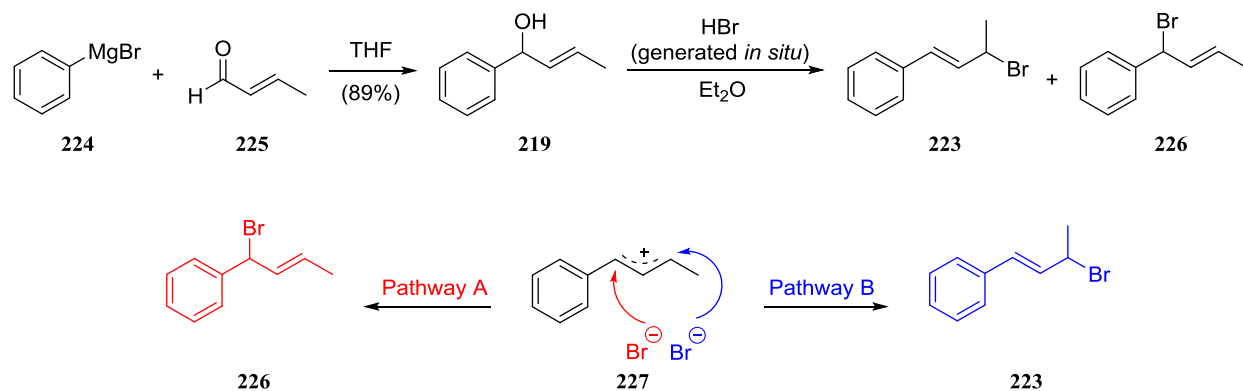
4.2 Preparation of the Phosphonate Ester Fragments for Aboa and Apoa Synthesis

The assembly of phosphonate **213** for Apoa synthesis was initially carried out by Alex Nguyen. The formation of bromide **223** should occur through S_N1 addition of bromide to the oxonium ion generated from **219**. White and Fife prepared *m*- and *p*-substituted cinnamyl bromides by combining benzyl alcohols with HBr in ether to give the rearranged allylic bromide in a S_N1 reaction (Scheme 4.2).² Hirabe *et al.* synthesized the unsubstituted cinnamyl bromide in an analogous fashion.³ The allylic chloride **221**, a highly relevant derivative, prepared via S_N1 reaction has also been reported.^{4,5}



Scheme 4.2 – Precedents for the Proposed S_N1 Reaction

Phosphonate **213** synthesis commenced with Grignard addition of phenylmagnesium bromide to crotonaldehyde which gave benzylic alcohol **219** in 89% yield (Scheme 4.3). The reaction of **219** in diethyl ether, saturated with anhydrous HBr, gave an inseparable mixture of regioisomeric bromides **223** and **226**. The desired allylic bromide **223** was accompanied by a second allylic bromide **226** obtained via S_N1 displacement. The **223/226** product distribution was 2.3/1.0 as indicated by ¹H NMR. Specifically, comparing integrals for the methyl protons in **223** and **226** led to this conclusion.

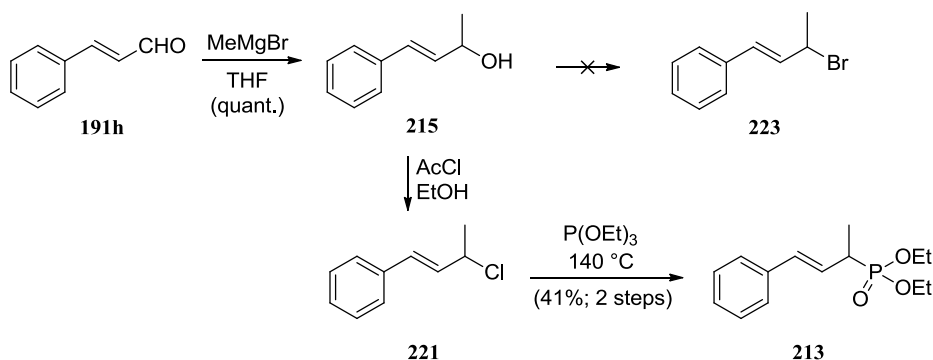


Scheme 4.3 – Competing Mechanistic Pathways for the Bromination Reaction

The revised synthesis of phosphonate **213** started with Grignard addition of methylmagnesium bromide to *trans*-cinnamaldehyde to form allylic alcohol **215** in quantitative yield (Scheme 4.4). Conversion of **215** to allylic bromide **223** with the use of AcBr/EtOH provided a similar mixture of bromides as observed in Scheme 4.3. Alternative bromination protocols including the use of CBr₄/PPh₃,⁶ CBr₄/PPh₃/imidazole,⁷ and (CH₃)₃SiCl/LiBr⁸ did not give the desired product. We resorted to the generation of allylic chloride **221** as reported by Yadav and Babu⁹ in near quantitative yield. The instability of the allylic chloride to silica precluded the use of chromatography to monitor the reaction or purify the product.

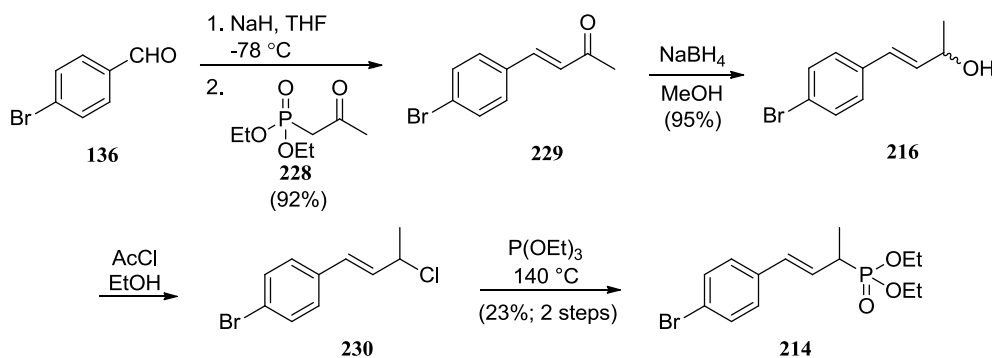
The poor regioselectivity in the bromination of **215** is in contrast to that observed from the corresponding chlorination. The bromide intermediate would likely benefit the subsequent Arbuzov

reaction due to the greater leaving group ability of Br^- relative to Cl^- . The modest yield for phosphonate ester **213** (41%) derived from the chlorination approach left a lot to be desired. However, **213** could be obtained in two steps (both conducted on gram scale) from commercially available starting material.



Scheme 4.4 – Synthesis of the Phosphonate Ester Fragment for Apoa

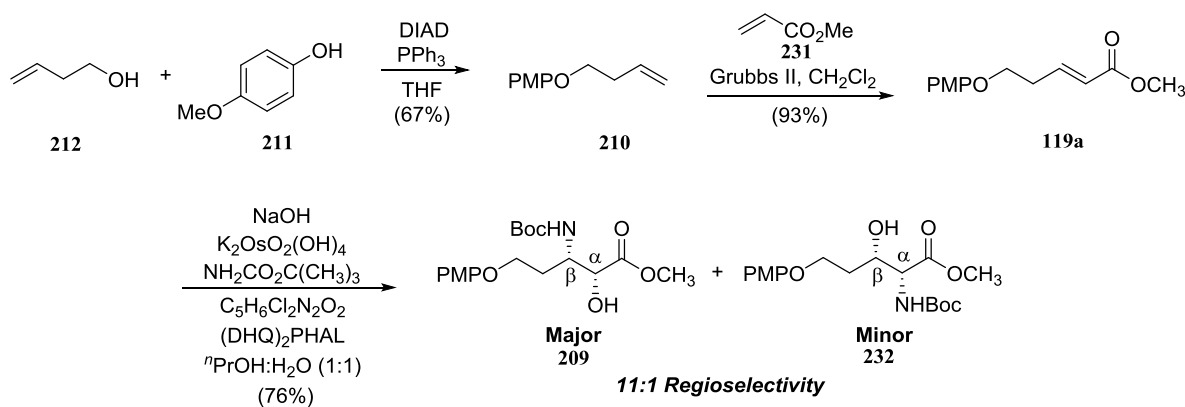
The synthesis of the phosphonate ester for Aboa is shown in Scheme 4.5. Wittig olefination between *p*-bromobenzaldehyde and diethyl (2-oxopropyl)phosphonate produced α,β -unsaturated ketone **229** which was reduced to the corresponding allylic alcohol **216** using NaBH_4 . Chlorination of **216** followed by the use of $\text{P}(\text{OEt})_3$ in the Arbuzov reaction as prescribed above formed the desired phosphonate ester **214**, albeit in significantly lower yield than for the non-brominated analog.



Scheme 4.5 – Synthesis of the Phosphonate Ester Fragment for Aboa

4.3 Preparation of the Aldehyde Fragment for Aboa and Apoa Synthesis

N-Boc protected amino alcohol **209** (Scheme 4.6) had been prepared previously by Bodkin and McLeod for their synthesis of 3- and 4-aminosugar derivatives.¹ Mitsunobu etherification of *p*-methoxyphenol and but-3-en-1-ol generated **210** which underwent cross metathesis with methyl acrylate to yield α,β -unsaturated methyl ester **119a**. In our hands, the SAH using the (DHQ)₂PHAL ligand afforded β -amino alcohol **209** in 76% yield. As mentioned previously, Bodkin and McLeod proposed that selectivity for the β -amino regioisomer originates from a mode of binding in which the *p*-methoxyphenyl group undergoes “stabilizing interactions with the methoxyquinoline rings of the catalyst.”



Scheme 4.6 – Synthesis of β -amino alcohol **209**

The purification of **209** proved to be very difficult for a number of reasons. In practice, two chromatographic steps were required for purification. The first chromatographic separation eliminated everything less polar than *tert*-butyl carbamate and more polar than the two regioisomeric products. A second chromatographic separation was necessary to remove *tert*-butyl carbamate from the mixture of regioisomers. Flash chromatography to completely separate the two regioisomers proved to be impossible using hexane/ethyl acetate mixtures. We resorted to preparative HPLC to achieve separation of the regioisomers. Chiral HPLC of regioisomerically pure **209** on a Daicel Chiralcel OD-H was used to determine levels of enantioselectivity. Peaks were assigned based on comparison of retention times put forth by McLeod and co-workers.¹ At this point, chiral HPLC showed the purified β -amino alcohol and

its enantiomer (Figure 4.1). Gratifyingly, the purified material was obtained with excellent enantioselectivity (98.50 %).

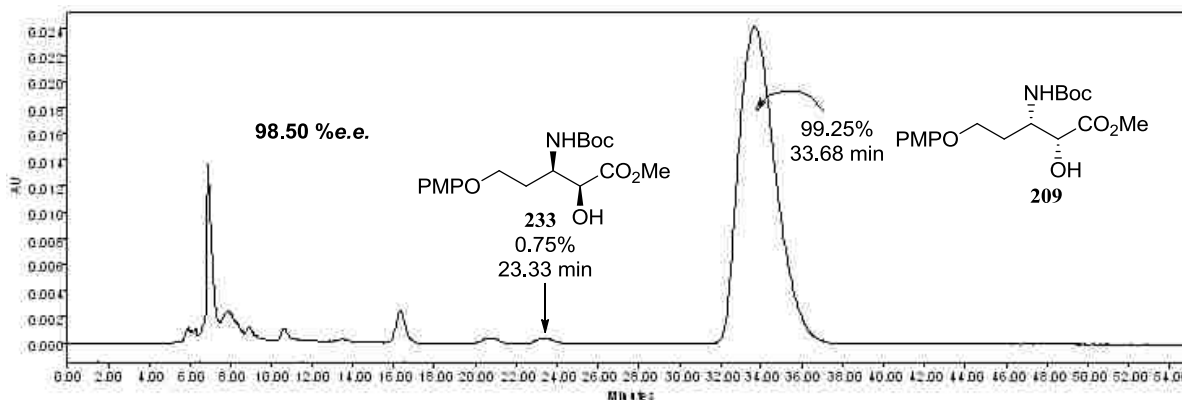


Figure 4.1 – Chiral HPLC Chromatogram for SAH Reaction Products after Preparative HPLC to Separate Regioisomers. Chiralcel OD-H (0.46 cm X 25 cm), Hex/Isopropanol = 9:1, flow rate 0.5 mL/min. Retention Time: 23.33, 33.68 min, Detection 270 nm

With information from Bodkin and McLeod, we were able to confirm the identity of the major regioisomer by ^1H NMR.¹ The α - and β -amino isomers show distinct chemical shifts for the N-H proton: when NH is immediately adjacent to CO_2Me , the NH resonates at δ 5.44 ppm while when in the β -position, the NH is at δ 4.80 ppm (Figure 4.2). The N-H proton of our amino alcohol resonates at 4.82 ppm, confirming that it is the “ β -regioisomer.”

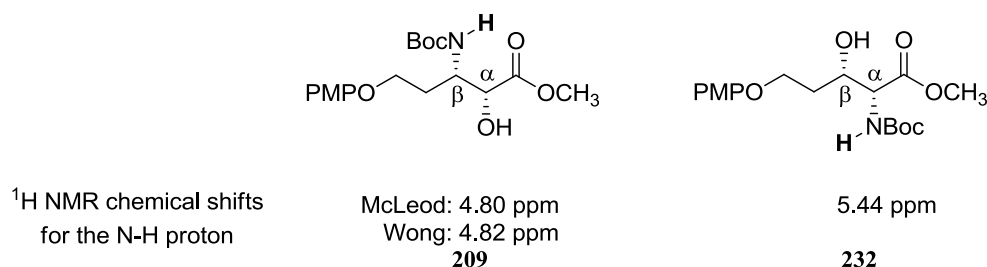
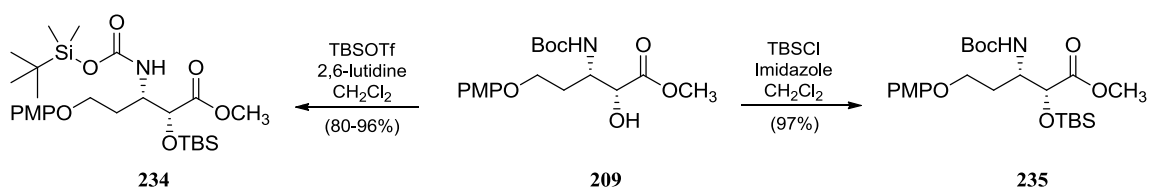


Figure 4.2 - ^1H NMR Chemical Shifts for the N-H Proton of **209** and its Regioisomer

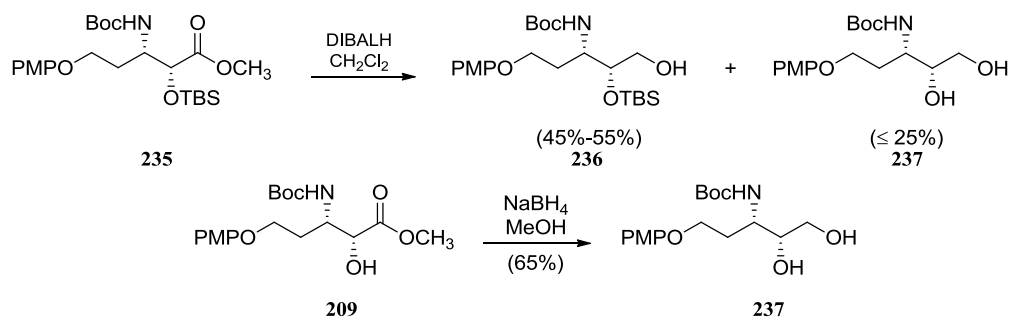
Protection of amino alcohol **209** as its TBS ether was expected to proceed smoothly using TBSOTf/2,6-lutidine. A similar protection was accomplished *en route* to the synthesis of *eHyAsn* (Scheme 2.16, chapter 2).¹⁰ The current reaction, unfortunately, produced compound **234** in 80-96% yield (Scheme 4.7). The ¹H NMR data of **234** showed the disappearance of a singlet (9H) around δ 1.5 ppm corresponding to the *tert*-butyl group of the Boc carbamate and the appearance of two singlets (9H each) around δ 1.0 ppm and four singlets (3H each) around δ 0.0 ppm that is suggestive of two *tert*-butyldimethylsilyl groups. This evidence, in conjunction with a peak corresponding to (M+H)⁺ at 542.2967 (C₂₆H₄₈NO₇Si₂) confirms the formation of compound **234**. Sakaitani and Ohfuné first reported that TBSOTf/2,6-lutidine can be used to convert the *N*-Boc group into the *N-tert*-butyldimethylsilyloxycarbonyl group.¹¹ The strong Lewis acidity of TBSOTf is responsible for the transcarbamylation of the Boc protecting group. We resorted to using the milder TBSCl/imidazole system and found that treatment of **209** with two equivalents of TBSCl and two equivalents of imidazole gave the desired silyl ether **235** in 18% yield. Increasing the number of equivalents of TBSCl and imidazole to five and eventually seven gave **235** in 85% and 97% yield respectively. On reflection, conducting the reaction under a high reagent concentration (*viz.* reduced quantities of DMF) would likely also lead to high yields.



Scheme 4.7 - TBS Protection of **209** Using TBSOTf and TBSCl

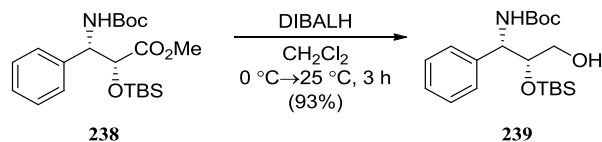
The reduction of methyl ester **235** was carried out using diisobutylaluminum hydride (DIBALH) in dichloromethane. While the reaction resulted in the isolation of the desired primary alcohol **236** in 45%-55% yield, an undesired diol **237** was also obtained, sometimes in as much as 25% yield (Scheme

4.8). To confirm the identity of diol **237**, compound **209** was reduced with NaBH₄/MeOH to generate the same offending diol. Indeed, ¹H NMR of the DIBALH side product matched that of the NaBH₄ reduction product.



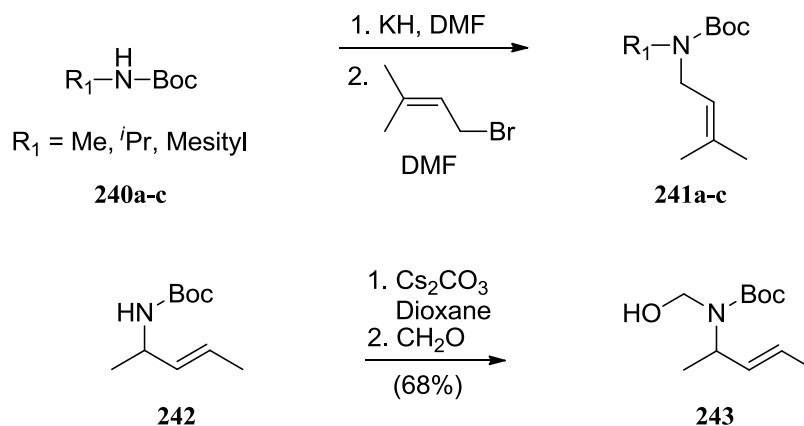
Scheme 4.8 – Results for the DIBALH Reduction of **235**

This outcome was disappointing because Kandula and Kumar reported reduction of a related α -silyloxy β -amino methyl ester in 93% yield (Scheme 4.9).¹²



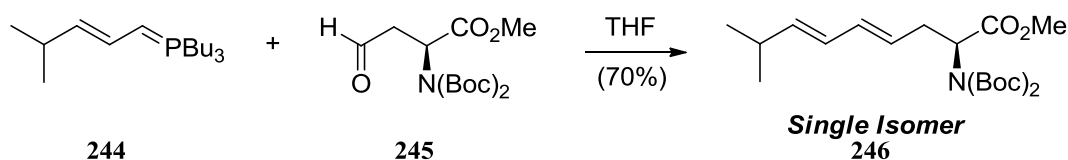
Scheme 4.9 - Kandula and Kumar *En Route* to (+)-L-733,060

Corey and Jones first reported the cleavage of TBS ethers under reductive and near-neutral conditions using DIBALH.¹³ Efforts to optimize the conditions to keep this side reaction to a minimum proved futile. Increasing the stoichiometry of the reducing agent (two or five equivalents) or varying the reaction temperature (-78 °C, -20 °C, 0 °C) did not significantly improve conversion. The low yields provided by the DIBALH reaction coupled with concerns about whether the acidic carbamate proton might interfere with the HWE reaction (Scheme 4.10)^{14,15} prompted us to reevaluate our protecting groups. We opted for full protection of the amino group, in order to remove the carbamate proton.



Scheme 4.10 – Precedents for Deprotonation of Acidic Carbamate Protons Followed by Addition Reactions

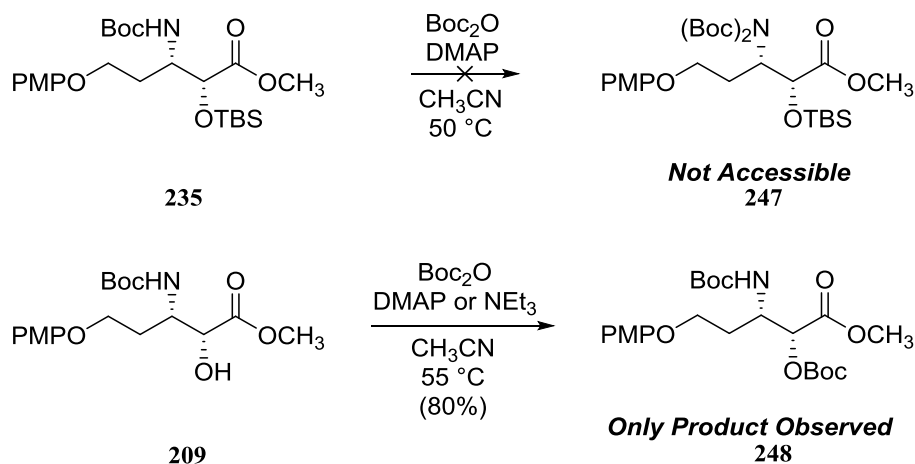
Ma and co-workers found that the use of an aldehyde containing a di-Boc-protected primary amine was critical for formation of the desired isomer **246** in the Wittig reaction (Scheme 4.11).¹⁶ The authors also note that the second Boc group “might increase the steric bulk of the substrate and prevent isomerization of the intermediate oxaphosphetane, thereby giving better stereoselectivity.” Thus, di-Boc protection provides significant advantages during Wittig-type reactions of amino aldehydes.



Scheme 4.11 - Example of an Aldehyde Containing a Di-Boc-Protected Primary Amine Used for an Olefination Reaction

Thus, we tried to introduce a second Boc group to **235**. The reaction of **235** with 2.3 equiv of Boc_2O and 0.3 equiv of DMAP in CH_3CN at 50°C failed to produce desired product **247** (Scheme 4.12). We were, however, able to recover the large remaining portion as unreacted starting material. Prolonged heating at an elevated temperature with additional Boc_2O did not improve conversion. We thought that

steric hindrance by the neighboring OTBS group might be contributing to the sluggish reaction. Unfortunately, treatment of aminoalcohol **209** with Boc₂O/DMAP or Boc₂O/NEt₃ led to carbonate formation exclusively. At this point, we were forced to conclude that **247** was inaccessible.

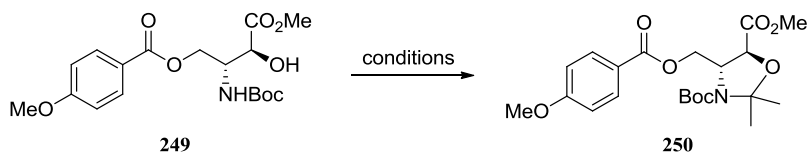


Scheme 4.12 – Attempted Synthesis of **247**

In surveying the literature, we came across the 2,2-dimethyloxazolidine protecting group.¹⁷ Generally formed under acid-catalyzed conditions, an oxazolidine group simultaneously protects the amine and the hydroxyl functionality. The benefits of using this protecting group are two-fold. First, the absence of the silyl ether should improve the subsequent DIBALH reaction. Also, the lack of an acidic carbamate proton should help the key HWE olefination.

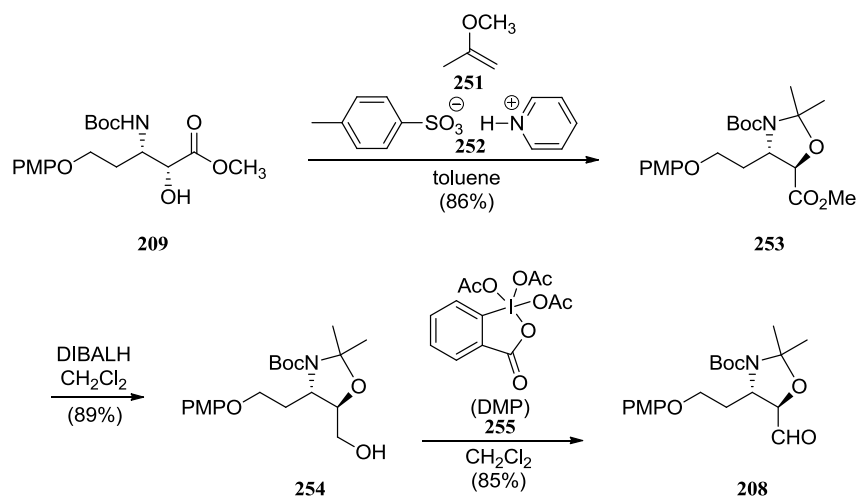
Hutton and co-workers optimized the protection of a related β -amino alcohol as its oxazolidine derivative (Table 4.1).¹⁷ The authors found that use of 2,2-dimethoxypropane and TsOH gave the product in poor yield (36%) and a significant amount of starting alcohol (40%). A different three carbon reagent, 2-methoxypropene (2-MP), along with TsOH provided better conversion (60%) and reduced starting material (22%). The reaction was further improved by using an alternative activating acid, PPTS, in conjunction with 2-MP to afford the product in 84% yield.

Table 4.1 – Hutton and Co-workers¹⁷ Optimization Study for Generation of Oxazolidine **250**



Reagent	Activating Acid	Solvent	Yield of 250 (%)	Recovered SM (%)
2,2-DMP	TsOH	Benzene	36	40
2-MP	TsOH	Benzene	60	22
2-MP	PPTS	Toluene	84	15

We decided to adopt the 2,2-dimethyloxazolidine protecting group for the reasons described above. Treatment of β -amino alcohol **209** with 2-MP/PPTS in toluene gave oxazolidine **253** (Scheme 4.13). This ester was then reduced to primary alcohol **254** using DIBALH in CH_2Cl_2 . The high yield for the reduction step further confirmed that the TBS protecting group was the problem in the previous conversion of **235** to **236**. Dess-Martin oxidation provided aldehyde **208** in good yield, setting the stage for the HWE olefination.



Scheme 4.13 - Completion of the Aldehyde Fragment for Apoa and Aboa Synthesis

4.4 Probing Anion Formation and the HWE Reaction

Before investing significant amounts of aldehyde **208** in the key step, it was prudent to probe the reactivity of phosphonate ester **213** and its commercially available desmethyl analog **256** (Figure 4.3).

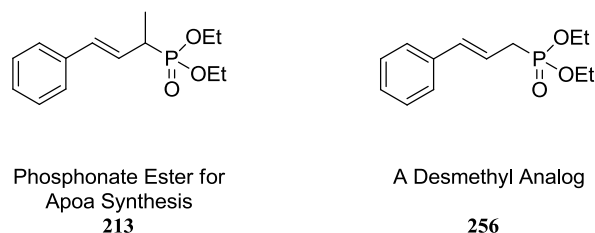
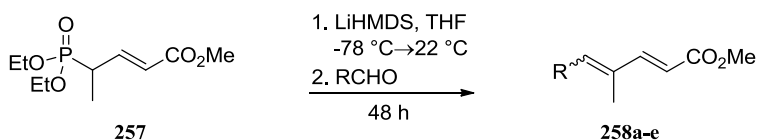


Figure 4.3 – Phosphonate Ester Fragment for Apoa and a Desmethyl Analog

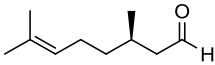
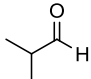
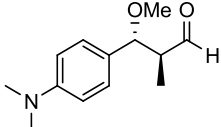
The initial choice of LiHMDS in THF was inspired by Helquist and co-workers' report that optimized HWE reactions with 4-methyl-substituted phosphonate **257** to access 4-methyldienoate derivatives (Table 4.2).¹⁸ In general, the double bond stereoselectivities are better in HWE reactions of aromatic aldehydes than aliphatic aldehydes. Increasing alkyl branching at the α -carbon of the aldehyde reduces *E*-selectivity. Employing the optimized conditions for the key step in a synthesis of trichostatic acid, phosphonate **257** reacted with an aldehyde to give dienoate **258e** in 71% yield as a 2:1 mixture of *E,E*- and *E,Z*-isomers.

Table 4.2 – Helquist and Co-workers'¹⁸ Access to 4-Methyldienoate Derivatives Using LiHMDS in HWE Reactions



Aldehyde	<i>E,E</i> / <i>E,Z</i> ^a	Yield (%) ^b
	92:8	82
	74:26	97

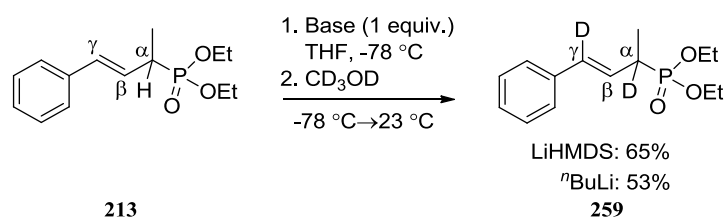
(Table 4.2 continued)

Aldehyde	<i>E,E/E,Z</i> ^a	Yield (%) ^b
	76:24	78
	40:60	80
	2:1	71

^aRatios were measured by integration of relevant peaks in the ¹H NMR of the crude product mixture.

^bYield of the purified product.

With phosphonate esters **213** and **256** in hand, we began investigations into formation of their anions and reaction with CD₃OD, *p*-bromobenzaldehyde (**136**) and Garner's aldehyde (**268**). The aldehydes used in the HWE reactions represent gradual steps upward in complexity leading ultimately to reaction between **213** and **208**. To test our technique for anion formation, CD₃OD was used as the first electrophile. The deprotonation of **213** (1.0 equiv. of LiHMDS in THF) and reaction with CD₃OD afforded an unexpected dideuterated product **259** (Scheme 4.14). A similar experiment, substituting *n*-BuLi (1.0 equiv.) as the base generated the same product in lower yield.



Scheme 4.14 - Formation of an Unexpected Dideuterated Product

The ¹H NMR spectrum and mass spectrometry [(M+H)⁺ at 271.1427, C₁₄H₂₀D₂O₃P] data is consistent with **259**. The ¹H NMR spectrum of **259** (red in Figure 4.4) showed the appearance of a doublet instead of a doublet of doublets around δ 1.40 ppm (effect on methyl group due to α -deuteration), disappearance of the multiplet around δ 2.8 ppm (α -deuteration), appearance of a doublet instead of a

multiplet around δ 6.2 ppm (effect on β -hydrogen due to α - and γ -deuteration), and disappearance of the multiplet around δ 6.5 ppm (γ -deuteration).

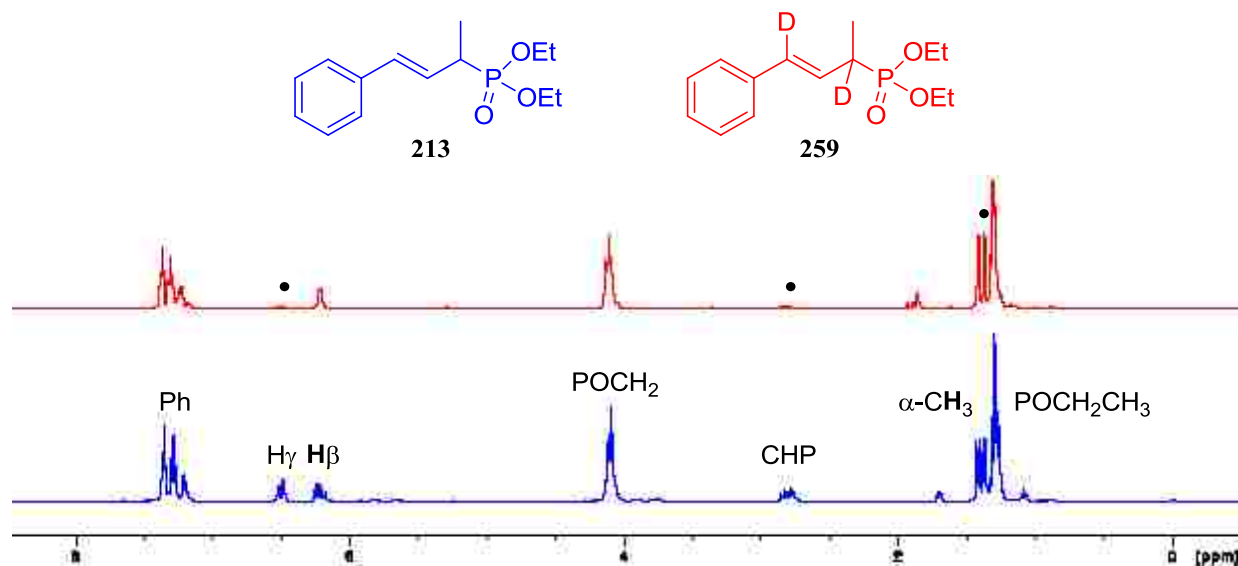
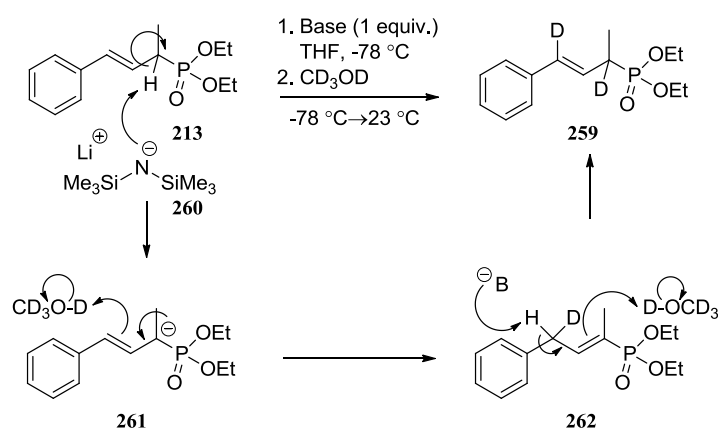


Figure 4.4 - ^1H NMR Spectra of Starting Apoa Phosphonate Ester (Blue) and Dideuterated Apoa Phosphonate Ester (Red)

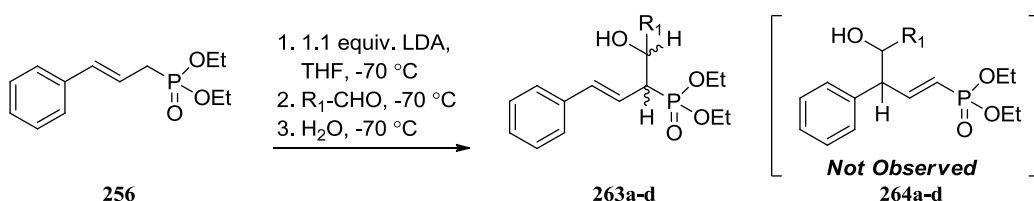
The mechanism of formation for **259** is proposed to occur as illustrated in Scheme 4.15. The use of one equivalent of base (LiHMDS or *n*-BuLi) led to deprotonation at the α -carbon of phosphonate ester **213**. Deuteration apparently occurred at the γ position. The hexamethyldisilazane or deuterated methoxide anion is then able to abstract the γ hydrogen leading to deuteration at the α position.



Scheme 4.15 – Proposed Mechanism for the Deuteration Product

The results were surprising, since Collignon and co-workers reported that products resulting from γ -reactivity of a related phosphonate ester were not observed.¹⁹ They prepared several 2-diethylphosphonyl homoallylic alcohols from addition of a lithiated allylic phosphonate to various aromatic and aliphatic aldehydes (Table 4.3). The deprotonation of phosphonate **256** (1.1 equiv. of LDA in THF), reaction with an aldehyde, and acid hydrolysis, all performed at $-70\text{ }^{\circ}\text{C}$, afforded the corresponding diastereomeric alcohol in high yield. Comparing **213** to **256**, however, the inductive effect of the methyl group makes H_α slightly less acidic. There was also the long stir time after anion trapping with CD_3OD but before work-up. We suspect that these two factors increase the likelihood for the formation of **259**. In addition, differences in electrophile (CD_3OD as opposed to RCHO) provide another likely explanation.

Table 4.3 – Collignon *et al.*¹⁹ Generation of 2-Diethylphosphonyl Homoallylic Alcohols Using LDA in HWE Reactions



Entry	R_1	<i>Erythro:Threo</i> Ratio ^a	Yield (%) ^b
1	Ph	33:67	85
2	4-ClC ₆ H ₄	30:70	84
3	<i>n</i> -Pr	36:64	88
4	<i>i</i> -Pr	15:85	93

^aDetermined by integration of ^{31}P NMR signals of product mixture.

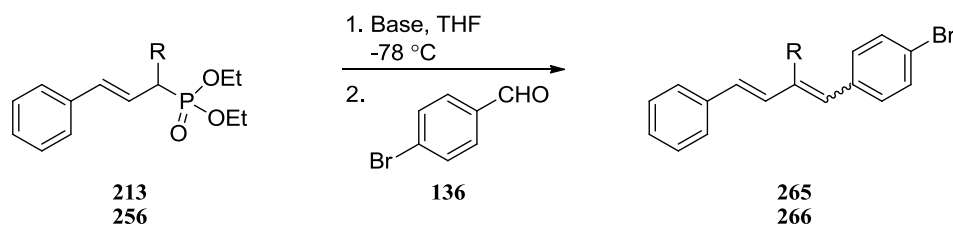
^bYield of purified product mixture.

p-Bromobenzaldehyde represents a more relevant electrophile. The reaction between **213** and *p*-bromobenzaldehyde, however, afforded conjugated product **265** in only 19% yield (Table 4.4). Lithium

hexamethyldisilazide is a more hindered and considerably weaker base than LDA (pK_a of 30 as opposed to 36). It was at this point we decided to switch bases to LDA.

Commercially available LDA was used to generate the anion from phosphonate ester **256**. This was reacted with *p*-bromobenzaldehyde to give conjugated diene **266** in 79% yield. Unfortunately, reacting **213** and *p*-bromobenzaldehyde with the use of LDA, only netted a 24% yield of product **265**. Even when stored cold, the shelf life of commercially available LDA does not justify the cost. At this point, we were committed to preparing LDA fresh for each HWE reaction.

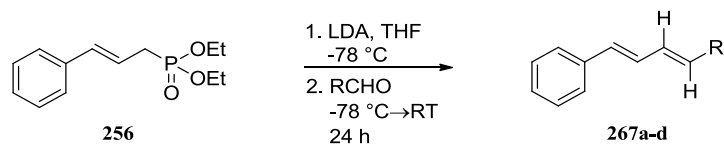
Table 4.4 - HWE Reaction of Commercially Available Bases with *p*-Bromobenzaldehyde



R	Base (Commercial)	Yield (%)
CH ₃	LiHMDS	19
H	LDA	79
CH ₃	LDA	24

Nicolaou and co-workers utilized (*E*)-diethyl cinnamylphosphonate in several instances *en route* to endiandric acids A-G (Table 4.5).²⁰ The deprotonation of phosphonate **256** with LDA and condensation with each aldehyde afforded the corresponding di-substituted olefin in good yield (75%-80%) and with excellent stereoselectivity (*E*:*Z* ≥ 20:1). The steric environment of the aldehyde demanded the use of an increasing amount of the lithio derivative of **256**.

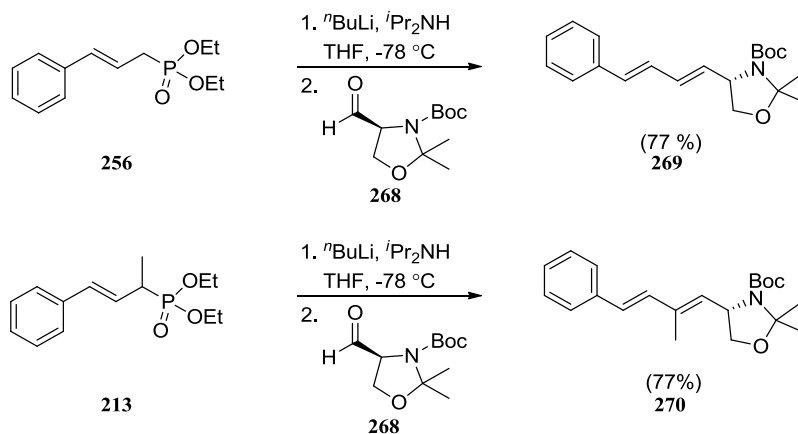
Table 4.5 – Nicolaou and Co-worker's²⁰ Use of (*E*)-Diethyl Cinnamylphosphonate *En Route* to Endiandric Acids A-G



Aldehyde	Equivalents of [<i>trans</i> -PhCH=CHCHP(O)(OEt) ₂] ⁻ Li ⁺	<i>E:Z</i>	Yield (%)
	1.1	≥ 20:1	78
	2.0	≥ 20:1	75
	3.0	≥ 20:1	80
	3.0	≥ 20:1	75

We next shifted our focus from aromatic to aliphatic aldehydes. We selected Garner's aldehyde to fill this role and prepared it via reduction/oxidation of the parent methyl ester.²¹ Garner's aldehyde has found considerable use as a chiral α -amino carbonyl compound for stereochemical studies and a precursor to biologically active compounds such as amino sugars and sphingosines.²¹⁻²³ Our interest in using this aldehyde as a model system is threefold. First, the oxazolidine protecting group and chiral α -substitution are in common with our real aldehyde. This should lead to a comparable HWE reactivity profile for both aldehydes involved. Lastly, the olefination products might serve as a model system to probe some of the subsequent FGIs. The reaction of **256** with Garner's aldehyde for 17 hours gave product **269** in 77% yield (Scheme 4.16). More importantly, reaction between **213** with Garner's

aldehyde for 18 hours gave product **270** in 77% yield as well. With the production of **270** in good yield, we were ready to perform the key HWE reaction between phosphonate ester **213** and aldehyde **208**.



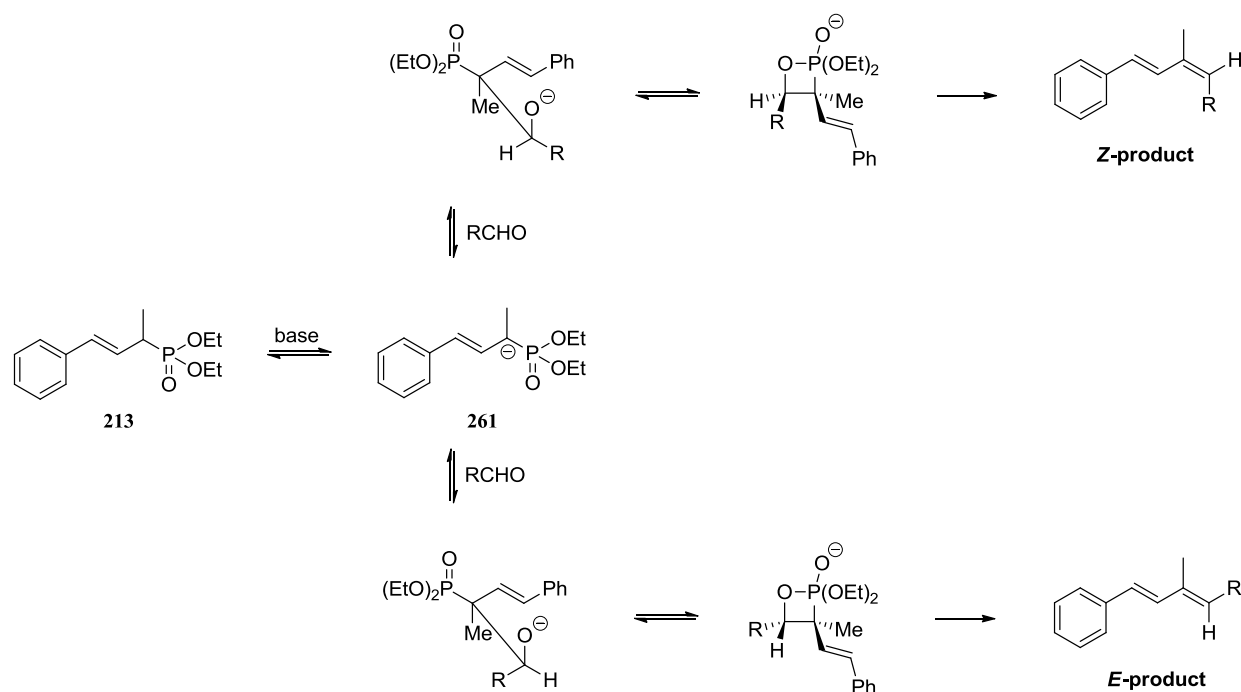
Scheme 4.16 - HWE Reaction of the Model and Apoa Phosphonate Ester with Garner's Aldehyde

4.5 The Key HWE Reaction

The mechanism of the HWE reaction is shown in Scheme 4.17. First, the phosphonate ester is deprotonated with a base to generate a phosphonate anion. The anion then attacks the carbonyl carbon of the aldehyde generating two possible betaine intermediates each of which can form a P-O bond to give their respective oxaphosphetanes. These compounds then go through a [2+2] cycloreversion to form an *E/Z* mixture of olefin products. Corey and co-workers noted that an electron-withdrawing group at the phosphonate-substituted carbon is necessary for elimination to occur.²⁴ Otherwise, the reaction halts after the initial nucleophilic addition step. *E*-olefins are formed preferentially in the HWE reaction, albeit to a lesser extent in the case of trisubstituted olefins.

The mechanism of this reaction contains several subtle features. Each step is reversible with the exception of the *syn*-elimination step. Phosphonate anion addition to the carbonyl is the rate-determining step. With the initial nucleophilic attack being reversible, the reaction should form the thermodynamically favored *E*-isomer predominantly. The oxaphosphetane that leads to the *E*-product will form faster due to decreased steric interactions. Ultimately, the *E/Z* ratio of the olefin isomers is

dependent upon the stereochemical outcome of the initial addition and upon the ability of the intermediates to equilibrate (reversibility of each step).

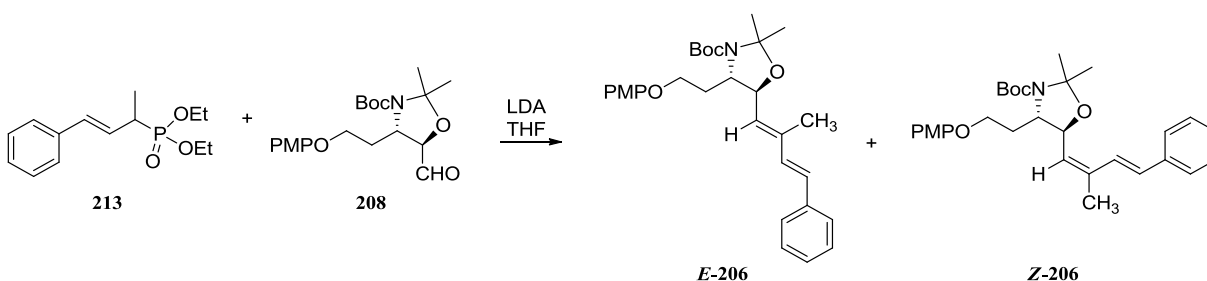


Scheme 4.17 – Mechanism of the HWE Reaction

The goal of any HWE reaction is to maximize yield and stereoselectivity through the screening of experimental variables. With suitable conditions for anion formation identified, the HWE reaction between **213** and **208** was initially run to check for proper oxaphosphetane/ β -hydroxyphosphonate generation. Anion formation with LDA for 30 minutes, reaction with aldehyde **208** for 30 minutes and acid hydrolysis (H_2O) all performed at $-78\text{ }^\circ\text{C}$ generated an oxaphosphetane/ β -hydroxyphosphonate species which was unstable to silica but verified by ESI-MS. The next step was to determine the temperature at which the oxaphosphetane/ β -hydroxyphosphonate irreversibly eliminates to give a *E/Z* mixture of olefin products. To accomplish this, the reaction mixture was allowed to warm to $0\text{ }^\circ\text{C}$ (from $-78\text{ }^\circ\text{C}$) and after 30 minutes, TLC analysis showed elimination adducts. Changing the concentration of various species did not improve the yield, however, the temperature of aldehyde addition ($-78\text{ }^\circ\text{C}$) boosted both yield and stereoselectivity indicating decomposition of the phosphonate at higher temperatures in the

absence of aldehyde. Comparing entries 1 and 3 in Table 4.6, two reactions run with the only difference being noted above led to a 30% yield (from 18%) and 3.9:1 *E/Z* ratio (from 3.1:1) of alkene products. The reaction was further refined when we opted for strict temperature control as opposed to our original temperature conditions (compare entries 1 and 4 in Table 4.6). These conditions led to an optimized 40% yield with a 4.5:1 *E/Z* ratio of olefin products. Holding the reaction temperature at -30 °C or -20 °C for 2 hours (instead of -40 °C) gave decreased yields and stereoselectivities.

Table 4.6 - Optimization Study for the HWE Reaction



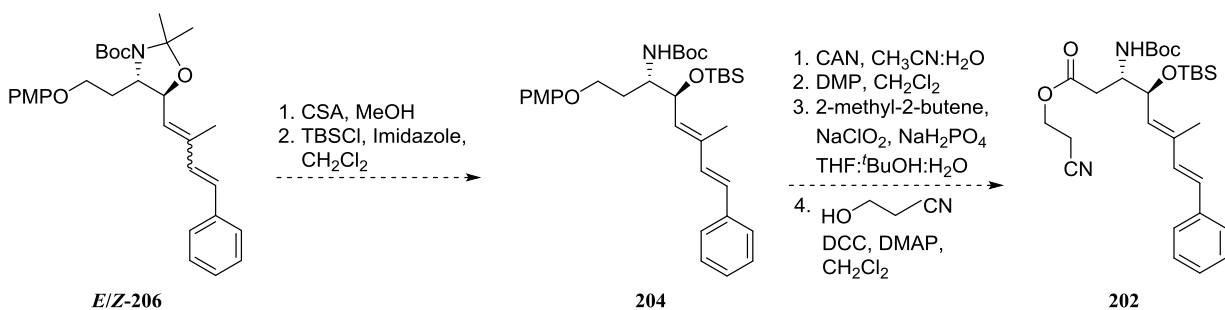
Trial	RCHO Addition Temperature	Reaction Temperature	Yield (%)	<i>E/Z</i> ratio
1	23 °C	-78 °C (2 h) → 0 °C (0.5 h)	18%	3.1:1
2	23 °C	-78 °C (2 h) → -40 °C (2 h) → 0 °C (0.5 h)	21%	3:1
3	-78 °C	-78 °C (2 h) → 0 °C (0.5 h)	30%	3.9:1
4	-78 °C	-78 °C (2 h) → -40 °C (2 h) → 0 °C (0.5 h)	40%	4.5:1

The ¹H NMR of the product indicated a mixture of *E* and *Z* isomers. It was not possible to separate the nonpolar *E/Z* isomers of **206**, even by HPLC. We hypothesized that division of the two isomers might best be achieved after deprotection of the oxazolidine group provided a more polar compound.

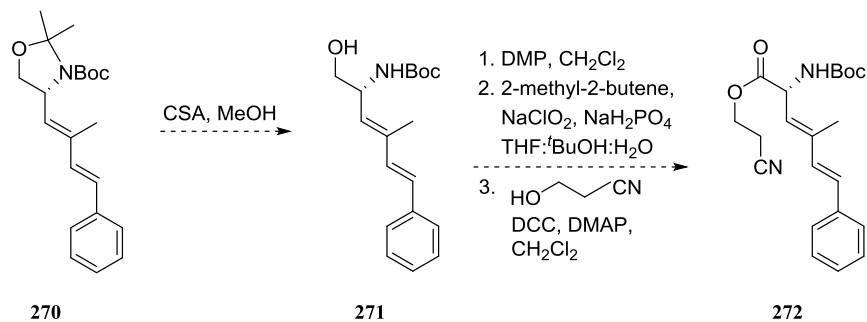
4.6 A Model System for Protecting Group Manipulations and Functional Group Interconversions

Since PMP ether *E/Z*-**206** is a valuable resource (longest linear sequence of 7 steps; 12% yield), we felt that **270** might serve as a useful model system to investigate the remaining steps in the synthesis (Scheme 4.18). Specifically, both compounds contain a conjugated diene and oxazolidine unit but **270** lacks a PMP ether group which is present in *E/Z*-**206**. Nonetheless, **270** can be subjected to further modifications that include oxazolidine removal to reveal a primary alcohol followed by full oxidation and protection of the carboxylic acid as its β -cyano ester derivative. Although not in exactly the same sequence, each reaction will be applied to advanced intermediate *E/Z*-**206**.

Apoa

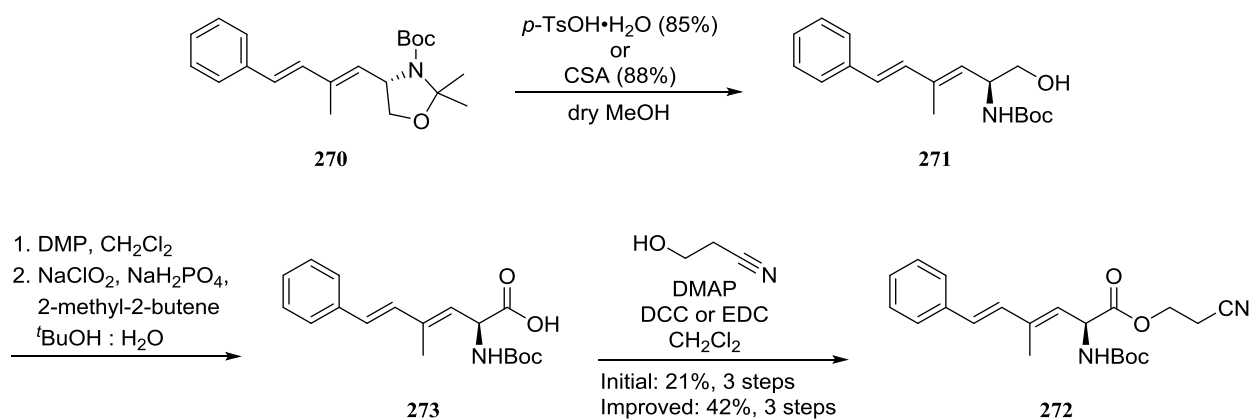


Model System



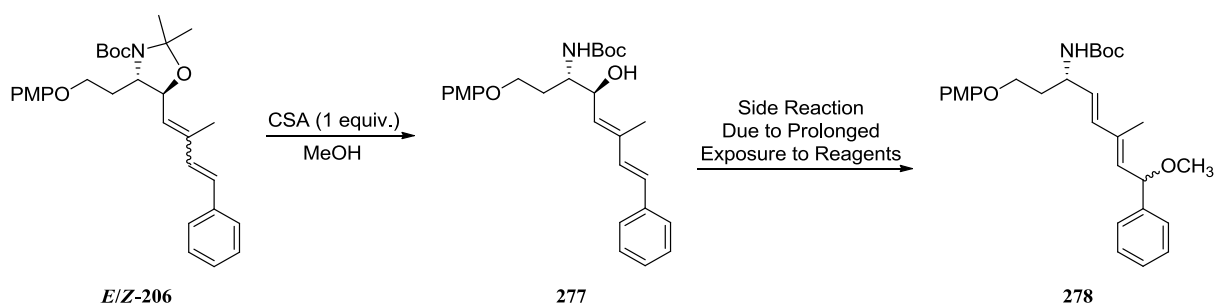
Scheme 4.18 – Comparison of the Model System to Apoa for Further Modifications

Both *p*-toluenesulfonic acid (*p*-TsOH) and camphorsulfonic acid (CSA) were equally effective in removing the oxazolidine group in **270** (Scheme 4.19). The resulting primary alcohol **271** was oxidized in two steps, first to an aldehyde using the Dess-Martin periodinane (DMP) and secondly to a carboxylic acid under Pinnick conditions. Under these mild oxidation conditions, the Boc protecting group and diene functionality remain intact providing good precedent for the real system. Protection of **273** using 3-hydroxypropane-nitrile/DMAP/DCC afforded the β -cyano ester **272** in 21% yield (three steps from **271**).



Scheme 4.19 – Initial and Improved Conditions for Reactions of Interest

Improvements were made to each of the last three steps. For the Dess-Martin oxidation, we took advantage of the report by Meyers and Schreiber that water increases the rate of the oxidation.²⁵ The reaction of water with DMP results in formation of an acetoxyiodinane oxide (Scheme 4.20) that is more efficient than DMP as a alcohol oxidant. A generally accepted explanation for this effect correlates increased electron-donating ability of a hydroxy substituent (instead of an acetoxy group) with rate of dissociation of an acetate ligand. To compare both methods, monitoring the reaction by TLC indicated significant amounts of starting material after six hours when dry CH_2Cl_2 was used. TLC analysis of the same oxidation performed with water-saturated CH_2Cl_2 suggested complete consumption of starting material after six hours.



Scheme 4.21 – Formation of a Side Product Following Oxazolidine Group Deprotection

To suppress the side reaction, we screened other acid sources (PPTS, *p*TsOH·H₂O, TFA) in combination with different solvents (EtOH, *i*PrOH). These reactions can be characterized as either too sluggish (lots of starting material present) or too fast (exclusive formation of the side product). We decided to refine the original conditions in an attempt to slow down the reaction. Reducing CSA to catalytic levels (10 mol %) in MeOH led to no reaction after 19 hours. The same reaction using a MeOH/THF solvent mixture led to a 44% yield of **277** as a *E/Z* mixture after 41 hours. Switching to a different solvent combination (1:1 ethylene glycol:THF) gave the same products in 39% yield after 19 hours. The reaction run in MeOH generates 2,2-dimethoxypropane as a by-product, however, the use of ethylene glycol produces 2,2-dimethyl-1,3-dioxolane as a by-product instead. Perhaps the intramolecular nature of the dioxolane formation led to faster reaction times. We recognized that this reaction would not achieve full conversion, however, losing product to the side reaction would be the worse alternative. The nonpolar starting material could be easily recovered via flash chromatography. Increasing the equivalents of CSA (20 mol %) or reaction temperature led to a major decrease in yield. Using 10 mole % CSA in 1:2 ethylene glycol:THF, we wanted to see how the yield varied with reaction time. The optimized reaction time is seven hours. As noted previously, separation of the *E/Z* isomers **206** was not possible after the olefination step. Separation of the *E* and *Z* isomers for the newly formed secondary alcohol, however, could be accomplished via flash chromatography resulting in the isolation of desired *E*-product **277** in 65% yield (95% BORSM, based on recovered starting material).

Once the oxazolidine protecting group was removed, two spots were discernible by TLC. Our intentions were to prove the *E*-stereochemistry of the C5-C6 olefin in **E-277**, but purity issues made assigning the minor *Z*-isomer a more prudent decision (Figure 4.5). To prove the *Z*-stereochemistry of the C5-C6 olefin in **Z-277**, we relied on ^1H , ^{13}C , and 2-D (ROESY, HSQC and HMBC) NMR spectroscopy.

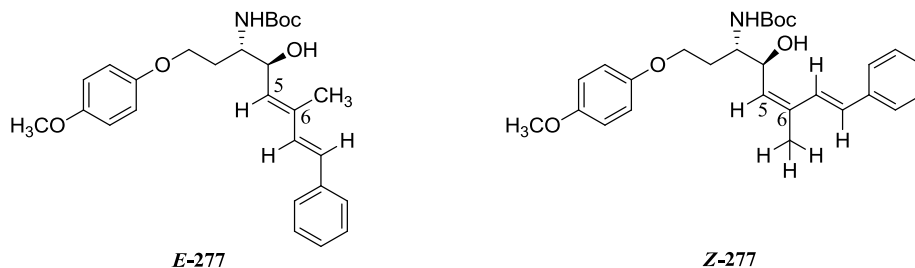


Figure 4.5 – Chemical Structures of **E-277** and **Z-277**

The isolation of TNM F by Fusetani and co-workers was accompanied by the structure determination of the component amino acids. Their structure elucidation of Aboa was discussed at length in §1.2 and includes the use of ROESY, COSY and HMBC NMR to establish the (*E,E*) stereochemistry of the Aboa diene. Tohdo's synthesis of Aboa included the use of nOe measurements to assign olefin configurations to key precursors. Tohdo reported that (*Z*)-diene **Z-132** showed an nOe correlation between the C5-H and the C6-CH₃ (Figure 4.6). The (*E*)-diene **E-132**, on the other hand, showed an nOe correlation between the C4-H and the C6-CH₃.

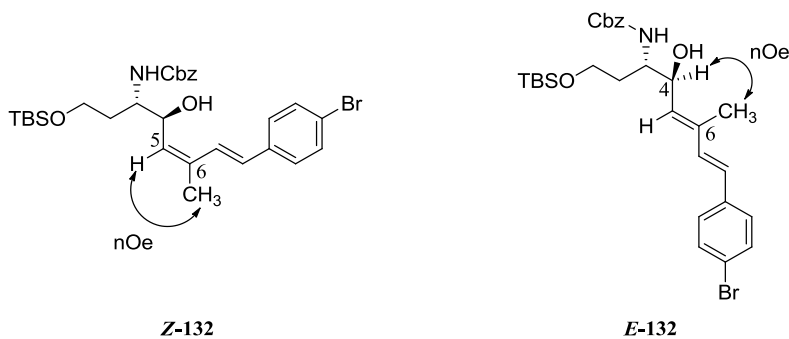


Figure 4.6 – Tohdo's Olefin Assignments Based on nOe Measurements of Precursors

Helquist and co-workers made diene configuration assignments on an assortment of HWE products (Figure 4.7) using ROESY NMR.

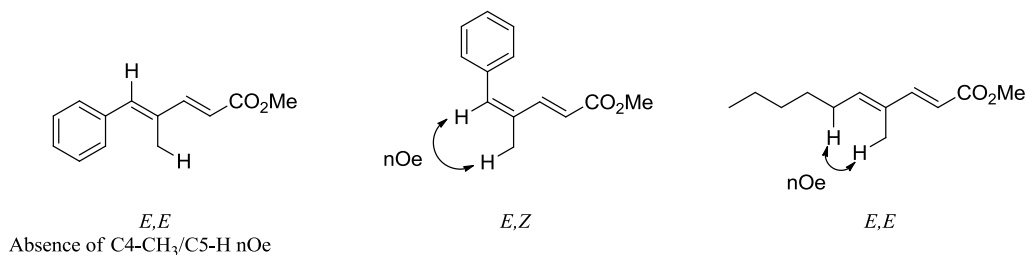


Figure 4.7 – Helquist’s Double Bond Assignments Based on ROESY NMR Results

With these results in mind, establishing *Z*-stereochemistry of the C5-C6 olefin in **Z-277** depends on assigning the ¹H NMR spectrum of the region in red for the molecule in Figure 4.8. The singlet at 2.00 ppm can be readily assigned to the proton labeled H6'. The ¹³C-¹H correlation spectrum (Figure 4.8, HSQC) revealed that H6' was attached to C6' that gives rise to a ¹³C resonance at 21.0 ppm. A long range ¹³C-¹H correlation spectrum (Figure 4.9, HMBC) shows a correlation of C6' to a doublet at 7.15 ppm and a doublet at 5.51 ppm which we label H7 and H5 respectively. The HSQC spectrum reveals that these proton signals show correlations to ¹³C resonances at 125.3 ppm (C7) and 129.7 ppm (C5) respectively. The remaining doublet in the olefinic region of the spectrum (H8, δ 6.65) is linked to a carbon that resonates at 131.2 ppm (C8) as seen in the HSQC spectrum. The *J* coupling constant between H7 and H8 was 16.0 Hz, further evidence that they are part of the same olefin and in the *trans* configuration. The HMBC spectrum revealed that the ¹³C resonance at 136.5 ppm showed correlation to H8 and H6' and as a result, is assigned to C6.

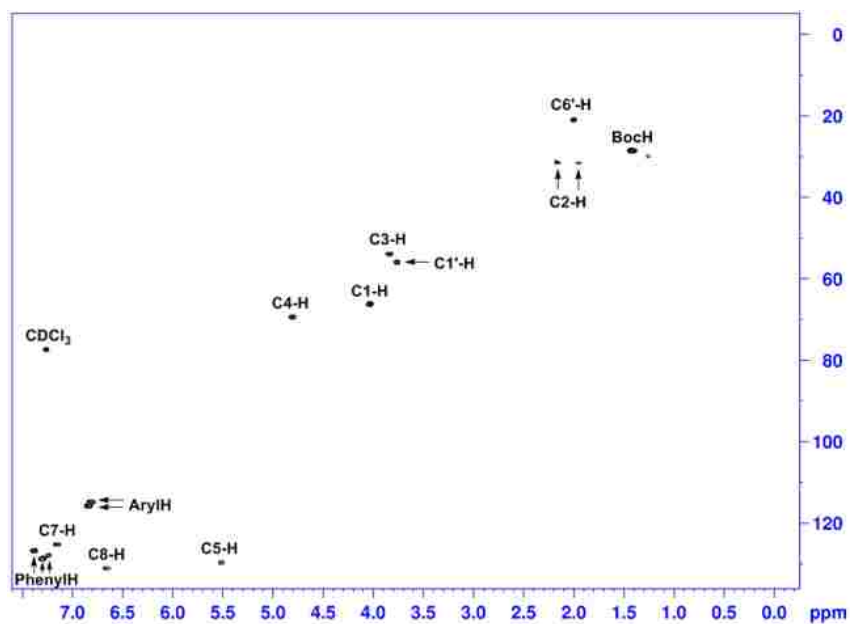
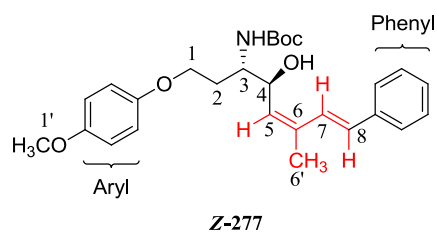


Figure 4.8 – HSQC spectrum of **Z-277**

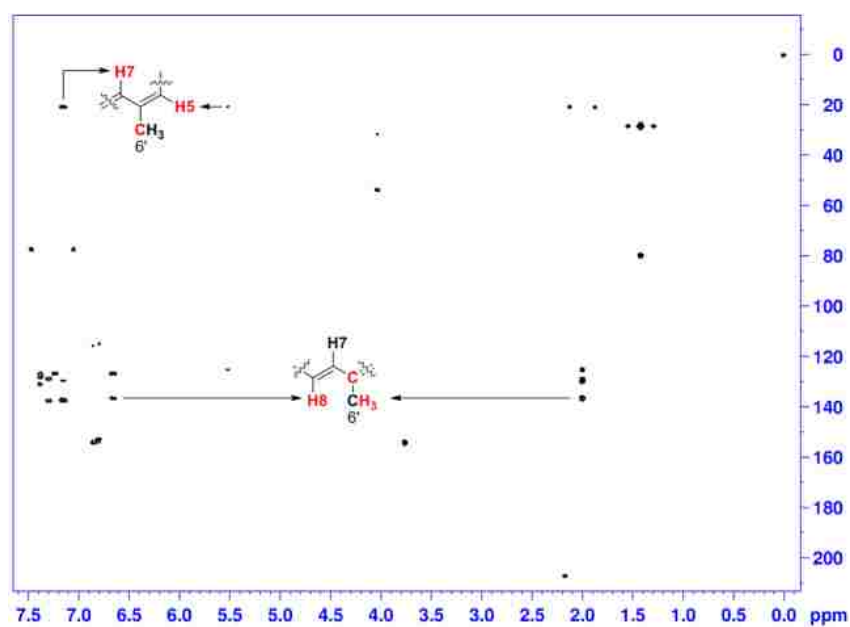


Figure 4.9 – HMBC spectrum of **Z-277**

With the assignment of the protons and carbons for the key diene region in place, we used the ROESY spectrum to resolve the stereochemistry of the C5-C6 olefin in **Z-277**. Examination of the ROESY spectrum (Figure 4.10) shows that H6' (methyl group) is correlated to H5 and H8. In addition, the H7 resonance showed a correlation to H4. Thus, the C5-C6 olefin in **Z-277** was assigned with *Z* stereochemistry. If we were dealing with the *E* version of the C5-C6 double bond, correlations of H5 to H7 and H6' to H8 would have been expected. The C7-C8 double bond geometry in **Z-277** can be confirmed using the same correlations in Figure 4.10 and the H7/H8 coupling constant ($J = 16.0$ Hz). Taken all together, the C7-C8 olefin was designated with *E* stereochemistry and **Z-277** had a (*5Z*, *7E*) configuration.

For the sake of fully characterizing the deprotected product, purity was of utmost importance. In this light, we utilized **Z-277** to prove the *Z*-stereochemistry of the C5-C6 double bond. We were also able to validate the C7-C8 *E*-olefin geometry. Table 4.7 contains ^1H and ^{13}C NMR data for **Z-277**.

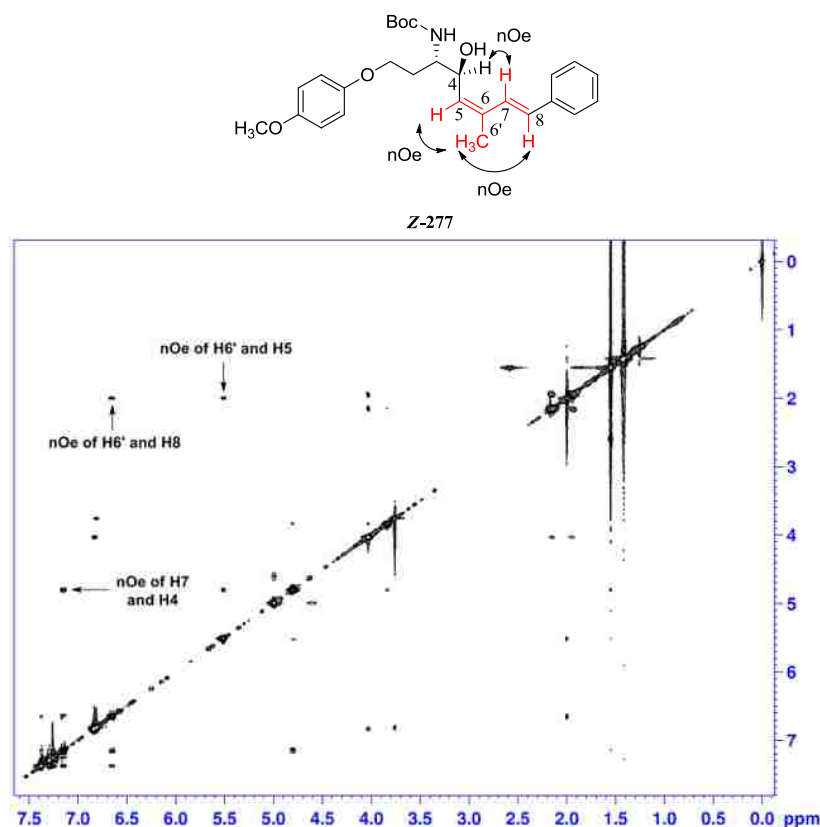
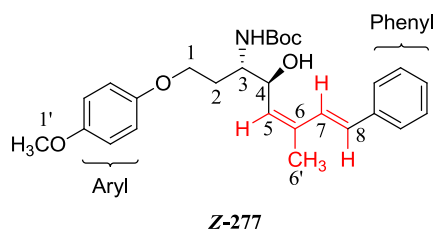


Figure 4.10 – ROESY spectrum of **Z-277**

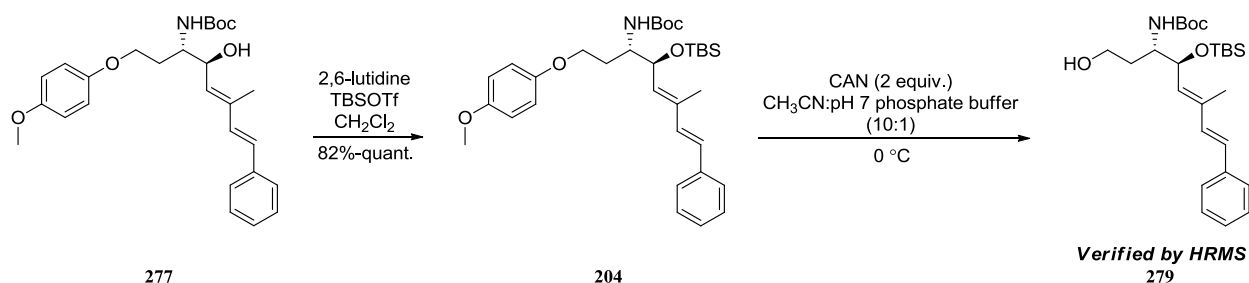
Table 4.7 – ^1H and ^{13}C NMR Data for **Z-277** in CDCl_3



Carbon Number	^{13}C (δ)	^1H (δ)	m	J (Hz)
1	66.3	4.03	t	5.7
2	31.1	1.89-1.98 2.10-2.16	m m	- -
3	53.9	3.80-3.87	m	-
4	69.4	4.77-4.84	m	-
5	129.7	5.51	d	8.6
6	136.5	-	-	-
7	125.3	7.15	d	16.0
8	131.2	6.65	d	16.0
1'	55.9	3.76	s	-
6'	21.0	2.00	s	-
Aryl	114.9, 115.9	6.78-6.87	m	-
Phenyl	126.9, 128.0, 128.8	7.20-7.41	m	-
-OH	-	2.59	br s	-
$\begin{array}{c} \text{—N—} \\ \\ \text{H} \end{array}$	-	5.00	d	6.9
Boc	28.5 79.9	1.42	s	-

*The carbonyl carbon from the Boc group and the quaternary carbons from the aryl group and phenyl group were not assigned

The protection of **277** as its TBS ether proceeded uneventfully. The ratio of secondary alcohol:TBSOTf:2,6-lutidine used was 1.0:1.5:3.0. This ratio was important because the use of only two equivalents of 2,6-lutidine resulted in a dramatic drop in yield. Next, oxidative cleavage of the *para*-methoxyphenyl protecting group to reveal primary alcohol **279** was investigated. Cerium ammonium nitrate (CAN) represents a popular reagent to effect the transformation.¹ The deprotection reactions were run using three milligrams of starting material, monitored by TLC, quenched, extracted and submitted for mass spectrometry analysis. These reactions, conducted at 0 °C, led to complete consumption of starting material after 25 minutes (TLC), however, no desired product was detected by mass spectrometry. Variations in experimental conditions including the manner in which the CAN reagent was added (as a solid or a solution) and/or buffering the reaction using NaHCO₃²⁶ or pyridine²⁷ did not change the outcome. Changing the reaction scale and solvent composition, however, produced the desired primary alcohol **279**, as verified by HRMS (C₂₆H₄₃NNaO₄Si, (M+Na)⁺ 484.2836, Scheme 4.22). This is not the first instance where performing a deprotection reaction via oxidation on a larger scale led to a completely different result (§2.8). The use of CH₃CN:pH 7 phosphate buffer instead of CH₃CN:H₂O as the reaction solvent is not surprising considering the acid-labile and oxidizable moieties present. Limited access to stocks of **204** has precluded optimization studies for the current reaction.

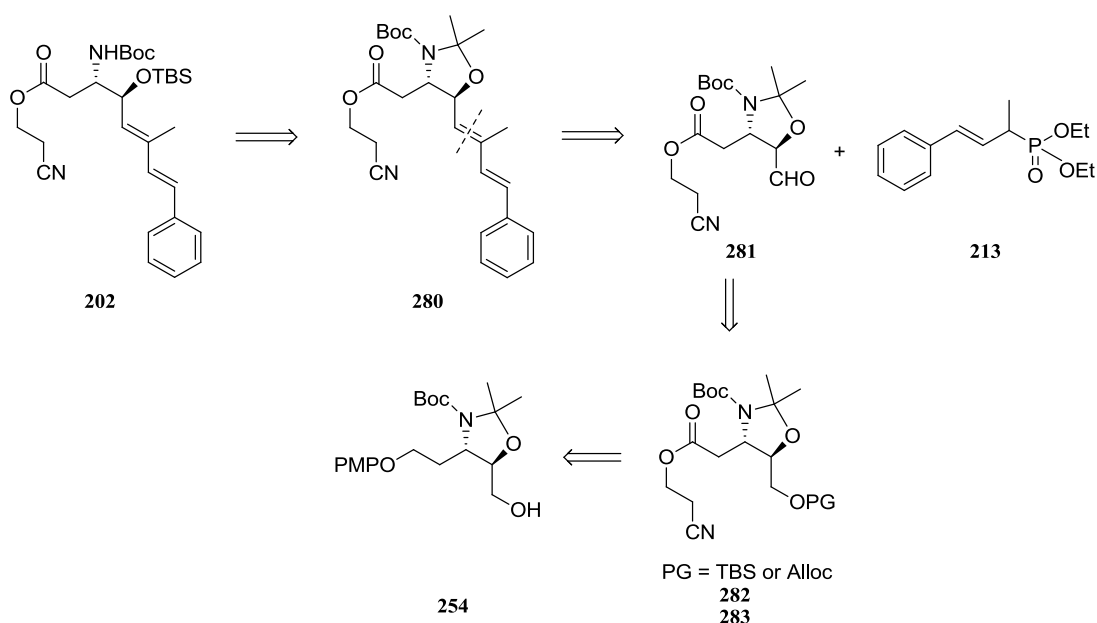


Scheme 4.22 - Formation of Primary Alcohol **279**

4.8 An Alternate Approach for the Synthesis of Apoa

We also briefly explored an approach whereby the conjugated system could potentially be introduced after the oxidative removal of the PMP group. Conceptually, the same reactions would be

utilized as Scheme 4.1 although not in exactly the same sequence. The key HWE step, as shown in Scheme 4.23, is now between aldehyde **281** and the same phosphonate ester **213**. Retrosynthetically, aldehyde **281** can potentially be accessed from an TBS/Alloc protected alcohol **282/283** which in turn can be further simplified to a primary alcohol **254** obtained from the previous route. Our efforts to synthesize aldehyde **281** from primary alcohol **254** are detailed in the following two sections. HWE reaction between **281** and **213** should provide a mixture of **280** favoring the *E*-isomer. Deprotection of the oxazolidine group followed by protection of the newly formed secondary alcohol as its TBS ether should generate our target compound **202**.

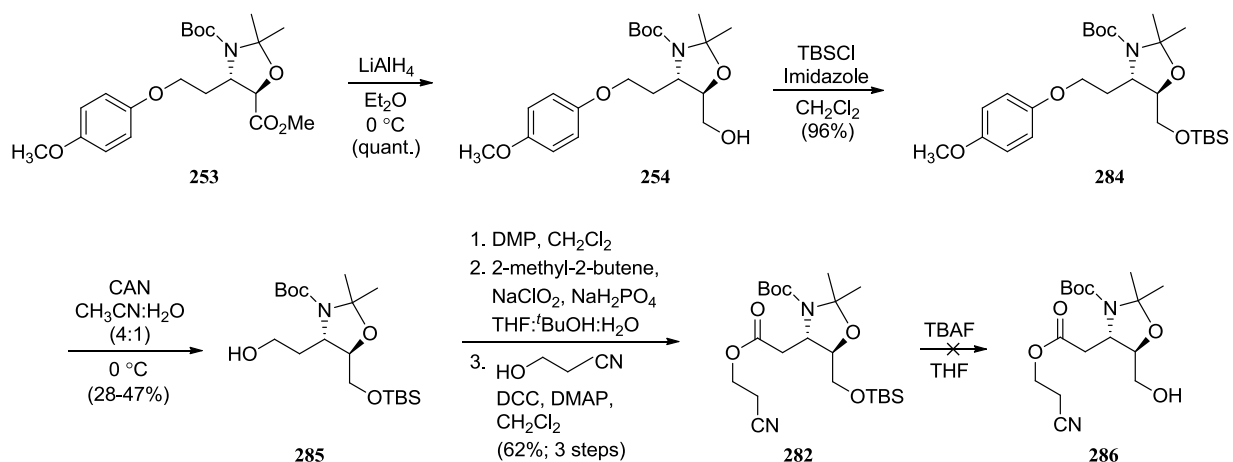


Scheme 4.23 - An Alternate Retrosynthesis of Apoa

4.9 Efforts to Synthesize Aldehyde **281** from **254** Through a TBS or Alloc Protected Intermediate

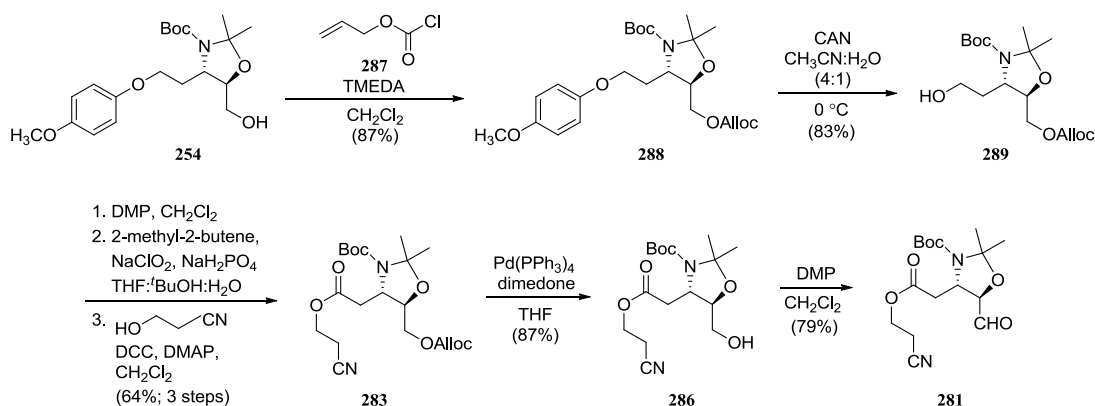
The revised synthesis is presented in Scheme 4.24. Reduction of the methyl ester in **253** using LiAlH_4 generated primary alcohol **254** in high yield. We used DIBALH for the same transformation earlier (Scheme 4.13), however, LiAlH_4 afforded comparable yields and faster reaction times. Protection of the primary alcohol as its TBS ether followed by deprotection of the PMP group produced a different

primary alcohol **285** in low yield. The low yield can be attributed to simultaneous removal of the TBS group as reported by Dattagupta and co-workers.²⁸ Nevertheless, oxidation first to an aldehyde using Dess-Martin periodinane and then to a carboxylic acid under Pinnick conditions provided a handle for β -cyano ethyl ester formation in 62% yield over three steps. We attempted to unmask the primary alcohol **286** via TBS ether cleavage using TBAF/THF, but, this resulted in decomposition products. It seems that the deprotection of the TBS group was not possible without affecting the β CE group, i.e., they were not truly orthogonal. The use of acidic conditions to deprotect the TBS group was ill-advised since the Boc and oxazolidine groups are acid labile. We resorted to switching protecting groups from TBS to Alloc since Alloc's palladium-based deprotection method was orthogonal to the PMP and β CE groups.



Scheme 4.24 – Attempted Synthesis of Primary Alcohol **286** Using a TBS Protecting Group

The most recent approach is presented in Scheme 4.25. These reactions are analogous to the ones presented in Scheme 4.24, yet, the Alloc group resulted in better yields for the reactions leading up to aldehyde **281**. Protection of the primary alcohol as its allyl carbonate followed by oxidative removal of the PMP group generating **289** in 83% yield. Two oxidations in succession followed by β -cyano ethyl ester formation under the conditions optimized earlier produced **283** in 64% yield over three steps. The Alloc group was rapidly removed (30 minutes) and the newly formed primary alcohol **286** was oxidized under Dess-Martin conditions to give aldehyde **281**, ready for HWE reaction.

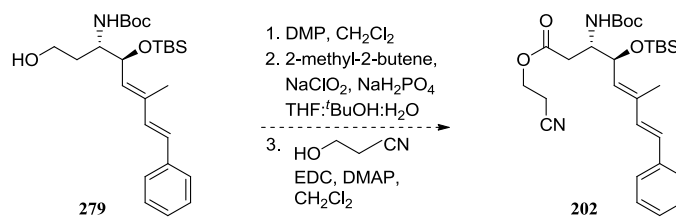


Scheme 4.25 - Synthesis of Aldehyde **281** Using a Alloc Protecting Group

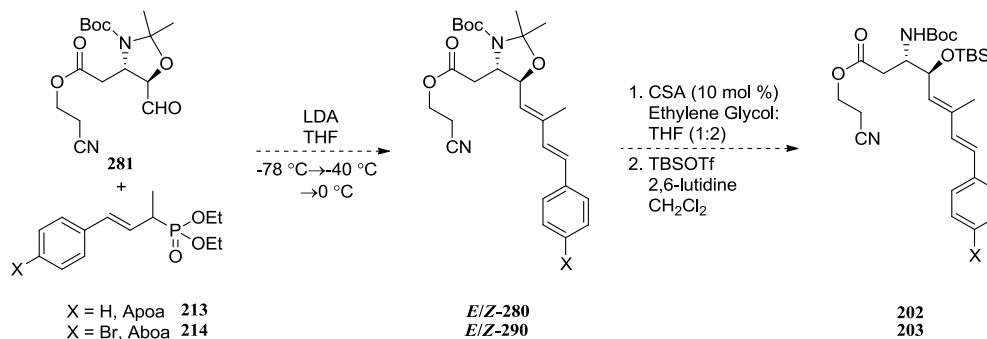
4.10 Future Work for the Completion of Apoa and Aboa

The production of target compounds **202** and **203** are now within reach via both approaches. According to Scheme 4.26, the third route would produce Apoa building block **202** pending primary alcohol **279** oxidation in two steps, first to an aldehyde using Dess-Martin periodinane and secondly to a carboxylic acid under Pinnick conditions followed by protection of the newly formed carboxylic acid as its β -cyano ester.

Apoa Synthesis Via the Third Route:



Apoa and Aboa Synthesis Through an Alternate Approach:



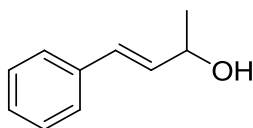
Scheme 4.26 – Plans to Complete Apoa and Aboa

Preliminary HWE reactions between **281** and **214** for the alternate approach led to a complex mixture of products. The desired product would be carried on to the next step. Once in hand, the oxazolidine group in *E/Z*-**209** can be removed and the resulting secondary alcohol can be protected as its TBS ether generating Aboa **203**.

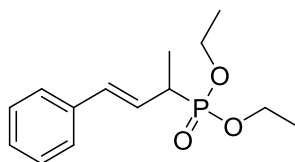
4.11 Experimental Section

General methods: as detailed in Chapter 2

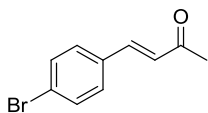
4.11.1 Experimental Procedures



(*E*)-4-phenylbut-3-en-2-ol (**215**). A solution of methylmagnesium bromide (27.2 mL, 1.4 M in toluene/THF (3:1), 38.1 mmol, 1.7 equiv.) was added to a solution of *trans*-cinnamaldehyde (2.86 mL, 22.7 mmol, 1.0 equiv.) in THF (25 mL) at 0 °C under N₂. The mixture was stirred for 30 min at 0 °C then warmed to rt and stirred for 23 h. The reaction was quenched by the addition of sat'd aq. NH₄Cl (60 mL). The mixture was extracted with diethyl ether (3 x 60 mL). The organic layers were combined and washed twice with H₂O (30 mL), dried with MgSO₄, filtered, and concentrated to give alcohol **215**. *R*_f 0.16 (5:1 Hex-EtOAc). ¹H NMR (CDCl₃, 400 MHz) δ 1.37 (d, *J* = 6.3 Hz, 3H), 1.68 (br s, 1H), 4.49 (app. p, *J* = 6.3 Hz, 1H), 6.26 (dd, *J* = 15.9, 6.3 Hz, 1H), 6.56 (d, *J* = 15.9 Hz, 1H), 7.24 (t, *J* = 7.3 Hz, 1H), 7.32 (t, *J* = 7.3 Hz, 2H), 7.38 (d, *J* = 7.3 Hz, 2H); ¹³C NMR (CDCl₃, 100 MHz) δ 23.3, 68.8, 126.4, 127.5, 128.5, 129.3, 133.5, 136.7.

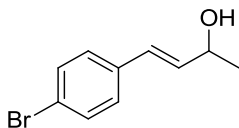


(*E*)-diethyl (4-phenylbut-3-en-2-yl)phosphonate (**213**).⁹ Acetyl chloride (3.26 mL, 3.60 g, 45.9 mmol, 8.0 equiv.) was added dropwise to a stirred solution of (*E*)-4-phenylbut-3-en-2-ol (0.85 g, 5.7 mmol, 1.0 equiv.) in dry EtOH (2.68 mL, 2.11 g, 45.9 mmol, 8.0 equiv.). The reaction mixture was stirred at rt for 1.5 h. The black solution was concentrated under reduced pressure to give the allylic chloride as a black oil (0.923 g, 97%) which was used without further purification. Triethyl phosphite (0.867 mL, 0.828 g, 5.0 mmol, 0.9 equiv.) was added to the residue and the resulting mixture stirred at 140 °C for 19 h. The reaction mixture was cooled to rt and applied directly to a flash column. Elution with 2:1 EtOAc/Hex afforded the title compound as a yellow oil (0.632 g, 41% over 2 steps). R_f 0.16 (1:1 Hex-EtOAc). ¹H NMR (CDCl₃, 400 MHz) δ 1.29 (app. q, J = 6.8 Hz, 6H), 1.40 (dd, J = 18.3, 7.1 Hz, 3H), 2.79 (dq, J = 23.1, 7.4 Hz, 1H), 4.10 (app. p, J = 7.2 Hz, 4H), 6.16-6.28 (m, 1H), 6.50 (dd, J = 15.9, 4.9 Hz, 1H), 7.20 (t, J = 7.1 Hz, 1H), 7.28 (t, J = 7.4 Hz, 2H), 7.36 (d, J = 7.4 Hz, 2H); ¹³C NMR (CDCl₃, 100 MHz) δ 14.0 (d, $^2J_{C-P}$ = 6.1 Hz), 16.5 (d, 3J = 5.7 Hz), 36.1 (d, $^1J_{C-P}$ = 139.6 Hz), 62.0 (d, 2J = 7.0 Hz), 62.2 (d, 2J = 7.1 Hz), 126.1 (d, $^2J_{C-P}$ = 10.3 Hz), 126.3 (d, $^5J_{C-P}$ = 1.6 Hz), 127.5, 128.5, 132.1 (d, $^3J_{C-P}$ = 13.9 Hz), 136.9 (d, $^4J_{C-P}$ = 3.2 Hz). HRMS (ESI-TOF) calcd for C₁₄H₂₂O₃P (M+H)⁺ 269.1301, obsd 269.1296.



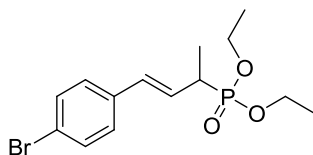
(*E*)-4-(4-bromophenyl)but-3-en-2-one (**229**).^{*} Sodium hydride (60% dispersion in mineral oil, 0.272 g, 6.8 mmol, 1.3 equiv.) was suspended in THF (10 mL) at 0 °C under N₂. After 10 min, a solution of diethyl (2-oxopropyl)phosphonate (1.14 mL, 5.9 mmol, 1.1 equiv.) was added and the mixture stirred at 0 °C for 30 min. A solution of 4-bromobenzaldehyde (1.00 g, 5.4 mmol, 1.0 equiv.) was added to the mixture and stirred for 2 h at 0 °C. The mixture was diluted with H₂O (40 mL) and extracted with Et₂O (3 x 100 mL). The organic layers were combined and washed with 5% HCl (2 x 40 mL), sat'd aq. NaHCO₃ (2 x 40 mL), brine (2 x 40 mL), dried over MgSO₄, filtered, and concentrated. The mixture was applied directly to a flash column, eluting with 10:1 Hex/EtOAc, to give ketone **229** as colorless crystals (1.12 g,

92%). R_f 0.30 (4:1 Hex-EtOAc). $^1\text{H NMR}$ (CDCl_3 , 400 MHz) δ 2.28 (s, 3H), 6.59 (d, $J = 16.3$ Hz, 1H), 7.28 (d, $J = 8.2$ Hz, 2H), 7.33 (d, $J = 16.3$ Hz, 1H), 7.40 (d, $J = 8.2$ Hz, 2H); $^{13}\text{C NMR}$ (CDCl_3 , 100 MHz) δ 27.6, 124.7, 127.5, 129.6, 132.1, 133.3, 141.8, 197.9.



(*E*)-4-(4-bromophenyl)but-3-en-2-ol (**216**).* A solution of (*E*)-4-(4-bromophenyl)but-3-en-2-one (100 mg, 0.44 mmol, 1.0 equiv.) was dissolved in dry methanol (1 mL) at 0 °C under N_2 . After 10 min, sodium borohydride (25 mg, 0.67 mmol, 1.5 equiv.) was added. The resulting mixture was stirred for 1.5 h at 0 °C, then neutralized by the dropwise addition of 5% HCl until pH of 7, as observed with UIP, mixture was diluted with H_2O (10 mL) and extracted with EtOAc (3 x 30 mL). The combined organic layers were filtered through MgSO_4 , and concentrated. The residue was applied to a flash column and eluting with (5:1 Hex/EtOAc) to afford the title compound as a colorless solid (96 mg, 95%). R_f 0.30 (3:1 Hex-EtOAc). $^1\text{H NMR}$ (CDCl_3 , 400 MHz) δ 1.37 (d, $J = 6.4$ Hz, 3H), 1.74 (s, 1H), 4.48 (app. p, $J = 6.2$ Hz, 1H), 6.25 (dd, $J = 15.9, 6.2$ Hz, 1H), 6.50 (d, $J = 15.9$ Hz, 1H), 7.23 (d, $J = 8.2$ Hz, 2H), 7.43 (d, $J = 8.2$ Hz, 2H); $^{13}\text{C NMR}$ (CDCl_3 , 100 MHz) δ 23.4, 68.7, 121.3, 128.0, 128.1, 131.7, 134.7, 135.7.

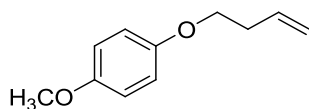
*Procedure and spectra courtesy of Alex Long Nguyen, LSU undergraduate, Summer 2010



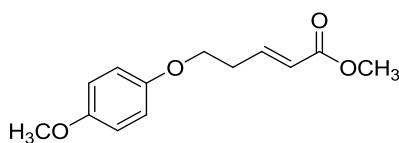
(*E*)-diethyl (4-(4-bromophenyl)but-3-en-2-yl)phosphonate (**214**). Acetyl chloride (903 μL , 998 mg, 12.7 mmol, 8.0 equiv.) was added dropwise to a stirred solution of (*E*)-4-(4-bromophenyl)but-3-en-2-ol (361 mg, 1.59 mmol, 1.0 equiv.) in dry EtOH (743 μL , 586 mg, 12.7 mmol, 8.0 equiv.). The reaction mixture was stirred at rt for 2 h. The black solution was concentrated under reduced pressure to give the

allylic chloride as a black oil (390 mg, quant.) that was used without further purification. Triethyl phosphite (249 μL , 238 mg, 1.43 mmol, 0.9 equiv.) was added to (*E*)-1-bromo-4-(3-chlorobut-1-enyl)benzene (390 mg, 1.59 mmol, 1.0 equiv.) and the resulting mixture stirred at 140 $^{\circ}\text{C}$ for 19 h. The reaction mixture was cooled to rt and applied directly to flash column. Elution with 2:1 EtOAc/Hex afforded the title compound as a yellow oil (127 mg, 23% over 2 steps). R_f 0.27 (2:1 EtOAc-Hex). ^1H NMR* (CDCl_3 , 250 MHz) δ 1.26-1.47 (m, 9H), 2.81 (dq, $J = 23.3, 7.2$ Hz, 1H), 4.14 (app. p, $J = 7.3$ Hz, 4H), 6.22 (ddd, $J = 15.9, 7.9, 6.3$ Hz, 1H), 6.45 (dd, $J = 15.9, 4.8$ Hz, 1H), 7.23 (d, $J = 8.4$ Hz, 2H), 7.42 (d, $J = 8.4$ Hz, 2H). HRMS (ESI-TOF) calcd for $\text{C}_{14}\text{H}_{21}\text{BrO}_3\text{P}$ ($\text{M}+\text{H}$) $^+$ 347.0406, obsd 347.0406.

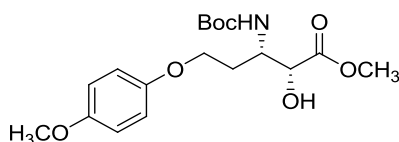
* ^1H NMR spectra of the title compound contaminated with $\text{P}(\text{OEt})_3$ in a ratio of 2:1 favoring **214**



1-(But-3-en-1-yloxy)-4-methoxybenzene (**210**). *p*-Methoxyphenol (860 mg, 6.9 mmol, 1.0 equiv.) was added to a stirred solution of 3-buten-1-ol (600 μL , 506 mg, 7.0 mmol, 1.0 equiv.) in dry THF (25 mL). Triphenylphosphine (2.36 g, 9.0 mmol, 1.3 equiv.) was added as a solid, in a single portion, followed by the dropwise addition of DIAD (1.91 mL, 1.96 g, 9.7 mmol, 1.4 equiv.). The reaction mixture was heated at reflux overnight, cooled to rt, concentrated, and applied directly to a flash column. Elution with 95:5 Hex/ Et_2O afforded the title compound as a colorless oil (825 mg, 67%). R_f 0.33 (95:5 Hex- Et_2O). ^1H NMR (CDCl_3 , 400 MHz) δ 2.52 (app. q, $J = 6.7$ Hz, 2H), 3.76 (s, 3H), 3.96 (t, $J = 6.7$ Hz, 2H), 5.07-5.20 (m, 2H), 5.90 (ddt, $J = 17.2, 10.3, 6.7$ Hz, 1H), 6.79-6.87 (m, 4H); ^{13}C NMR (CDCl_3 , 100 MHz) δ 33.7, 55.7, 67.9, 114.6, 115.6, 116.9, 134.6, 153.0, 153.8. HRMS (ESI-TOF) calcd for $\text{C}_{11}\text{H}_{15}\text{O}_2$ ($\text{M}+\text{H}$) $^+$ 179.1067, obsd 179.1062.

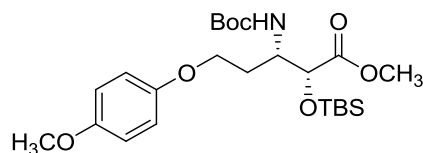


(*E*)-Methyl 5-(4-methoxyphenoxy)pent-2-enoate (**119a**). Methyl acrylate (1.25 mL, 1.18 g, 13.7 mmol, 1.9 equiv.) was added dropwise to a stirred solution of Grubbs' second generation catalyst (305 mg, 0.36 mmol, 5 mol %) in dry CH₂Cl₂ (40 mL). After stirring for 15 min, a solution of 1-(but-3-en-1-yloxy)-4-methoxybenzene (1.29 g, 7.2 mmol, 1.0 equiv.) in dry CH₂Cl₂ (20 mL) was added dropwise. The reaction mixture was heated at reflux for 4 h, cooled to rt, concentrated, and applied directly to a flash column. Elution with 92:8 Hex/EtOAc → 4:1 Hex/EtOAc afforded the title compound as a black oil (1.587 g, 93%). *R*_f 0.34 (4:1 Hex-EtOAc). ¹H NMR (CDCl₃, 400 MHz) δ 2.63 (app. q, *J* = 6.4 Hz, 2H), 3.72 (s, 3H), 3.74 (s, 3H), 4.00 (t, *J* = 6.3 Hz, 2H), 5.95 (d, *J* = 15.7 Hz, 1H), 6.81 (app. s, 4H), 7.03 (dt, *J* = 15.7, 6.4 Hz, 1H); ¹³C NMR (CDCl₃, 100 MHz) δ 32.0, 51.3, 55.5, 66.4, 114.5, 115.4, 122.7, 145.0, 152.5, 153.8, 166.5. HRMS (ESI-TOF) calcd for C₁₃H₁₆NaO₄ (M+Na)⁺ 259.0941, obsd 259.0941.

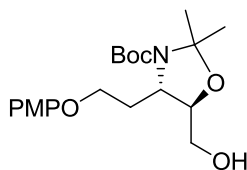


(2*R*,3*S*)-Methyl-3-((*tert*-butoxycarbonyl)amino)-2-hydroxy-5-(4-methoxyphenoxy)pentanoate (**209**). Sodium hydroxide (212 mg, 5.3 mmol, 3.0 equiv.) in H₂O (12.45 mL) was added to a stirred solution of *tert*-butyl carbamate (620 mg, 5.3 mmol, 3.0 equiv.) in *n*-PrOH (4.15 mL). The addition of 1,3-dichloro-5,5-dimethylhydantoin (695 mg, 3.5 mmol, 2.0 equiv.) was followed by the dropwise addition of a solution of (DHQ)₂PHAL (69 mg, 0.088 mmol, 5 mol %) in *n*-PrOH (4.15 mL). After stirring for 15 min, a solution of (*E*)-methyl 5-(4-methoxyphenoxy)pent-2-enoate (417 mg, 1.8 mmol, 1.0 equiv.) in *n*-PrOH (4.15 mL) was added, followed immediately by potassium osmate dihydrate (33 mg, 0.088 mmol, 5 mol %). The reaction mixture was stirred at rt for 21 h. Sodium sulfite (1.83 g, 8.2 equiv.) was added and the mixture stirred for 1 h. The resulting mixture was diluted with H₂O (16.6 mL) and extracted with EtOAc (4 x 40 mL). The combined organic layers were dried with MgSO₄, filtered, and concentrated to afford a 11:1 mixture of regioisomers. Purification by flash chromatography (column 1: 95:5 CH₂Cl₂/MeOH to isolate *R*_f 0.48, column 2: 3:1 Hex/EtOAc to isolate *R*_f 0.10) afforded the title

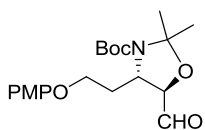
compound as a white solid (493 mg, 76%). R_f 0.10 (3:1 Hex-EtOAc). $[\alpha]_D^{25}$ -64.4 (c 1.8, CH_2Cl_2) Lit,¹ $[\alpha]_D$ -67 (c 1.8, CH_2Cl_2). ^1H NMR (CDCl_3 , 400 MHz) δ 1.32 (br s, 1H), 1.39 (s, 9H), 1.94-2.15 (m, 2H), 3.74 (s, 3H), 3.77 (s, 3H), 3.99 (t, J = 6.0 Hz, 2H), 4.27 (s, 1H), 4.31 (app. t, J = 7.1 Hz, 1H), 5.11 (d, J = 9.6 Hz, 1H), 6.77-6.87 (m, 4H); ^{13}C NMR (CDCl_3 , 100 MHz) δ 28.0, 31.7, 50.5, 52.5, 55.5, 65.5, 72.2, 79.4, 114.4, 115.5, 152.7, 153.7, 155.3, 173.7. HRMS (ESI-TOF) calcd for $\text{C}_{18}\text{H}_{27}\text{NNaO}_7$ ($\text{M}+\text{Na}$)⁺ 392.1680, obsd 392.1677.



(2*R*,3*S*)-Methyl-3-((*tert*-butoxycarbonyl)amino)-2-((*tert*-butyldimethylsilyl)oxy)-5-(4-methoxyphenoxy)pentanoate (**235**). Imidazole (252 mg, 3.7 mmol, 7.0 equiv.) was added to a stirred solution of (2*R*,3*S*)-methyl 3-((*tert*-butoxycarbonyl)amino)-2-hydroxy-5-(4-methoxyphenoxy)pentanoate (195 mg, 0.53 mmol, 1.0 equiv.) in dry CH_2Cl_2 (5.0 mL) at rt under N_2 . After stirring for 30 min, TBSCl (557 mg, 3.7 mmol, 7.0 equiv.) was added in a single portion. The reaction mixture was stirred overnight at rt, concentrated, and purified via flash chromatography (6:1 Hex/EtOAc) to provide the title compound as a colorless oil (248 mg, 97%). R_f 0.26 (5:1 Hex-EtOAc). $[\alpha]_D^{25}$ -47.6 (c 1.0, CHCl_3). ^1H NMR (CDCl_3 , 400 MHz) δ 0.08 (s, 3H), 0.12 (s, 3H), 0.94 (s, 9H), 1.40 (s, 9H), 1.86-2.09 (m, 2H), 3.71 (s, 3H), 3.76 (s, 3H), 3.93-4.04 (m, 2H), 4.19-4.29 (m, 1H), 4.33 (app. d, J = 2.0 Hz, 1H), 4.89 (d, J = 9.9 Hz, 1H), 6.78-6.87 (m, 4H); ^{13}C NMR (CDCl_3 , 100 MHz) δ -5.5, -4.9, 18.3, 25.7, 28.2, 32.3, 51.4, 51.9, 55.6, 66.0, 73.6, 79.3, 114.5, 115.6, 153.0, 153.8, 155.3, 172.2. HRMS (ESI-TOF) calcd for $\text{C}_{24}\text{H}_{42}\text{NO}_7\text{Si}$ ($\text{M}+\text{H}$)⁺ 484.2725, obsd 484.2712.

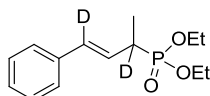


(4*S*,5*R*)-*tert*-butyl-5-(hydroxymethyl)-4-(2-(4-methoxyphenoxy)ethyl)-2,2-dimethyloxazolidine-3-carboxylate (**254**). Diisobutylaluminum hydride (2.53 mL, 1 M in CH₂Cl₂, 2.53 mmol, 5.0 equiv.) was added to a stirred solution of (4*S*,5*R*)-3-*tert*-butyl 5-methyl 4-(2-(4-methoxyphenoxy)ethyl)-2,2-dimethyloxazolidine-3,5-dicarboxylate (0.207 g, 0.51 mmol, 1.0 equiv.) in dry CH₂Cl₂ (5 mL) at -78 °C. The mixture was stirred at -78 °C for 30 min and then warmed to rt for 4.5 h. The colorless solution was cooled to 0 °C and quenched by the dropwise addition of MeOH (5 mL). A solution of sat'd aq. potassium sodium tartrate (5 mL) was added to the reaction mixture at rt and stirred vigorously overnight. The aqueous layer was extracted with EtOAc (5 x 50 mL). The combined organic layers were dried with MgSO₄, filtered, concentrated, and purified via flash chromatography (2:1 Hex/EtOAc) to provide the title compound as a yellow oil (166 mg, 86%). *R*_f 0.22 (2:1 Hex-EtOAc). [α]_D²⁵ +5.2 (*c* 0.75, CHCl₃). ¹H NMR (CDCl₃, 400 MHz, 330 K) δ 1.48 (s, 9H), 1.51 (s, 3H), 1.61 (s, 3H), 1.97 (t, *J* = 6.0 Hz, 1H), 2.05-2.16 (m, 1H), 2.25-2.38 (m, 1H), 3.61-3.68 (m, 1H), 3.69-3.74 (m, 1H), 3.76 (s, 3H), 3.88 (ddd, *J* = 8.1, 5.0, 2.8 Hz, 1H), 3.95-4.05 (m, 2H), 4.2 (q, *J* = 5.0 Hz, 1H), 6.81 (app. s, 4H); ¹³C NMR (CDCl₃, 100 MHz, 323 K) δ 27.2, 28.1, 28.5, 33.0, 55.8, 57.4, 63.7, 66.2, 80.2, 80.8, 94.4, 115.0, 115.6, 152.0, 153.0, 154.3. HRMS (ESI-TOF) calcd for C₂₀H₃₂NO₆ (M+H)⁺ 382.2224, obsd 382.2232.

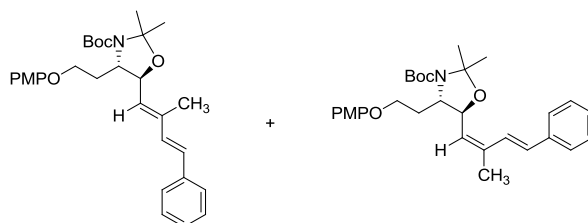


(4*S*,5*R*)-*tert*-butyl-5-formyl-4-(2-(4-methoxyphenoxy)ethyl)-2,2-dimethyloxazolidine-3-carboxylate (**208**). Dess-Martin periodinane (91 mg, 0.21 mmol, 1.3 equiv.) was added to a stirred solution of (4*S*,5*R*)-*tert*-butyl 5-(hydroxymethyl)-4-(2-(4-methoxyphenoxy)ethyl)-2,2-dimethyloxazolidine-3-carboxylate (63 mg, 0.17 mmol, 1.0 equiv.) in dry CH₂Cl₂ (1 mL) at rt. The colorless suspension was stirred at rt for 4.5 h. The reaction mixture was quenched with a mixture of sat'd aq. solutions of NaHCO₃ and Na₂S₂O₃ (4:1, 5 mL) and stirred vigorously for 1 h. The aqueous layer was extracted with CH₂Cl₂ (3 x 35 mL). The combined organic layers were washed with a mixture of

sat'd aq. solutions of NaHCO_3 and $\text{Na}_2\text{S}_2\text{O}_3$ (4:1, 5 mL), dried with MgSO_4 , filtered, concentrated, and purified via flash chromatography (2:1 Hex/EtOAc) to provide the title compound as a yellow oil (46 mg, 74%). R_f Streaking. $[\alpha]_{\text{D}}^{25} +11.7$ (c 0.35, CHCl_3). $^1\text{H NMR}$ (CDCl_3 , 400 MHz, 330 K) δ 1.47 (s, 9H), 1.57 (s, 3H), 1.61 (s, 3H), 2.08-2.19 (m, 1H), 2.26-2.37 (m, 1H), 3.75 (s, 3H), 3.96-4.07 (m, 2H), 4.34 (dt, $J = 8.8, 2.4$ Hz, 1H), 4.46 (d, $J = 2.4$ Hz, 1H), 6.80 (app. s, 4H), 9.78 (s, 1H). HRMS (ESI-TOF) calcd for $\text{C}_{20}\text{H}_{29}\text{NNaO}_6$ ($\text{M}+\text{Na}$) $^+$ 402.1887, obsd 402.1875.



α,γ Deuteration of (*E*)-diethyl (4-phenylbut-3-en-2-yl)phosphonate (**259**). Lithium hexamethyldisilazide (332 μL , 1 M in THF, 0.33 mmol, 1.0 equiv.) was added dropwise to a stirred solution of (*E*)-diethyl (4-phenylbut-3-en-2-yl)phosphonate (89 mg, 0.33 mmol, 1.0 equiv.) in dry THF (1.5 mL) at -78 $^\circ\text{C}$. After stirring for 1 h, CD_3OD (500 μL , excess) was added dropwise. The cold bath (-78 $^\circ\text{C}$) was removed and the reaction mixture stirred for 21 h at rt. The contents were quenched with sat'd aq. NH_4Cl (1.0 mL) and extracted with EtOAc (2 x 10 mL). The combined organic layers were washed with H_2O (8.0 mL) and brine (8.0 mL), dried with MgSO_4 , filtered, and concentrated. Purification by flash chromatography (2:1 EtOAc/Hex) afforded the title compound as a colorless oil (58 mg, 65%). R_f 0.16 (1:1 Hex-EtOAc). $^1\text{H NMR}$ (CDCl_3 , 400 MHz) δ 1.26-1.35 (m, 6H), 1.39 (d, $J = 18.3$ Hz, 3H), 4.12 (app. p, $J = 7.0$ Hz, 4H), 6.22 (d, $J = 5.0$ Hz, 1H), 7.14-7.41 (m, 5H); $^{13}\text{C NMR}$ (CDCl_3 , 100 MHz) δ 13.9 (d, $^2J_{\text{C-P}} = 6.3$ Hz), 16.5 (d, $^3J = 5.6$ Hz), 36.1 (d, $^1J_{\text{C-P}} = 139.5$ Hz), 62.0 (d, $^2J = 7.0$ Hz), 62.2 (d, $^2J = 7.1$ Hz), 125.9 (d, $^2J_{\text{C-P}} = 10.3$ Hz), 126.2, 127.5, 128.5, 132.1 (d, $^3J_{\text{C-P}} = 14.1$ Hz), 136.8 (d, $^4J_{\text{C-P}} = 3.3$ Hz). HRMS (ESI-TOF) calcd for $\text{C}_{14}\text{H}_{20}\text{D}_2\text{O}_3\text{P}$ ($\text{M}+\text{H}$) $^+$ 271.1427, obsd 271.1427.

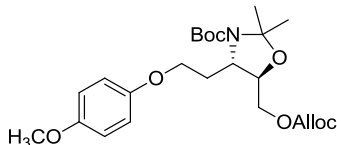


Lithium diisopropylamide was prepared according to the following procedure: Diisopropylamine (128 μ L, 92.4 μ g, 0.9 mmol, 2.5 equiv.) was dissolved in dry THF (1.0 mL) and cooled to -78 $^{\circ}$ C. After stirring for 10 min, n BuLi (418 μ L, 2.16 M in Hexanes,^{†,29} 0.9 mmol, 2.5 equiv.) was added dropwise and the mixture stirred for 15 min at -78 $^{\circ}$ C.

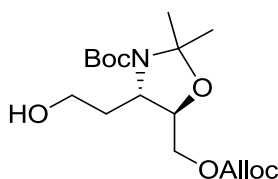
E/Z mixture of (4*S*,5*S*)-*tert*-butyl 4-(2-(4-methoxyphenoxy)ethyl)-2,2-dimethyl-5-((3*E*)-2-methyl-4-phenylbuta-1,3-dien-1-yl)oxazolidine-3-carboxylate (***E/Z*-206**). A solution of phosphonate ester **213** (242 mg, 0.9 mmol, 2.5 equiv.) in dry THF (2.0 mL) was transferred by cannula to the solution of LDA and stirred for 30 min at -78 $^{\circ}$ C. A solution of aldehyde **208** (137 mg, 0.36 mmol, 1.0 equiv.) in dry THF (2.5 mL) at -78 $^{\circ}$ C was transferred by cannula to the reaction mixture and stirring continued for 2 h at -78 $^{\circ}$ C. The reaction mixture was warmed to -40 $^{\circ}$ C, stirred for 2 h, warmed to 0 $^{\circ}$ C and stirred for 45 min. The reaction was quenched with H₂O (5.0 mL) at 0 $^{\circ}$ C and extracted with EtOAc (3 x 40 mL). The combined organic layers were dried with MgSO₄, filtered and concentrated. Purification by flash chromatography (8:1 Hex/EtOAc) gave the title compound as an inseparable 4.5:1 *E/Z* mixture (70 mg, 40%). *R*_f 0.16 (12:1 Hex/EtOAc). ¹H NMR* (CDCl₃, 400 MHz, 328 K) δ 1.49 (1.48)* (s, 9H), 1.53 (s, 3H), 1.63 (s, 3H), 1.98 (1.99)* (d, *J* = 0.8 Hz, 3H), 2.19-2.27 (m, 2H), 3.72 (3.73)* (s, 3H), 3.75-3.81 (m, 1H), 3.99 (t, *J* = 6.2 Hz, 2H), 5.18 (4.96)* (dd, *J* = 8.6, 6.0 Hz, 1H), 5.49 (5.67)* (d, *J* = 8.7 Hz, 1H), 6.55-6.83 (m, 6H), 7.17-7.44 (m, 5H); ¹³C NMR (CDCl₃, 100 MHz, 328 K) δ 13.1, 20.6, 26.8, 28.5, 55.8, 61.4, 65.5 (65.6)*, 75.0 (76.1)*, 80.0, 94.1, 114.8 (114.8)*, 115.6 (115.5)*, 125.5, 126.5, 126.8, 127.8, 128.4, 128.6, 131.2, 132.9, 137.5, 137.9, 152.3, 153.1, 154.0. HRMS (ESI-TOF) calcd for C₃₀H₄₀NO₅ (M+H)⁺ 494.2901, obsd 494.2899.

*where discernible peaks were attributable to the *Z*-isomer, these are reported in parentheses with an asterisk

[†]1,3-diphenylacetone *p*-tosylhydrazone (291 mg, 0.77 mmol) was dissolved in anhydrous THF (8 mL) and cooled to 0 $^{\circ}$ C under N₂. n Butyllithium (2.5 M in Hex) was added slowly until a deep yellow color persisted (titer = 0.77/0.36 = 2.16 M)

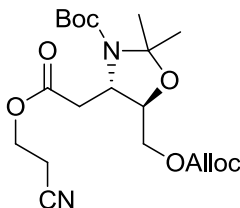


(4*S*,5*R*)-*tert*-butyl-5-[(allyloxycarbonyl)oxy]methyl-4-(2-(4-methoxyphenoxy)ethyl)-2,2-dimethyloxazolidine-3-carboxylate (**288**). Tetramethylethylenediamine (33 μ L, 25.6 μ g, 0.22 mmol, 0.6 equiv.) was added dropwise to a stirred solution of (4*S*,5*R*)-*tert*-butyl 5-(hydroxymethyl)-4-(2-(4-methoxyphenoxy)ethyl)-2,2-dimethyloxazolidine-3-carboxylate (141 mg, 0.37 mmol, 1.0 equiv.) in dry CH_2Cl_2 (3.7 mL) at 0 $^\circ\text{C}$. After stirring for 10 min, allyl chloroformate (43 μ L, 0.41 mmol, 1.1 equiv.) was added dropwise. The reaction mixture was stirred for 1 h at 0 $^\circ\text{C}$, diluted with CH_2Cl_2 (100 mL) and washed with H_2O (50 mL). The organic layer was dried with MgSO_4 , filtered, and concentrated. Purification by flash chromatography (3:1 Hex/EtOAc) afforded the title compound as a colorless oil (149 mg, 87%). R_f 0.43 (3:1 Hex/EtOAc). ^1H NMR (CDCl_3 , 400 MHz) δ 1.48 (s, 9H), 1.51 (s, 3H), 1.56-1.65 (m, 3H), 2.03-2.16 (m, 1H), 2.17-2.42 (m, 1H), 3.76 (s, 3H), 3.87-3.95 (m, 1H), 3.96-4.04 (m, 2H), 4.21 (dd, $J = 11.1, 6.4$ Hz, 1H), 4.24-4.30 (m, 1H), 4.37 (br s, 1H), 4.58 (d, $J = 5.7$ Hz, 2H), 5.22-5.28 (m, 1H), 5.29-5.37 (m, 1H), 5.89 (ddt, $J = 17.2, 10.8, 5.8$ Hz, 1H), 6.82 (app. s, 4H). HRMS (ESI-TOF) calcd for $\text{C}_{24}\text{H}_{36}\text{NO}_8$ ($\text{M}+\text{H}$) $^+$ 466.2435, obsd 466.2436.



(4*S*,5*R*)-*tert*-butyl-5-[(allyloxycarbonyl)oxy]methyl-4-(2-hydroxyethyl)-2,2-dimethyloxazolidine-3-carboxylate (**289**). Cerium (IV) ammonium nitrate (1.17 g, 2.1 mmol, 2.0 equiv.) was added to a stirred solution of (4*S*,5*R*)-*tert*-butyl 5-[(allyloxycarbonyl)oxy]methyl-4-(2-(4-methoxyphenoxy)ethyl)-2,2-dimethyloxazolidine-3-carboxylate (497 mg, 1.1 mmol, 1.0 equiv.) in $\text{CH}_3\text{CN}/\text{H}_2\text{O}$ (4:1, 22 mL) at 0 $^\circ\text{C}$. The reaction mixture was stirred for 10 min at 0 $^\circ\text{C}$, quenched with sat'd aq. NaHCO_3 (10 mL) and extracted with EtOAc (3 x 120 mL). The combined organic layers were dried with MgSO_4 , filtered and

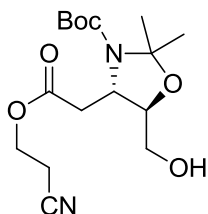
concentrated. Purification by flash chromatography (3:1 Hex/EtOAc → 2:1 Hex/EtOAc) afforded the title compound as a yellow oil (318 mg, 83%). R_f 0.17 (2:1 Hex/EtOAc). ^1H NMR (CDCl_3 , 400 MHz) δ 1.50 (s, 9H), 1.59 (s, 3H), 1.61 (s, 3H), 1.79-1.97 (m, 2H), 3.50-3.76 (m, 2H), 4.06-4.16 (m, 2H), 4.19 (app. s, 1H), 4.20 (app. s, 1H), 4.64 (dt, $J = 5.8, 1.2$ Hz, 2H), 5.24-5.31 (m, 1H), 5.32-5.41 (m, 1H), 5.87-5.99 (m, 1H). HRMS (ESI-TOF) calcd for $\text{C}_{17}\text{H}_{30}\text{NO}_7$ ($\text{M}+\text{H}$) $^+$ 360.2017, obsd 360.2018.



(4*S*,5*R*)-*tert*-butyl-5-[(allyloxycarbonyl)oxy]methyl-4-(2-(2-cyanoethoxy)-2-oxoethyl)-2,2-dimethyloxazolidine-3-carboxylate (**283**). Dess-Martin periodinane (468 mg, 1.1 mmol, 1.3 equiv.) was added to a stirred solution of (4*S*,5*R*)-*tert*-butyl 5-[(allyloxycarbonyl)oxy]methyl-4-(2-hydroxyethyl)-2,2-dimethyloxazolidine-3-carboxylate (305 mg, 0.85 mmol, 1.0 equiv.) in dry CH_2Cl_2 (23 mL) at rt. The colorless suspension was stirred at rt for 1 h, quenched with sat'd aq. NaHCO_3 (5 mL) and stirred for 1 h. The mixture was extracted with CH_2Cl_2 (3 x 100 mL). The combined organic layers were dried with MgSO_4 , filtered, concentrated to 5 mL, and filtered through a silica plug (washing well with 2:1 Hex/EtOAc) to give an intermediate aldehyde (312 mg) which was used without further purification.

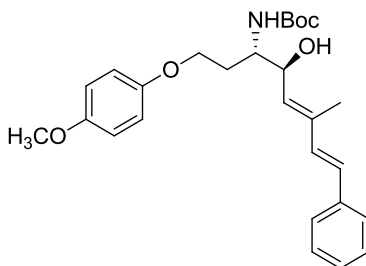
2-Methyl-2-butene (4.62 mL, 90% technical grade, 0.044 mol, 50.0 equiv.) was dissolved in THF (20 mL) and added dropwise to a stirred solution of crude aldehyde (312 mg, 0.87 mmol, 1.0 equiv.) in t -BuOH (45 mL). After stirring for 10 min, a solution containing NaClO_2 (790 mg, 8.7 mmol, 10.0 equiv.) and NaH_2PO_4 (786 mg, 6.6 mmol, 7.5 equiv.) in H_2O (20 mL) was added dropwise to the reaction mixture via glass pipette. The contents were stirred at rt for 16 h, diluted with H_2O (50 mL) and extracted with EtOAc (4 x 50 mL). The combined organic layers were dried with MgSO_4 , filtered and concentrated to give an intermediate carboxylic acid (317 mg theoretical) which was used without further purification.

3-Hydroxypropionitrile (115 μ L, 120 μ g, 1.7 mmol, 2.0 equiv.) was added to a stirred solution of crude carboxylic acid (317 mg theoretical, 0.85 mmol, 1.0 equiv.) in dry CH_2Cl_2 (12 mL) at rt. 4-Dimethylaminopyridine (10 mg, 0.082 mmol, 10 mol %) was added as a CH_2Cl_2 solution followed by DCC (193 mg, 0.94 mmol, 1.1 equiv.). The reaction mixture was stirred for 21 h at rt, filtered through a Celite® plug in a Pasteur pipette (washing well with CH_2Cl_2) and concentrated. Purification by flash chromatography (3:1 Hex/EtOAc) afforded the title compound as a colorless oil (233 mg, 64% over 3 steps). R_f 0.16 (3:1 Hex/EtOAc). ^1H NMR (CDCl_3 , 400 MHz) δ 1.48 (s, 9H), 1.51 (s, 3H), 1.58 (s, 3H), 2.52-2.66 (m, 1H), 2.73 (t, $J = 6.4$ Hz, 2H), 2.89-3.13 (m, 1H), 4.04-4.37 (m, 6H), 4.64 (d, $J = 5.8$ Hz, 2H), 5.29 (dd, $J = 10.4, 1.2$ Hz, 1H), 5.37 (dd, $J = 17.2, 1.2$ Hz, 1H), 5.87-6.00 (m, 1H). HRMS (ESI-TOF) calcd for $\text{C}_{20}\text{H}_{31}\text{N}_2\text{O}_8$ ($\text{M}+\text{H}$)⁺ 427.2075, obsd 427.2071.

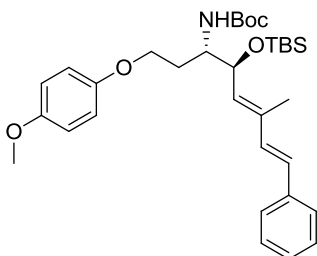


(4*S*,5*R*)-*tert*-butyl-4-(2-(2-cyanoethoxy)-2-oxoethyl)-5-(hydroxymethyl)-2,2-dimethyloxazolidine-3-carboxylate (**286**). Dimedone (730 mg, 5.2 mmol, 10.0 equiv.) was added to a stirred solution of (4*S*,5*R*)-*tert*-butyl-5-[(allyloxycarbonyl)oxy]methyl-4-(2-(2-cyanoethoxy)-2-oxoethyl)-2,2-dimethyloxazolidine-3-carboxylate (222 mg, 0.52 mmol, 1.0 equiv.) in dry THF (7.5 mL) at rt. After stirring for 10 min, $\text{Pd}(\text{PPh}_3)_4$ (60 mg, 0.052 mmol, 10 mol %) was added in a single portion. The reaction mixture was stirred for 30 min at rt, diluted with CH_2Cl_2 (120 mL) and washed with sat'd aq. NaHCO_3 (3 x 100 mL). The organic layer was dried with MgSO_4 , filtered, and concentrated. Purification by flash chromatography (3:2 Hex/EtOAc \rightarrow 1:1 Hex/EtOAc) afforded the title compound as a colorless oil (154 mg, 87%). R_f 0.17 (1:1 Hex/EtOAc). ^1H NMR (CDCl_3 , 400 MHz) δ 1.48 (s, 9H), 1.51 (s, 3H), 1.59 (br s, 3H), 2.01 (t, $J = 6.2$ Hz, 1H), 2.52-2.66 (m, 1H), 2.72 (t, $J = 6.2$ Hz, 2H), 2.89-3.16 (m, 1H),

3.68 (app. p, $J = 5.8$ Hz, 1H), 3.73-3.82 (m, 1H), 3.98-4.19 (m, 2H), 4.31 (t, $J = 6.2$ Hz, 2H). HRMS (ESI-TOF) calcd for $C_{16}H_{26}N_2NaO_6$ ($M+Na$)⁺ 365.1683, obsd 365.1683.



Tert-butyl-((3*S*,4*S*,5*E*,7*E*)-4-hydroxy-1-(4-methoxyphenoxy)-6-methyl-8-phenylocta-5,7-dien-3-yl)carbamate (**277**). Camphorsulfonic acid (940 μ g, 4.0 μ mol, 10 mol %) was dissolved in dry THF (125 μ L) and added dropwise to a stirred solution of *E/Z*-**206** (20 mg, 0.04 mmol, 1.0 equiv.) in ethylene glycol:THF (1:1, 250 μ L). The reaction mixture was stirred at rt for 7 h, quenched with sat'd aq. $NaHCO_3$ (250 μ L) and extracted with EtOAc (3 x 15 mL). The combined organic layers were dried with $MgSO_4$, filtered and concentrated. Purification by flash chromatography (3:1 Hex/EtOAc) afforded the title compound as a colorless oil (12 mg, 65%) (also recovered 6 mg of *E/Z*-**206**, 95% BORSM). R_f 0.26 (2:1 Hex/EtOAc). HRMS (ESI-TOF) calcd for $C_{27}H_{35}NNaO_5$ ($M+Na$)⁺ 476.2407, obsd 476.2405.



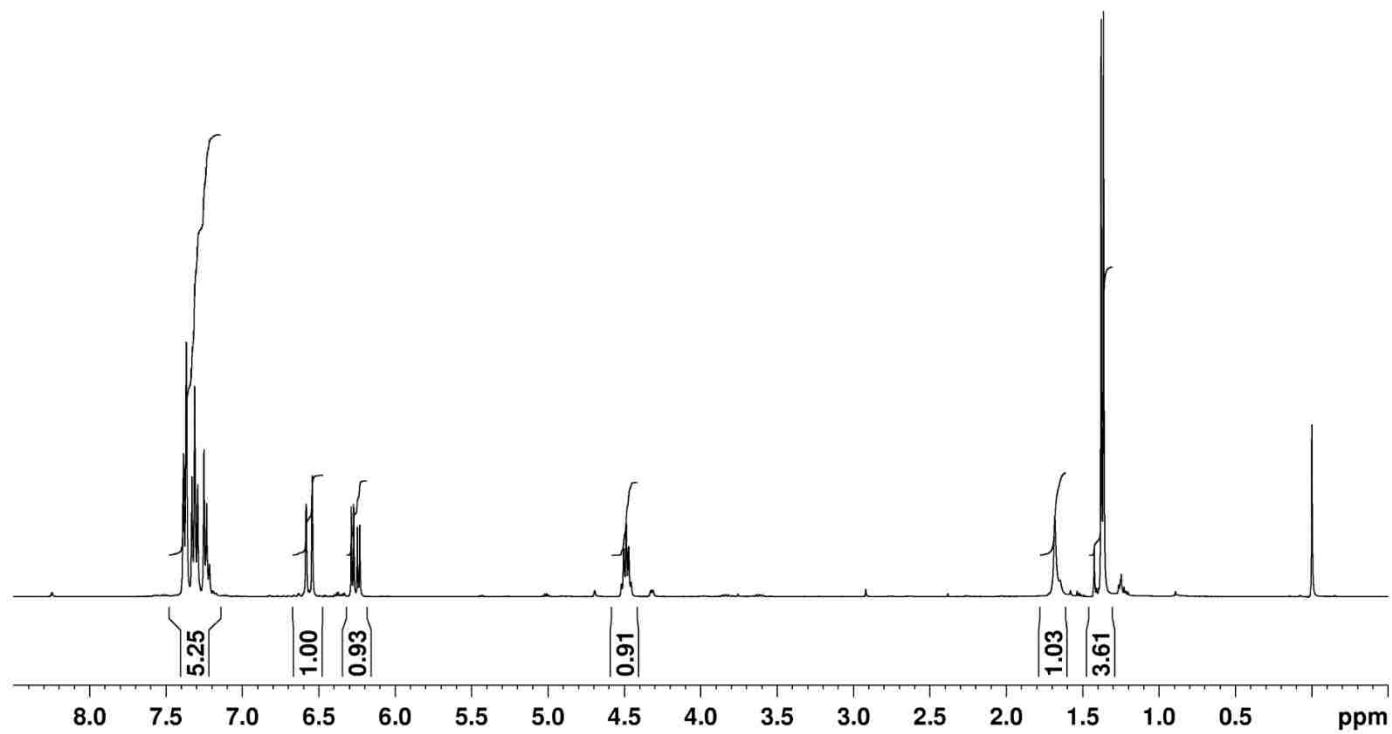
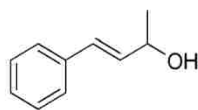
Tert-butyl-((3*S*,4*S*,5*E*,7*E*)-4-((*tert*-butyldimethylsilyl)oxy)-1-(4-methoxyphenoxy)-6-methyl-8-phenylocta-5,7-dien-3-yl)carbamate (**204**). 2,6-Lutidine (14 μ L, 13.0 μ g, 0.12 mmol, 3.0 equiv.) was added dropwise to a stirred solution of *tert*-butyl ((3*S*,4*S*,5*E*,7*E*)-4-hydroxy-1-(4-methoxyphenoxy)-6-methyl-8-phenylocta-5,7-dien-3-yl)carbamate (18 mg, 0.04 mmol, 1.0 equiv.) in dry CH_2Cl_2 (1.0 mL) at rt under N_2 . After stirring for 10 min, TBSOTf (14 μ L, 17.2 μ g, 0.06 mmol, 1.5 equiv.) was added

dropwise. The reaction mixture was stirred overnight at rt, concentrated, and applied directly to flash column. Elution with 3:1 Hex/EtOAc afforded the title compound as a colorless oil (18 mg, 82%). R_f 0.43 (5:1 Hex/EtOAc). HRMS (ESI-TOF) calcd for $C_{33}H_{49}NNaO_5Si$ ($M+Na$)⁺ 590.3272, obsd 590.3257.

4.11.2 Spectra

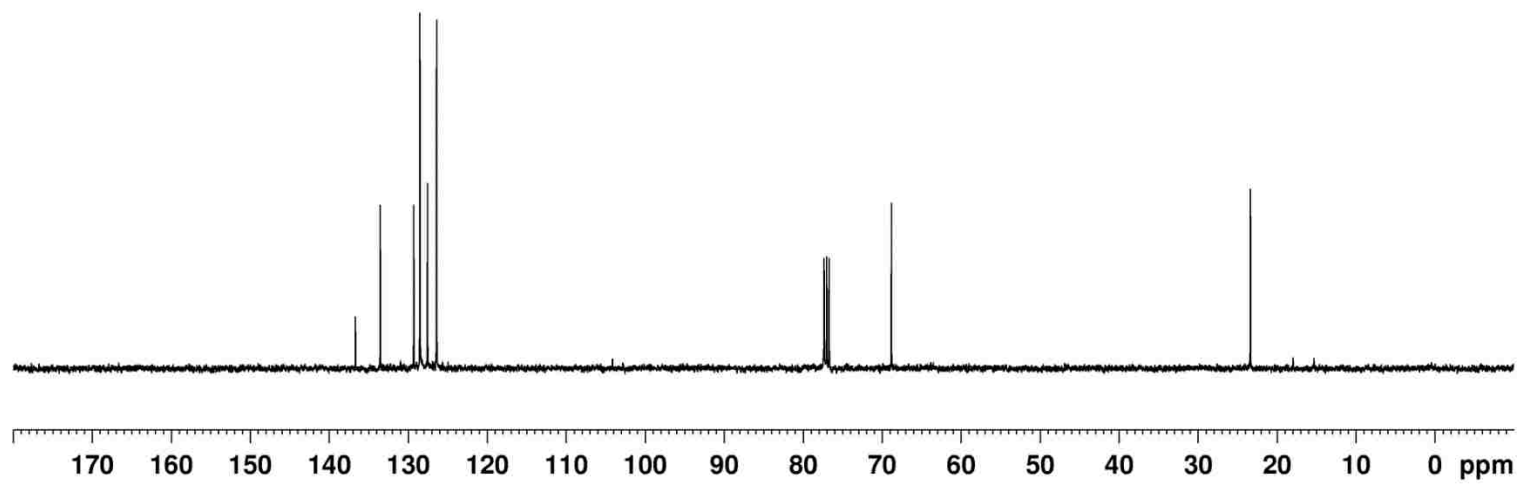
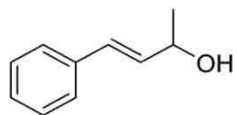
Compound **215** - ^1H NMR spectrum

LN-MeMgBr+trans-cinnamaldehyde in CDCl_3 (400 MHz)



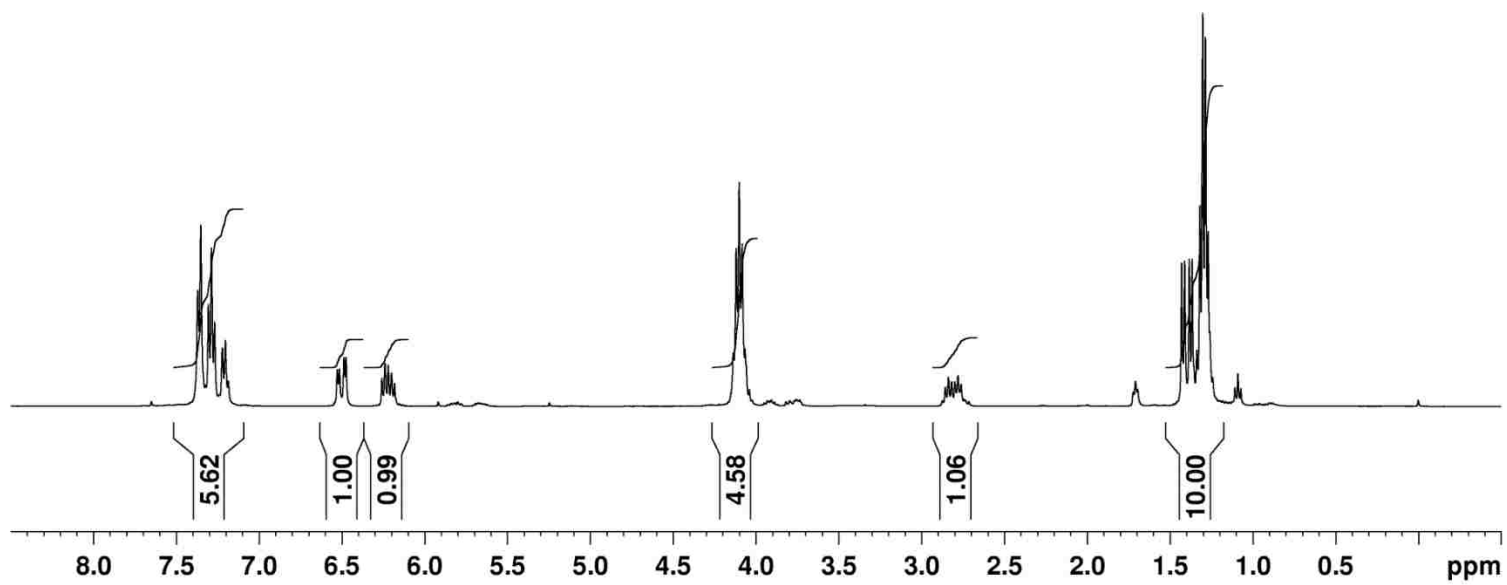
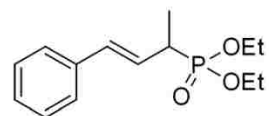
Compound **215** - ^{13}C NMR spectrum

LN's-MeMgBr+trans-cinnamaldehyde



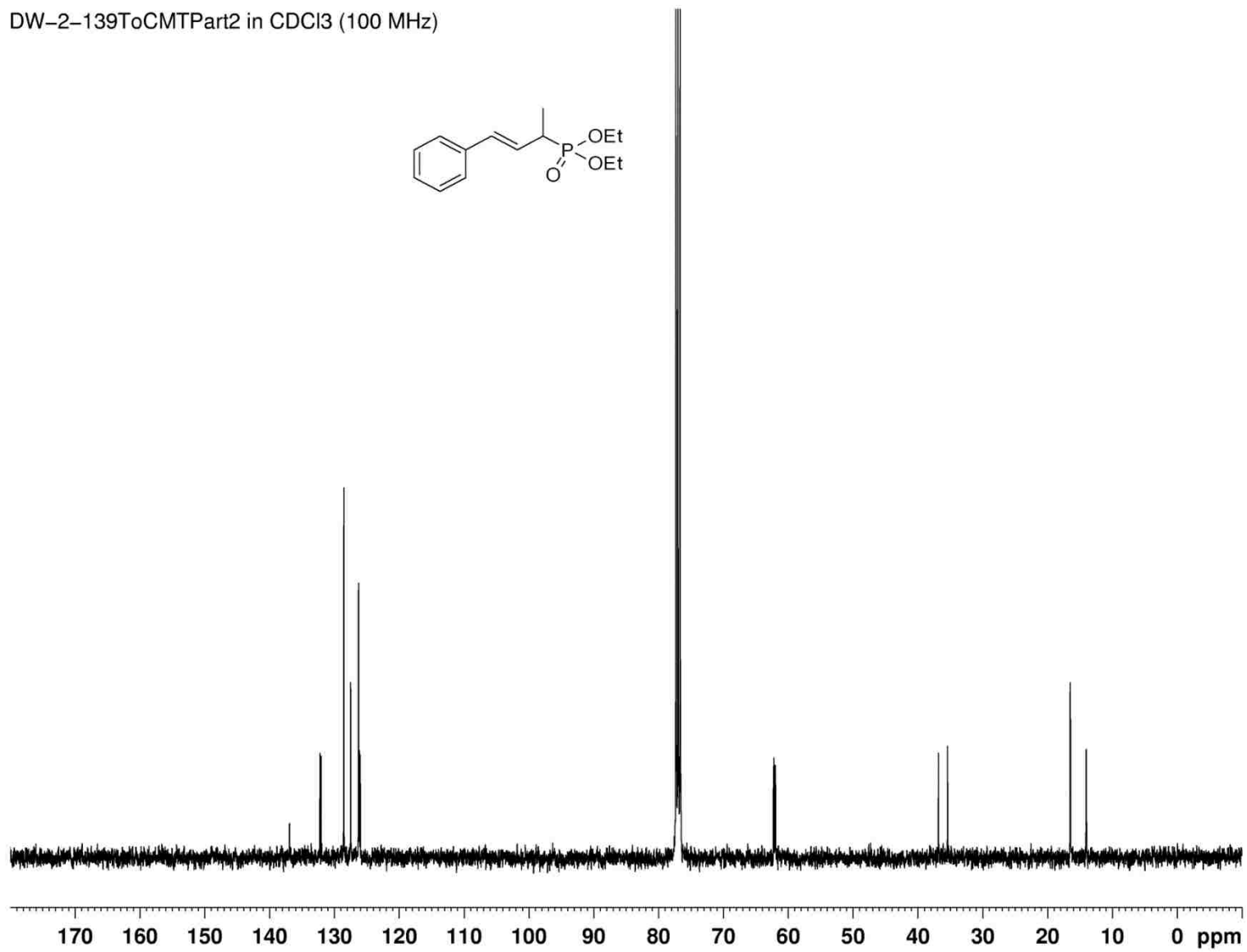
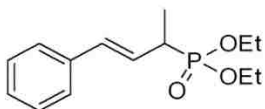
Compound **213** - ^1H NMR spectrum

DW-2-139ToCMT in CDCl_3 (400 MHz)

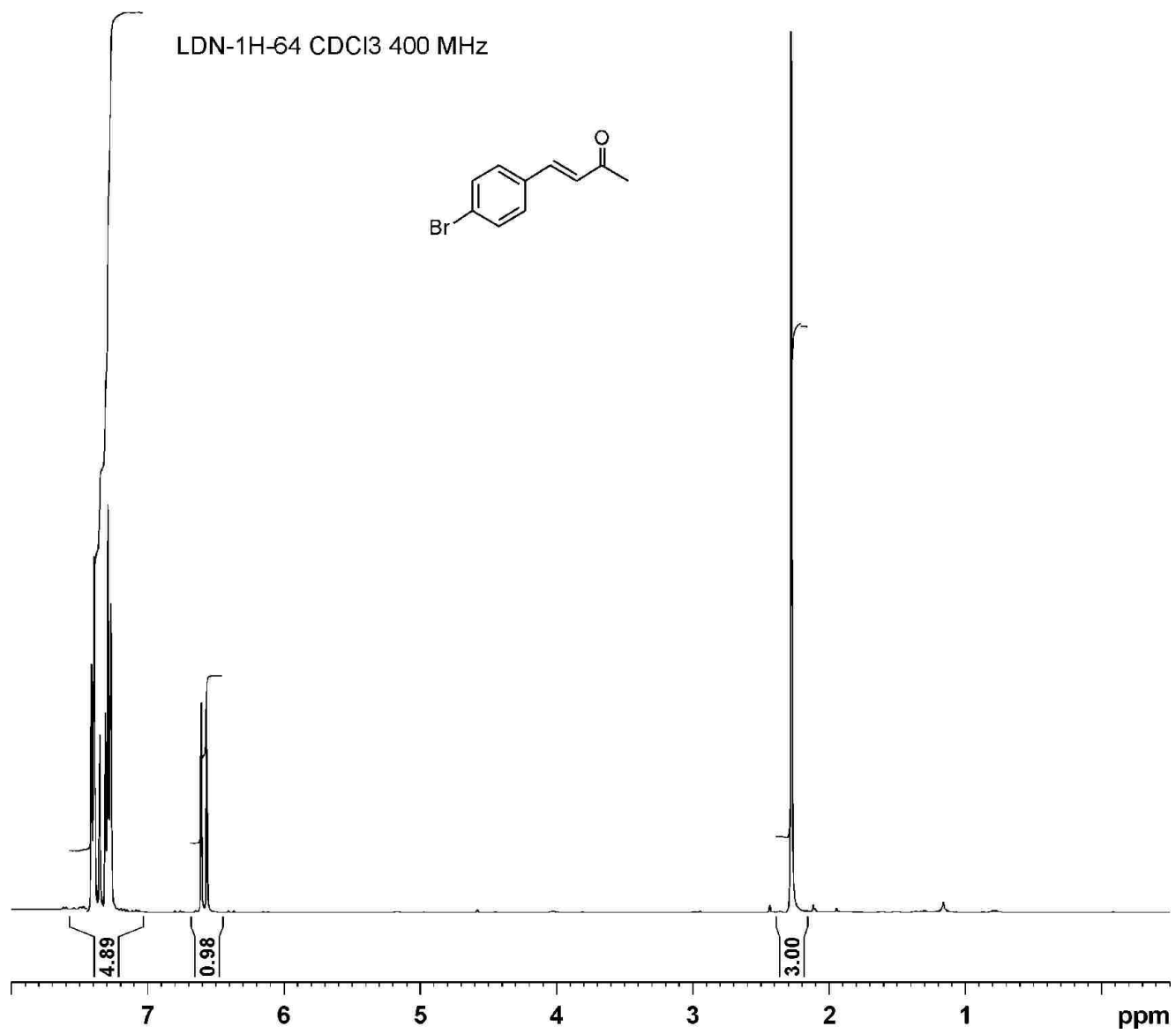


Compound **213** - ^{13}C NMR spectrum

DW-2-139ToCMTPart2 in CDCl_3 (100 MHz)

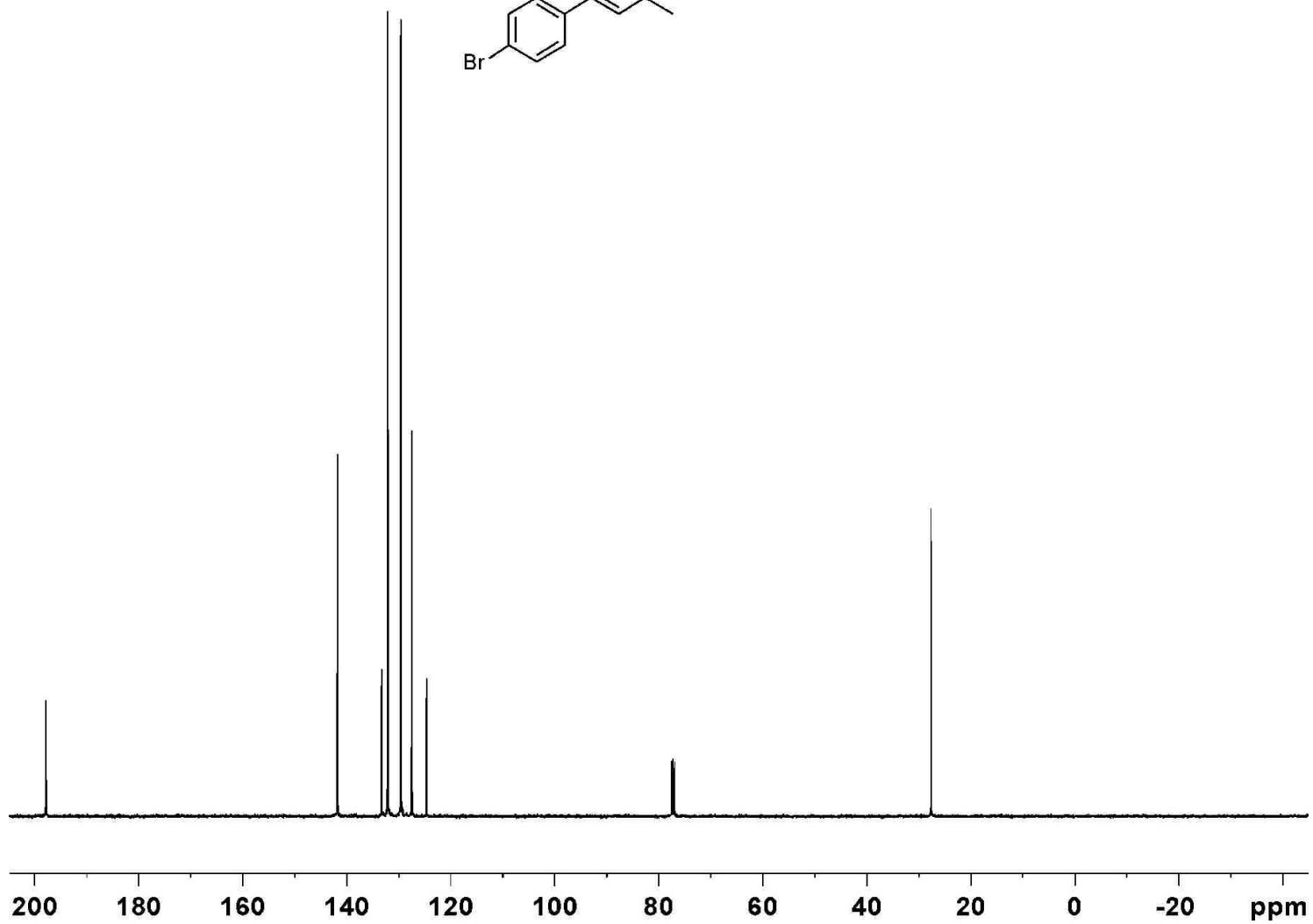
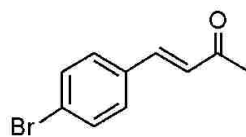


Compound **229** - ^1H NMR spectrum

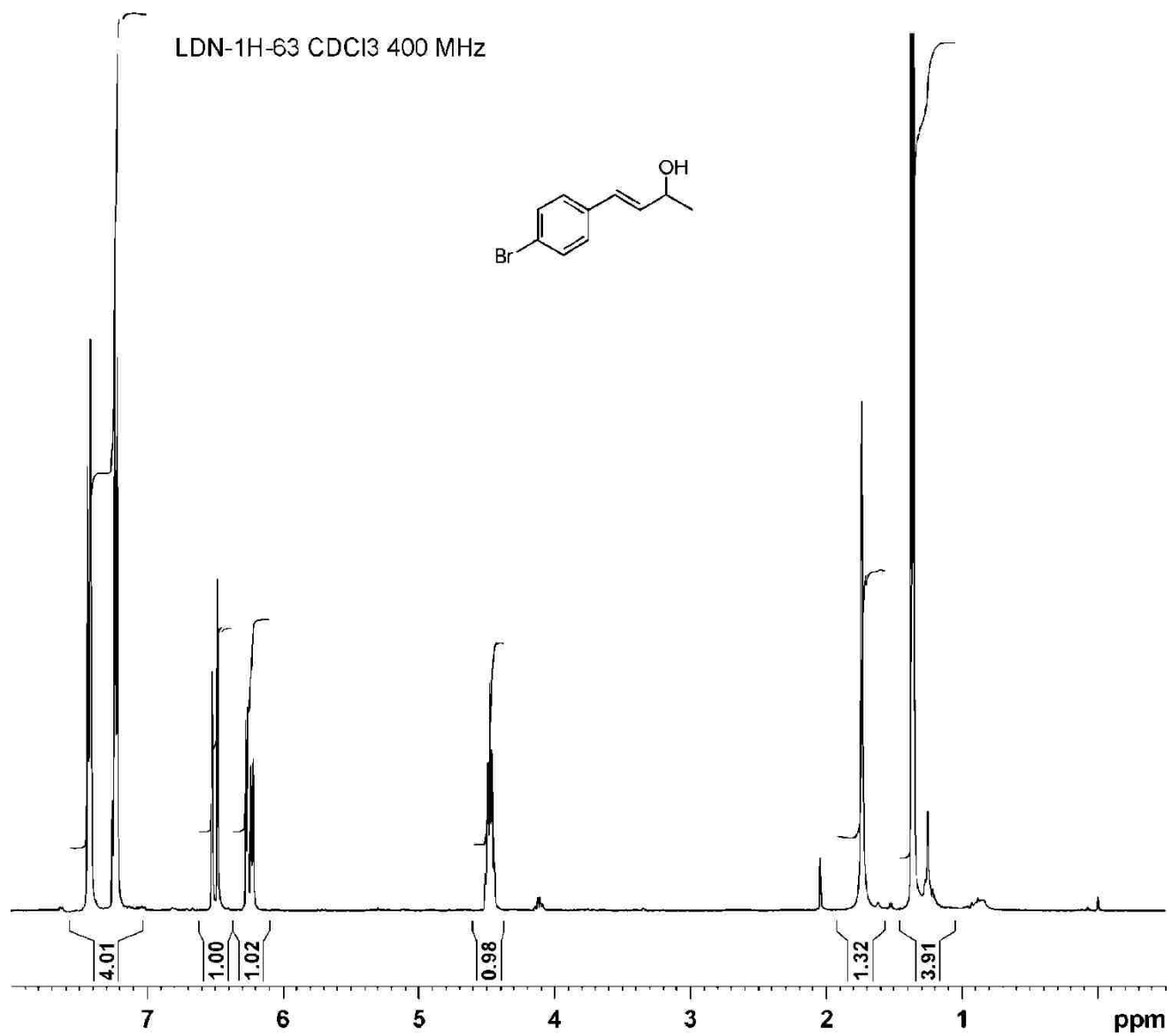


Compound **229** - ^{13}C NMR spectrum

LDN-1-64 Carbon CDCl_3 400 MHz

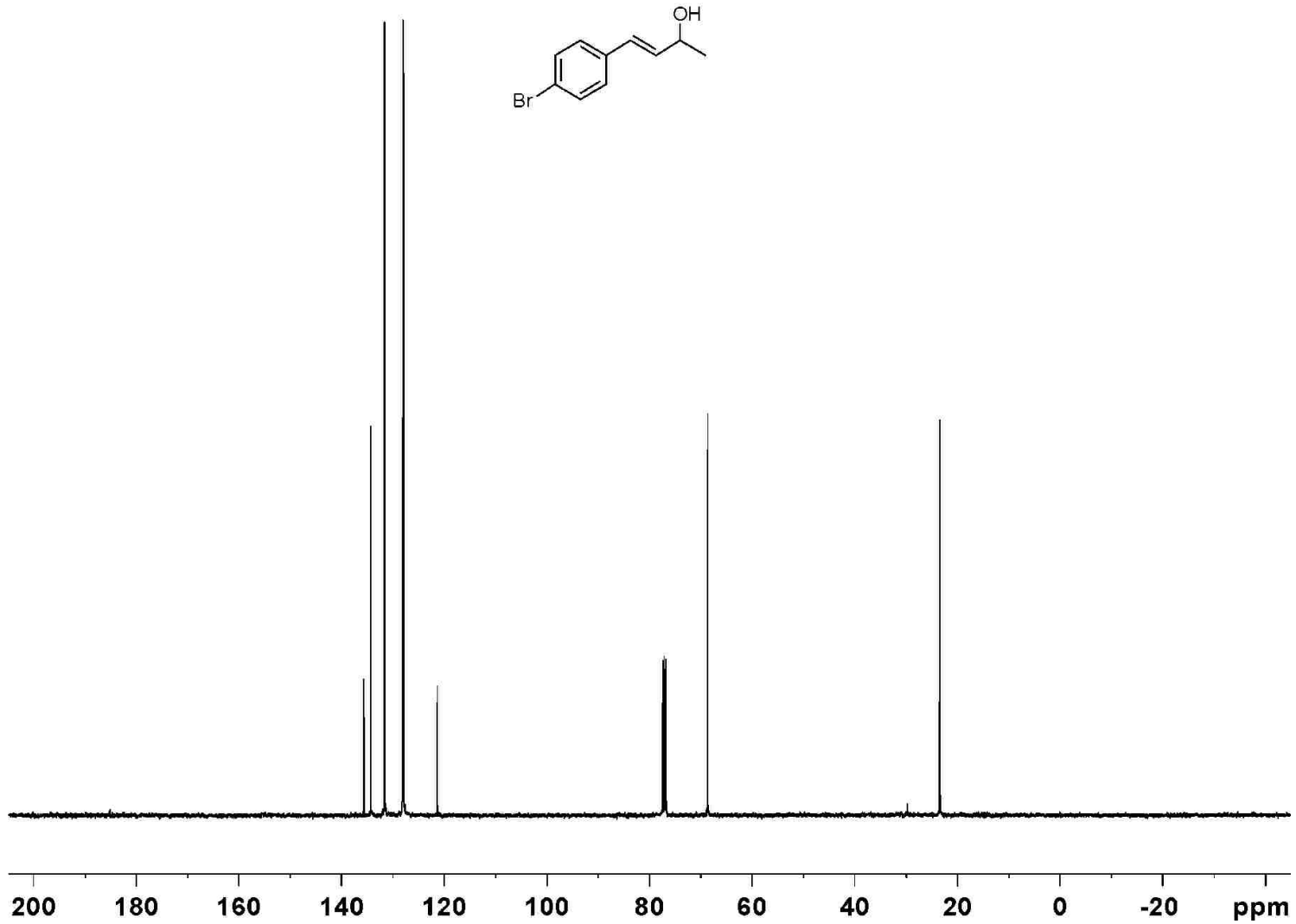
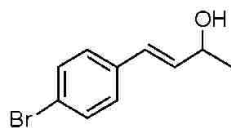


Compound **216** - ^1H NMR spectrum



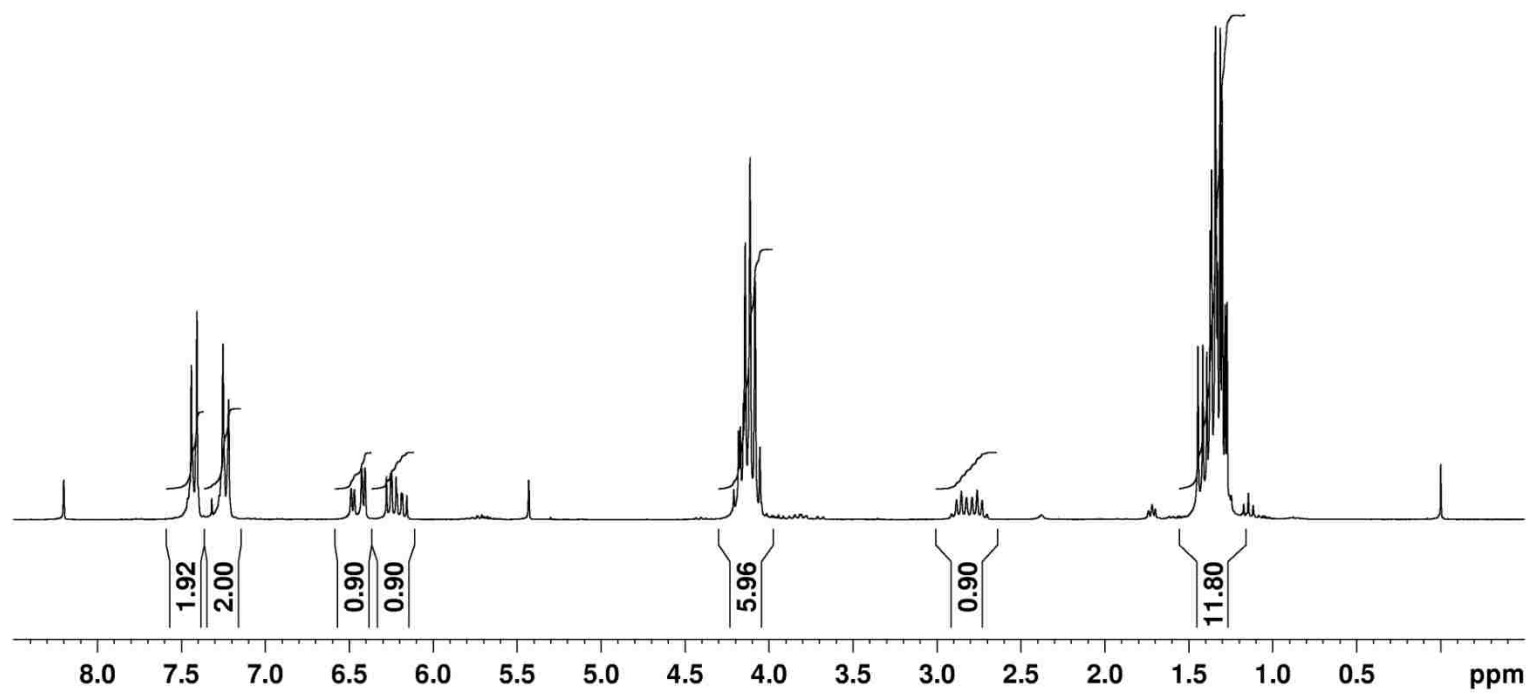
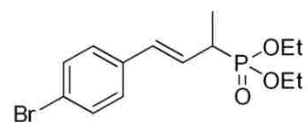
Compound **216** - ^{13}C NMR spectrum

LDN-1-63 Carbon CDCl_3 400 MHz



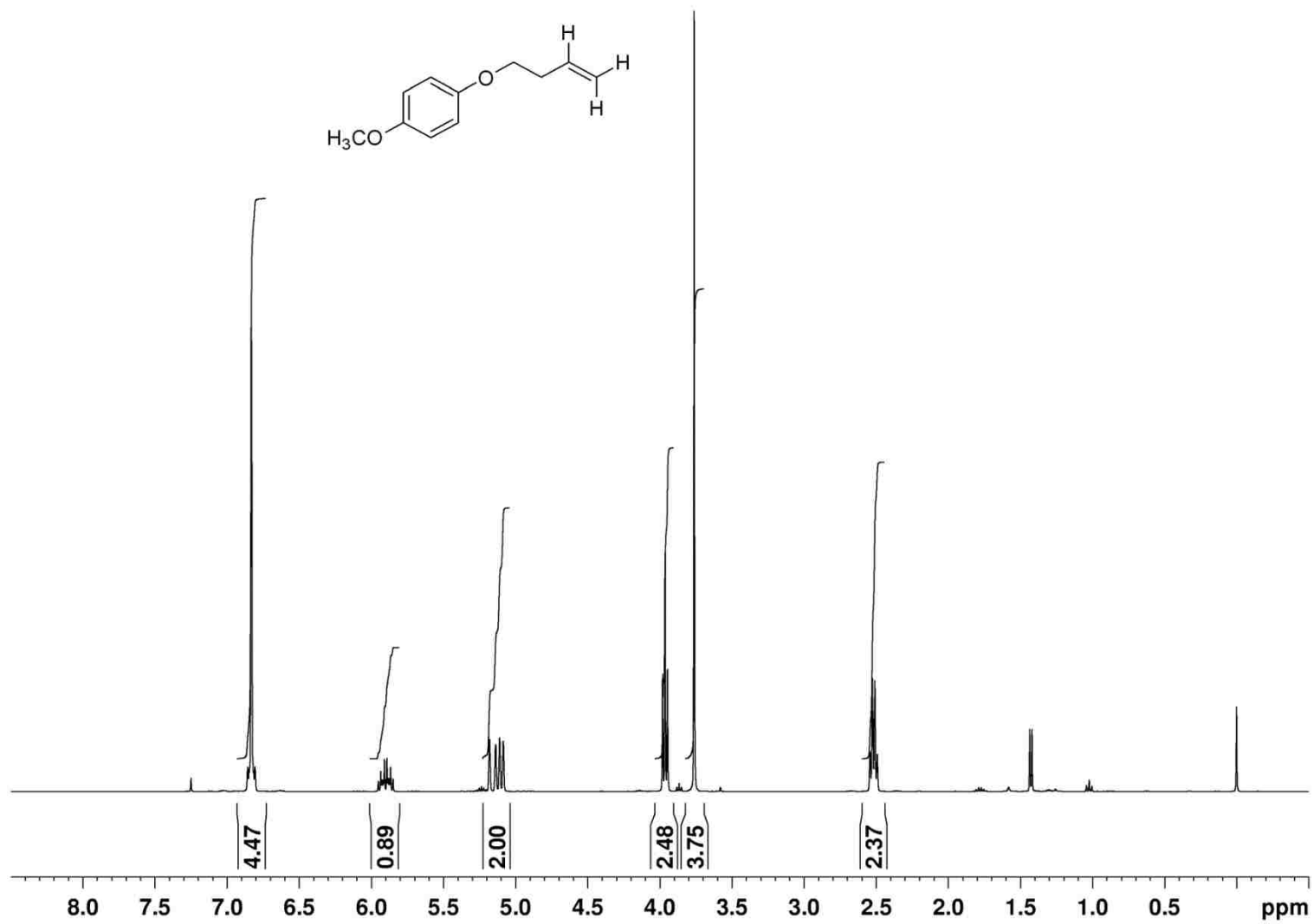
Compound **214** - ^1H NMR spectrum

DW-3-042Part2 in CDCl_3 (250 MHz)



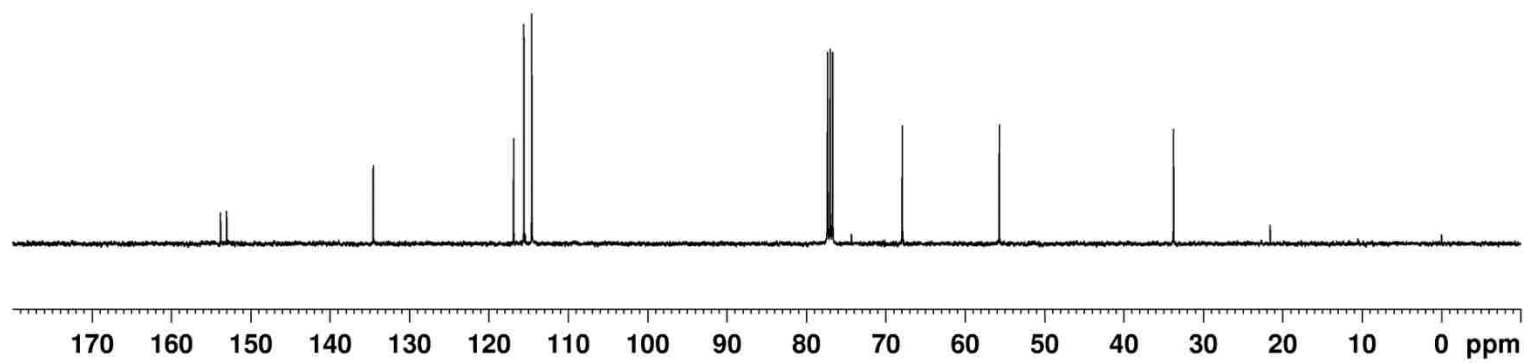
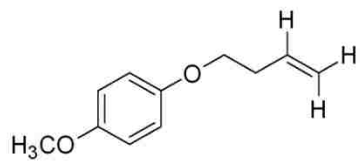
Compound **210** - ^1H NMR spectrum

DW-2-065 in CDCl_3 (400 MHz)



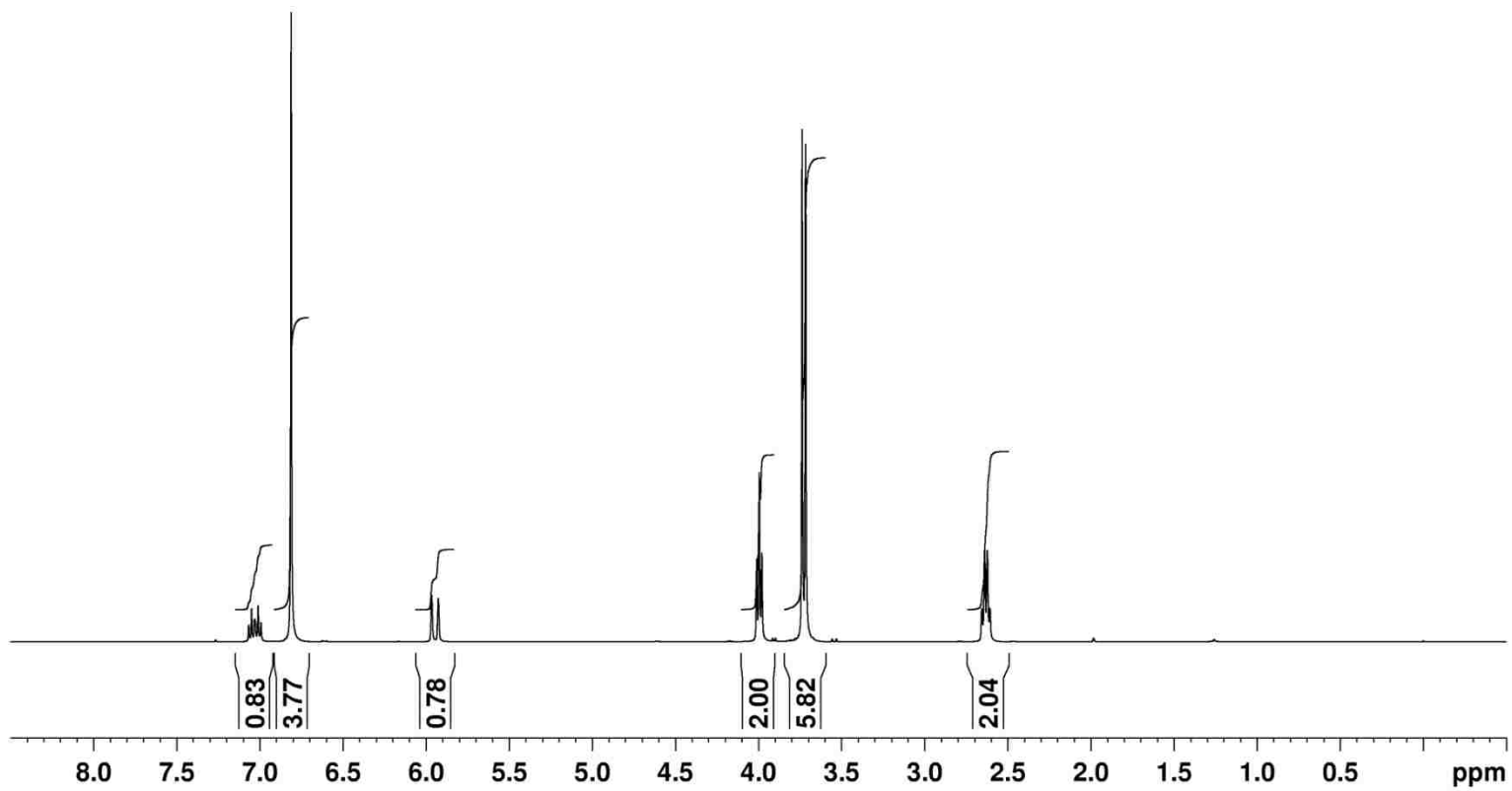
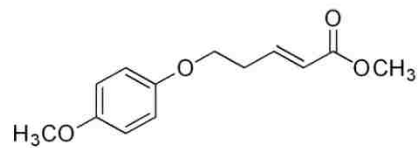
Compound **210** - ^{13}C NMR spectrum

DW-2-065 in CDCl_3 (100 MHz)



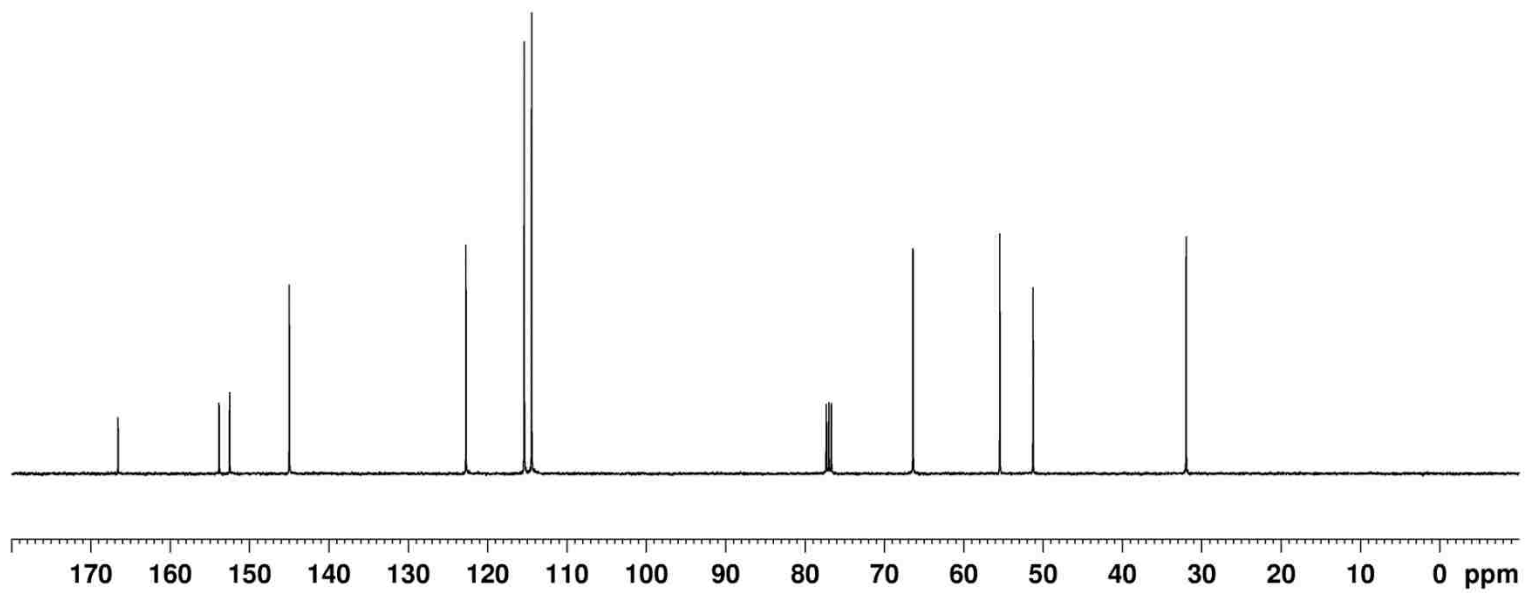
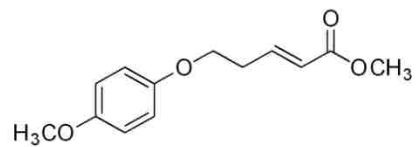
Compound **119a** - ^1H NMR spectrum

DW-2-066 in CDCl_3 (400 MHz)



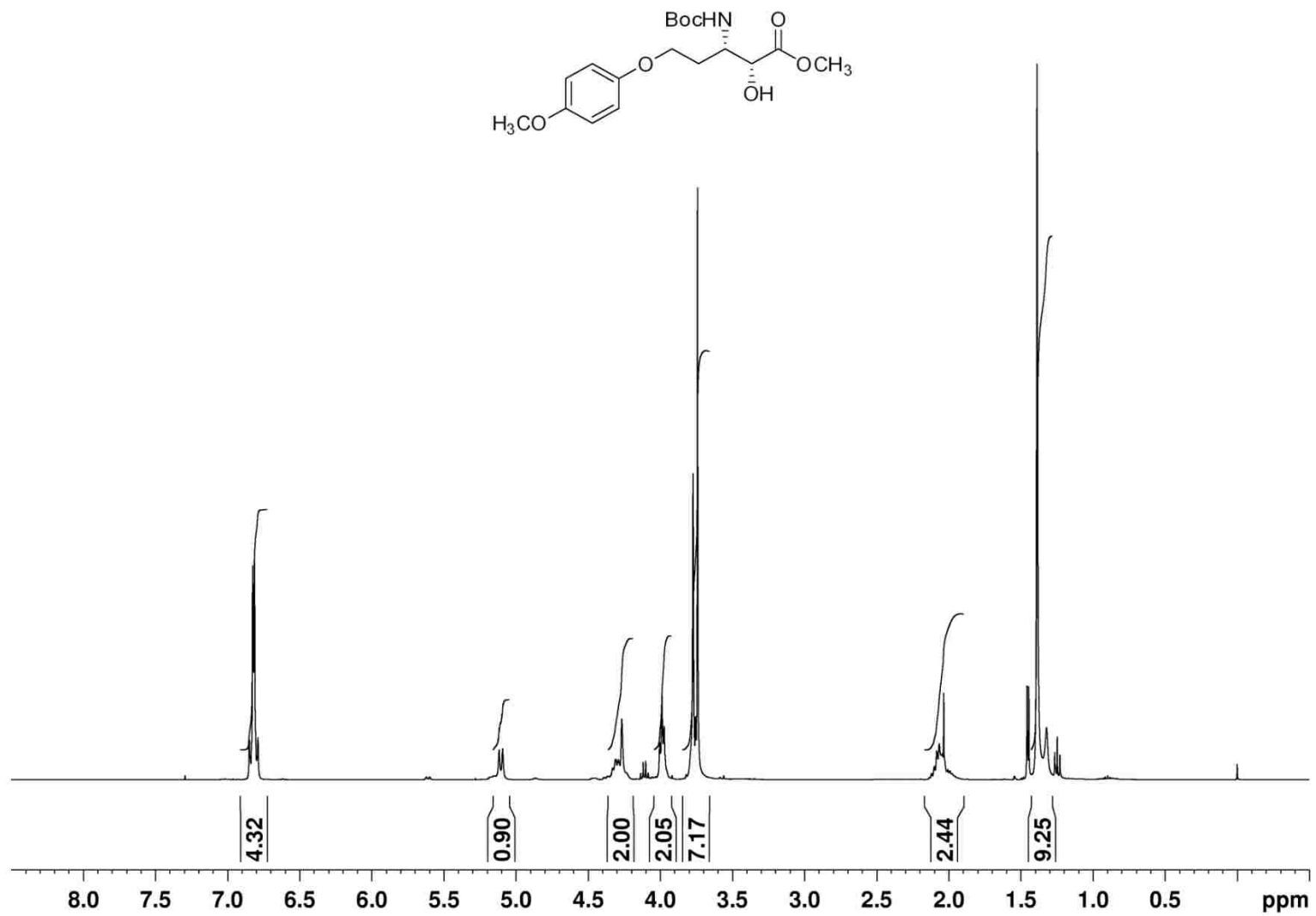
Compound **119a** - ^{13}C NMR spectrum

DW-2-066 in CDCl_3 (100 MHz)



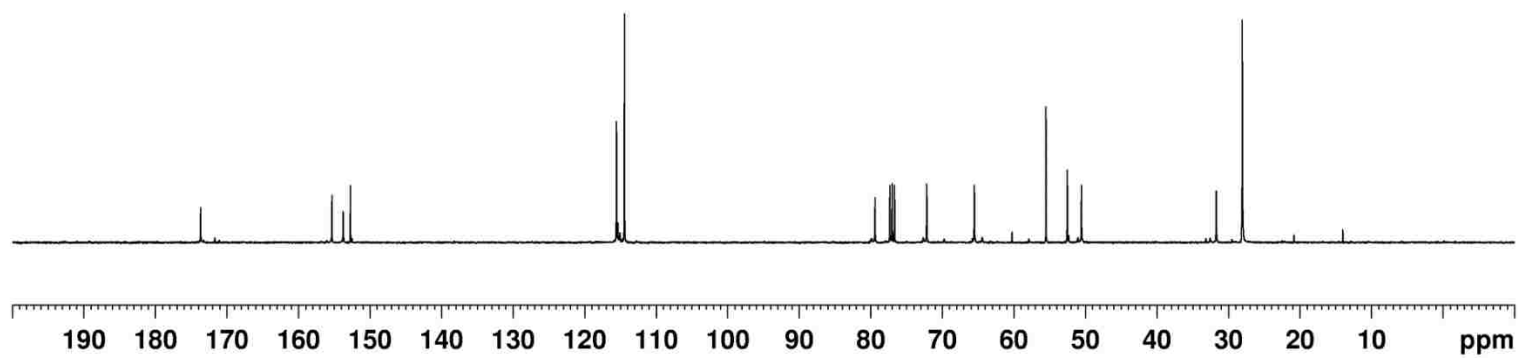
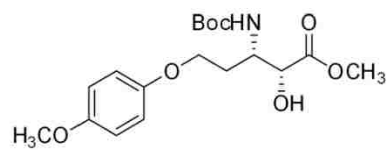
Compound **209** - ^1H NMR spectrum

DW-2-067 in CDCl_3 (400 MHz)



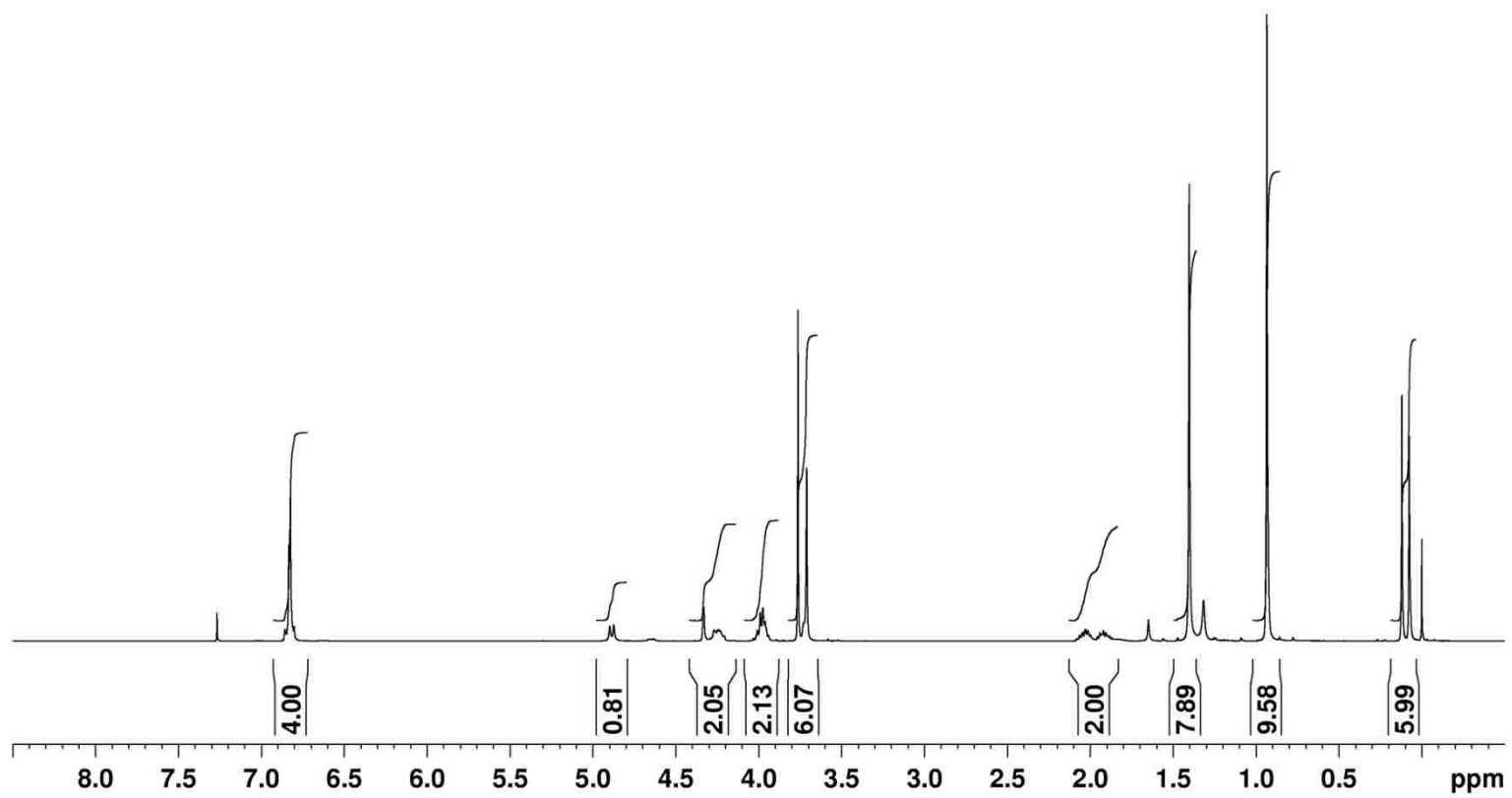
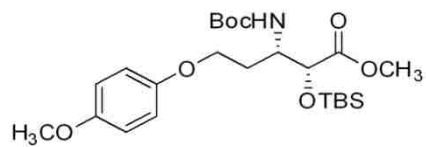
Compound **209** - ^{13}C NMR spectrum

DW-2-067 in CDCl_3 (100 MHz)



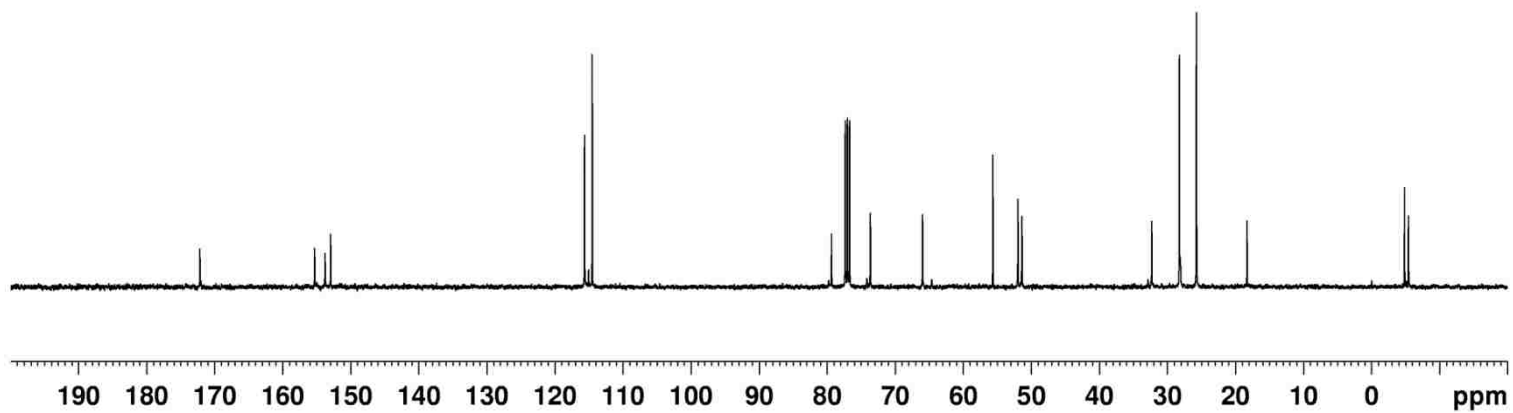
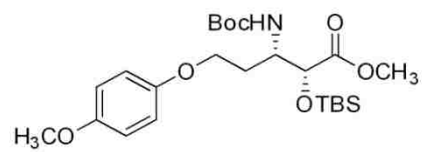
Compound **235** - ^1H NMR spectrum

DW-2-115 in CDCl_3 (400 MHz)



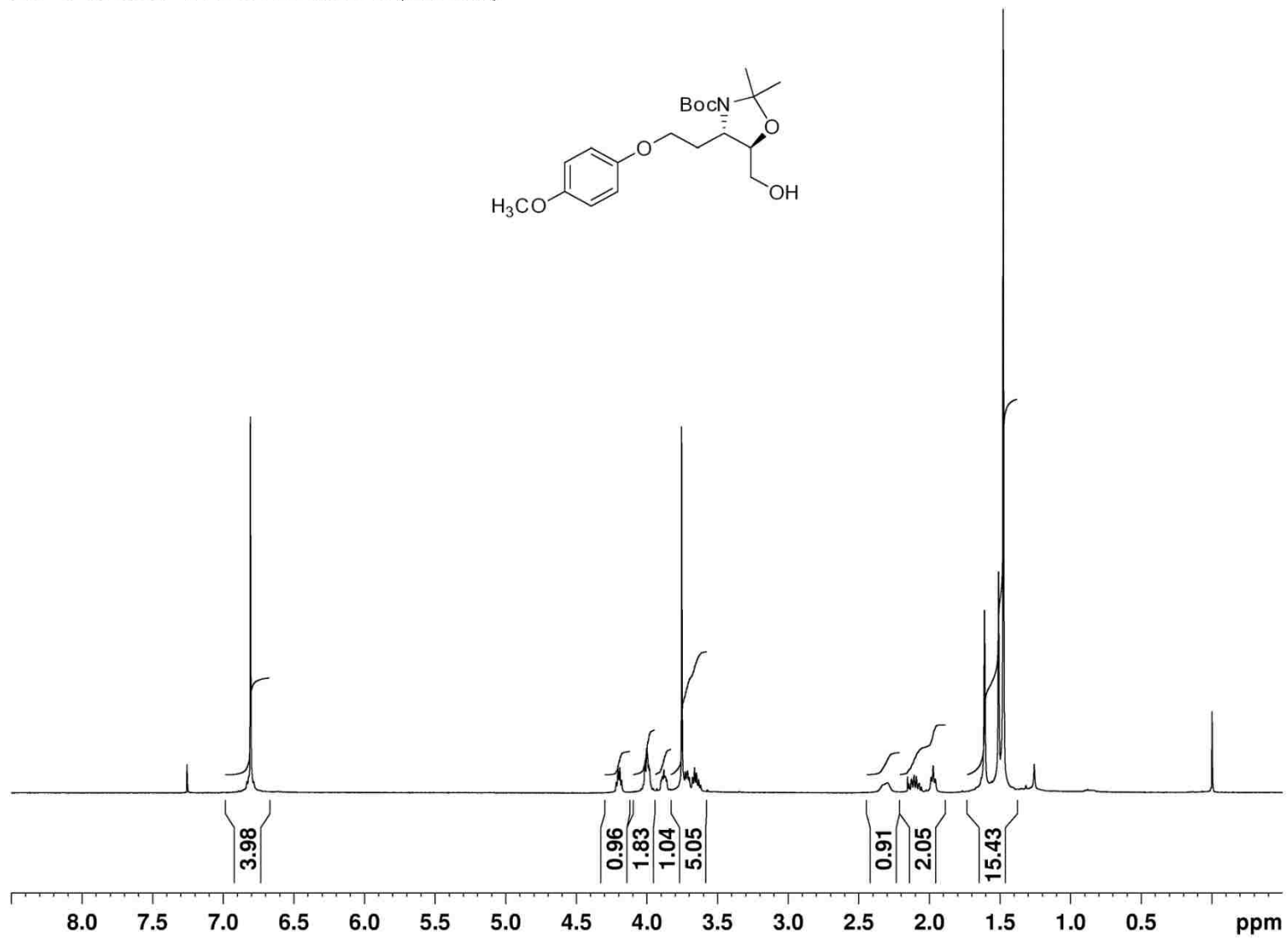
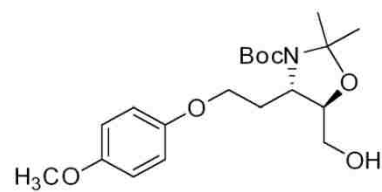
Compound **235** - ^{13}C NMR spectrum

DW-2-114 in CDCl_3 (100 MHz)



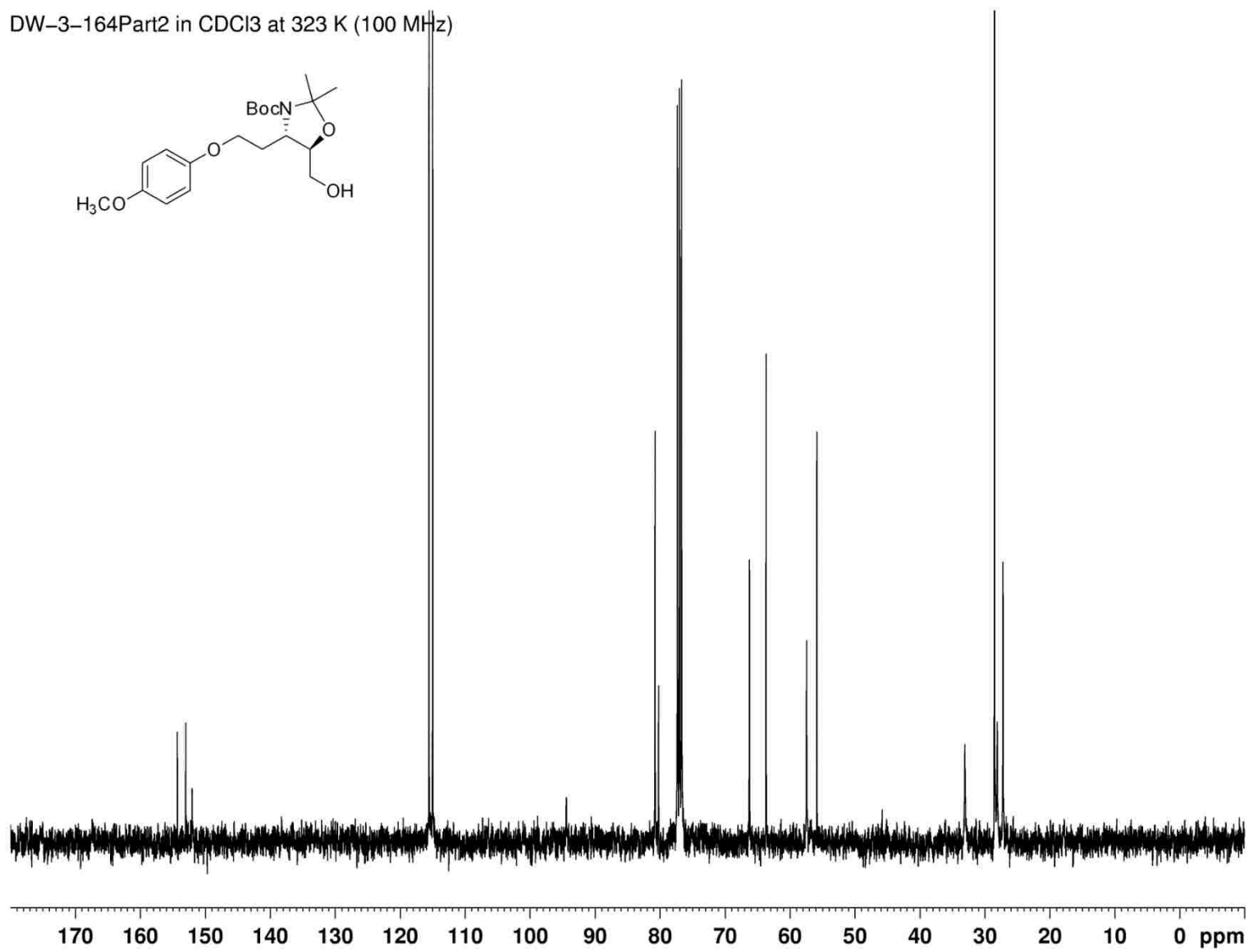
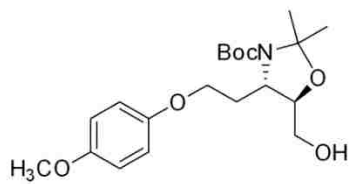
Compound **254** - ^1H NMR spectrum

DW-3-034.330-1H in CDCl_3 at 330 K (400 MHz)



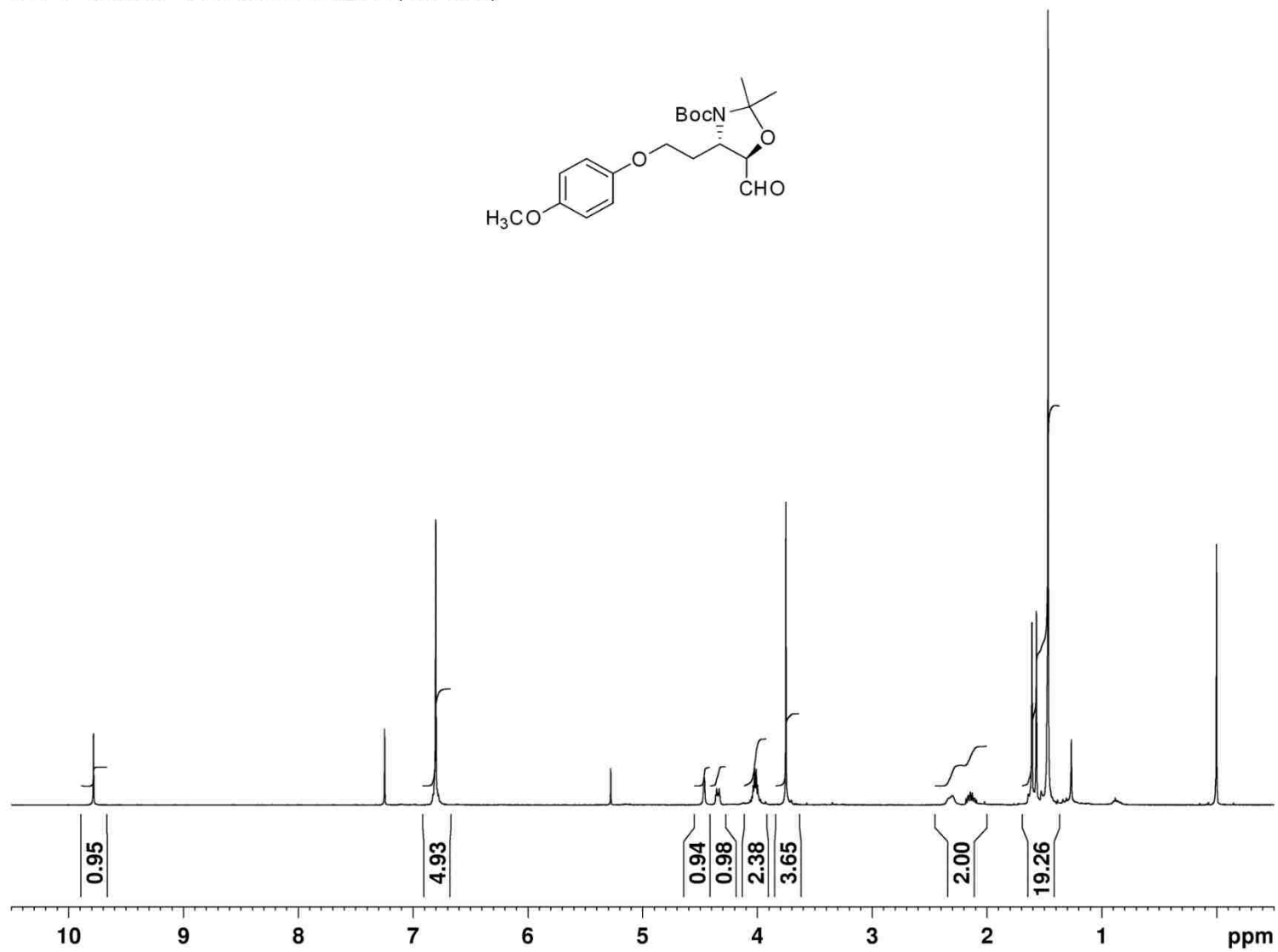
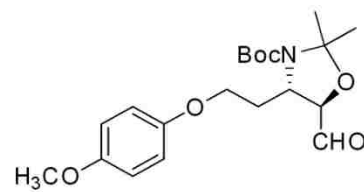
Compound **254** - ^{13}C NMR spectrum

DW-3-164Part2 in CDCl_3 at 323 K (100 MHz)



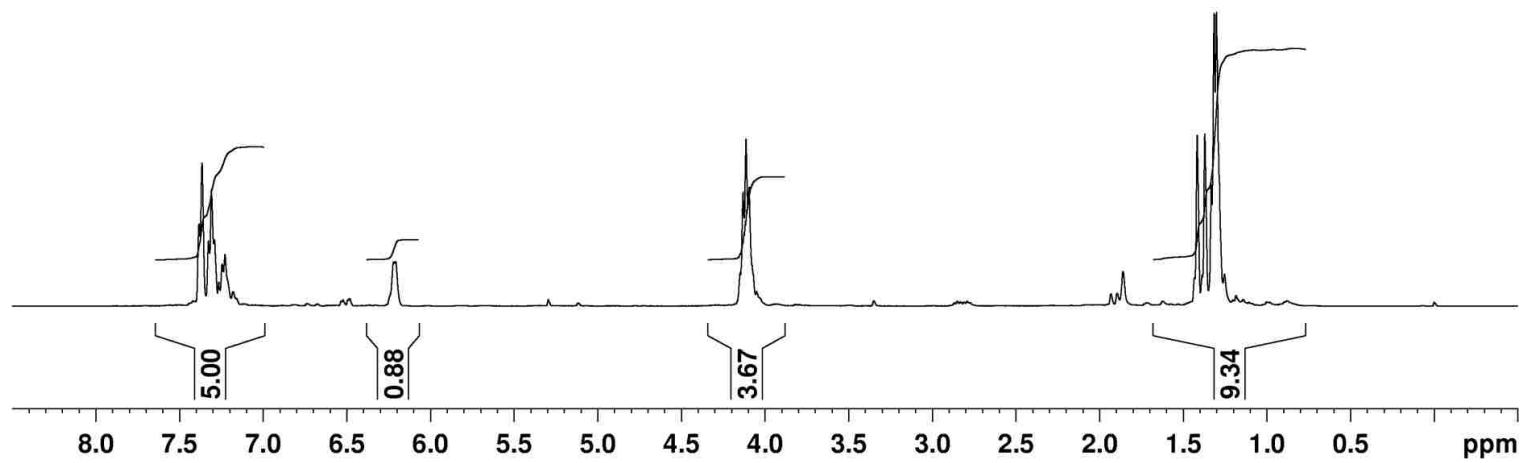
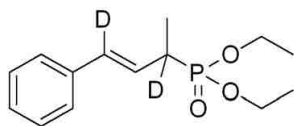
Compound **208** - ^1H NMR spectrum

DW-3-036.330-1H in CDCl_3 at 330 K (400 MHz)



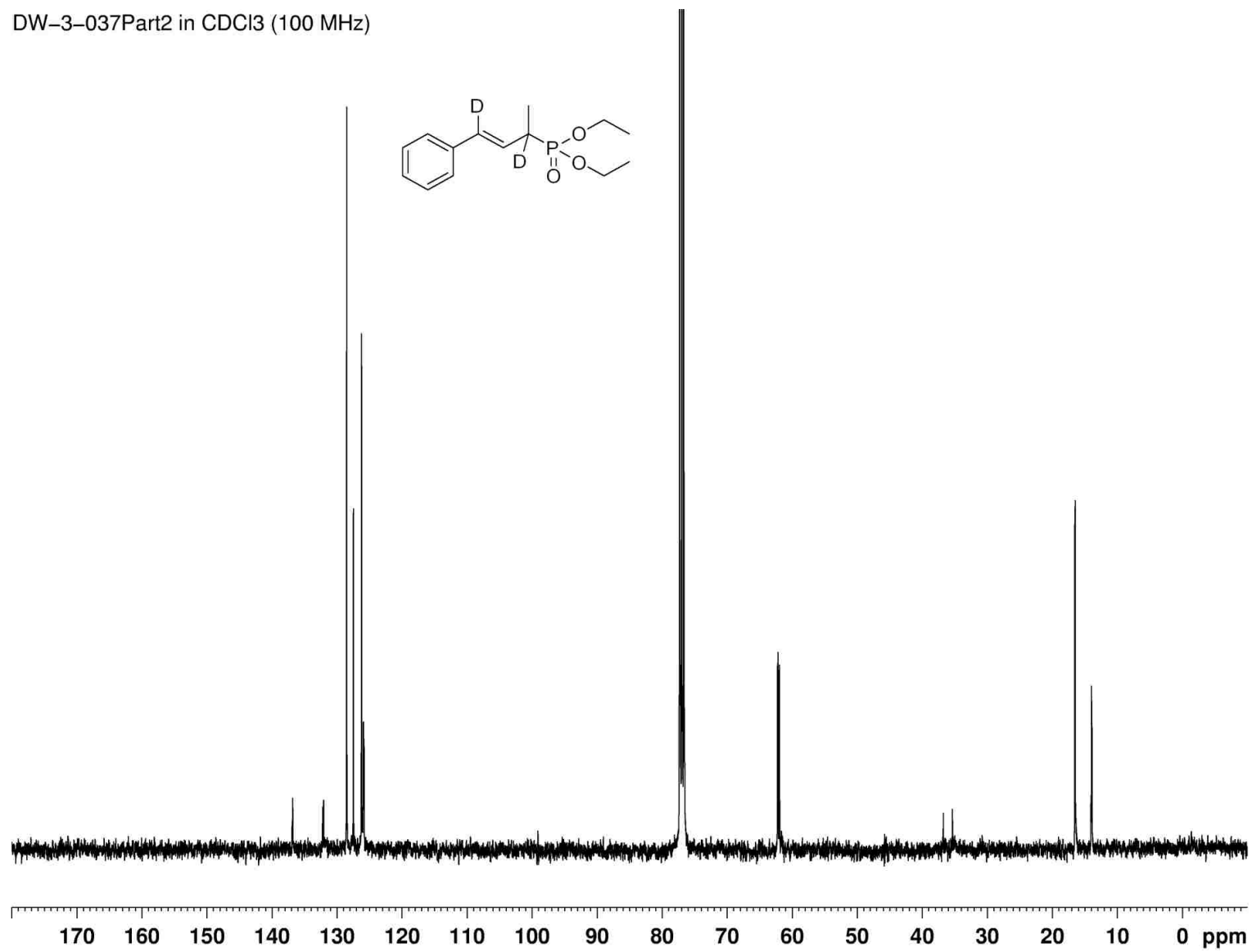
Compound **259** - ^1H NMR spectrum

DW-2-148 Purified in CDCl_3 (400 MHz)



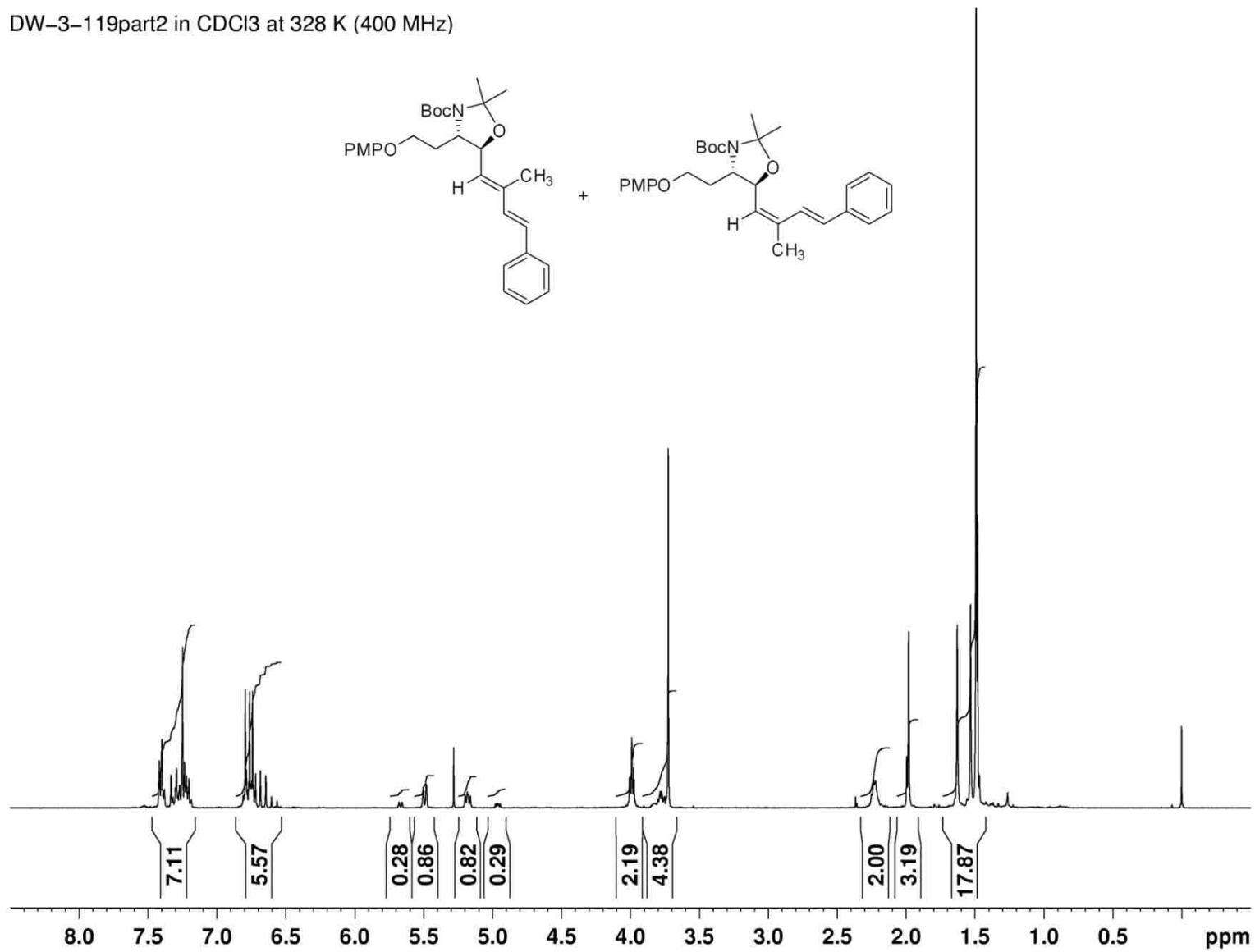
Compound **259** - ^{13}C NMR spectrum

DW-3-037Part2 in CDCl_3 (100 MHz)



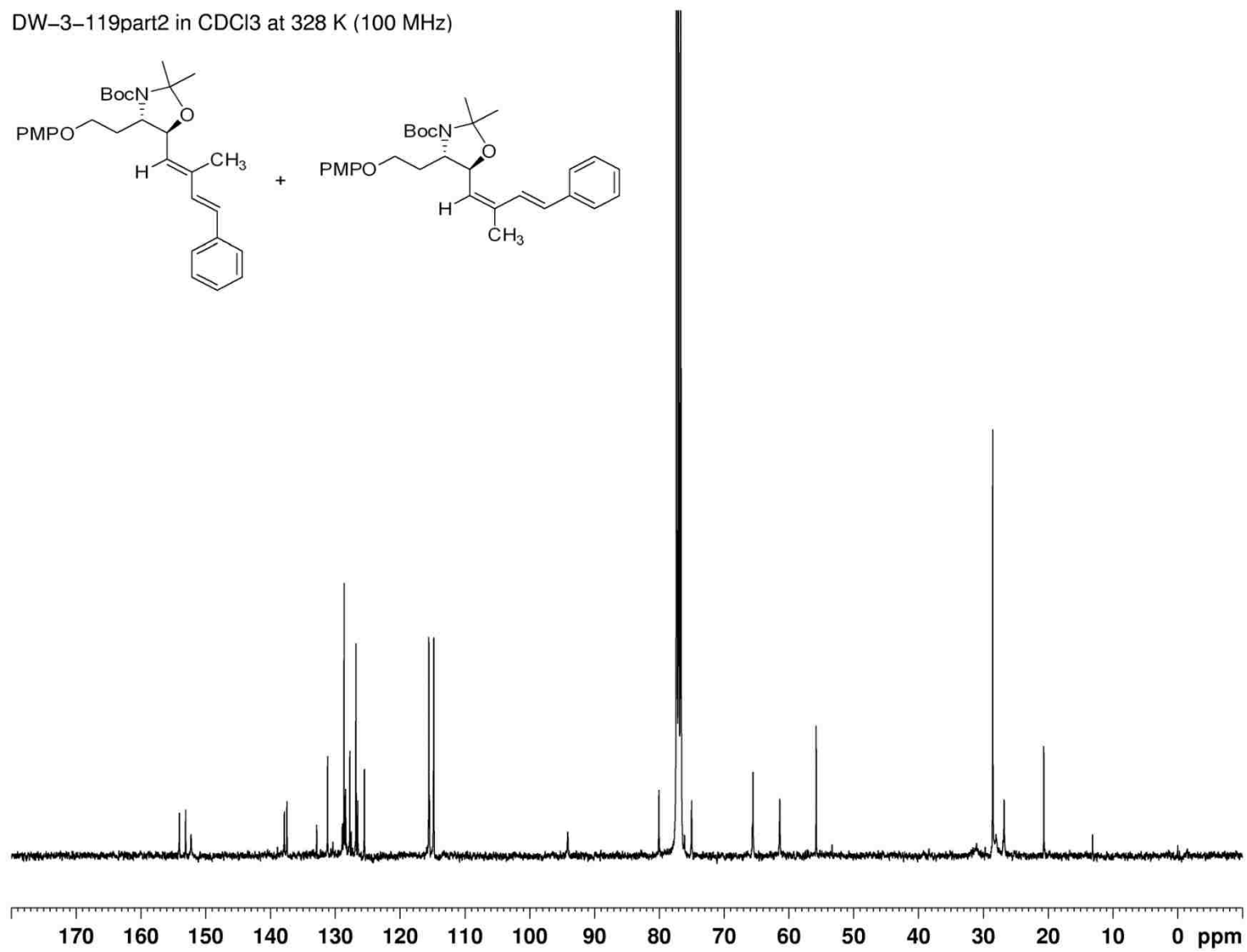
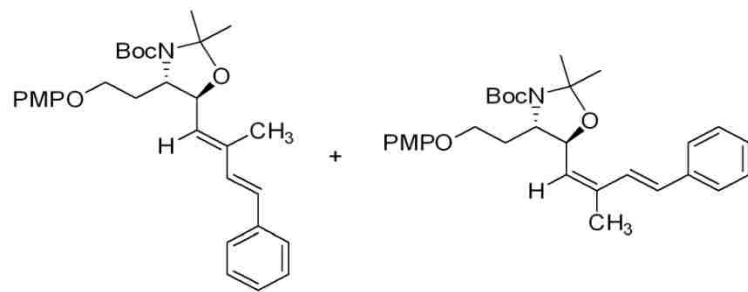
Compound *E/Z*-206 - ^1H NMR spectrum

DW-3-119part2 in CDCl_3 at 328 K (400 MHz)



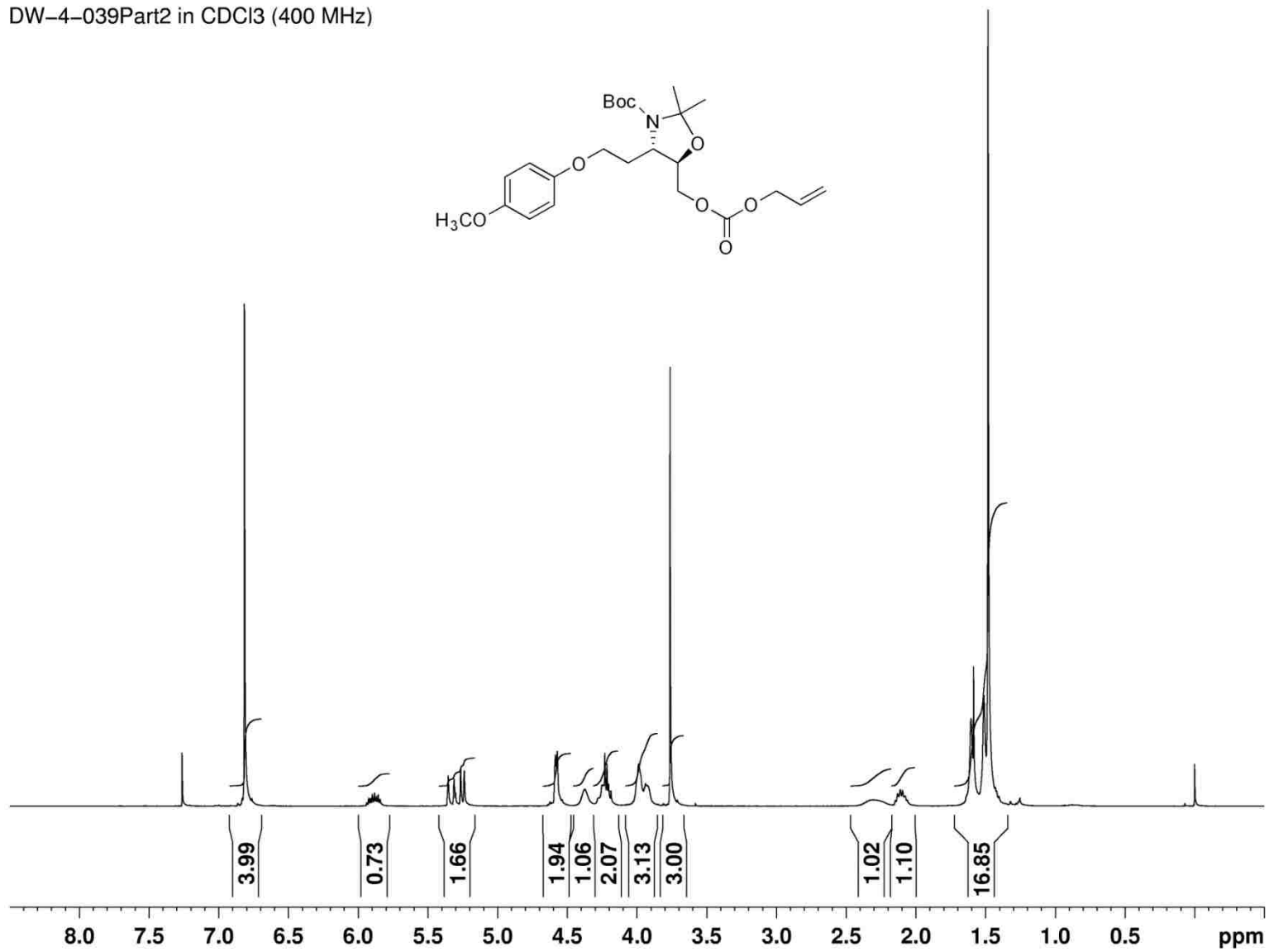
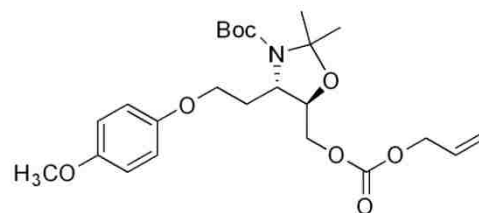
Compound *E/Z*-206 - ^{13}C NMR spectrum

DW-3-119part2 in CDCl_3 at 328 K (100 MHz)



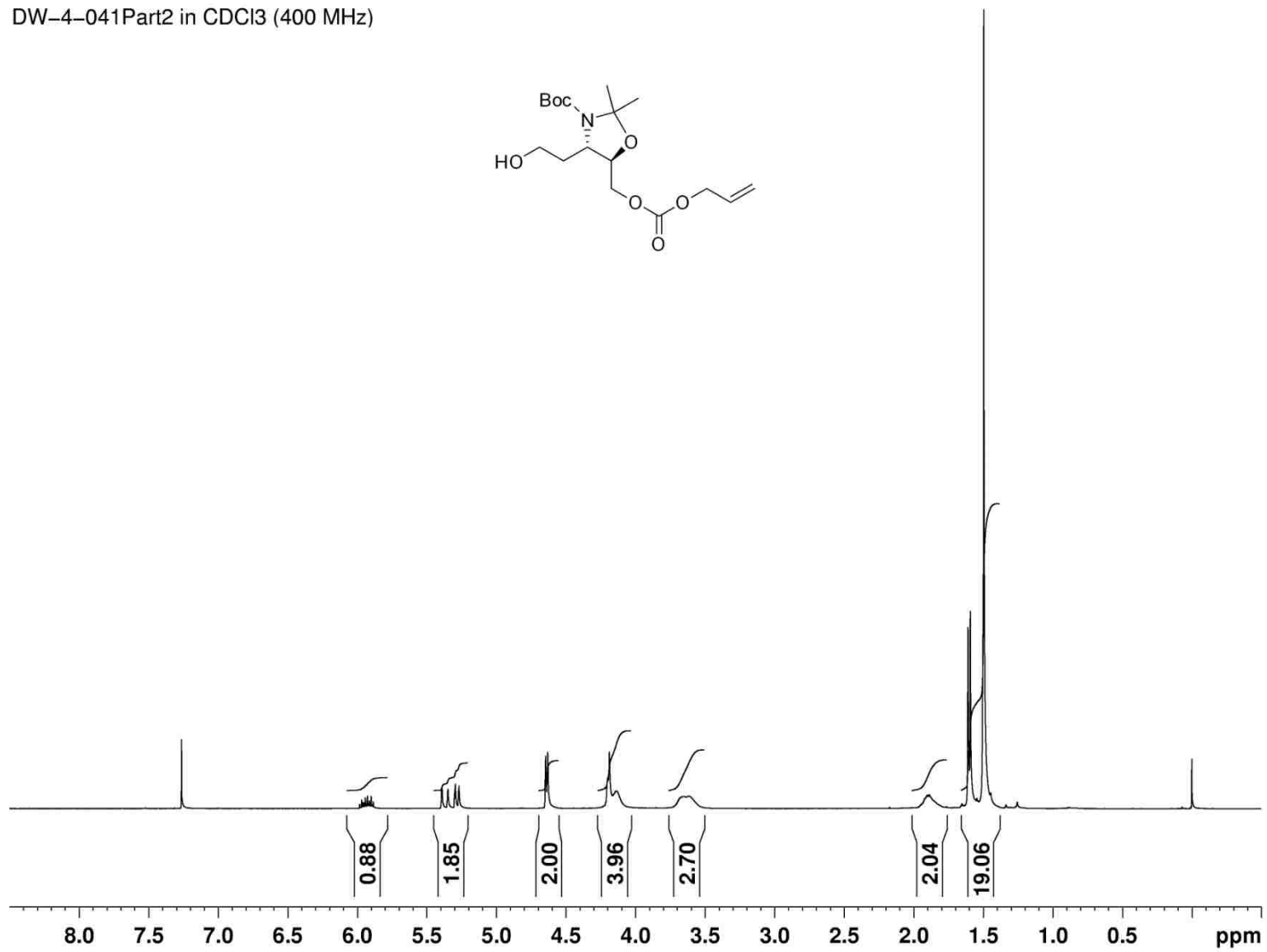
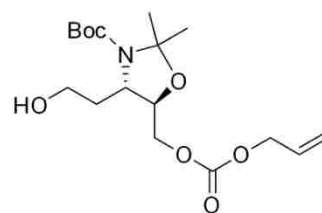
Compound **288** - ^1H NMR spectrum

DW-4-039Part2 in CDCl_3 (400 MHz)



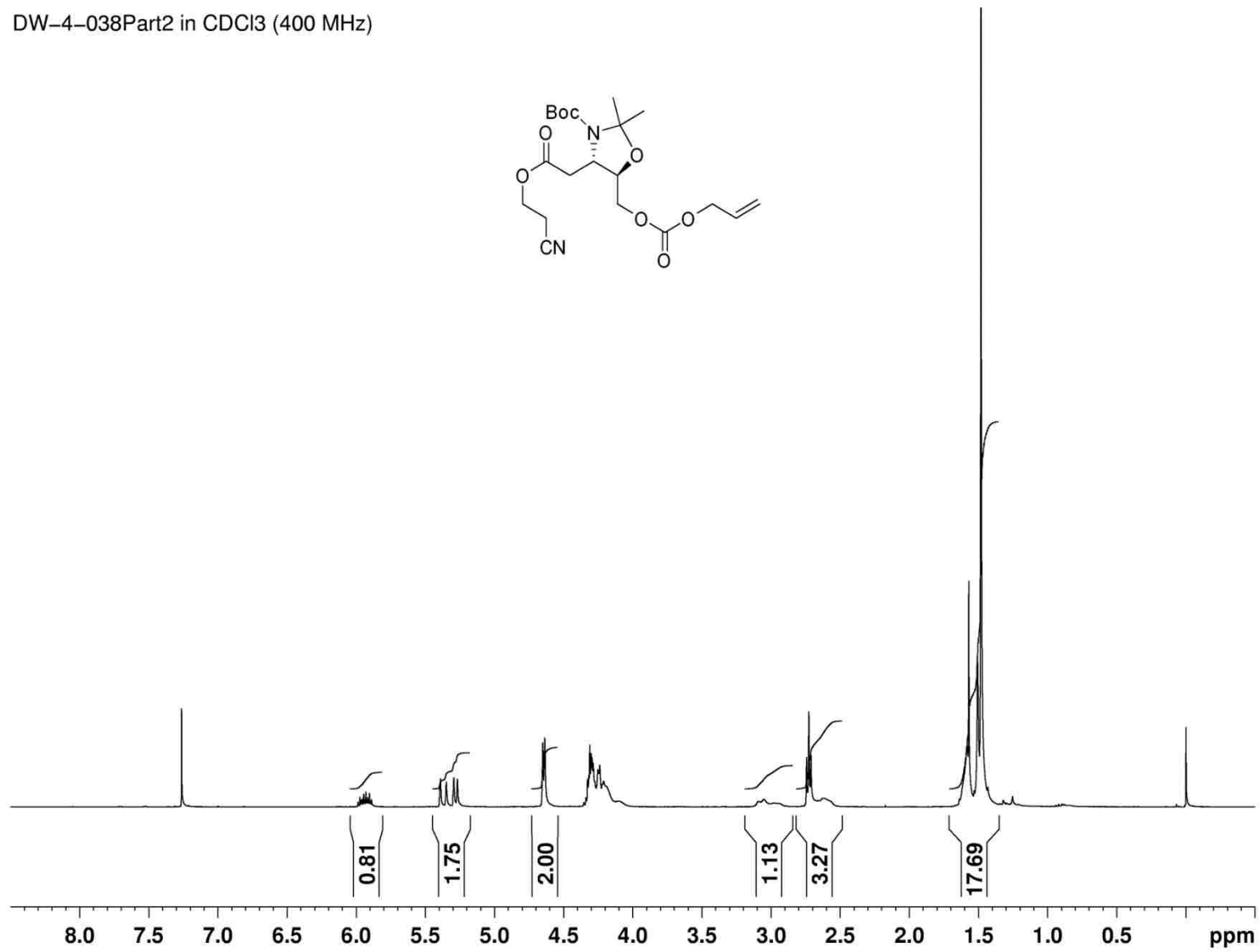
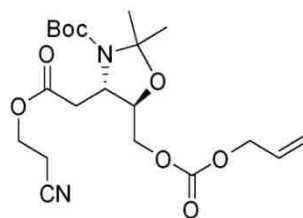
Compound **289** - ^1H NMR spectrum

DW-4-041Part2 in CDCl_3 (400 MHz)



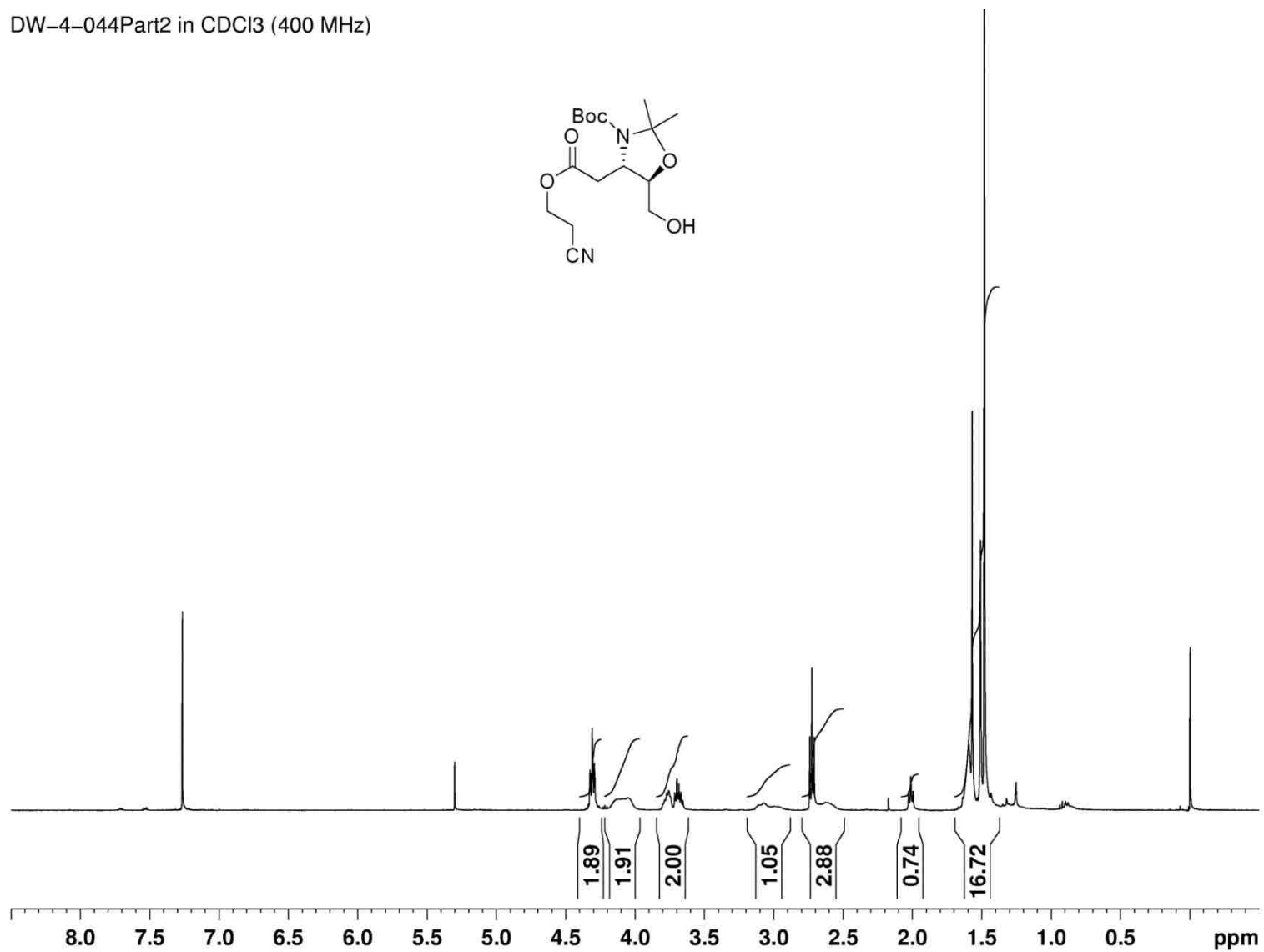
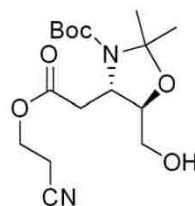
Compound **283** - ^1H NMR spectrum

DW-4-038Part2 in CDCl_3 (400 MHz)



Compound **286** - ^1H NMR spectrum

DW-4-044Part2 in CDCl_3 (400 MHz)



4.12 References

1. Bodkin, J. A.; Bacskay, G. B.; McLeod, M. D.: The Sharpless asymmetric aminohydroxylation reaction: optimising ligand/substrate control of regioselectivity for the synthesis of 3- and 4-aminosugars. *Org. Biomol. Chem.* **2008**, *6*, 2544–2553.
2. White, W. N.; Fife, W. K.: The *ortho*-Claisen rearrangement. IV. The rearrangement of X-cinnamyl *p*-tolyl ethers. *J. Am. Chem. Soc.* **1961**, *83*, 3846-3853.
3. Hirabe, T.; Nojima, M.; Kusabayashi, S.: Lithium aluminum hydride reduction of allylic substrates. Notable leaving group effects on the product regiochemistry. *J. Org. Chem.* **1984**, *49*, 4084-4086.
4. Roy, S.; Das, T.; Saha, M.; Chaudhuri, S. K.; Bhar, S.: Cyanuric chloride-mediated synthesis of allylic chloride-*ipso*- versus *tele*-substitution. *Synth. Commun.* **2007**, *37*, 4367-4370.
5. Fuchter, M. J.; Levy, J. N.: One-pot formation of allylic chlorides from carbonyl derivatives. *Org. Lett.* **2008**, *10*, 4919-4922.
6. Maigrot, N.; Mazaleyrat, J. P.; Welvert, Z.: High diastereoselectivity in the reaction of alpha-aminonitriles bearing an (*S*)-(+)-2-methoxymethylpyrrolidine group with Grignard reagents. *J. Chem. Soc., Chem. Commun.* **1984**, 40-41.
7. Lewandowska, E.; Lalama, J.; Yuan, C. S.; Wnuk, S. F.: Open-chain carbocyclic analogs of adenosine with dihalovinyl unit as potential inhibitors of *S*-adenosyl-L-homocysteine hydrolase. *Nucleosides Nucleotides Nucleic Acids.* **2003**, *22*, 1747-1755.
8. Kiyooka, S.; Shahid, K. A.; Goto, F.; Okazaki, M.; Shuto, Y.: Regulated-stereoselective construction of thirteen stereogenic centers necessary for the frame of (+)-discodermolide, based on iterative Lewis acid-promoted aldol reactions. *J. Org. Chem.* **2003**, *68*, 7967-7978.
9. Yadav, V. K.; Babu, K. G.: Acetyl chloride-ethanol brings about a remarkably efficient conversion of allyl acetates into allyl chlorides. *Tetrahedron.* **2003**, *59*, 9111-9116.
10. Wong, D.; Taylor, C. M.: Asymmetric synthesis of *erythro*- β -hydroxyasparagine. *Tetrahedron Lett.* **2009**, *50*, 1273-1275.
11. Sakaitani, M.; Ohfuné, Y.: Syntheses and reactions of silyl carbamates. 1. Chemoselective transformation of amino protecting groups via *tert*-butyldimethylsilyl carbmates. *J. Org. Chem.* **1990**, *55*, 870-876.
12. Kandula, S. R. V.; Kumar, P.: An asymmetric aminohydroxylation route to (+)-L-733,060. *Tetrahedron: Asymmetry.* **2005**, *16*, 3579-3583.

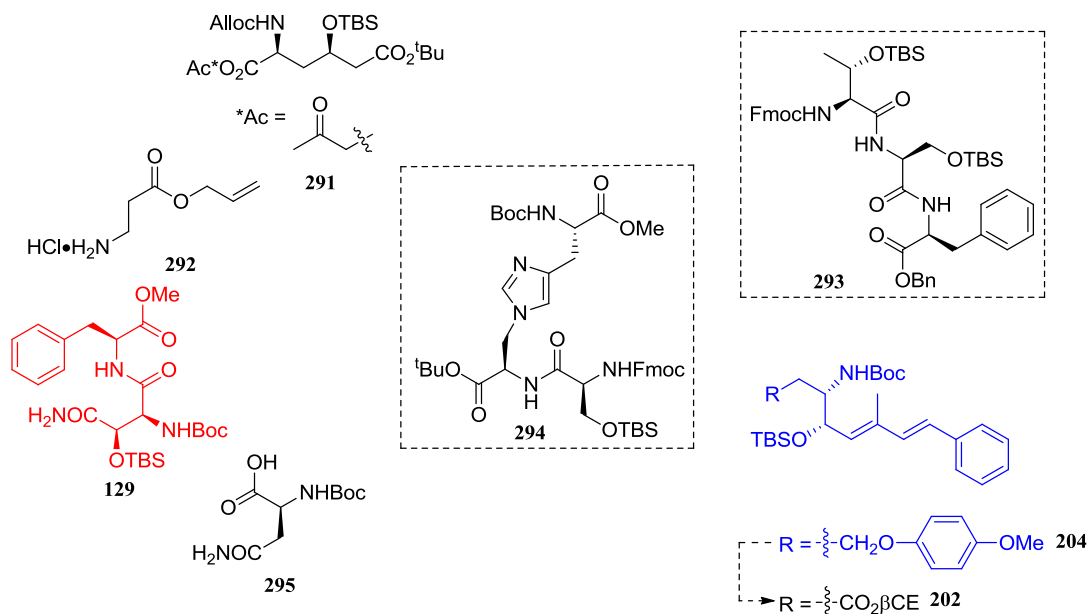
13. Corey, E. J.; Jones, G. B.: Reductive cleavage of *tert*-butyldimethylsilyl ethers by diisobutylaluminum hydride. *J. Org. Chem.* **1992**, *57*, 1028-1029.
14. Nanchen, S.; Pfaltz, A.: Chiral phosphino- and (phosphinooxy)-substituted *N*-heterocyclic carbene ligands and their application in iridium-catalyzed asymmetric hydrogenation. *Helv. Chim. Acta.* **2006**, *89*, 1559-1573.
15. Van Benthem, R. A. T. M.; Hiemstra, H.; Longarela, G. R.; Speckamp, W. N.: Formamide as a superior nitrogen nucleophile in palladium (II) mediated synthesis of imidazolidines. *Tetrahedron Lett.* **1994**, *35*, 9281-9284.
16. Li, W.; Gan, J.; Ma, D.: Total synthesis of piperazimycin A: a cytotoxic cyclic hexadepsipeptide. *Angew. Chem. Int. Ed.* **2009**, *48*, 8891-8895.
17. Shuter, E. C.; Duong, H.; Hutton, C. A.; McLeod, M. D.: The enantioselective synthesis of APTO and AETD: polyhydroxylated beta-amino acid constituents of the microsclerodermin cyclic peptides. *Org. Biomol. Chem.* **2007**, *5*, 3183-3189.
18. Markiewicz, J. T.; Schauer, D. J.; Lofstedt, J.; Corden, S. J.; Wiest, O.; Helquist, P.: Synthesis of 4-methyldienoates using a vinylogous Horner-Wadsworth-Emmons reagent. Application to the synthesis of trichostatic acid. *J. Org. Chem.* **2010**, *75*, 2061-2064.
19. Al-Badri, H.; About-Jaudet, E.; Collignon, N.: Efficient synthesis of substituted 2-diethylphosphonylbuta-1,3-dienes. *Synthesis.* **1994**, 1072-1078.
20. Nicolaou, K. C.; Petasis, N. A.; Zipkin, R. E.; Uenishi, J.: The endiandric acid cascade. Electrocyclizations in organic synthesis. 1. Stepwise, stereocontrolled total synthesis of endiandric acids A and B. *J. Am. Chem. Soc.* **1982**, *104*, 5555-5557.
21. Garner, P.: Stereocontrolled addition to a penaldic acid equivalent-an asymmetric-synthesis of *threo*-beta-hydroxy-L-glutamic acid. *Tetrahedron Lett.* **1984**, *25*, 5855-5858.
22. Garner, P.; Park, J. M.: The synthesis and configurational stability of differentially protected beta-hydroxy-alpha-amino aldehydes. *J. Org. Chem.* **1987**, *52*, 2361-2364.
23. Garner, P.; Park, J. M.; Malecki, E.: A stereodivergent synthesis of *D-erythro*-sphingosine and *D-threo*-sphingosine from L-serine. *J. Org. Chem.* **1988**, *53*, 4395-4398.
24. Corey, E. J.; Kwiatkowski, G. T.: The synthesis of olefins from *O,O'*-dialkyl alpha-lithioalkylphosphonothioate esters. *J. Am. Chem. Soc.* **1966**, *88*, 5654-5656.
25. Meyer, S. D.; Schreiber, S. L.: Acceleration of the Dess-Martin oxidation by water. *J. Org. Chem.* **1994**, *59*, 7549-7552.
26. Clausen, M. H.; Madsen, R.: Synthesis of hexasaccharide fragments of pectin. *Chem. Eur. J.* **2003**, *9*, 3821-3832.

27. Mahapatra, T.; Das, T.; Nanda, S.: Asymmetric synthesis of stagonolide-D and stagonolide-G. *Bull. Chem. Soc. Jpn.* **2011**, *84*, 511-519.
28. DattaGupta, A.; Singh, R.; Singh, V. K.: A mild and efficient method for the cleavage of *tert*-butyldimethylsilyl and tetrahydropyranyl ethers by ceric ammonium nitrate in methanol. *Synlett.* **1996**, 69-71.
29. Lipton, M. F.; Sorensen, C. M.; Sadler, A. C.; Shapiro, R. H.: A convenient method for the accurate estimation of concentrations of alkyllithium reagents. *J. Organomet. Chem.* **1980**, *186*, 155-158.

CHAPTER 5: PEPTIDE FRAGMENT ASSEMBLY FOR THEONELLAMIDE C

5.1 Introduction

The efforts described in the previous chapters have resulted in the production of *eHyAsn* through a key Sharpless aminohydroxylation reaction (Chapter 2, red fragment in Figure 5.1) and an advanced intermediate **204** of Apoa via a crucial HWE reaction (Chapter 4, blue fragment in Figure 5.1). Recall from Chapter 1 that these non-natural amino acids are constituents of the bicyclic peptide TNM C. Originally demonstrated to be cytotoxic against mouse leukemia cells (P388 and L1210), the theonellamides have emerged as a new class of ergosterol-binding anti-fungal agent.¹⁻⁴



Completed Synthesis from Chapter 2

Work from Chapter 4 - An Advanced Intermediate of Apoa

Peptide Fragment Assembly in Chapter 5

Figure 5.1 – Summary of Synthetic Work Presented

5.2 Peptide and Peptide-Based Drugs

Peptides play a crucial role in the fundamental functions of life, and as such they have attracted considerable attention for their potential therapeutic use. Historically, peptides were not popular drug

candidates. For a number of years, peptide-based therapies were reserved for treatment of hormone disease states.⁵ Also, many peptides lack oral availability and the pharmaceutical industry, in the past, heavily favored oral therapies (the exception being the treatment of Type I diabetes with insulin). The introduction of drugs based on genetic engineering and recombinant technology in the late 1980s caused a resurgence of interest in peptides.⁵ The technologies provided insight to previously untreatable medical conditions and in doing so, catalyzed the industry's acceptance of developing drugs that could not be orally administered. Genome sequencing efforts at the dawn of the 21st century brought with them the potential to identify a range of new targets.⁶ As genomic and proteomic technologies continue to mature, a more complete picture of protein-protein interactions as targets in drug design will eventually lead to more widespread application of these as therapeutic targets. As a result, peptides should benefit greatly and command even more attention as therapeutic agents.

The use of peptides as drugs comes with a number of potential benefits as well as some drawbacks.⁷ A primary advantage stems from peptides' binding to their targets with high specificity leading to high potencies and few toxicology issues. However, potential disadvantages of peptides include proteolytic instability, low oral bioavailability, poor membrane permeability and rapid clearance from the body. The molecular weight gap between small molecules and protein-based drugs can potentially be filled by peptides because their specificity and potency mimic protein-based drugs but are smaller and more cost effective to manufacture using chemical synthesis. The synthesis of small linear peptides is now routinely accomplished and large peptides containing < 50 common amino acid residues has never been more synthetically feasible. Many challenges remain, however, such as the synthesis of peptides containing α,α -dialkyl amino acids **I-III** and *N*-alkyl amino acids **298-300** (Figure 5.2). Also, peptide macrocyclization of small-to-medium sized rings **301-302** can be extremely difficult due to an entropically disfavored pre-cyclization conformation.⁸ Fortunately, modern strategies to facilitate macrocyclization of peptide-containing molecules such as ring contractions,⁹ azide-alkyne cycloadditions¹⁰ and ring-closing metathesis¹¹ are in constant development. Cyclization of larger peptides

(greater than seven amino acids) are less challenging. Peptide research for developing synthetic analogs of natural peptides with desirable pharmacokinetic and pharmacological properties is maturing. The demand for more stringent safety standards has modified the field of drug development, bringing into favor more peptide-based drugs.

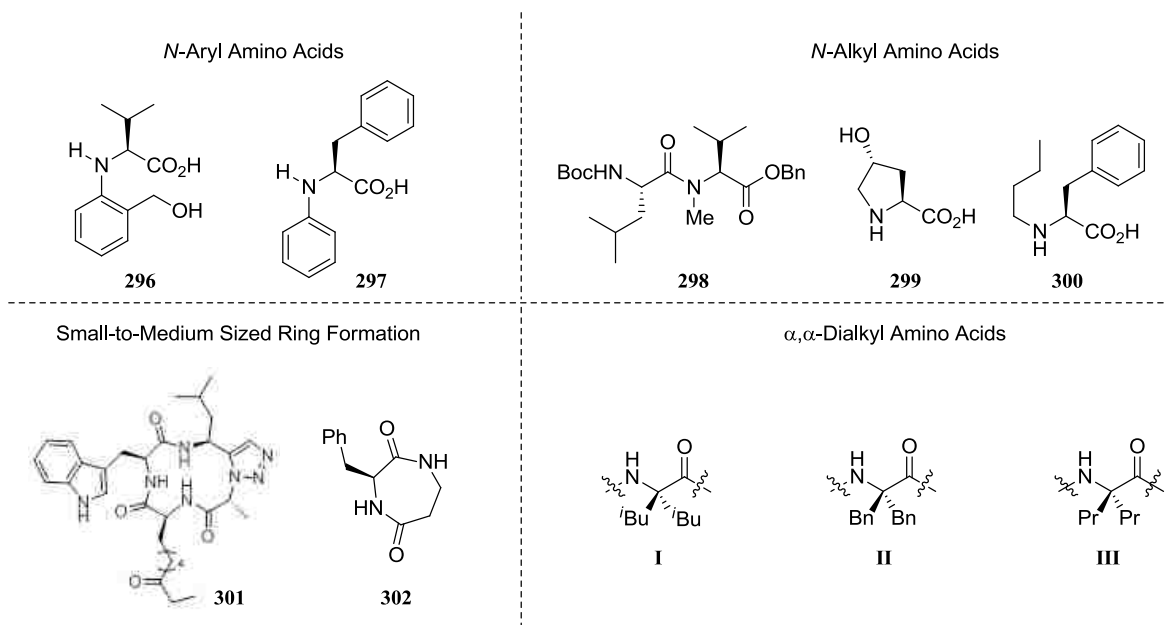


Figure 5.2 – Challenging Motifs in Peptide Chemistry

Natural peptides such as oxytocin **303**, cyclosporine **304** and vancomycin **305** are approved peptide drugs (Figure 5.3). The mammalian neurohypophysial hormone oxytocin **303**, a peptide of nine amino acids, plays roles during and after childbirth. The nonapeptide is also implicated in behaviors such as pair bonding and social recognition. Synthetic oxytocin, Pitocin™, is commercially produced according to a chemical synthesis originally developed by Boissonnas.¹² The cyclic nonribosomal peptide, cyclosporine **304**, is used as an immunosuppressant for organ transplant therapy. Interestingly, this drug is suitable for oral consumption largely due to three structural features: (1) a cyclic backbone that guards against proteolytic cleavage, (2) decrease in the number of amide hydrogen bond donors via seven *N*-methyl groups, (3) four amide NH protons restrained by four intramolecular hydrogen bonds to

diminish their hydrogen bonding potential for water solvation.^{13,14} The filamentous fungus *Tolypocladium inflatum*, through the submerged fermentation process, produces cyclosporine on a commercial scale.¹⁵ Vancomycin **305**, a glycopeptide antibiotic traditionally viewed as a drug of last resort, is used to treat infections caused by Gram-positive bacteria. The antibiotic's mode of action, to inhibit cell wall biosynthesis, is to bind to terminal D-alanyl-D-alanine moieties, thus preventing the incorporation of *N*-acetylmuramic acid/*N*-acetylglucosamine peptide subunits into a peptidoglycan matrix.¹⁶ Commercial production of vancomycin relies on *Amycolatopsis orientalis* cultures, an organism from the soil of Borneo.¹⁷ The multitude of oxytocin,¹⁸ cyclosporine^{19,20} and vancomycin^{21,22} total syntheses attests to the importance of these peptide drugs.

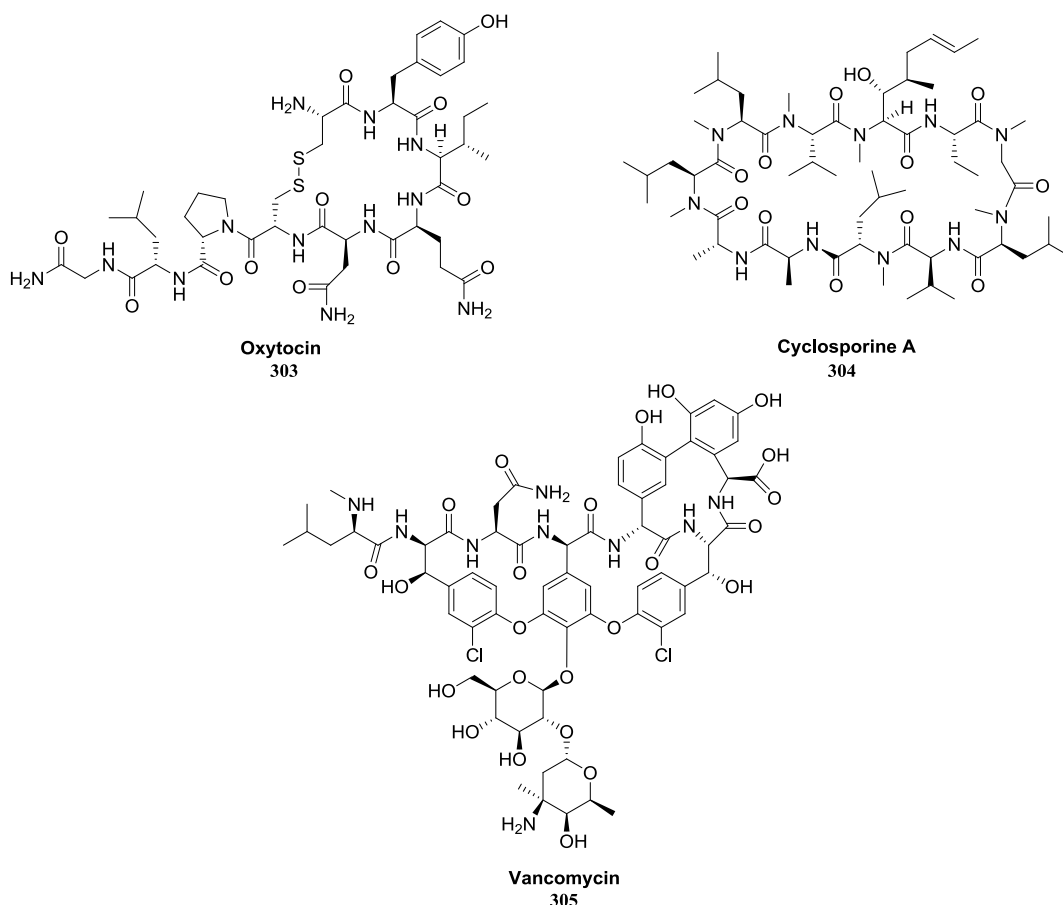
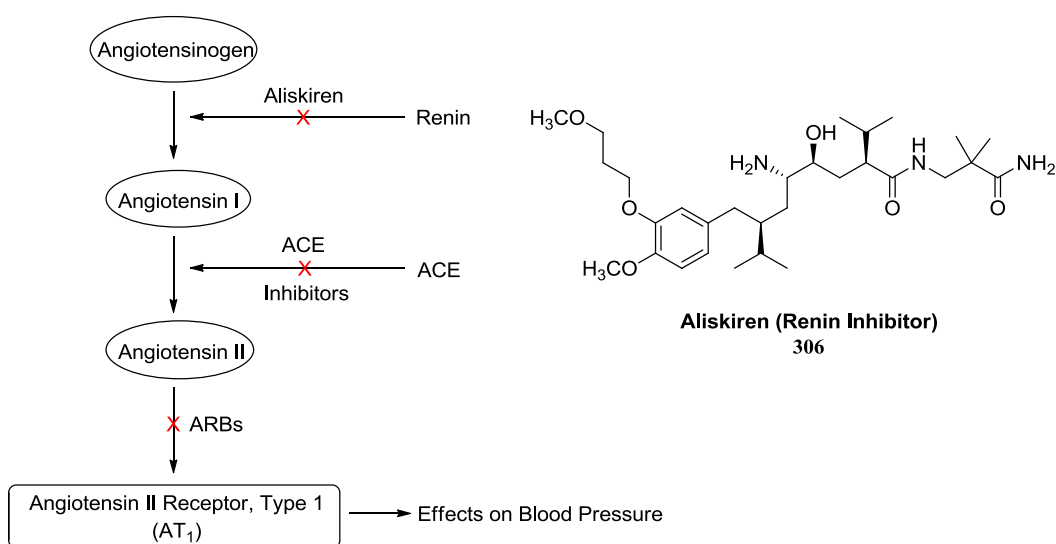


Figure 5.3 – Natural Peptides as Approved Peptide Drugs

Peptides produced by chemical synthesis have also been brought to market. Aliskiren **306**, for example, is in the renin inhibitor drug class and was approved for the treatment of hypertension in 2007 (Scheme 5.1).²³ By understanding the renin-angiotensin system (RAS), the enzyme renin was designated as the most logical drug target in the cascade. The difficulty in targeting renin, primarily due to a previously unrecognized subpocket ($S3^{SP}$) distinct for renin,²⁴ led to the earlier development of angiotensin-converting-enzyme inhibitors (ACE, prevents conversion of angiotensin I into angiotensin II) and angiotensin II receptor blockers (ARBs, specific for the angiotensin II type 1 receptor).



Scheme 5.1 – Inhibition of RAS can Occur at Three Different Stages

Chemical development of renin inhibitors over the course of two decades paved the way for aliskiren **306**. According to Figure 5.4, the compound interacts with several binding pockets ($S1$, $S1'$, $S2'$, $S3$ and $S3^{SP}$) around the active site of renin, but binding to the $S3^{SP}$ subpocket which stretches from the $S3$ binding site is critical for effective renin inhibition.²⁴ A synthon approach led to an innovative synthetic route for commercial production of aliskiren at an acceptable cost level (Scheme 5.2).²³ Three building blocks **307-309** were synthesized, two of which were generated using enzyme- or metal-catalyzed reactions. The fragments were coupled in a stepwise fashion with the latent vicinal amino alcohol moiety installed via a diastereoselective halolactonization. Coincidentally, aliskiren shares some

structural features with TNM C. These include an amide bond and the aforementioned vicinal amino alcohol moiety.

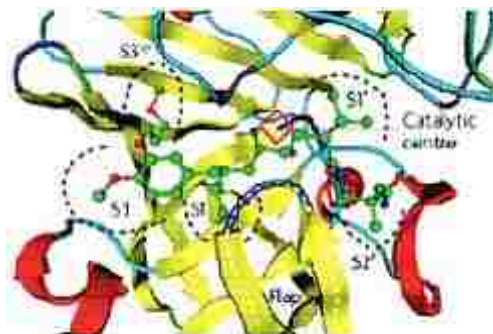
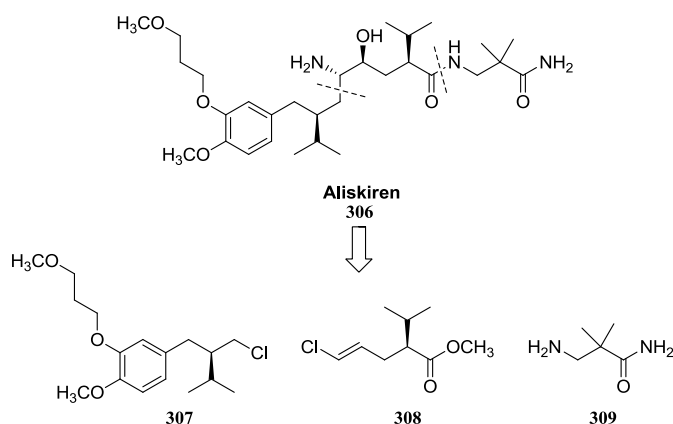


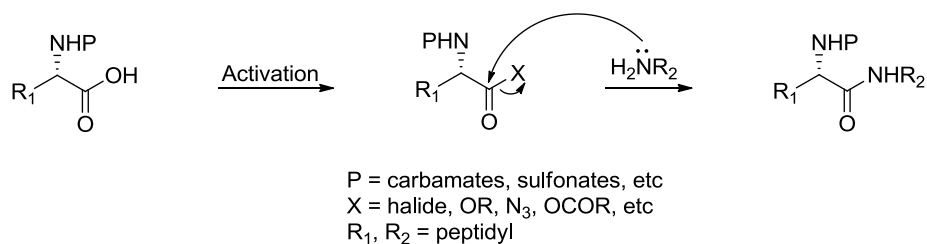
Figure 5.4 – Graphic Depiction of Aliskiren Binding to the Active Site of Renin. Copyright 2008, Nature Publishing Group, reprinted with permission (p. 256).



Scheme 5.2 – The Retrosynthetic Analysis for Commercial Production of Aliskiren. Copyright 2008, Nature Publishing Group, reprinted with permission (p. 256).

5.3 How to Make an Amide Bond

Amide bond formation between an amine and a carboxylic acid is a condensation reaction. The union of these two functional groups does not occur readily at room temperature. The expulsion of water only takes place at high temperatures, conditions generally incompatible with the presence of other functionalities. Therefore, activation of a carboxylic acid, a process that converts the -OH of the acid into a good leaving group, before treatment with the amine is necessary (Scheme 5.3).



Scheme 5.3 – Amide Bond Formation Via Activation

Carboxy components can be activated as shelf-stable reagents (some esters), an isolable compound of intermediate stability (acyl halides and azides), or as transient intermediates.^{25,26} All of the aforementioned species can undergo direct aminolysis to give an amide or react with a second nucleophile to give a more stable anhydride or ester whose aminolysis, in-turn, affords the peptide.

The acid chloride method for peptide synthesis was presented by Emil Fischer in 1903.²⁷ In the intervening years, carbodiimides,²⁸ active esters, anhydrides^{29,30} and phosphonium or iminium salts³¹ have emerged as useful coupling reagents. The plethora of coupling reagents available for amide bond formation, however, makes an optimal reagent selection for a given application difficult (Figure 5.5).

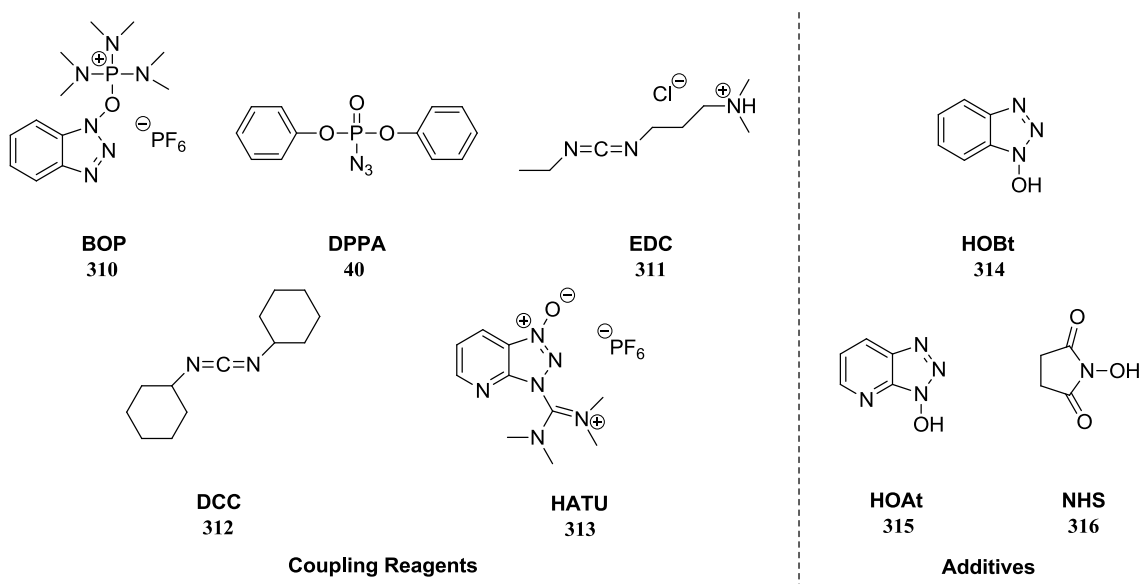


Figure 5.5 – Common Peptide Coupling Reagents and Additives Used in This and Previous Chapters

Unfortunately, the large number of potential substrates and their assorted challenges renders the idea of a universal coupling reagent naive. Some reagents do perform well in general and differences are typically small. HATU **313** and EDC **311**/HOBt **314** reagents offer generally excellent reactivity and rapid coupling times for many substrates. Many other reagents, however, could be superior for specialized situations, since they might be more efficient or do a better job preserving stereochemical purity. While some of the reagents in Figure 5.5 were discussed in the synthesis of the *e*HyAsn-Phe dipeptide (§2.9), the remaining reagents will be discussed here in chapter 5 in the context of TNM C peptide fragment assembly.

5.4 Retrosynthesis for the Eastern Hemisphere of TNM C

At this point, we were ready to assemble the peptide fragments associated with TNM C's eastern hemisphere. The partial synthesis of TNM F by Shioiri *et al.* offered a cautionary tale which influenced some of our decisions regarding our TNM C eastern hemisphere assembly strategy.^{32,33} Some elements of their TNM F eastern hemisphere **317** strategy that stood out included a highly linear fragment approach leading to their choice of cyclization site and the high number of hydroxyl groups left unprotected during peptide ligation which both contributed to a poor chemical yield for the cyclization step (Figure 5.6).

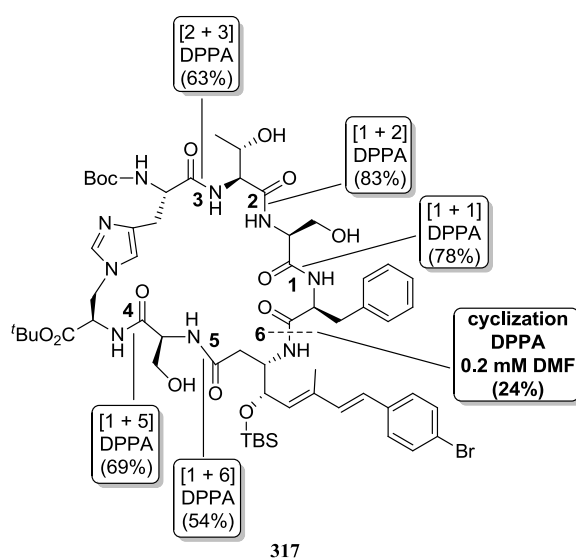
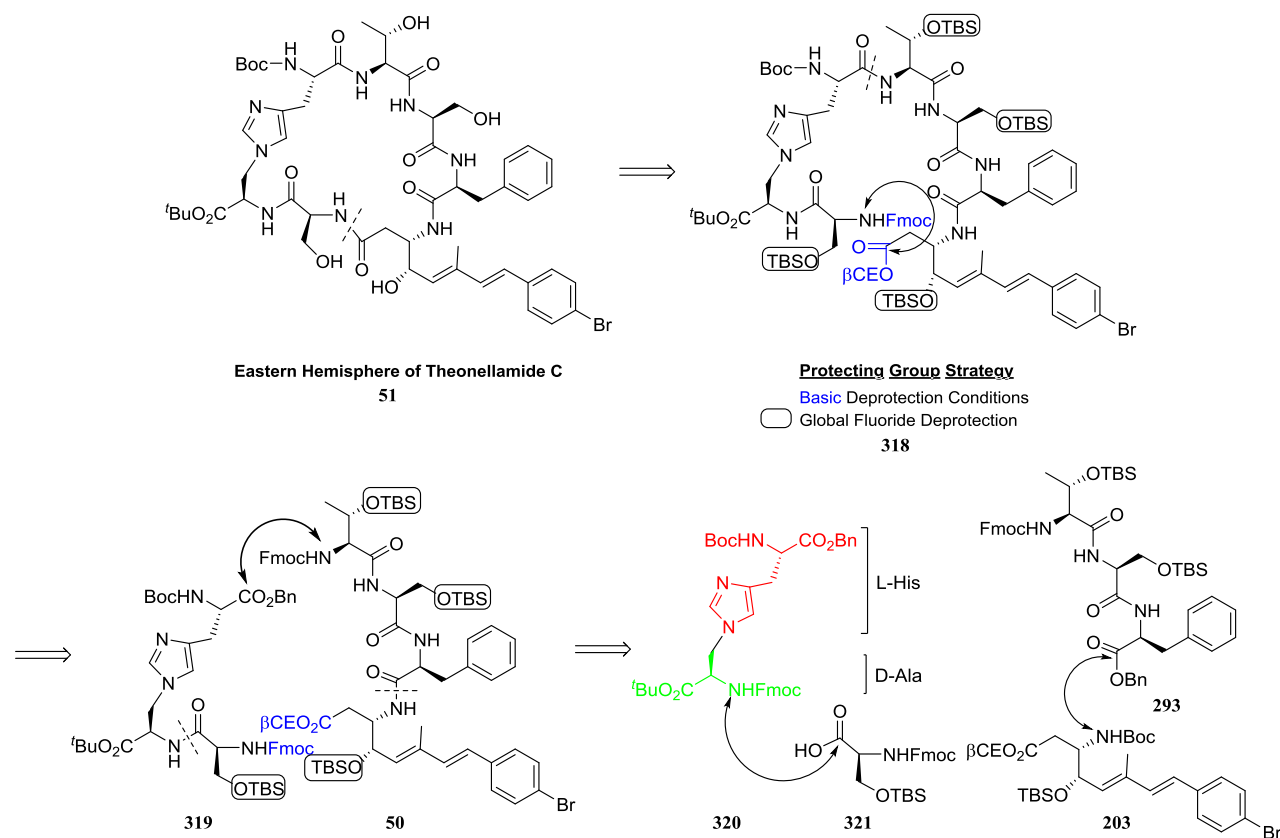


Figure 5.6 – Synthesis of the Eastern Hemisphere of TNM F by Shioiri *et al.*^{32,33}
11 Steps (5 Deprotections and 6 Couplings) → 3.6% Overall Yield

Our TNM C eastern hemisphere **51** strategy (Scheme 5.4) included protection of all four hydroxyl groups as their TBS ethers leading to a global fluoride deprotection scenario. The site chosen for cyclization is ideal, since the C-terminal Aboa residue (a β -amino acid) does not contain a $C\alpha$ stereocenter and therefore is not susceptible to epimerization during peptide bond formation (*vide infra*, §5.5). Also, the linear heptapeptide contains τ -HAL, a potential turn-inducing component to help promote cyclization. The other major disconnection, according to Scheme 5.4, is between the τ -HAL/*allo*-Thr residues, leading to the Fmoc-Ser(OTBS)- τ -HAL-OBn acid fragment **319** and Fmoc-*allo*-Thr(OTBS)-Ser(OTBS)-Phe-Aboa(OTBS)-O β CE tetrapeptide amine **50**.



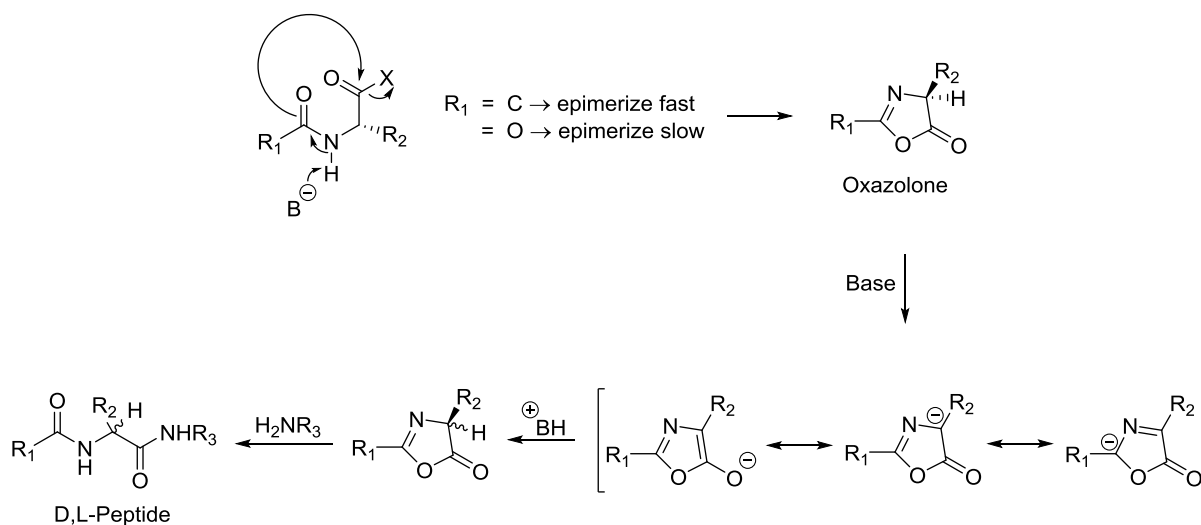
Scheme 5.4 - Eastern Hemisphere of TNM C: Retrosynthesis and Protecting Group Strategy

The structural complexity of TNM C demanded a fragment condensation approach. Our proposed synthesis is highly convergent, driven by the relative value of synthetic amino acid residues. The synthesis of tetrapeptide **50** required the preparation and ligation of the Fmoc-*allo*-Thr(OTBS)-

Ser(OTBS)-Phe-OBn tripeptide and the Aboa residue. Tripeptide **293**, in-turn, can be generated from coupling of commercially available amino acids Fmoc-*allo*-Thr(O^tBu)-OH, H-Ser(O^tBu)-OH and HCl·Phe-OBn in a stepwise fashion followed by hydroxyl protecting group exchange (O^tBu → OTBS). The Fmoc-Ser(OTBS)- τ -HAL-OBn fragment called for base-mediated deprotection of the D-Ala-NH₂ (green, Scheme 5.4) of orthogonally protected τ -HAL (supplied by Chyree Batton) and coupling the resulting free amino group to Fmoc-Ser(OTBS)-OH **321**.

5.5 The Risk of Epimerization During Fragment Condensation

For coupling of peptide fragments, the advantages of carboxylic acid activation are tempered somewhat by the possibility of epimerization of the C-terminal amino acid at C α (with few exceptions). Although other pathways have been noted, the most important mechanism of “racemization” involves oxazolone formation (Scheme 5.5).³⁴⁻³⁷ This intermediate results from competing intramolecular attack of the carbonyl function of the preceding amide group at the activated carboxyl group. After deprotonation, the oxazolone generates an aromatic species resulting in epimerization of the C-terminal residue. The oxazolone ring can also be opened by amines to produce peptide bonds.

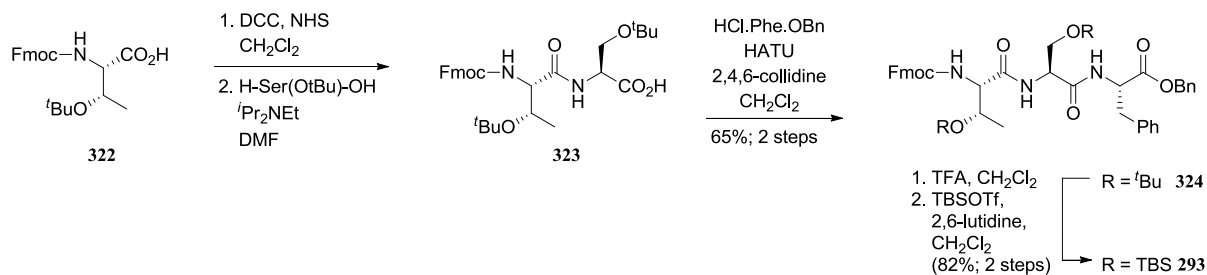


Scheme 5.5 – Mechanism of Racemization: Oxazolone Formation

The rate of peptide coupling relative to the rate of epimerization is enhanced by using amino acids protected with carbamate groups ($R_1 = \text{alkoxy}$). Should oxazolone formation occur, no enolization takes place since this configurationally robust intermediate then undergoes aminolysis to generate the desired peptide. When $R_1 = \text{alkyl}$ or peptidyl, enolization of the chirally unstable oxazolone intermediate ensues to produce diastereomeric products.

5.6 Synthesis of the Fmoc-*allo*-Thr(OTBS)-Ser(OTBS)-Phe-OBn Tripeptide

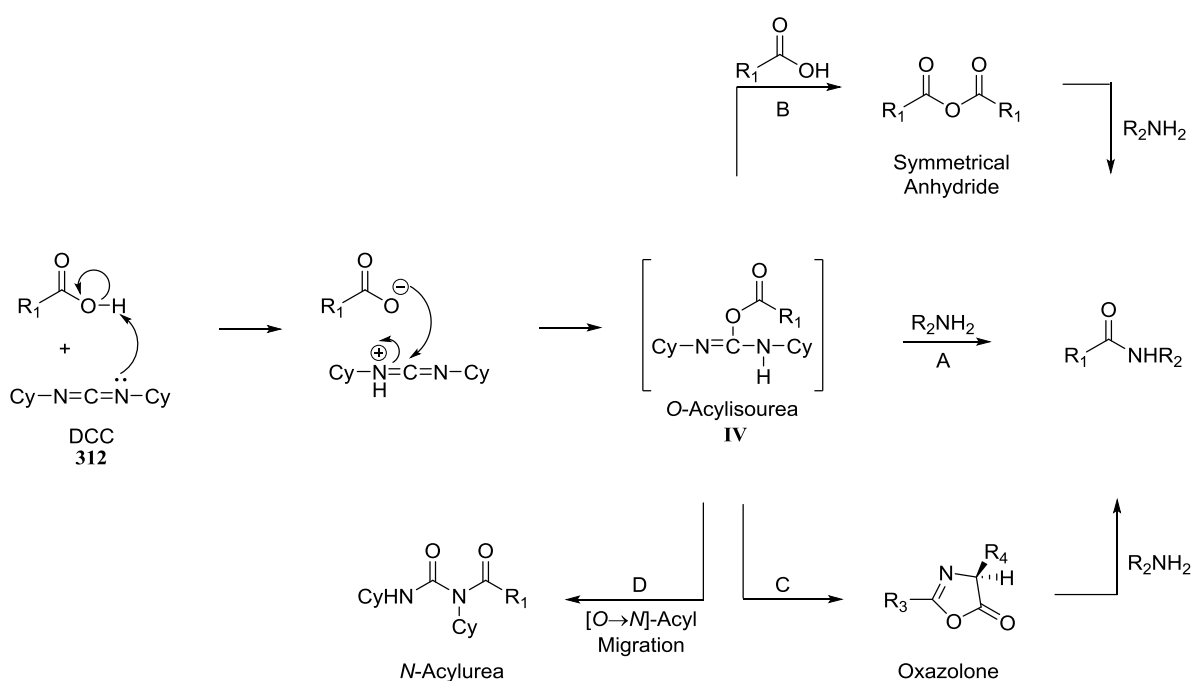
A number of years ago, Taylor *et al.* described the use of a carbodiimide method to prepare *N*-Fmoc protected dipeptide acids which did not require purification.³⁸ Therefore, we decided to start the preparation of the Fmoc-*allo*-Thr(OTBS)-Ser(OTBS)-Phe-OBn tripeptide **293** for the eastern hemisphere of TNM C using the same carbodiimide method. Amino acids **1** (Fmoc-*allo*-Thr(O^tBu)-OH), **2** (H-Ser(O^tBu)-OH), and **3** (HCl·Phe-OBn) were commercially available and readily coupled in a stepwise fashion (Scheme 5.6).



Scheme 5.6 - Fmoc-*allo*-Thr(OTBS)-Ser(OTBS)-Phe-OBn Tripeptide Construction

Sheehan and Hess reported the use of carbodiimides for peptide synthesis in 1955.²⁸ The mechanism begins with protonation of the carbodiimide moiety of dicyclohexylcarbodiimide (DCC, **312**) by the carboxylic acid. The carboxylate anion then attacks the activated reagent to generate an *O*-acylisourea **IV**. At this point, the highly reactive intermediate **IV** can go through at least four possible pathways (Scheme 5.7).^{35,39-41} Formation of the peptide can occur from three of these pathways. These

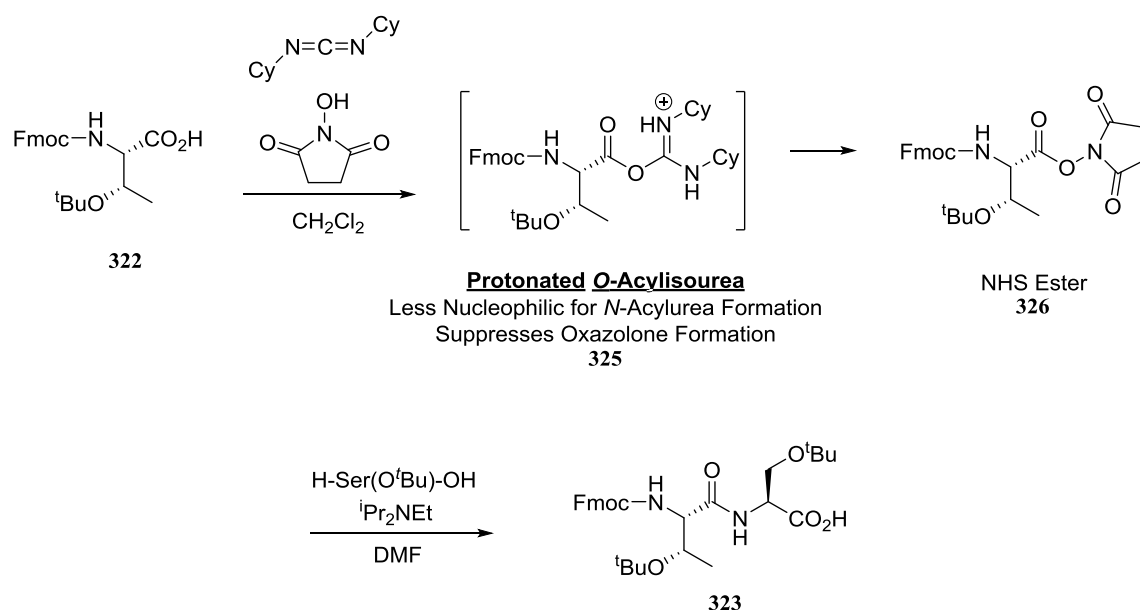
include direct aminolysis of the *O*-acylisourea with an amine (Path A) or aminolysis of a symmetrical anhydride or oxazolone intermediate generated from **IV** (Paths B and C respectively). The least desirable side reaction, *N*-acylurea formation, arises from intramolecular nucleophilic attack of the imino moiety in **IV** leading to *O*→*N*-acyl migration. This side reaction competes with aminolysis and diminishes the coupling yields. The proportion of this side product is heavily influenced by experimental conditions. *N*-acylurea generation is suppressed at lower temperatures⁴² and when low polarity solvents are used⁴³ (e.g., dichloromethane and benzene).



Scheme 5.7 – Reaction Mechanism for Carbodiimide-Mediated Peptide Ligation

N-Hydroxysuccinimide (NHS) or 1,2,3-benzotriazol-1-ol (HOBt) boosts the efficiency of carbodiimide-governed reactions by suppressing both *N*-acylurea formation and epimerization during peptide coupling.^{44,45} *N*-Hydroxysuccinimide exerts its positive effects via protic properties (pKa 6.09). It reduces the nucleophilicity of *O*-acylisourea by partial protonation thereby inhibiting the intramolecular reaction (Scheme 5.8). It also mitigates oxazolone generation by protonation of *O*-acylisourea which

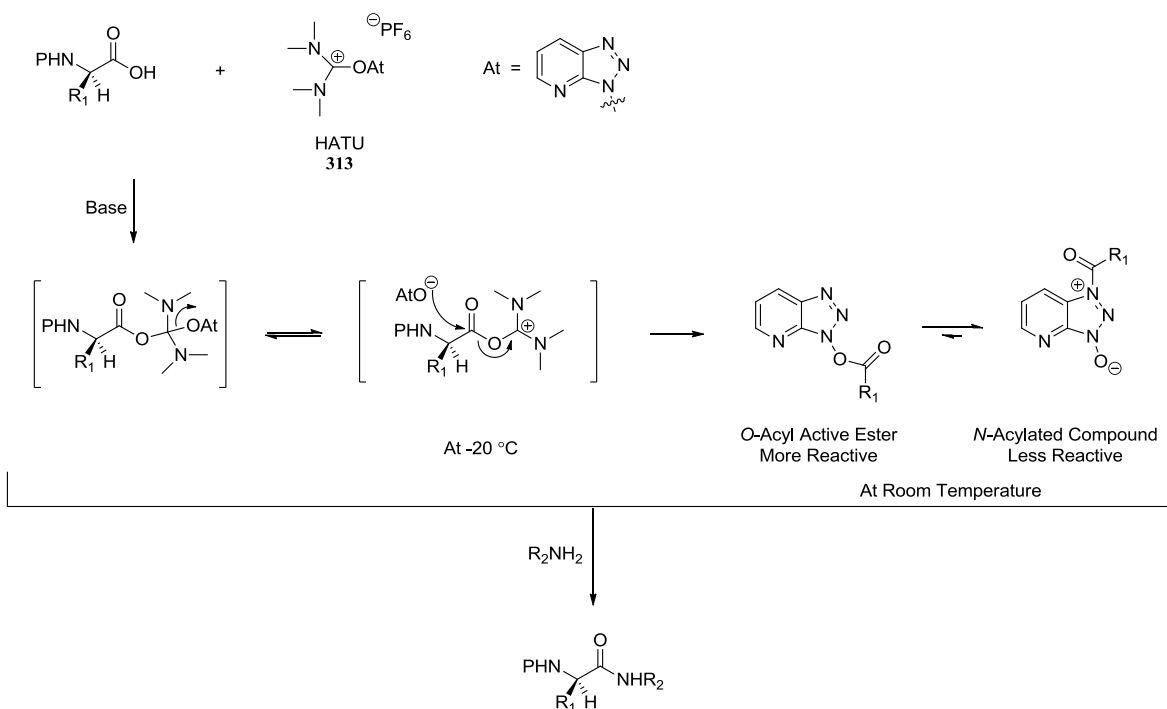
produces a better electrophile which in turn expedites its consumption. Fmoc-*allo*-Thr(O^tBu)-OH **322** was activated as its NHS ester **326** that reacted readily with H-Ser(O^tBu)-OH to form the Fmoc-*allo*-Thr(O^tBu)-Ser-OH dipeptide **323**. The by-product formed, *N,N'*-dicyclohexylurea (DCU), can be eliminated by filtration, although traces of it are difficult to remove.



Scheme 5.8 - Fmoc-*allo*-Thr(O^tBu)-Ser(O^tBu)-OH Dipeptide Formation Via DCC/NHS Activation

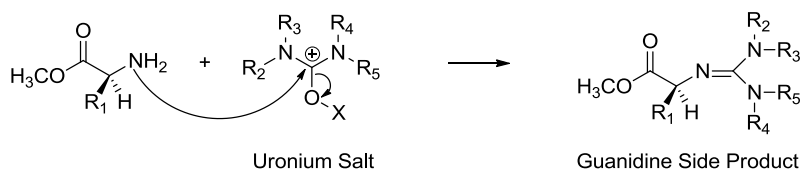
Continuing with TNM C fragment assembly, the coupling reagent HATU was used to link the free acid dipeptide to HCl-Phe-OBn to produce the Fmoc-*allo*-Thr(O^tBu)-Ser(O^tBu)-Phe-OBn tripeptide **324** in 65% yield over two steps (Scheme 5.6). HATU **313**, when used with a judicious choice of amine base is a superior reagent combination for sterically demanding couplings that gives very low levels of racemization.^{46,47} Carpino and co-workers established this through loss of chirality studies using a variety of coupling reagents/bases in DMF to form the sensitive Cbz-Phe-Val-Pro-NH₂ tripeptide via [2+1] coupling. In the case of onium-derived reagents, epimerization levels decreased in the order of BOP > HBTU > HDTU > HATU > HAPyU.

The mechanism of HATU coupling starts with the use of a tertiary amine to form the carboxylate ion from a carboxylic acid (Scheme 5.9). Attack on the uronium/guandinium reagent leads to the carboxyl uronium salt (detected by NMR at $-20\text{ }^{\circ}\text{C}^{46}$), which is converted into an active ester that is thought to be the prevailing species undergoing aminolysis.



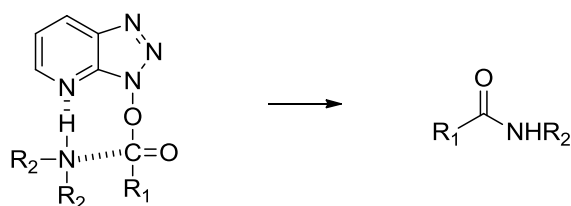
Scheme 5.9 – HATU Activation and Coupling

Not surprisingly, side reactions can occur when an aminium/uronium salt is used as a coupling reagent. Excess uronium reagent or slow preactivation of the amino acid may provide an opportunity for nucleophilic attack of the amino group on the positively charged carbon atom of the uronium salt to produce a guanidino derivative (Scheme 5.10).⁴⁸



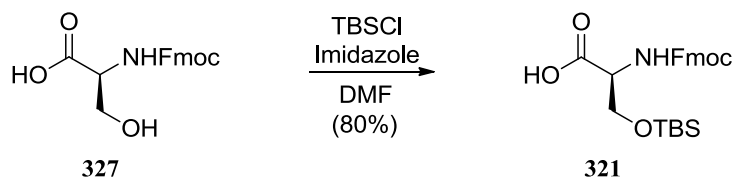
Scheme 5.10 – Side Reaction Associated with the Use of HATU

Carpino *et al.* showed that the additive, HOAt **315**, used in combination with a carbodiimide, consistently gave excellent results⁴⁹ and it is no coincidence that the coupling reagent HATU was based on this additive. Hydroxyazabenzotriazole esters lead to faster, more efficient coupling than activated esters made from NHS or HOBt. This observation stems from the ring nitrogen atom at position 7 which provides two effects to increase reactivity. The nitrogen atom provides an electron-withdrawing effect which improves the quality of the leaving group. Moreover, neighboring group participation is now possible (Scheme 5.11). HATU is a powerful reagent, however, care must be incurred because it is considerably more expensive than other routinely used coupling reagents.



Scheme 5.11 – Neighboring Group Participation: H-Bonding Accelerates Rate of Coupling of OAt Esters

In keeping with our global fluoride deprotection strategy, we replaced both *O*Bu protecting groups with their TBS counterparts (Scheme 5.6). The decision to introduce the more robust TBS ethers at the tripeptide stage, as opposed to after tetrapeptide formation was revealed in §2.9. Recall that γ -hydroxyacids (Ahad and Aboa) can form γ -lactones under acidic conditions (refer to Scheme 2.19 for a general example).¹ According to Scheme 5.4, we also needed to protect the hydroxyl group in Fmoc-Ser-OH **327** (commercially available) as its TBS ether. As prescribed by Palumbo *et al.*, this was accomplished in high yield (Scheme 5.12).⁵⁰



Scheme 5.12 - TBS Protection of the Hydroxyl Group in Fmoc-Ser-OH

5.7 Synthetic Efforts Towards the Eastern Hemisphere of TNM C: a β -Phe Analog

Ultimately, we want to produce three monocycles related to the eastern hemisphere of TNM C for analog development and structure activity relationship studies. Since the Aboa and Apoa residues (blue in Figure 5.7) were not yet available, we therefore sought to synthesize a β -Phe (green in Figure 5.7) containing analog **328** as this would generate a macrocycle with the same ring size.

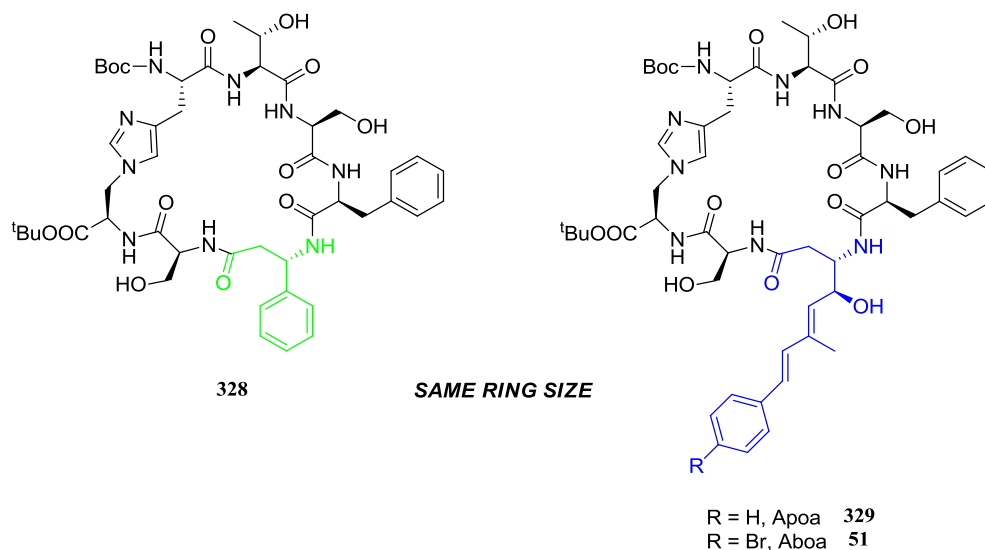
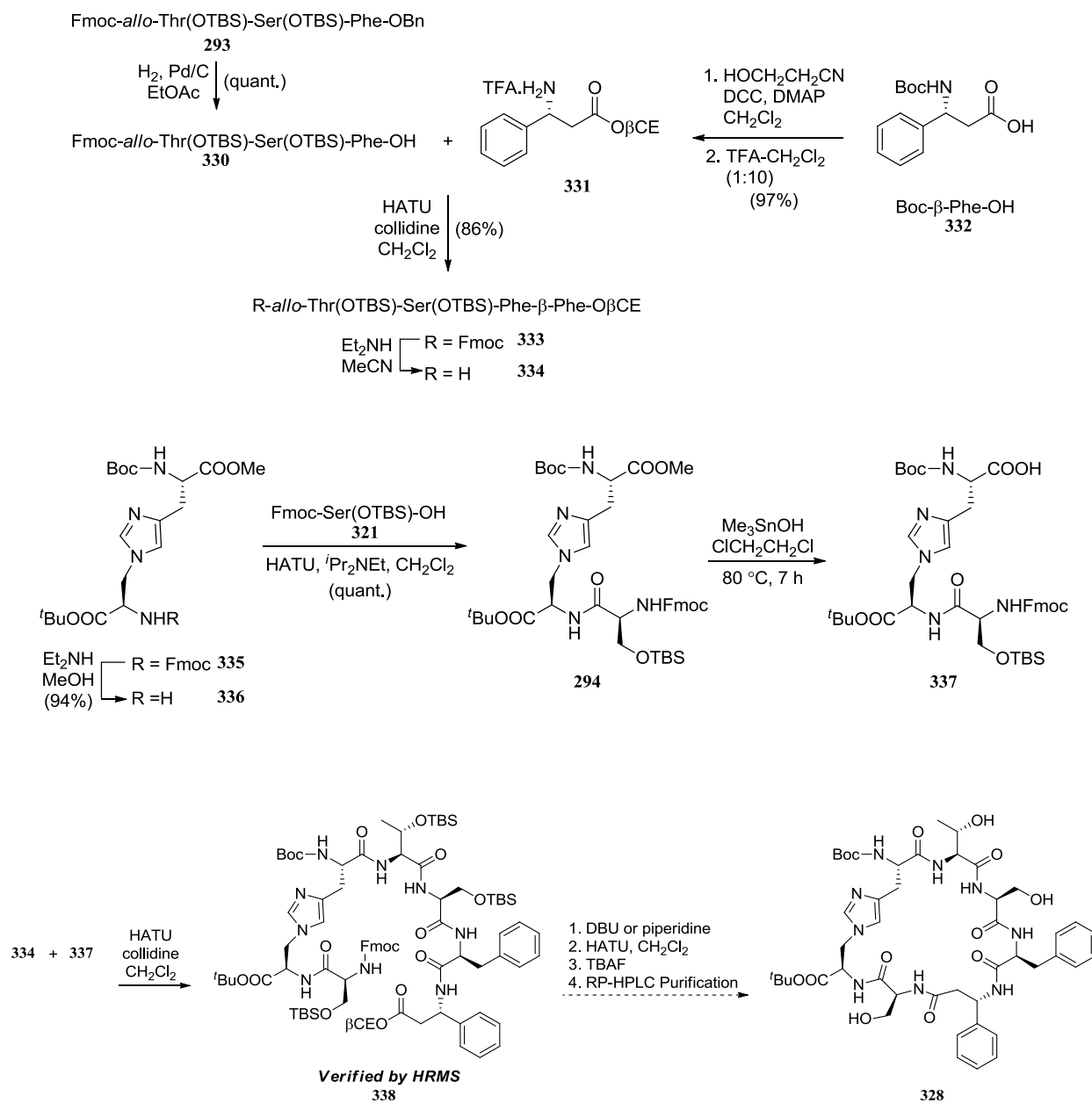


Figure 5.7 – Three Macrocycles Related to the Eastern Hemisphere of TNM C

Synthetic efforts toward the β -Phe containing analog **328** were conducted by Carol Taylor (Scheme 5.13). Boc- β -Phe-OH **332** was protected as its β CE ester followed by Boc removal to give TFA salt **331**. Tripeptide **293** underwent hydrogenolysis to expose the free carboxylic acid **330** in quantitative yield. Coupling of **330** and **331** using HATU/collidine generated the Fmoc-*allo*-Thr(OTBS)-Ser(OTBS)-Phe- β -Phe-O β CE tetrapeptide **333** in high yield. The τ -HAL-Ser fragment, was acquired after Fmoc deprotection of **335** (supplied by Chyree Batton) using diethylamine and ligation of the resulting free amine to Fmoc-Ser(OTBS)-OH **321** using HATU/ i Pr₂NEt. Formation of the cyclization precursor required coupling partners derived from Fmoc deprotection of **333** (NHET₂) and deprotection of the methyl ester in **294** (trimethyltin hydroxide). While the methyl ester in **294** could be removed cleanly, the

“tripeptide” substrate reacted sluggishly and for future purposes, the methyl ester in **294** will be supplanted with a benzyl ester group (supplied by Chyree Batton). The deprotected crude products were coupled using HATU/collidine to produce the linear “heptapeptide” **338** (verified by HRMS).



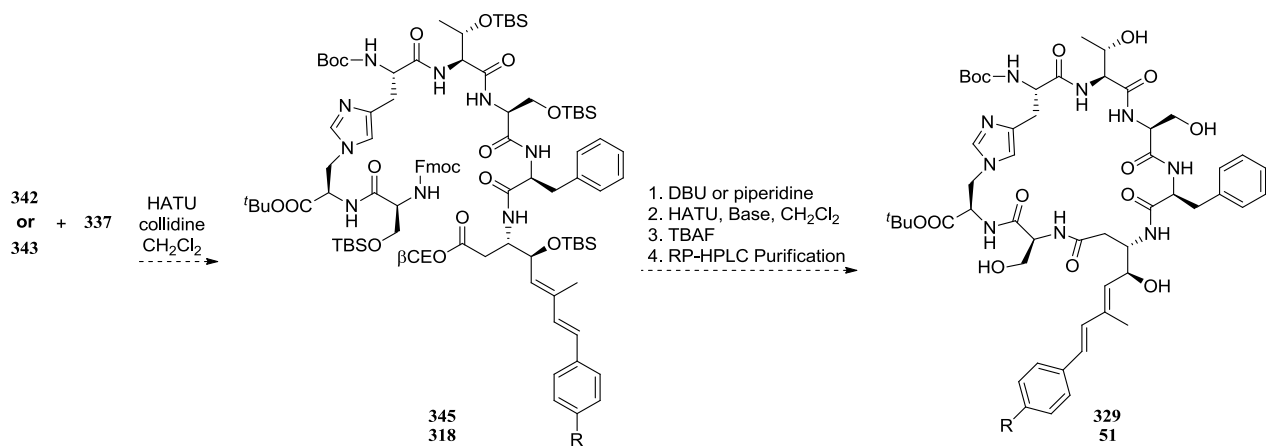
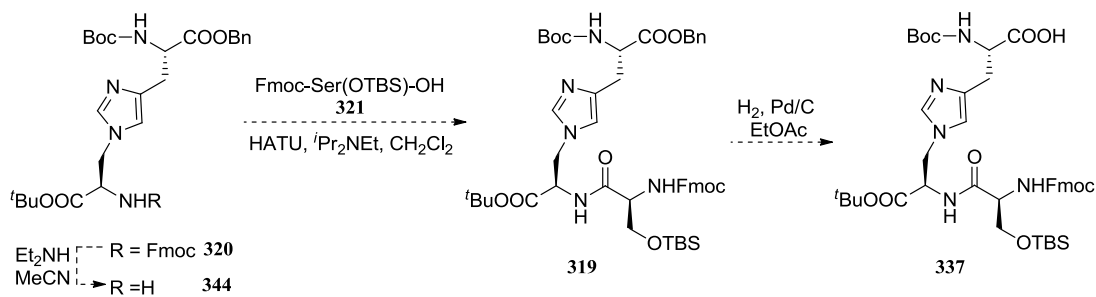
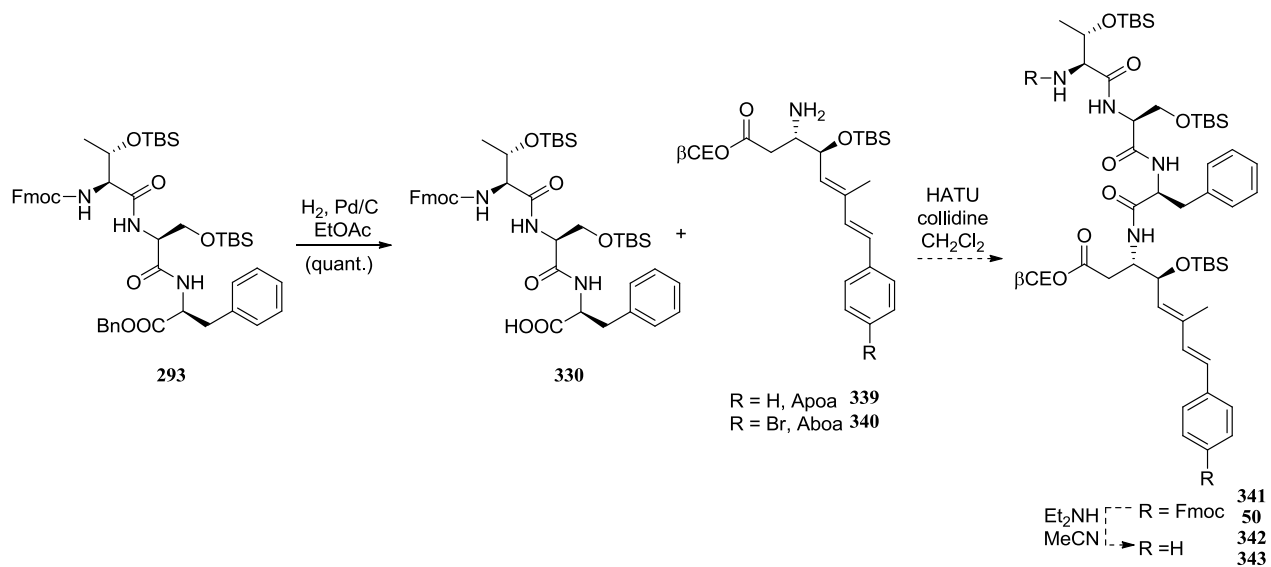
Scheme 5.13 – Progress Toward the Eastern Hemisphere of TNM C: a β -Phe Analog

The fact that both the Fmoc and β CE ester groups are base labile led us to screen various bases in the hope of finding a reagent to effect simultaneous removal. The deprotections were performed using Fmoc-Phe-O β CE and while diethylamine and potassium carbonate individually removed Fmoc and the β CE ester respectively, DBU or piperidine worked well in rapid fashion to afford the desired product. Using this knowledge, exposing the linear “heptapeptide” **338** to DBU or piperidine should reveal the *N*- and *C*-terminus of the β -Phe containing monocycle. Whether the deprotected crude product can undergo HATU-mediated cyclization in tandem remains to be seen, however, macrocycle formation should be conducted under high dilution conditions. Global desilylation with tetrabutylammonium fluoride (TBAF) followed by purification via reversed phase HPLC should provide the β -Phe containing analog **328**.

5.8 Future Work and Perspectives

5.8.1 Future Work: Construction of Both Naturally Occurring Theonellamide Eastern Hemispheres, The Apoa and Aboa Containing Congeners

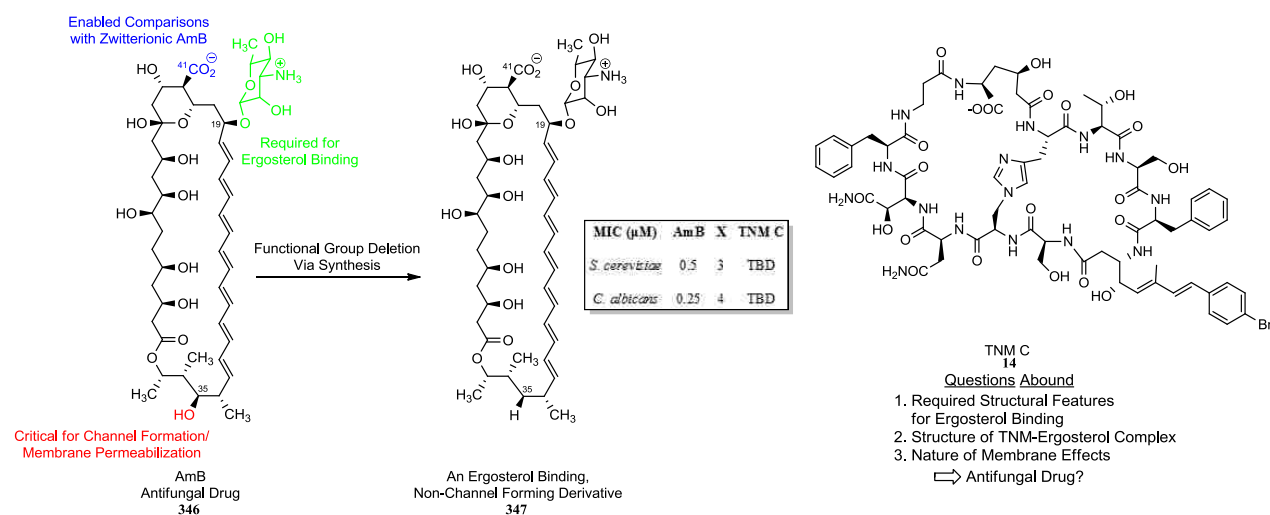
Efforts to produce the Apoa- or Aboa-containing eastern hemisphere of a naturally occurring theonellamide are on hold until either residue is available. According to Scheme 5.14, once **339** or **340** is complete, the deprotection and coupling conditions outlined above for the β -Phe analog can be readily applied towards the assembly of both congeners. Cyclization investigations performed on the β -Phe analog should provide us with the knowledge to carry out cyclization reactions using the Apoa- and Aboa-containing compounds.



Scheme 5.14 – Plans to Complete Both Theonellamide Eastern Hemispheres

5.8.2 Future TNM C Perspectives: Utilizing the Amphotericin B Blueprint

Recent work by Burke and co-workers has elucidated amphotericin B's (AmB, **346**) mode of action in killing yeast.^{51,52} For decades, it was believed that channel formation was essential for the fungicidal effect of AmB. The mechanism of action (MOA) is much simpler, however, AmB just needs to bind to the cell's ergosterol. To test this theory, an AmB derivative **347** was generated that could bind ergosterol but could not form ion channels. All of the available evidence suggests that the C35-OH (red in Scheme 5.15) is critical for channel formation. The ergosterol binding, non-channel forming derivative **347** was similarly potent to AmB against *S. cerevisiae* and *C. albicans* cells.



Scheme 5.15 - Linking AmB's Past to TNM C's Future

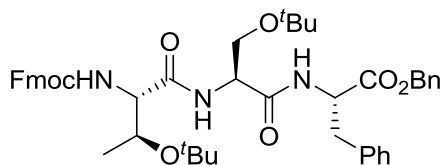
The TNMs represent a mechanistically distinct class of ergosterol binders.^{3,4} What has been established is that the TNMs recognize 3 β -hydroxysterols (ergosterol, cholesterol, etc.) to induce overproduction of 1,3- β -D-glucan by Rho1 activation leading to cytotoxic membrane damage.⁴ What is less clear though, is the portion of the peptide that binds to ergosterol in lipid bilayers, the resulting TNM-ergosterol complex and the associated membrane morphological changes leading to membrane damage. The current understanding of the TNMs mode of action is still in its infancy while knowledge regarding

AmB's MOA continues to mature. Comparisons between the two, however, are inevitable. The synthesis of the three macrocycles proposed in §5.7 and §5.8.1 may provide an opportunity to identify the minimal chemical structure required for the TNMs biological activity. Specifically, all three macrocycles will be tested against the same species of yeast cells as AmB (*S. cerevisiae* and *C. albicans*). Ultimately, the discovery that simple AmB binding to an essential lipid (ergosterol) is an antimicrobial MOA could have drug discovery implications for the TNMs.

5.9 Experimental Section

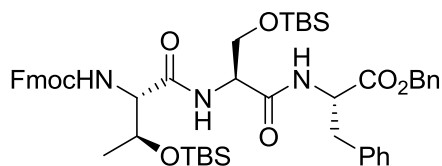
General methods: as detailed in Chapter 2

5.9.1 Experimental Procedures



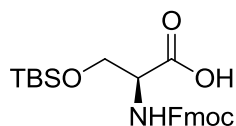
Fmoc-*allo*-Thr(O^tBu)-Ser(O^tBu)-Phe-OBn (**324**). *N*-Hydroxysuccinimide (29 mg, 0.25 mmol, 1.0 equiv.), followed immediately by DCC (52 mg, 0.25 mmol, 1.0 equiv.), were added to a solution of Fmoc-*allo*-Thr(O^tBu)-OH (100 mg, 0.25 mmol, 1.0 equiv.) in anhydrous CH₂Cl₂ (4.0 mL) at 0 °C under N₂. The mixture was warmed to RT and stirred for 4 h, filtered to remove the dicyclohexylurea (washing well with CH₂Cl₂) and concentrated to ½ of the original reaction volume. After standing in the freezer for 4 h, the reaction was filtered again (washing twice with CH₂Cl₂). The filtrate was concentrated and the intermediate NHS ester dissolved in dry DMF (1.0 mL) and cooled to 0 °C under N₂. After 10 min, H-Ser(O^tBu)-OH (41 mg, 0.25 mmol, 1.0 equiv.) was added to the reaction mixture, followed by the dropwise addition of DIPEA (50 μL, 39 mg, 0.30 mmol, 1.2 equiv.). The mixture was warmed to RT and stirred overnight under N₂. The mixture was diluted with EtOAc (25 mL) and washed with 2 M HCl (25 mL). The aqueous layer was washed with EtOAc (25 mL) again and the combined organic layers washed with H₂O (40 mL), dried over MgSO₄, filtered and concentrated to give Fmoc-*allo*-Thr(O^tBu)-Ser(O^tBu)-

OH (108 mg, 80% yield) that was used directly in the next step without further purification. Fmoc-*allo*-Thr(O'Bu)-Ser(O'Bu)-OH (108 mg, 0.2 mmol, 1.1 equiv.) was dissolved in anhydrous CH₂Cl₂ (3.0 mL) and cooled to 0 °C under N₂. After 10 min, HCl.Phe.OBn (53 mg, 0.2 mmol, 1.0 equiv.) was added to the reaction mixture, followed by the dropwise addition of 2,4,6-collidine (53 μL, 48 mg, 0.40 mmol, 2.0 equiv.). After the addition of HATU (76 mg, 0.2 mmol, 1.1 equiv.), the contents were warmed to RT and stirred overnight under N₂. The reaction mixture was concentrated and the residue purified via column chromatography (2:1 Hex/EtOAc → 1:1 Hex/EtOAc) to produce Fmoc-*allo*-Thr(O'Bu)-Ser(O'Bu)-Phe-OBn as a colorless foam (124 mg; 64% over 2 steps). *R*_f 0.18 (2:1 Hex-EtOAc); [α]^{25.0}_D +18.2 (*c* 1.0, CHCl₃). ¹H NMR (CDCl₃, 400 MHz) δ 1.11 (s, 9H), 1.16 (s, 9H), 1.12-1.19 (m, 3H), 3.06 (dd, *J* = 13.9, 6.2 Hz, 1H), 3.12 (dd, *J* = 13.9, 5.8 Hz, 1H), 3.29 (app. t, *J* = 8.3 Hz, 1H), 3.79 (dd, *J* = 8.3, 3.7 Hz, 1H), 3.97 (br, 1H), 4.15 (br, 1H), 4.22 (t, *J* = 6.8 Hz, 1H), 4.28 (br, 1H), 4.41 (br, 1H), 4.45 (dd, *J* = 10.4, 6.8 Hz, 1H), 4.90 (app. q, *J* = 6.5 Hz, 1H), 5.08 (d, *J* = 12.2 Hz, 1H), 5.13 (d, *J* = 12.2 Hz, 1H), 5.51 (br, 1H), 7.00-7.04 (m, 2H), 7.11 (d, *J* = 6.4 Hz, 1H), 7.13-7.19 (m, 3H), 7.25-7.41 (m, 8H), 7.58 (d, *J* = 5.7 Hz, 2H), 7.75 (d, *J* = 7.5 Hz, 2H); ¹³C NMR (CDCl₃, 100 MHz) δ 19.2, 27.3, 28.3, 37.9, 47.1, 52.8, 53.5, 60.8, 61.0, 67.1, 67.2, 67.5, 74.2, 74.7, 120.0, 125.0, 125.1, 126.9, 127.0, 127.7, 128.4 [2C], 128.5, 129.2, 135.2, 135.9, 141.3, 143.8, 156.5, 169.7, 170.0, 170.9. HRMS (ESI) calcd for C₄₆H₅₆N₃O₈ (M+H)⁺ 778.4061, obsd 778.4071.



Fmoc-*allo*-Thr(OTBS)-Ser(OTBS)-Phe-OBn (**293**). Trifluoroacetic acid (0.70 mL) was added to anhydrous CH₂Cl₂ (0.70 mL) and cooled to 0 °C under N₂. After 10 min, Fmoc-*allo*-Thr(O'Bu)-Ser(O'Bu)-Phe-OBn (100 mg, 0.13 mmol, 1.0 equiv.) was added as a solid in a single portion and the reaction mixture stirred at rt for 2.25 h. The reaction mixture was concentrated and the diol (111 mg) isolated by column chromatography (95:5 CH₂Cl₂/MeOH). The intermediate diol (111 mg, 0.17 mmol,

1.0 equiv.) was dissolved in anhydrous CH₂Cl₂ (2.0 mL) and cooled to 0 °C under N₂. After 10 min, 2,6-lutidine (267 μL, 247 mg, 2.3 mmol, 13.8 equiv.) was added dropwise to the reaction mixture, followed by TBDMSOTf (264 μL, 304 mg, 1.2 mmol, 6.9 equiv.). The mixture was stirred overnight at RT under N₂. The reaction mixture was concentrated and the residue purified via column chromatography (5:1 Hex/EtOAc) to produce Fmoc-*allo*-Thr(OTBS)-Ser(OTBS)-Phe-OBn as a colorless foam (94 mg, 82% over 2 steps). $[\alpha]^{25.0}_D +24.6$ (*c* 1.0, CHCl₃). ¹H NMR (CDCl₃, 400 MHz) δ -0.04 (2 X s, 12H), 0.76 (s, 9H), 0.79 (s, 9H), 1.09 (d, *J* = 4.6 Hz, 3H), 2.97 (dd, *J* = 13.9, 6.5 Hz, 1H), 3.05 (dd, *J* = 13.9, 6.5 Hz, 1H), 3.47 (app. t, *J* = 8.4 Hz, 1H), 3.97 (d, *J* = 7.0 Hz, 1H), 4.02-4.22 (m, 3H), 4.13 (t, *J* = 6.7 Hz, 1H), 4.28 (br, 1H), 4.40 (dd, *J* = 10.2, 6.7 Hz, 1H), 4.80 (dd, *J* = 14.1, 6.7 Hz, 1H), 5.00 (d, *J* = 12.2 Hz, 1H), 5.05 (d, *J* = 12.2 Hz, 1H), 5.36 (br, 1H), 6.89-6.97 (m, 3H), 7.08-7.26 (m, 9H), 7.31 (t, *J* = 7.5 Hz, 2H), 7.48 (t, *J* = 7.0 Hz, 2H) 7.69 (d, *J* = 7.6 Hz, 2H); ¹³C NMR (CDCl₃, 100 MHz) δ -5.6 [2C], -5.0, -4.7, 17.9, 18.1, 19.5, 25.7, 25.8, 38.0, 47.1, 53.7, 54.1, 61.4, 62.4, 67.0, 67.4, 68.5, 120.0, 125.0, 126.9, 127.1, 127.7, 128.3, 128.4, 128.5, 129.1, 135.2, 135.9, 141.3, 143.6, 143.7, 156.7, 169.3, 169.6, 170.8. HRMS (ESI) calcd for C₅₀H₆₈N₃O₈Si₂ (M+H)⁺ 894.4539, obsd 894.4540.



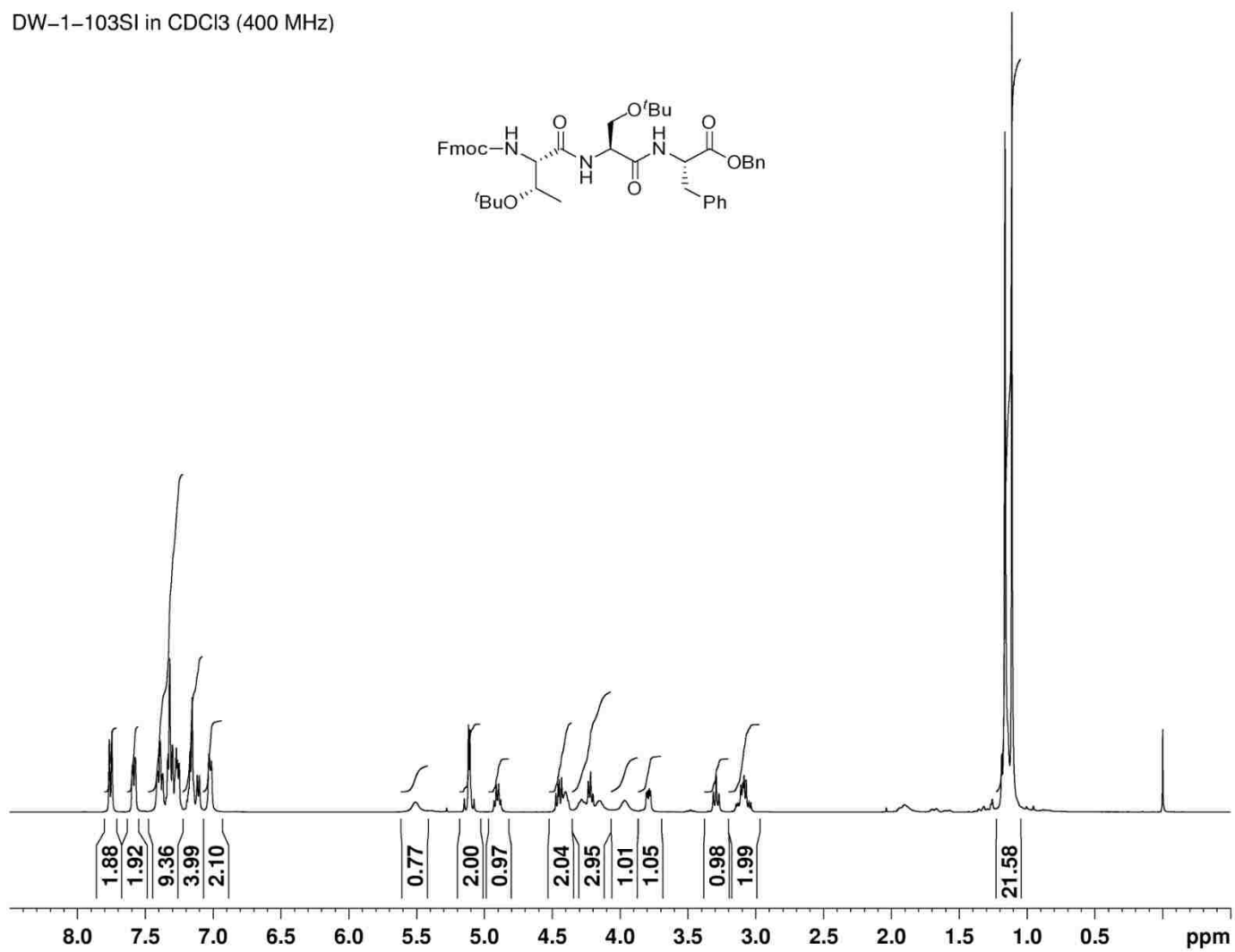
Fmoc-Ser(OTBS)-OH (**321**). Imidazole (459 mg, 6.7 mmol, 6.0 equiv.) was added to a stirred solution of Fmoc-Ser-OH (368 mg, 1.1 mmol, 1.0 equiv.) in dry DMF (3.7 mL) at 0 °C under N₂. After stirring for 30 min at 0 °C, TBSCl (779 mg, 5.2 mmol, 4.6 equiv.) was added in a single portion. The reaction mixture was stirred for 1 h at 0 °C, warmed to rt and stirred overnight. The reaction mixture was cooled to 0 °C, quenched by the dropwise addition of 1 M HCl (7.4 mL) and warmed to rt. The contents were extracted with Et₂O (2 x 30 mL) and the combined organic layers were concentrated. The residue was diluted with 10 % LiCl (7.4 mL) and extracted with Et₂O (2 x 30 mL). The combined organic layers were dried with MgSO₄, filtered and concentrated. Purification by flash chromatography (4:1 Hex/EtOAc

→ 9:1 CH₂Cl₂/MeOH) afforded the title compound as a colorless oil (398 mg, 80%). *R_f* 0.40 (9:1 CH₂Cl₂/MeOH). ¹H NMR and ¹³C NMR spectra are in good agreement with Palumbo and co-workers.⁵⁰

5.9.2 Spectra

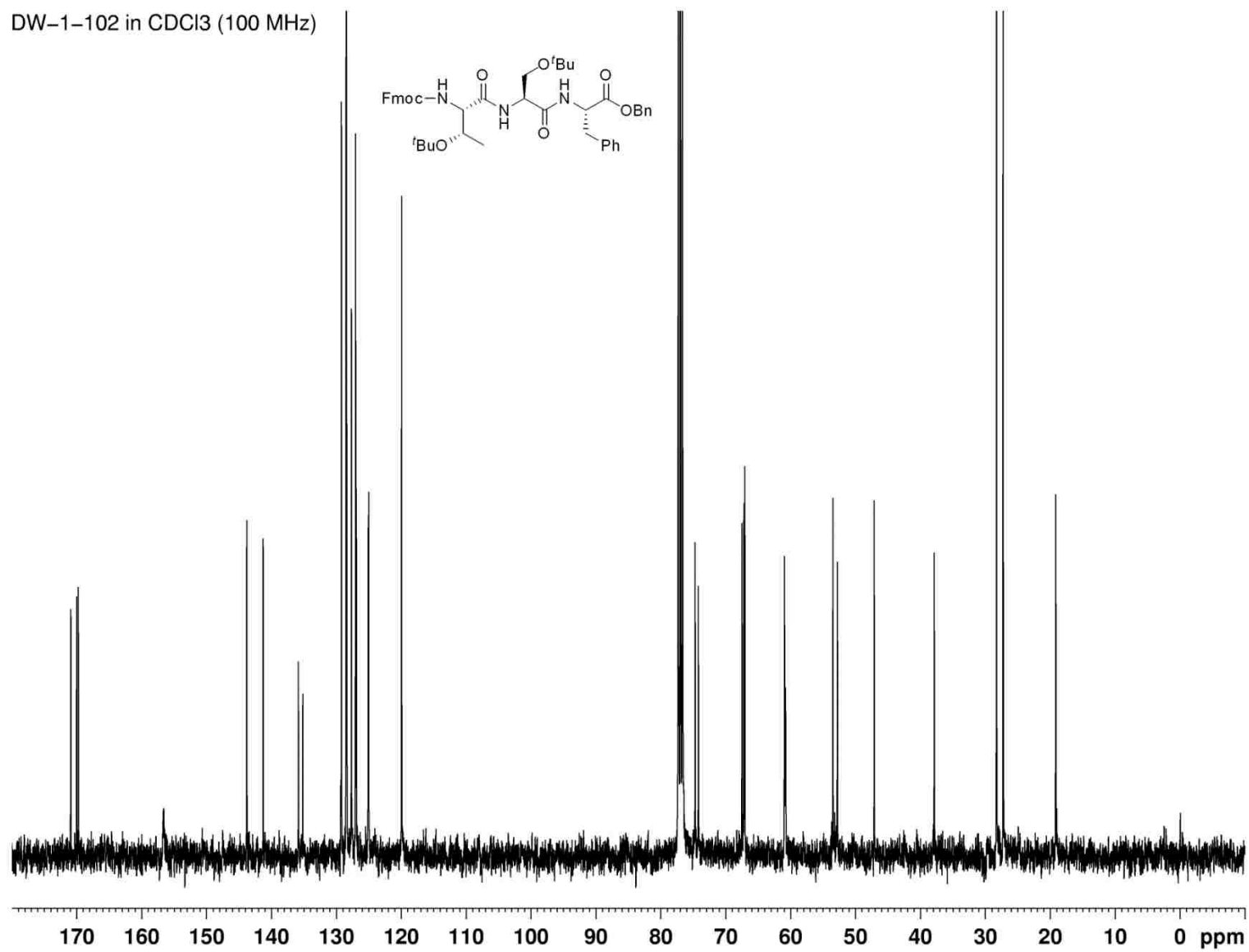
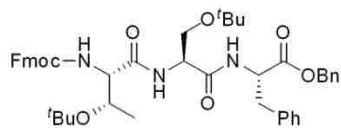
Compound **324** - ^1H NMR spectrum

DW-1-103SI in CDCl_3 (400 MHz)



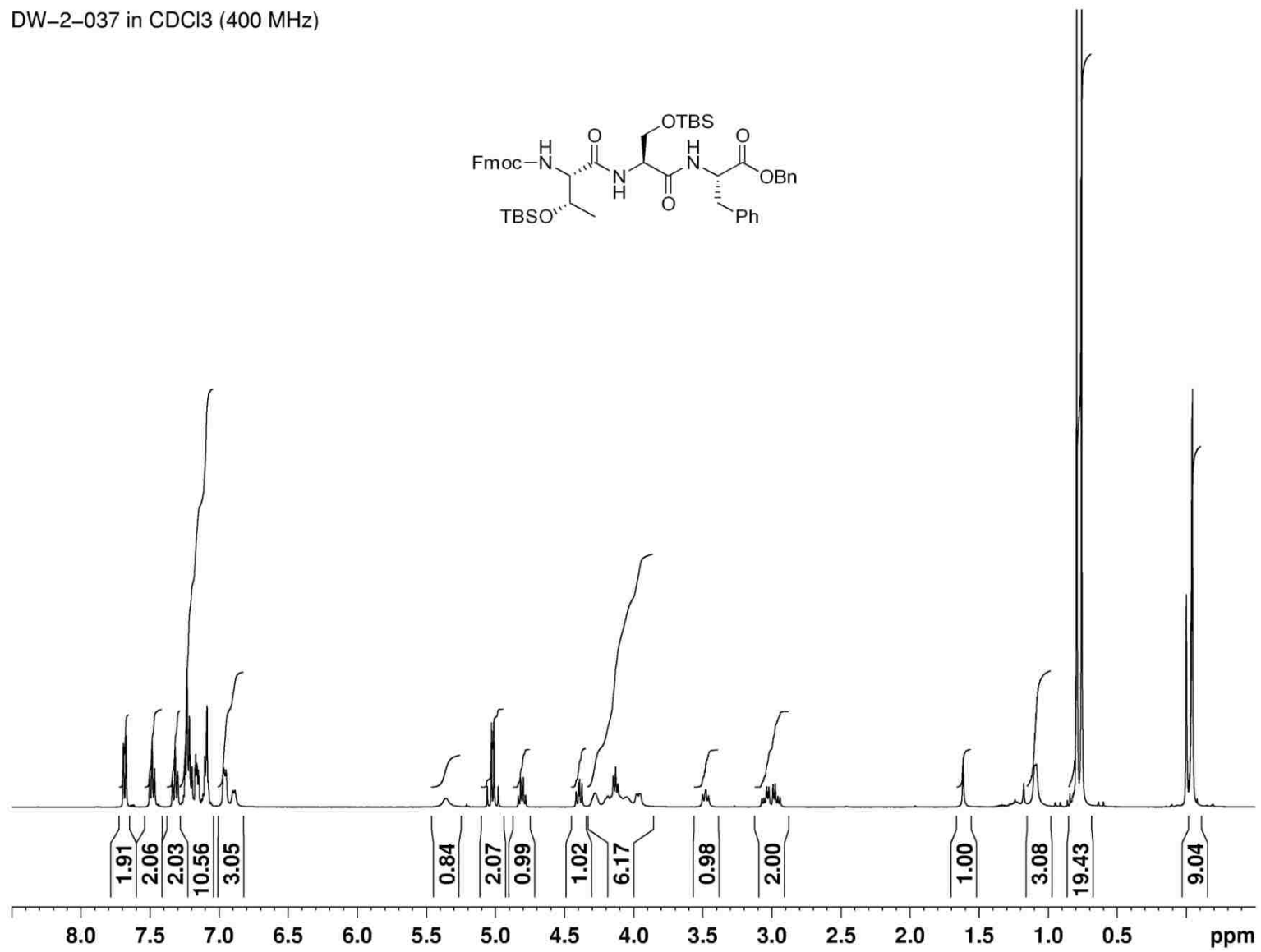
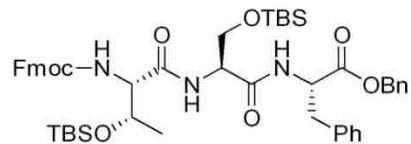
Compound **324** - ^{13}C NMR spectrum

DW-1-102 in CDCl_3 (100 MHz)



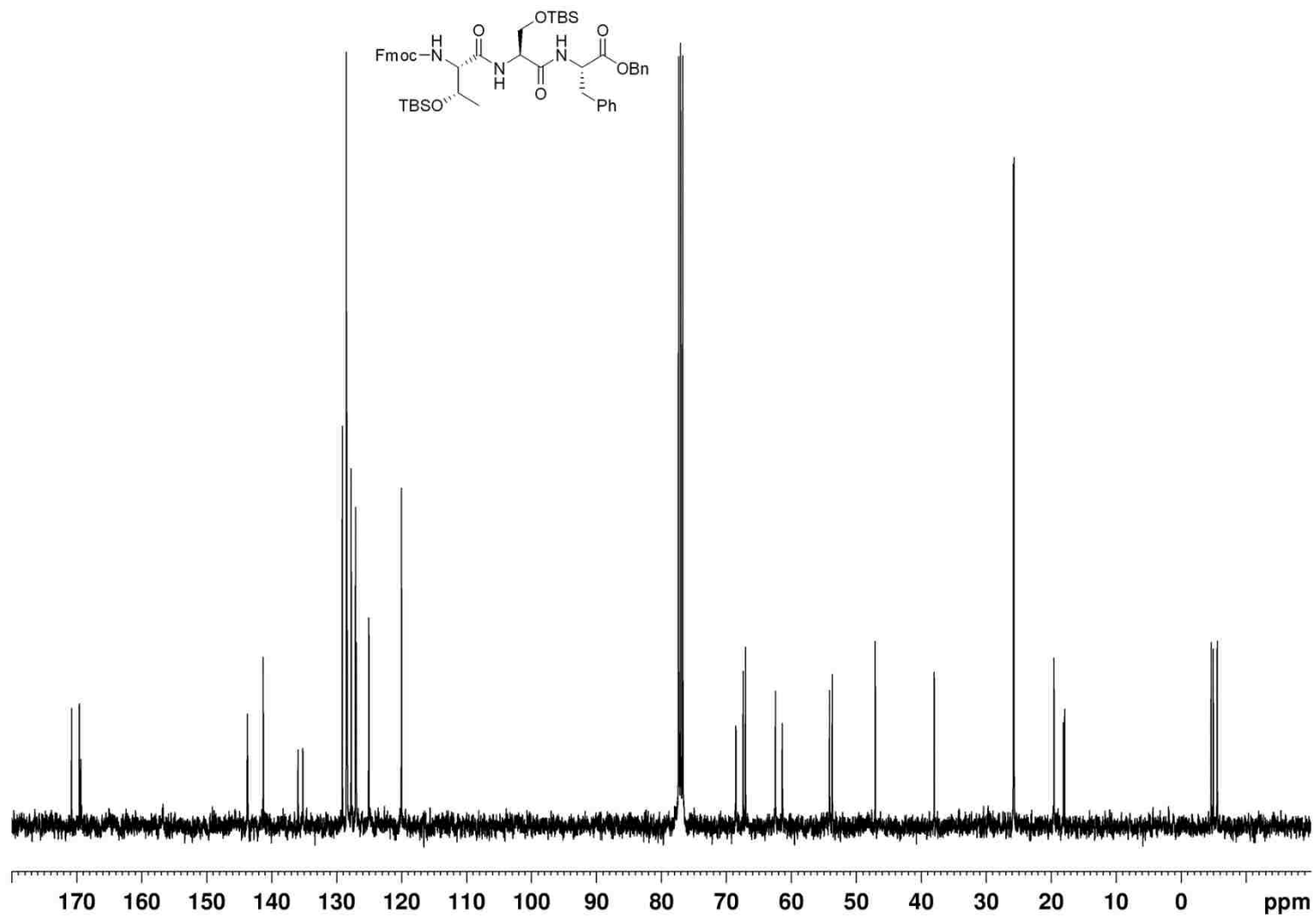
Compound **293** - ^1H NMR spectrum

DW-2-037 in CDCl_3 (400 MHz)



Compound **293** - ^{13}C NMR spectrum

DW-2-037 in CDCl_3 (100 MHz)



5.10 References

1. Matsunaga, S.; Fusetani, N.; Hashimoto, K.; Walchli, M.: Theonellamide F. A novel antifungal bicyclic peptide from a marine sponge *Theonella* sp. *J. Am. Chem. Soc.* **1989**, *111*, 2582-2588.
2. Matsunaga, S.; Fusetani, N.: Theonellamides A-E, cytotoxic bicyclic peptides, from a marine sponge *Theonella* sp. *J. Org. Chem.* **1995**, *60*, 1177-1181.
3. Ho, C. H.; Magtanong, L.; Barker, S. L.; Gresham, D.; Nishimura, S.; Natarajan, P.; Koh, J. L. Y.; Porter, J.; Gray, C. A.; Andersen, R. J.; Giaever, G.; Nislow, C.; Andrews, B.; Botstein, D.; Graham, T. R.; Yoshida, M.; Boone, C.: A molecular barcoded yeast ORF library enables mode-of-action analysis of bioactive compounds. *Nat. Biotechnol.* **2009**, *27*, 369-377.
4. Nishimura, S.; Arita, Y.; Honda, M.; Iwamoto, K.; Matsuyama, A.; Shirai, A.; Kawasaki, H.; Kakeya, H.; Kobayashi, T.; Matsunaga, S.; Yoshida, M.: Marine antifungal theonellamides target β -hydroxysterol to activate Rho1 signaling. *Nat. Chem. Biol.* **2010**, *6*, 519-526.
5. Lax, R.: The future of peptide development in the pharmaceutical industry. *PharManufacturing: Int. Pept. Rev.* **2010**, 10-15.
6. Craik, D. J.; Fairlie, D. P.; Liras, S.; Price, D.: The future of peptide-based drugs. *Chem. Biol. Drug Des.* **2013**, *81*, 136-147.
7. Mason, J. M.: Design and development of peptides and peptide mimetics as antagonists for therapeutic intervention. *Future Med. Chem.* **2010**, *2*, 1813-1822.
8. White, C. J.; Yudin, A. K.: Contemporary strategies for peptide macrocyclization. *Nat. Chem.* **2011**, *3*, 509-524.
9. Meutermans, W. D. F.; Golding, S. W.; Bourne, G. T.; Miranda, L. P.; Dooley, M. J.; Alewood, P. F.; Smythe, M. L.: Synthesis of difficult cyclic peptides by inclusion of a novel photolabile auxiliary in a ring contraction strategy. *J. Am. Chem. Soc.* **1999**, *121*, 9790-9796.
10. Rostovtsev, V. V.; Green, L. G.; Fokin, V. V.; Sharpless, K. B.: A stepwise Huisgen cycloaddition process: copper(I)-catalyzed regioselective "ligation" of azides and terminal alkynes. *Angew. Chem. Int. Ed.* **2002**, *41*, 2596-2599.
11. Miller, S. J.; Blackwell, H. E.; Grubbs, R. H.: Application of ring-closing metathesis to the synthesis of rigidified amino acids and peptides. *J. Am. Chem. Soc.* **1996**, *118*, 9606-9614.
12. Boissonnas, R. A.; Guttmann, S.; Jaquenoud, P. A.; Waller, J. P.: Une nouvelle synthese de l'oxytocine. *Helv. Chim. Acta.* **1955**, *38*, 1491-1507.
13. Veber, D. F.; Johnson, S. R.; Cheng, H. Y.; Smith, B. R.; Ward, K. W.; Kopple, K. D.: Molecular properties that influence the oral bioavailability of drug candidates. *J. Med. Chem.* **2002**, *45*, 2615-2623.

14. White, T. R.; Renzelman, C. M.; Rand, A. C.; Rezai, T.; McEwen, C. M.; Gelev, V. M.; Turner, R. A.; Linington, R. G.; Leung, S. S. F.; Kalgutkar, A. S.; Bauman, J. N.; Zhang, Y.; Liras, S.; Price, D. A.; Mathiowetz, A. M.; Jacobson, M. P.; Lokey, R. S.: On-resin *N*-methylation of cyclic peptides for discovery of orally bioavailable scaffolds. *Nat. Chem. Biol.* **2011**, *7*, 810-817.
15. Irum, W.; Anjum, T.: Production enhancement of cyclosporin 'A' by *Aspergillus terreus* through mutation. *Afr. J. Biotechnol.* **2012**, *11*, 1736-1743.
16. Watanakunakorn, C.: Mode of action and *in-vitro* activity of vancomycin. *J. Antimicrob. Chemother.* **1984**, *14*, 7-18.
17. Jung, H. M.; Kim, S. Y.; Moon, H. J.; Oh, D. K.; Lee, J. K.: Optimization of culture conditions and scale-up to pilot and plant scales for vancomycin production by *Amycolatopsis orientalis*. *Appl. Microbiol. Biotechnol.* **2007**, *77*, 789-795.
18. Vigneaud, V. D.; Ressler, C.; Swan, J. M.; Roberts, C. W.; Katsoyannis, P. G.: The synthesis of oxytocin. *J. Am. Chem. Soc.* **1954**, *76*, 3115-3121.
19. Wu, X.; Stockdill, J. L.; Wang, P.; Danishefsky, S. J.: Total synthesis of cyclosporine: access to *N*-methylated peptides via isonitrile coupling reactions. *J. Am. Chem. Soc.* **2010**, *132*, 4098-4100.
20. Wenger, R. M.: Synthesis of cyclosporine. Total syntheses of 'cyclosporin A' and 'cyclosporin H', two fungal metabolites isolated from the species *Tolypocladium inflatum* gams. *Helv. Chim. Acta.* **1984**, *67*, 502-525.
21. Nicolaou, K. C.; Boddy, C. N. C.; Li, H.; Koumbis, A. E.; Hughes, R.; Natarajan, S.; Jain, N. F.; Ramanjulu, J. M.; Brase, S.; Solomon, M. E.: Total synthesis of vancomycin-part 2: retrosynthetic analysis, synthesis of amino acid building blocks and strategy evaluations. *Chem. Eur. J.* **1999**, *5*, 2602-2621.
22. Boger, D. L.; Miyazaki, S.; Kim, S. H.; Wu, J. H.; Castle, S. L.; Loiseleur, O.; Jin, Q.: Total synthesis of the vancomycin aglycon. *J. Am. Chem. Soc.* **1999**, *121*, 10004-10011.
23. Jensen, C.; Herold, P.; Brunner, H. R.: Aliskiren: the first renin inhibitor for clinical treatment. *Nat. Rev. Drug Discovery.* **2008**, *7*, 399-410.
24. Rahuel, J.; Rasetti, V.; Maibaum, J.; Rueger, H.; Goschke, R.; Cohen, N. C.; Stutz, S.; Cumin, F.; Fuhrer, W.; Wood, J. M.; Grutter, M. G.: Structure-based drug design: the discovery of novel nonpeptide orally active inhibitors of human renin. *Chem. Biol.* **2000**, *7*, 493-504.
25. Li, P.; Xu, J. C.: The development of highly efficient onium-type peptide coupling reagents based upon rational molecular design. *J. Pept. Res.* **2001**, *58*, 129-139.
26. Carpino, L. A.; Beyermann, M.; Wenschuh, H.; Bienert, M.: Peptide synthesis via amino acid halides. *Acc. Chem. Res.* **1996**, *29*, 268-274.

27. Fischer, E.: Synthese von polypeptiden. *Ber. Dtsch. Chem. Ges.* **1903**, *36*, 2982-2992.
28. Sheehan, J. C.; Hess, G. P.: A new method of forming peptide bonds. *J. Am. Chem. Soc.* **1955**, *77*, 1067-1068.
29. Vaughan, J. R.: Acylalkylcarbonates as acylating agents for the synthesis of peptides. *J. Am. Chem. Soc.* **1951**, *73*, 3547.
30. Wieland, T.; Sehring, R.: Eine neue peptid-synthese. *Liebigs Ann.* **1950**, *569*, 122-129.
31. Gawne, G.; Kenner, G. W.; Sheppard, R. C.: Acyloxyphosphonium salts as acylating agents. Synthesis of peptides. *J. Am. Chem. Soc.* **1969**, *91*, 5669-5671.
32. Tohdo, K.; Hamada, Y.; Shioiri, T.: Synthesis of the southern hemisphere of theonellamide F, a bicyclic dodecapeptide of marine origin. *Synlett.* **1994**, *4*, 247-249.
33. Tohdo, K.; Hamada, Y.; Shioiri, T.: Synthesis of the northern hemisphere of theonellamide F, a bicyclic dodecapeptide of marine origin. *Synlett.* **1994**, *4*, 250.
34. Jones, J. H.; Witty, M. J.: Formation of 2-benzyloxyoxazol-5(4*H*)-ones from benzyloxycarbonyl-amino-acids. *J. Chem. Soc., Perkin Trans. 1.* **1979**, 3203-3206.
35. Benoiton, N. L.; Chen, F. M. F.: 2-Alkoxy-5(4*H*)-oxazolones from *N*-alkoxycarbonylamino acids and their implication in carbodiimide-mediated reactions in peptide-synthesis. *Can. J. Chem.* **1981**, *59*, 384-389.
36. Benoiton, N. L.; Chen, F. M. F.: Reaction of *N*-*t*-butoxycarbonylamino acid anhydrides with tertiary amines and carbodiimides. New precursors for 2-*t*-butoxyoxazol-5(4*H*)-one and *N*-acylureas. *J. Chem. Soc., Chem. Commun.* **1981**, 1225-1227.
37. Chen, F. M. F.; Benoiton, N. L.: The preparation and reactions of mixed anhydrides of *N*-alkoxycarbonylamino acids. *Can. J. Chem.* **1987**, *65*, 619-625.
38. Taylor, C. M.; Weir, C. A.: Synthesis of the repeating decapeptide unit of Mefp1 in orthogonally protected form. *J. Org. Chem.* **2000**, *65*, 1414-1421.
39. Benoiton, N. L.; Chen, F. M. F.: Not the alkoxy-carbonylamino-acid *O*-acylisourea. *J. Chem. Soc., Chem. Commun.* **1981**, 543-545.
40. Słebioda, M.; Wodecki, Z.; Kolodziejczyk, A. M.: Formation of optically pure *N*-acyl-*N,N'*-dicyclohexylurea in *N,N'*-dicyclohexylcarbodiimide-mediated peptide-synthesis. *Int. J. Pept. Protein Res.* **1990**, *35*, 539-541.
41. Rebek, J.; Feitler, D.: Mechanism of carbodiimide reaction. II. Peptide-synthesis on solid-phase. *J. Am. Chem. Soc.* **1974**, *96*, 1606-1607.

42. Helferich, B.; Boshagen, H.: Synthese einiger peptide aus histidin, valin und leucin. *Chem. Ber.* **1959**, *92*, 2813-2827.
43. Anderson, G. W.: Racemization by the dicyclohexylcarbodiimide method of peptide synthesis. *J. Am. Chem. Soc.* **1958**, *80*, 2902-2903.
44. Wunsch, E.; Drees, F.: Darstellung der sequenz 22-29. *Chem. Ber.* **1966**, *99*, 110-120.
45. Konig, W.; Geiger, R.: A new method for synthesis of peptides-activation of carboxyl group with dicyclohexylcarbodiimide using 1-hydroxybenzotriazoles as additives. *Chem. Ber.* **1970**, *103*, 788-798.
46. Ehrlich, A.; Heyne, H. U.; Winter, R.; Beyermann, M.; Haber, H.; Carpino, L. A.; Bienert, M.: Cyclization of *all*-L-pentapeptides by means of 1-hydroxy-7-azabenzotriazole-derived uronium and phosphonium reagents. *J. Org. Chem.* **1996**, *61*, 8831-8838.
47. Hale, K. J.; Lazarides, L.: Synthetic route to the GE3 cyclodepsipeptide. *Org. Lett.* **2002**, *4*, 1903-1906.
48. Albericio, F.; Bofill, J. M.; El-Faham, A.; Kates, S. A.: Use of onium salt-based coupling reagents in peptide synthesis. *J. Org. Chem.* **1998**, *63*, 9678-9683.
49. Carpino, L. A.: 1-Hydroxy-7-azabenzotriazole. An efficient peptide coupling additive. *J. Am. Chem. Soc.* **1993**, *115*, 4397-4398.
50. Palumbo, A. M.; Tepe, J. J.; Reid, G. E.: Mechanistic insights into the multistage gas-phase fragmentation behavior of phosphoserine- and phosphothreonine-containing peptides. *J. Proteome Res.* **2008**, *7*, 771-779.
51. Palacios, D. S.; Dailey, I.; Siebert, D. M.; Wilcock, B. C.; Burke, M. D.: Synthesis-enabled functional group deletions reveal key underpinnings of amphotericin B ion channel and antifungal activities. *Proc. Natl. Acad. Sci. USA.* **2011**, *108*, 6733-6738.
52. Gray, K. C.; Palacios, D. S.; Dailey, I.; Endo, M. M.; Uno, B. E.; Wilcock, B. C.; Burke, M. D.: Amphotericin primarily kills yeast by simply binding ergosterol. *Proc. Natl. Acad. Sci. USA.* **2012**, *109*, 2234-2239.

APPENDIX: LETTERS OF PERMISSION

Figure 1.3 – Page 3

JOHN WILEY AND SONS LICENSE
TERMS AND CONDITIONS
Oct 07, 2013

This is a License Agreement between Douglas D Wong ("You") and John Wiley and Sons ("John Wiley and Sons") provided by Copyright Clearance Center ("CCC"). The license consists of your order details, the terms and conditions provided by John Wiley and Sons, and the payment terms and conditions.

All payments must be made in full to CCC. For payment instructions, please see information listed at the bottom of this form.

License Number	3240250945025
License date	Oct 01, 2013
Licensed content publisher	John Wiley and Sons
Licensed content publication	Angewandte Chemie International Edition
Licensed content title	Lithistid Sponges: Star Performers or Hosts to the Stars
Licensed copyright line	© 1998 WILEY-VCH Verlag GmbH, Weinheim, Fed. Rep. of Germany
Licensed content author	Carole A. Bewley,D. John Faulkner
Licensed content date	Dec 17, 1998
Start page	2162
End page	2178
Type of use	Dissertation/Thesis
Requestor type	University/Academic
Format	Print and electronic
Portion	Figure/table
Number of figures/tables	1
Original Wiley figure/table number(s)	Cover Page Figure
Will you be translating?	No
Total	0.00 USD
Terms and Conditions	

ELSEVIER LICENSE
TERMS AND CONDITIONS

Oct 07, 2013

This is a License Agreement between Douglas D Wong ("You") and Elsevier ("Elsevier") provided by Copyright Clearance Center ("CCC"). The license consists of your order details, the terms and conditions provided by Elsevier, and the payment terms and conditions.

All payments must be made in full to CCC. For payment instructions, please see information listed at the bottom of this form.

Supplier	Elsevier Limited The Boulevard, Langford Lane Kidlington, Oxford, OX5 1GB, UK
Registered Company Number	1982084
Customer name	Douglas D Wong
Customer address	1634 Cora Dive BATON ROUGE, LA 70815
License number	3231031145509
License date	Sep 16, 2013
Licensed content publisher	Elsevier
Licensed content publication	Tetrahedron
Licensed content title	Histidinoalanine: a crosslinking amino acid
Licensed content author	Carol M. Taylor, Weihua Wang
Licensed content date	10 September 2007
Licensed content volume number	63
Licensed content issue number	37
Number of pages	15
Start Page	9033
End Page	9047
Type of Use	reuse in a thesis/dissertation
Portion	figures/tables/illustrations
Number of figures/tables/illustrations	1
Format	both print and electronic
Are you the author of this Elsevier article?	No
Will you be translating?	No
Order reference number	
Title of your thesis/dissertation	Synthetic Efforts Toward the Eastern Hemisphere of Theonellamide C
Expected completion date	Sep 2013
Estimated size (number of pages)	250

Elsevier VAT number	GB 494 6272 12
Permissions price	0.00 USD
VAT/Local Sales Tax	0.0 USD / 0.0 GBP
Total	0.00 USD
Terms and Conditions	

SPRINGER LICENSE
TERMS AND CONDITIONS

Oct 07, 2013

This is a License Agreement between Douglas D Wong ("You") and Springer ("Springer") provided by Copyright Clearance Center ("CCC"). The license consists of your order details, the terms and conditions provided by Springer, and the payment terms and conditions.

All payments must be made in full to CCC. For payment instructions, please see information listed at the bottom of this form.

License Number	3231050373145
License date	Sep 16, 2013
Licensed content publisher	Springer
Licensed content publication	Marine Biotechnology
Licensed content title	Accumulation of H ⁺ in Vacuoles Induced by a Marine Peptide Toxin, Theonellamide F, in Rat Embryonic 3Y1 Fibroblasts
Licensed content author	Shun-ichi Wada
Licensed content date	Jan 1, 2002
Volume number	4
Issue number	6
Type of Use	Thesis/Dissertation
Portion	Figures
Author of this Springer article	No
Order reference number	
Title of your thesis / dissertation	Synthetic Efforts Toward the Eastern Hemisphere of Theonellamide C
Expected completion date	Sep 2013
Estimated size(pages)	250
Total	0.00 USD
Terms and Conditions	

ELSEVIER LICENSE
TERMS AND CONDITIONS

Oct 07, 2013

This is a License Agreement between Douglas D Wong ("You") and Elsevier ("Elsevier") provided by Copyright Clearance Center ("CCC"). The license consists of your order details, the terms and conditions provided by Elsevier, and the payment terms and conditions.

All payments must be made in full to CCC. For payment instructions, please see information listed at the bottom of this form.

Supplier	Elsevier Limited The Boulevard, Langford Lane Kidlington, Oxford, OX5 1GB, UK
Registered Company Number	1982084
Customer name	Douglas D Wong
Customer address	1634 Cora Dive BATON ROUGE, LA 70815
License number	3231051147969
License date	Sep 16, 2013
Licensed content publisher	Elsevier
Licensed content publication	Bioorganic & Medicinal Chemistry
Licensed content title	Chemical-genomic profiling: Systematic analysis of the cellular targets of bioactive molecules
Licensed content author	Kerry Andrusiak, Jeff S. Piotrowski, Charles Boone
Licensed content date	15 March 2012
Licensed content volume number	20
Licensed content issue number	6
Number of pages	9
Start Page	1952
End Page	1960
Type of Use	reuse in a thesis/dissertation
Intended publisher of new work	other
Portion	figures/tables/illustrations
Number of figures/tables/illustrations	1
Format	both print and electronic
Are you the author of this Elsevier article?	No
Will you be translating?	No

Order reference number	
Title of your thesis/dissertation	Synthetic Efforts Toward the Eastern Hemisphere of Theonellamide C
Expected completion date	Sep 2013
Estimated size (number of pages)	250
Elsevier VAT number	GB 494 6272 12
Permissions price	0.00 USD
VAT/Local Sales Tax	0.0 USD / 0.0 GBP
Total	0.00 USD
Terms and Conditions	

ELSEVIER LICENSE
TERMS AND CONDITIONS

Oct 07, 2013

This is a License Agreement between Douglas D Wong ("You") and Elsevier ("Elsevier") provided by Copyright Clearance Center ("CCC"). The license consists of your order details, the terms and conditions provided by Elsevier, and the payment terms and conditions.

All payments must be made in full to CCC. For payment instructions, please see information listed at the bottom of this form.

Supplier	Elsevier Limited The Boulevard,Langford Lane Kidlington,Oxford,OX5 1GB,UK
Registered Company Number	1982084
Customer name	Douglas D Wong
Customer address	1634 Cora Dive BATON ROUGE, LA 70815
License number	3231061386164
License date	Sep 16, 2013
Licensed content publisher	Elsevier
Licensed content publication	Cell
Licensed content title	Exploring the Mode-of-Action of Bioactive Compounds by Chemical-Genetic Profiling in Yeast
Licensed content author	Ainslie B. Parsons,Andres Lopez,Inmar E. Givoni,David E. Williams,Christopher A. Gray,Justin Porter,Gordon Chua,Richelle Sopko,Renee L. Brost,Cheuk-Hei Ho,Jiyi Wang,Troy Ketela,Charles Brenner,Julie A. Brill,G. Esteban Fernandez,Todd C. Lorenz, et al.
Licensed content date	11 August 2006
Licensed content volume number	126
Licensed content issue number	3
Number of pages	15
Start Page	611
End Page	625
Type of Use	reuse in a thesis/dissertation
Intended publisher of new work	other
Portion	figures/tables/illustrations

Number of figures/tables/illustrations	1
Format	both print and electronic
Are you the author of this Elsevier article?	No
Will you be translating?	No
Order reference number	
Title of your thesis/dissertation	Synthetic Efforts Toward the Eastern Hemisphere of Theonellamide C
Expected completion date	Sep 2013
Estimated size (number of pages)	250
Elsevier VAT number	GB 494 6272 12
Permissions price	0.00 USD
VAT/Local Sales Tax	0.0 USD / 0.0 GBP
Total	0.00 USD
Terms and Conditions	

a in Figure 1.10 – Page 18; Figure 1.11 – Page 19; Figure 1.12 – Page 20

NATURE PUBLISHING GROUP LICENSE
TERMS AND CONDITIONS

Oct 07, 2013

This is a License Agreement between Douglas D Wong ("You") and Nature Publishing Group ("Nature Publishing Group") provided by Copyright Clearance Center ("CCC"). The license consists of your order details, the terms and conditions provided by Nature Publishing Group, and the payment terms and conditions.

All payments must be made in full to CCC. For payment instructions, please see information listed at the bottom of this form.

License Number	3231070400850
License date	Sep 16, 2013
Licensed content publisher	Nature Publishing Group
Licensed content publication	Nature Biotechnology
Licensed content title	A molecular barcoded yeast ORF library enables mode-of-action analysis of bioactive compounds
Licensed content author	Cheuk Hei Ho, Leslie Magtanong, Sarah L Barker, David Gresham, Shinichi Nishimura et al.
Licensed content date	Apr 6, 2009
Volume number	27
Issue number	4
Type of Use	reuse in a thesis/dissertation
Requestor type	academic/educational
Format	print and electronic
Portion	figures/tables/illustrations
Number of figures/tables/illustrations	2
Figures	Figure 4 and Figure 5
Author of this NPG article	no
Your reference number	
Title of your thesis / dissertation	Synthetic Efforts Toward the Eastern Hemisphere of Theonellamide C
Expected completion date	Sep 2013
Estimated size (number of pages)	250
Total	0.00 USD

NATURE PUBLISHING GROUP LICENSE
TERMS AND CONDITIONS

Oct 07, 2013

This is a License Agreement between Douglas D Wong ("You") and Nature Publishing Group ("Nature Publishing Group") provided by Copyright Clearance Center ("CCC"). The license consists of your order details, the terms and conditions provided by Nature Publishing Group, and the payment terms and conditions.

All payments must be made in full to CCC. For payment instructions, please see information listed at the bottom of this form.

License Number	3231070928532
License date	Sep 16, 2013
Licensed content publisher	Nature Publishing Group
Licensed content publication	Nature Chemical Biology
Licensed content title	Marine antifungal theonellamides target 3 β -hydroxysterol to activate Rho1 signaling
Licensed content author	Shinichi Nishimura, Yuko Arita, Miyuki Honda, Kunihiko Iwamoto, Akihisa Matsuyama, Atsuko Shirai
Licensed content date	Jun 13, 2010
Volume number	6
Issue number	7
Type of Use	reuse in a thesis/dissertation
Requestor type	academic/educational
Format	print and electronic
Portion	figures/tables/illustrations
Number of figures/tables/illustrations	5
Figures	Figure 1 and Figure 2 and Figure 3 and Figure 4 and Figure 5
Author of this NPG article	no
Your reference number	
Title of your thesis / dissertation	Synthetic Efforts Toward the Eastern Hemisphere of Theonellamide C
Expected completion date	Sep 2013
Total	0.00 USD

JOHN WILEY AND SONS LICENSE
TERMS AND CONDITIONS

Oct 07, 2013

This is a License Agreement between Douglas D Wong ("You") and John Wiley and Sons ("John Wiley and Sons") provided by Copyright Clearance Center ("CCC"). The license consists of your order details, the terms and conditions provided by John Wiley and Sons, and the payment terms and conditions.

All payments must be made in full to CCC. For payment instructions, please see information listed at the bottom of this form.

License Number	3231041230956
License date	Sep 16, 2013
Licensed content publisher	John Wiley and Sons
Licensed content publication	Chemistry - A European Journal
Licensed content title	Recent Developments in Methodology for the Direct Oxyamination of Olefins
Licensed copyright line	Copyright © 2011 WILEY-VCH Verlag GmbH & Co. KGaA, Weinheim
Licensed content author	Timothy J. Donohoe, Cedric K. A. Callens, Aida Flores, Adam R. Lacy, Akshat H. Rathi
Licensed content date	Dec 16, 2010
Start page	58
End page	76
Type of use	Dissertation/Thesis
Requestor type	University/Academic
Format	Print and electronic
Portion	Figure/table
Number of figures/tables	1
Original Wiley figure/table number(s)	Scheme 2
Will you be translating?	No
Total	0.00 USD
Terms and Conditions	

ELSEVIER LICENSE
TERMS AND CONDITIONS

Oct 07, 2013

This is a License Agreement between Douglas D Wong ("You") and Elsevier ("Elsevier") provided by Copyright Clearance Center ("CCC"). The license consists of your order details, the terms and conditions provided by Elsevier, and the payment terms and conditions.

All payments must be made in full to CCC. For payment instructions, please see information listed at the bottom of this form.

Supplier	Elsevier Limited The Boulevard, Langford Lane Kidlington, Oxford, OX5 1GB, UK
Registered Company Number	1982084
Customer name	Douglas D Wong
Customer address	1634 Cora Dive BATON ROUGE, LA 70815
License number	3231090403007
License date	Sep 16, 2013
Licensed content publisher	Elsevier
Licensed content publication	Tetrahedron
Licensed content title	The asymmetric aminohydroxylation route to GABOB and homoserine derivatives
Licensed content author	Michael Harding, Jennifer A. Bodkin, Fatiah Issa, Craig A. Hutton, Anthony C. Willis, Malcolm D. McLeod
Licensed content date	24 January 2009
Licensed content volume number	65
Licensed content issue number	4
Number of pages	13
Start Page	831
End Page	843
Type of Use	reuse in a thesis/dissertation
Intended publisher of new work	other
Portion	figures/tables/illustrations
Number of figures/tables/illustrations	2
Format	both print and electronic
Are you the author of this Elsevier article?	No
Will you be translating?	No

Order reference number	
Title of your thesis/dissertation	Synthetic Efforts Toward the Eastern Hemisphere of Theonellamide C
Expected completion date	Sep 2013
Estimated size (number of pages)	250
Elsevier VAT number	GB 494 6272 12
Permissions price	0.00 USD
VAT/Local Sales Tax	0.0 USD / 0.0 GBP
Total	0.00 USD
Terms and Conditions	

ELSEVIER LICENSE
TERMS AND CONDITIONS

Oct 07, 2013

This is a License Agreement between Douglas D Wong ("You") and Elsevier ("Elsevier") provided by Copyright Clearance Center ("CCC"). The license consists of your order details, the terms and conditions provided by Elsevier, and the payment terms and conditions.

All payments must be made in full to CCC. For payment instructions, please see information listed at the bottom of this form.

Supplier	Elsevier Limited The Boulevard, Langford Lane Kidlington, Oxford, OX5 1GB, UK
Registered Company Number	1982084
Customer name	Douglas D Wong
Customer address	1634 Cora Dive BATON ROUGE, LA 70815
License number	3231970893435
License date	Sep 18, 2013
Licensed content publisher	Elsevier
Licensed content publication	Tetrahedron Letters
Licensed content title	Asymmetric synthesis of <i>erythro</i> - β -hydroxyasparagine
Licensed content author	Douglas Wong, Carol M. Taylor
Licensed content date	25 March 2009
Licensed content volume number	50
Licensed content issue number	12
Number of pages	3
Start Page	1273
End Page	1275
Type of Use	reuse in a thesis/dissertation
Intended publisher of new work	other
Portion	figures/tables/illustrations
Number of figures/tables/illustrations	1
Format	both print and electronic
Are you the author of this Elsevier article?	Yes
Will you be translating?	No
Order reference number	
Title of your thesis/dissertation	Synthetic Efforts Toward the Eastern Hemisphere of Theonellamide C

Expected completion date	Sep 2013
Estimated size (number of pages)	250
Elsevier VAT number	GB 494 6272 12
Permissions price	0.00 USD
VAT/Local Sales Tax	0.0 USD / 0.0 GBP
Total	0.00 USD
Terms and Conditions	

Scheme 3.8 – Page 86

Dear Douglas,

You have our permission to use the figure from page 416 in "Fundamentals of Asymmetric Catalysis" by Walsh and Kowzowski in your dissertation, as cited below. Please list full copyright information (book's title, authors, copyright year, publisher) and "All rights reserved, used with permission from the publisher."

Thanks and good luck with your defense!

Jane Ellis
USB

NATURE PUBLISHING GROUP LICENSE
TERMS AND CONDITIONS

Oct 07, 2013

This is a License Agreement between Douglas D Wong ("You") and Nature Publishing Group ("Nature Publishing Group") provided by Copyright Clearance Center ("CCC"). The license consists of your order details, the terms and conditions provided by Nature Publishing Group, and the payment terms and conditions.

All payments must be made in full to CCC. For payment instructions, please see information listed at the bottom of this form.

License Number	3231100813834
License date	Sep 16, 2013
Licensed content publisher	Nature Publishing Group
Licensed content publication	Nature Reviews Drug Discovery
Licensed content title	Aliskiren: the first renin inhibitor for clinical treatment
Licensed content author	Chris Jensen, Peter Herold and Hans Rudolf Brunner
Licensed content date	Mar 14, 2008
Volume number	7
Issue number	5
Type of Use	reuse in a thesis/dissertation
Requestor type	academic/educational
Format	print and electronic
Portion	figures/tables/illustrations
Number of figures/tables/illustrations	2
Figures	Figure 3 and Figure 4
Title of your thesis / dissertation	Synthetic Efforts Toward the Eastern Hemisphere of Theonellamide C
Expected completion date	Sep 2013
Estimated size (number of pages)	250
Total	0.00 USD

THE VITA

Douglas D. Wong received his Bachelor of Science degree in Chemistry in 2003 from LSU. He was introduced to organic chemistry research as an undergraduate in the laboratory of Professor Robert M. Strongin where he synthesized a chemosensor for the HPLC postcolumn detection of mono- and oligosaccharides. In the fall of 2006, Douglas was accepted into the doctoral program in the chemistry department at LSU where he is currently a doctoral candidate in organic chemistry working under the direction of Professor Carol M. Taylor. His graduate dissertation work involved efforts toward some of the required amino acid residues of theonellamide C and the eastern hemisphere. Douglas is a member of the American Chemical Society.